LEABHARLANN CHOLÁISTE NA TRÍONÓIDE, BAILE ÁTHA CLIATH | TRINITY COLLEGE LIBRARY DUBLIN
Ollscoil Átha Cliath | The University of Dublin

Terms and Conditions of Use of Digitised Theses from Trinity College Library Dublin

Copyright statement

All material supplied by Trinity College Library is protected by copyright (under the Copyright and Related Rights Act, 2000 as amended) and other relevant Intellectual Property Rights. By accessing and using a Digitised Thesis from Trinity College Library you acknowledge that all Intellectual Property Rights in any Works supplied are the sole and exclusive property of the copyright and/or other IPR holder. Specific copyright holders may not be explicitly identified. Use of materials from other sources within a thesis should not be construed as a claim over them.

A non-exclusive, non-transferable licence is hereby granted to those using or reproducing, in whole or in part, the material for valid purposes, providing the copyright owners are acknowledged using the normal conventions. Where specific permission to use material is required, this is identified and such permission must be sought from the copyright holder or agency cited.

Liability statement

By using a Digitised Thesis, I accept that Trinity College Dublin bears no legal responsibility for the accuracy, legality or comprehensiveness of materials contained within the thesis, and that Trinity College Dublin accepts no liability for indirect, consequential, or incidental, damages or losses arising from use of the thesis for whatever reason. Information located in a thesis may be subject to specific use constraints, details of which may not be explicitly described. It is the responsibility of potential and actual users to be aware of such constraints and to abide by them. By making use of material from a digitised thesis, you accept these copyright and disclaimer provisions. Where it is brought to the attention of Trinity College Library that there may be a breach of copyright or other restraint, it is the policy to withdraw or take down access to a thesis while the issue is being resolved.

Access Agreement

By using a Digitised Thesis from Trinity College Library you are bound by the following Terms & Conditions. Please read them carefully.

I have read and I understand the following statement: All material supplied via a Digitised Thesis from Trinity College Library is protected by copyright and other intellectual property rights, and duplication or sale of all or part of any of a thesis is not permitted, except that material may be duplicated by you for your research use or for educational purposes in electronic or print form providing the copyright owners are acknowledged using the normal conventions. You must obtain permission for any other use. Electronic or print copies may not be offered, whether for sale or otherwise to anyone. This copy has been supplied on the understanding that it is copyright material and that no quotation from the thesis may be published without proper acknowledgement.

Finite Element and Experimental Analysis of the Micro-Form Rolling Process

Emmet Cregan

SUBMITTED IN FULFILLMENT OF THE REQUIREMENTS FOR THE DEGREE OF DOCTOR OF PHILOSOPHY AT UNIVERSITY OF DUBLIN, TRINITY COLLEGE DUBLIN, IRELAND, MARCH 2007.

Supervisor: **Professor John Monaghan**

The work presented in this thesis was conducted at the Department of Mechanical and Manufacturing Engineering, University of Dublin, Trinity College, Ireland.

TRINITY COLLEGE
05 JUL 2007
LIBRARY DUBLIN
THOSS
8120

DECLARATION

Date: March 2007

Author: Emmet Cregan

Title: Finite Element and Experimental Analysis of the Micro-Form Rolling Process

Department: Mechanical & Manufacturing Engineering

Degree: Ph.D.

Year: 2007

I declare that the present work was not submitted as an exercise for a degree to any other another University. This thesis consists entirely of my own work, except where references indicate otherwise.

I agree that the Library may lend or copy the thesis upon request. This permission covers only single copies made for study purposes, subject to normal conditions of acknowledgement.

Signature of Author: 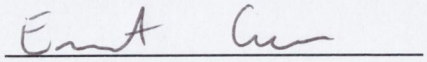

Emmet Cregan

The observations made during this research which, to the best knowledge of the author have not been previously mentioned in literature, were as follows:

- Loss of contact between the die and workpiece when rolling small diameter parts and the subsequent deviation of the workpiece groove geometry from the die geometry was predicted using FEA and observed experimentally.
- Literature predicted a laminar strain pattern in the workpiece in which the maximum values were located at the workpiece surface. The laminar pattern was confirmed during this research and, using 3D FEA, it was for the first time attributed to the rotational nature of the form rolling process.
- Die designs that prevented the formation of axial and helical laps on form rolled parts were designed and tested.
- The novel 'one-die rolling' process was trialled and proved to be a viable process.

Finite Element and Experimental Analysis of the Micro-Form Rolling Process

Emmet Cregan[1]

1. Dept. of Mechanical & Manufacturing Engineering, Trinity College Dublin, Ireland.

SUMMARY

With the greater miniaturisation of products, there is an increasing requirement for micro-parts and micro-fasteners. Currently, the majority of these micro-parts are manufactured using micro-machining processes. Micro-forming is the ideal method for the mass production of these micro-parts due to its advantages of high production rates and improved material properties. However, uncertainties relating to forming at the micro-scale have prevented its universal uptake. This project aims to address some of these uncertainties.

Form rolling is a rotary cold forming process in which the workpiece is rotated between a pair of flat dies. It can be used to form complex shapes on axisymmetric metal parts. Micro-parts are those with at least two sub-millimetre dimensions and the parts form rolled during this research fall into this category.

This research aims to establish a better understanding of the effects that workpiece diameter, material, area reduction and die geometry have on the micro-form rolling process and the quality of the formed parts. Particular regard was placed on the occurrence of internal failures, which are largely dependent on the area reduction experienced by the part during the forming process.

Micro-form rolling trials using a variety of die/workpiece combinations were carried out on a machine purchased specifically for this research. The rolled parts were mounted sectioned and investigated under a microscope to determine the presence, location and magnitude of defects.

The Elasto-plastic FE packages DEFORM 2D and 3D were used to model the micro-form rolling process. The stress distributions present in the workpiece during rolling were also examined to determine a better understanding of the mechanics of the process. Signs of failure were also monitored e.g. in some simulations high damage values indicated that internal failure was likely to ensue.

ACKNOWLEDGEMENTS

Firstly, I must thank my supervisor Professor John Monaghan for giving me the opportunity to carry out this research and for his subsequent advice and support during the intervening three years.

I would also like to thank Materials Ireland for their financial and technical support. In particular I would like to mention Toman MacGinley for bringing my computer back from the brink and answering all my technical questions, Ray Walsh for aiding me in the early and uncertain days of testing, Michael Murphy for his support throughout the project and Ioan Butan who has such an attraction to form rolling that he has decided to take it up full time.

From the Manufacturing Engineering Department at Trinity, I must mention J.J. Ryan for milling smaller than he has ever milled before in making the die sets used in this project, Peter O'Reilly who helped me with the materials testing part of the project and Dermot Geraghty and Paul Normoyle for their assistance in developing sensor based monitoring equipment.

I would also like to express my gratitude to Jim Ryall and Ali Pasalar from Hi-Life Tools for their advice, time and resources in the design and manufacture of micro-form rolling dies.

Of course, I must also mention the people with whom I have shared an office with during my time at Trinity. These include George who was also a form roller and provided me with a lot of information about the process, Kevin, Alan, Saeid, Daniela and Dave who were always willing to go for a coffee and a chat when I needed a break.

Finally I must thank my parents Eleanor and John, my sister Jill and my brother Brendan and my friends for their encouragement and their belief that one day I would finish this thesis.

5.1 Form Rolling 43
5.1.1 **Mechanics of the process** 43
5.1.2 **Empirical Analysis of the process** 49
5.1.3 **Failures associated with Form Rolling** 54
5.1.4 **Lap Formation during the Form Rolling process** 62
5.1.5 **Tool Design** 66
5.2 The Forming and Machining of Micro-Parts 70
5.2.1 **The 'Size Effect' in Micro-Forming** 70
5.2.2 **The Size Effect in the Machining of Micro-Forming Tooling** ..... **Error! Bookmark not defined.**
5.3 Theory of Similarity ..... **Error! Bookmark not defined.**
5.4 The FEA of Form Rolling and Micro-Forming ..... **Error! Bookmark not defined.**
5.4.1 **The Application of FEA in the Analysis of Form Rolling** ..... **Error! Bookmark not defined.**
5.4.2 **The Application of FEA to Micro-Forming** ..... **Error! Bookmark not defined.**
5.5 Fracture and Damage Criteria ..... **Error! Bookmark not defined.**
5.5.1 **Fracture Surfaces** ..... **Error! Bookmark not defined.**
5.5.2 **Damage Criteria** ..... **Error! Bookmark not defined.**
CHAPTER 6 ..... **Error! Bookmark not defined.**
WORK PROGRAMME ..... **Error! Bookmark not defined.**
6.1. Die Design ..... **Error! Bookmark not defined.**
6.1.1 **Dies to Investigate the size effect** ..... **Error! Bookmark not defined.**
6.1.2 **Dies to Investigate the Effect of Die Geometry** ..... **Error! Bookmark not defined.**
6.2 Die Manufacture ..... **Error! Bookmark not defined.**
6.2.1 **Milled Die Manufacture** ..... **Error! Bookmark not defined.**
6.2.2 **Ground Die Manufacture** ..... **Error! Bookmark not defined.**
6.2.3 **Die Material** ..... **Error! Bookmark not defined.**
6.2.4 **Heat Treatment of Micro-Form Rolling Dies** ..... **Error! Bookmark not defined.**
6.3 Form Rolling Trials ..... **Error! Bookmark not defined.**
6.3.1 **The EWM AF3 Micro Thread / Form Roller** ..... **Error! Bookmark not defined.**
6.3.2 **Blued Dies** ..... **Error! Bookmark not defined.**
6.3.3 **Form Rolling Trials** ..... **Error! Bookmark not defined.**
6.3.4 **Workpiece Materials** ..... **Error! Bookmark not defined.**
6.3.5 **One-Die Rolling Trials** ..... **Error! Bookmark not defined.**
6.4 Investigation of Form Rolled Parts ..... **Error! Bookmark not defined.**
6.4.1 **Mounting of the Rolled Specimen** ..... **Error! Bookmark not defined.**
6.4.2 **Polishing of the Mounted Specimen** ..... **Error! Bookmark not defined.**
6.4.3 **Etching the Specimen** ..... **Error! Bookmark not defined.**
6.4.4 **Microscopy of Micro-Form Rolled Parts and Micro-Form Rolling dies** ..... **Error! Bookmark not defined.**
6.5 Determining Accuracy and Dimensions of the Die Sets ..... **Error! Bookmark not defined.**
6.6 FEA of Form Rolling Process ..... **Error! Bookmark not defined.**
6.6.1 **2D Simulation Methods** ..... **Error! Bookmark not defined.**
6.6.2 **3D Simulation Methods** ..... **Error! Bookmark not defined.**

TABLE OF CONTENTS

LIST OF FIGURES XIII
LIST OF TABLES XIX
NOMENCLATURE XXI
CHAPTER 1 1
INTRODUCTION 1
CHAPTER 2 5
PROJECT OBJECTIVES 5
2.1 The Project Objective 7
2.2 Sub-Objectives 8
2.2.1 **Determine the Limitations of Micro-Form Rolling** 8
2.2.2 **Determine the effect of Miniaturisation on the Form Rolling Process** 8
2.2.3 **Determine the effect of Die Geometry and Manufacturing Method on the Micro-Form Rolling Process** 9
2.2.4 **Determine the effect of Workpiece Material on Micro-Form Rolling** 9
2.2.5 **Develop a Tooling Design Analysis Method** 9
2.2.6 **Develop the One-Die Rolling Process** 10
CHAPTER 3 11
THE BASICS OF MICRO AND MACRO-FORM ROLLING 11
3.1 The Basics of Micro-Forming 13
3.1.1 **Micro-parts** 13
3.1.2 **Introduction to the 'size effect'** 14
3.2 The Basics of the Form Rolling Process 16
3.2.1 **History of Form Rolling** 16
3.2.2 **Components Produced using the Form Rolling Process** 16
3.2.3 **Advantages of Form Rolling** 17
3.2.4 **Varieties of Form Rolling Die Configurations** 18
3.2.5 **Micro-Form Rolling Machines** 19
3.2.6 **The Form Rolling Process Using Flat Dies** 19
3.2.7 **Penetration Rate** 23
3.2.8 **Workpiece Rotation and the Waveform** 24
3.2.9 **Velocities and Torsional stresses in the Form Rolling Process** 26
3.2.10 **Form Rolling Like Processes** 29
3.2.11 **Advantages/Disadvantages of Micro-Form Rolling** 29
3.2.12 **One-Die Rolling** 31
CHAPTER 4 33
METAL FORMING AND THE FINITE ELEMENT METHOD 33
4.1 Overview of DEFORM software 35
4.2 Modelling of a Form Rolling Process using DEFORM 36
4.2.1 **Von Mises Yield Criteria** 36
4.2.2 **Prandtl-Reuss Flow Rule** 36
4.2.3 **Isotropic Hardening** 37
4.2.4 **Contact Conditions** 37
4.3 Creating a Meshed Object in DEFORM 37
4.4 State variables in DERORM FEA package 38
4.4.1 **Graphical Representation of the State Variables** 38
4.4.2 **Definition of State Variables** 40
CHAPTER 5 41
LITERATURE REVIEW 41

7.8.1 **Laminar Strain Pattern in a Form Rolled Part as Predicted by FEA Error! Bookmark not defined.**

7.8.2 **Stress Distribution in a Form Rolled part as predicted by FEA.... Error! Bookmark not defined.**

7.9 Development of a Larger Waveform on One Side of the Workpiece Error! Bookmark not defined.

7.10 One-Die Rolling ..... Error! Bookmark not defined.

7.10.1 **Importance of the Viability of One-Die Rolling for Micro-Form Rolling ..... Error! Bookmark not defined.**

7.10.2 **Development of Workpiece Shape during One-Die Rolling..... Error! Bookmark not defined.**

7.10.3 **Possibility of Lap Formation..... Error! Bookmark not defined.**

7.10.4 **Quality of Parts Produced using One-Die Rolling. Error! Bookmark not defined.**

7.10.5 **Advantages and Disadvantages of the One-Die Rolling Process.... Error! Bookmark not defined.**

CHAPTER 8..... **Error! Bookmark not defined.**

CONCLUSIONS ..... **Error! Bookmark not defined.**

CHAPTER 9..... **Error! Bookmark not defined.**

FUTURE WORK ..... **Error! Bookmark not defined.**

REFERENCES ..... Error! Bookmark not defined.

APPENDIX: FORM ROLLING MACHINE SETUP SHEET.... Error! Bookmark not defined.

APPENDIX: CONFERENCE PROCEEDINGS..... Error! Bookmark not defined.

APPENDIX: POSTER PRESENTATION ..... Error! Bookmark not defined.

CHAPTER 7 139
RESULTS AND DISCUSSION 139
7.1 The size effect 141
7.1.1 **The size effect in Micro-Form Rolling** 141
7.1.2 **The size effect in the Grinding of Micro-Form Rolling Dies** 142
7.2 Limitations of Micro-Form Rolling 143
7.2.1 **Accuracy of Milled Dies** 143
7.2.2 **Limitations Associated with Machine Adjustability** 146
7.2.3 **The Limitations of Measurement Accuracy and its Effect on FEA Simulations** 147
7.3 The Quality of Milled Die Sets 150
7.3.1 **Steps on the Sidewall of the Milled Die Sets** 150
7.3.2 **Burrs** 151
7.4 The Quality of Micro-Form Rolled Parts 153
7.4.1 **The Surface Quality of Form Rolled Parts** 153
7.4.2 **Loss of Die-Workpiece contact on the Groove Sidewall** 161
7.5 Internal Defects in Micro-Form Rolled Parts 172
7.5.1 **Axial Workpiece Failures Located Away from the Groove** 172
7.5.2 **Workpiece Failures Due to the Forming of the Groove** 175
7.5.3 **Explaining the Development of Internal Failures Using FEA Damage Values** 177
7.6 Micro-Form Rolling and FEA 179
7.6.1 **Undesired Rotation of the Workpiece in 3D FEA** 180
7.6.2 **2D Sequential versus Single Stroke Simulation** 184
7.6.3 **Limitations of 2D FEA** 188
7.7 Rolling Loads Predicted by FEA Simulations 192
7.8 Stress and Strain Distributions Predicted using FEA 195
7.8.1 **Laminar Strain Pattern in a Form Rolled Part as Predicted by FEA** 195
7.8.2 **Stress Distribution in a Form Rolled part as predicted by FEA** 202
7.9 Development of a Larger Waveform on One Side of the Workpiece 212
7.10 One-Die Rolling 218
7.10.1 **Importance of the Viability of One-Die Rolling for Micro-Form Rolling** 218
7.10.2 **Development of Workpiece Shape during One-Die Rolling** 223
7.10.3 **Possibility of Lap Formation** 224
7.10.4 **Quality of Parts Produced using One-Die Rolling** 225
7.10.5 **Advantages and Disadvantages of the One-Die Rolling Process** 227
CHAPTER 8 229
CONCLUSIONS 229
CHAPTER 9 237
FUTURE WORK 237
REFERENCES 241
APPENDIX: FORM ROLLING MACHINE SETUP SHEET 245
APPENDIX: CONFERENCE PROCEEDINGS 246
APPENDIX: POSTER PRESENTATION 249

LIST OF FIGURES

Figure 1.1: Photograph showing a range of micro-parts [2] 3
Figure 1.2: A turned brass pin, machined using a Kugler Micro Turning machine, which could potentially be produced using the micro-form rolling process [6]. 4
Figure 2.1: Flow chart representation of Project Objectives and Tasks 7
Figure 3.1: 2mm ø stainless steel micro-form rolled part 13
Figure 3.2: Increasing proportion of surface grains with miniaturisation [9] 14
Figure 3.3: Decreasing flow strength with miniaturisation [10] 15
Figure 3.4: Photograph of a complex form rolled part 17
Figure 3.5: Photograph of a selection of form rolled parts 17
Figure 3.6: Diagrams of a variety of form rolling die configuration [13] 18
Figure 3.7: Diagram of the form rolling process and plan of a form rolling die 19
Figure 3.8: Diagram illustrating the change in the feature geometry along the length of a form rolling die 20
Figure 3.9: The geometry of a form rolled workpiece 21
Figure 3.10: Schematic of the geometric details and nomenclature for form rolling dies . 22
Figure 3.11: Description of the various die angles found on a form rolling die 24
Figure 3.12: Generation of a waveform on the workpiece due to the combination of area reduction and rotation it experiences during form rolling 25
Figure 3.13: Velocities of the dies and the workpiece during the form rolling Process 26
Figure 3.14: Velocity components of the rotating workpiece 27
Figure 3.15: Determining the tangential velocity of the workpiece 28
Figure 3.16: Die setup for one-die rolling compared with traditional form rolling 31
Figure 4.1: Mesh concentrated in the region of deformation using three mesh density windows 38
Figure 4.2: Graphical methods of representing state variables in the DEFORM post-processor 39
Figure 5.1: A comparison of form rolling and Transverse Helical Rolling 44
Figure 5.2: Regions of stress in Transverse Helical Rolled workpiece[29] 45
Figure 5.3: Transverse cross section of workpieces, into which M12 bolts were screwed before rolling [29] 46
Figure 5.4: Longitudinal sections of composite workpieces showing the development of axial rupture with increasing area reduction [34] 47
Figure 5.5: Increased frictional force when the billet length is increased 48
Figure 5.6: Radial sections of constrained workpieces showing the development of axial rupture with increased diameter reduction[34] 48
Figure 5.7: Analysing form rolling as a wedge reducing process 52
Figure 5.8: Relation between plane strain indentation pressure and H/l for a block of thickness H indented by flat rigid indenters of width l [45]. 56
Figure 5.9: Alligatoring or crocodiling failure [45] 57
Figure 5.10: Chevron failure in drawn wire [45] 57
Figure 5.11: Slip line field of transverse rolling section [46] 58
Figure 5.12: Workpieces at different levels of H/l. 59
Figure 5.13: Simplified contact forces between tool and workpiece [46] 59
Figure 5.14: Void development [23] 60
Figure 5.15: Failures within a form rolled part [23] 61
Figure 5.16: Internal stresses generated in a workpiece during form rolling [23] 61
Figure 5.17: Schematic of Toyoda form rolling machine and die [47] 62
Figure 5.18: Small 'fish-skin' or axial lap on a form rolled part[47] 63

LIST OF FIGURES

Figure 1.1: Photograph showing a range of micro-parts [2] 3
Figure 1.2: A turned brass pin, machined using a Kugler Micro Turning machine, which could potentially be produced using the micro-form rolling process [6]. 4
Figure 2.1: Flow chart representation of Project Objectives and Tasks 7
Figure 3.1: 2mm ø stainless steel micro-form rolled part 13
Figure 3.2: Increasing proportion of surface grains with miniaturisation [9] 14
Figure 3.3: Decreasing flow strength with miniaturisation [10] 15
Figure 3.4: Photograph of a complex form rolled part 17
Figure 3.5: Photograph of a selection of form rolled parts 17
Figure 3.6: Diagrams of a variety of form rolling die configuration [13] 18
Figure 3.7: Diagram of the form rolling process and plan of a form rolling die 19
Figure 3.8: Diagram illustrating the change in the feature geometry along the length of a form rolling die 20
Figure 3.9: The geometry of a form rolled workpiece 21
Figure 3.10: Schematic of the geometric details and nomenclature for form rolling dies 22
Figure 3.11: Description of the various die angles found on a form rolling die 24
Figure 3.12: Generation of a waveform on the workpiece due to the combination of area reduction and rotation it experiences during form rolling 25
Figure 3.13: Velocities of the dies and the workpiece during the form rolling Process 26
Figure 3.14: Velocity components of the rotating workpiece 27
Figure 3.15: Determining the tangential velocity of the workpiece 28
Figure 3.16: Die setup for one-die rolling compared with traditional form rolling 31
Figure 4.1: Mesh concentrated in the region of deformation using three mesh density windows 38
Figure 4.2: Graphical methods of representing state variables in the DEFORM post-processor 39
Figure 5.1: A comparison of form rolling and Transverse Helical Rolling 44
Figure 5.2: Regions of stress in Transverse Helical Rolled workpiece[29] 45
Figure 5.3: Transverse cross section of workpieces, into which M12 bolts were screwed before rolling [29] 46
Figure 5.4: Longitudinal sections of composite workpieces showing the development of axial rupture with increasing area reduction [34] 47
Figure 5.5: Increased frictional force when the billet length is increased 48
Figure 5.6: Radial sections of constrained workpieces showing the development of axial rupture with increased diameter reduction[34] 48
Figure 5.7: Analysing form rolling as a wedge reducing process 52
Figure 5.8: Relation between plane strain indentation pressure and H/l for a block of thickness H indented by flat rigid indenters of width l [45]. 56
Figure 5.9: Alligatoring or crocodiling failure [45] 57
Figure 5.10: Chevron failure in drawn wire [45] 57
Figure 5.11: Slip line field of transverse rolling section [46] 58
Figure 5.12: Workpieces at different levels of H/l. 59
Figure 5.13: Simplified contact forces between tool and workpiece [46] 59
Figure 5.14: Void development [23] 60
Figure 5.15: Failures within a form rolled part [23] 61
Figure 5.16: Internal stresses generated in a workpiece during form rolling [23] 61
Figure 5.17: Schematic of Toyoda form rolling machine and die [47] 62
Figure 5.18: Small 'fish-skin' or axial lap on a form rolled part[47] 63

Figure 6.7: The path taken by the grinding wheel when grinding the die **Error! Bookmark not defined.**
Figure 6.8: Trenches in the die as a result of the grinding process ... **Error! Bookmark not defined.**
Figure 6.9: Working area and overview of EWM AF3 form roller .. **Error! Bookmark not defined.**
Figure 6.10: Form rolling machine adjustments ..... **Error! Bookmark not defined.**
Figure 6.11: Adjusting the starting position of the moving die ..... **Error! Bookmark not defined.**
Figure 6.12: Adjusting the height of the stationary die ..... **Error! Bookmark not defined.**
Figure 6.13: Blued dies used to illustrate die/workpiece contact..... **Error! Bookmark not defined.**
Figure 6.14: Geometries of the die sets used in this research ..... **Error! Bookmark not defined.**
Figure 6.15: Sectioned form rolled workpieces showing internal failures[23]..... **Error! Bookmark not defined.**
Figure 6.16: Grinding of mounted From Rolled parts..... **Error! Bookmark not defined.**
Figure 6.17: Photographs of a micro-form rolled part obtained using a Scanning Electron Microscope (SEM) and an optical microscope. 1mm ø Stainless steel part rolled with the 2mm ground die set to an area reduction of 92%..... **Error! Bookmark not defined.**
Figure 6.18: x, y and z axis relative to die ..... **Error! Bookmark not defined.**
Figure 6.19: Converting the 3D form rolling process into a 2D simulation ..... **Error! Bookmark not defined.**
Figure 6.20: 2D simplification of 3D process ..... **Error! Bookmark not defined.**
Figure 6.21: Sectioning the die to create die profiles to be used in 2D FEA simulations ..... **Error! Bookmark not defined.**
Figure 6.22: Die Profiles used in 2D FEA simulations ..... **Error! Bookmark not defined.**
Figure 6.23: Image of 2D FEA form rolling simulation..... **Error! Bookmark not defined.**
Figure 6.24: Images of 3D FEA with rotating dies ..... **Error! Bookmark not defined.**
Figure 6.25: Images of 3D FEA with translating die ..... **Error! Bookmark not defined.**
Figure 6.26: Pictures of parts modelled using 3D FEA with translating die ..... **Error! Bookmark not defined.**
Figure 6.27: Plots of boundaries between tensile and compressive regions..... **Error! Bookmark not defined.**
Figure 6.28: Stress Regions within a form rolled workpiece..... **Error! Bookmark not defined.**
Figure 6.29: FEA of micro form-rolling damage ..... **Error! Bookmark not defined.**
Figure 6.30: Roughened surface on the workpiece due to the EDM finish on the tooling ..... **Error! Bookmark not defined.**
Figure 6.31: Improvement of surface quality with rolling.. **Error! Bookmark not defined.**
Figure 6.32 The scale of deformation on 0.45mm diameter wire due to traction surfaces created using 60 grit and 120 grit shot blasting..... **Error! Bookmark not defined.**
Figure 6.33: Blued dies demonstrating a lack of contact between the workpiece and the traction surfaces of the dies ..... **Error! Bookmark not defined.**
Figure 6.34: Photograph of a die with a raised area for the application of the EDM traction surface ..... **Error! Bookmark not defined.**
Figure 6.35: EDM prong used to selectively apply EDM traction surface to form rolling dies ..... **Error! Bookmark not defined.**
Figure 6.36: Photograph of grit blasted traction surface .... **Error! Bookmark not defined.**

Figure 6.15: Sectioned form rolled workpieces showing internal failures[23] 114
Figure 6.16: Grinding of mounted From Rolled parts 115
Figure 6.17: Photographs of a micro-form rolled part obtained using a Scanning Electron Microscope (SEM) and an optical microscope. 1mm ø Stainless steel part rolled with the 2mm ground die set to an area reduction of 92% 117
Figure 6.18: x, y and z axis relative to die 118
Figure 6.19: Converting the 3D form rolling process into a 2D simulation 119
Figure 6.20: 2D simplification of 3D process 120
Figure 6.21: Sectioning the die to create die profiles to be used in 2D FEA simulations 121
Figure 6.22: Die Profiles used in 2D FEA simulations 121
Figure 6.23: Image of 2D FEA form rolling simulation 122
Figure 6.24: Images of 3D FEA with rotating dies 123
Figure 6.25: Images of 3D FEA with translating die 124
Figure 6.26: Pictures of parts modelled using 3D FEA with translating die 126
Figure 6.27: Plots of boundaries between tensile and compressive regions 127
Figure 6.28: Stress Regions within a form rolled workpiece 127
Figure 6.29: FEA of micro form-rolling damage 128
Figure 6.30: Roughened surface on the workpiece due to the EDM finish on the tooling 129
Figure 6.31: Improvement of surface quality with rolling 130
Figure 6.32 The scale of deformation on 0.45mm diameter wire due to traction surfaces created using 60 grit and 120 grit shot blasting 131
Figure 6.33: Blued dies demonstrating a lack of contact between the workpiece and the traction surfaces of the dies 132
Figure 6.34: Photograph of a die with a raised area for the application of the EDM traction surface 132
Figure 6.35: EDM prong used to selectively apply EDM traction surface to form rolling dies 133
Figure 6.36: Photograph of grit blasted traction surface 134
Figure 6.37: Photographs of EDM surface 134
Figure 6.38: The excessive wear experienced by dies made from P20 during the form rolling of stainless steel 135
Figure 6.39: Start of groove positioned at the front of the die 136
Figure 6.40: Release pocket in die to release wire after rolling 137
Figure 6.41: The change in the length of the die feature with miniaturisation 137
Figure 7.1: Heterogeneous deformation on the free surface of the workpiece 141
Figure 7.2: Increased roughness of large diameter wires 142
Figure 7.3: Accuracy of Machining – problems due to machining tolerances 143
Figure 7.4: The location of the maximum damage values in the workpiece when the die geometry is created using measurements and a trace of a photograph 148
Figure 7.5: Difference in the geometries obtained from measurements and trace 149
Figure 7.6: Photographs from stereo-microscope and SEM illustrating the machining lines on the die sidewalls 150
Figure 7.7: The improvement of die shape with the reduction of machining cut size 150
Figure 7.8: Evidence of burrs on dies – photographs from stereo-microscope 151
Figure 7.9: Photographs illustrating the effect of workpiece miniaturisation. The parts have diameters ranging from 0.45mm to 2mm 154
Figure 7.10: Illustrating the effect of increasing area reduction and die manufacturing method. Parts (a) and (b) were formed using ground dies while parts (c) and (d) were formed using milled dies. Parts (b) was formed using the same die set as part

Figure 7.18: The angle of the workpiece sidewall as predicted using an axisymmetric assumption ..... **Error! Bookmark not defined.**
Figure 7.19: The angle of the workpiece sidewall as predicted using a plain strain assumption ..... **Error! Bookmark not defined.**
Figure 7.20: SEM photographs showing that the groove geometry is independent of workpiece diameter when a narrow flat is used..... **Error! Bookmark not defined.**
Figure 7.21: SEM photographs showing that the groove geometry changes with workpiece diameter when a wide flat is used ..... **Error! Bookmark not defined.**
Figure 7.22: Contact conditions and the geometry of the workpiece when it is in contact with the die sidewall..... **Error! Bookmark not defined.**
Figure 7.23: Contact conditions and the geometry of the workpiece after it losses contact with the die sidewall..... **Error! Bookmark not defined.**
Figure 7.24: The axial velocity of the workpiece before and after it loses contact with the die sidewall ..... **Error! Bookmark not defined.**
Figure 7.25: Photograph showing the proportion of the workpiece that is rolled between the dies..... **Error! Bookmark not defined.**
Figure 7.26: Mannesmann failure on the end of a 1mm diameter stainless steel workpiece rolled with 1mm milled dies: (a) and (b) are photographs of a transverse section while (c) is a photograph of an axial section ..... **Error! Bookmark not defined.**
Figure 7.27: Mannesmann failure located immediately outside the groove region of a failed 1mm diameter stainless steel workpiece rolled with 2mm milled dies.. **Error! Bookmark not defined.**
Figure 7.28: Stainless steel wire with internal failure ..... **Error! Bookmark not defined.**
Figure 7.29: Ductile fracture surface of failed form rolled titanium part **Error! Bookmark not defined.**
Figure 7.30: Damage plots showing the variation of damage with die penetration.... **Error! Bookmark not defined.**
Figure 7.31: Alignment of workpiece axis and die movement under correct operating conditions ..... **Error! Bookmark not defined.**
Figure 7.32: Undesired rotation of the deforming workpiece around point of symmetry ..... **Error! Bookmark not defined.**
Figure 7.33: The position of the knurling on the die and a close up of the knurled surface. ..... **Error! Bookmark not defined.**
Figure 7.34: Picture showing the friction strips in an FEA simulation ... **Error! Bookmark not defined.**
Figure 7.35: A ½ symmetry model showing the axial boundary conditions used to prevent unwanted workpiece rotation..... **Error! Bookmark not defined.**
Figure 7.36: Graph of radial die load for sequential and single stroke simulation ..... **Error! Bookmark not defined.**
Figure 7.37: Stress Distribution in workpiece for sequential and single stroke simulation ..... **Error! Bookmark not defined.**
Figure 7.38: The shape of a workpiece following sequential and single stroke simulation ..... **Error! Bookmark not defined.**
Figure 7.39: Situations in which sequential or single stroke simulations are appropriate ..... **Error! Bookmark not defined.**
Figure 7.40: Die/workpiece contact conditions in 2D FEA simulations of the form rolling process..... **Error! Bookmark not defined.**
Figure 7.41: Flow into die trenches as predicted by 3D FEA..... **Error! Bookmark not defined.**

Figure 7.38: The shape of a workpiece following sequential and single stroke simulation 187
Figure 7.39: Situations in which sequential or single stroke simulations are appropriate 188
Figure 7.40: Die/workpiece contact conditions in 2D FEA simulations of the form rolling process 189
Figure 7.41: Flow into die trenches as predicted by 3D FEA 190
Figure 7.42: FEA simulation showing the drop in rolling load after ½ a revolution 192
Figure 7.43: The segmented die used to calculate the load in several die regions 193
Figure 7.44: Drop in rolling load as recorded by the composite die 193
Figure 7.45: Variation in the die/workpiece contact areas during the first half workpiece rotation 194
Figure 7.46: Illustration of the laminar strain pattern typical of a form Rolled part. In this instance it is a 1mm stainless steel workpiece rolled with the 2mm milled die set to an area reduction of 60% 195
Figure 7.47: Illustration of the laminar strain pattern typically found in the sidewall of a From Rolled workpiece. In this instance it is a 1mm stainless steel workpiece Rolled with the 2mm milled die set to an area reduction of 60% 196
Figure 7.48: Distributions of the strains predicted by plane strain and axisymmetric FEA simulations 196
Figure 7.49: The maximum principal strains predicted by 2D and 3D FEA form rolling Simulations 197
Figure 7.50: The distortion of a tracking line located along the diameter of the workpiece due to tangential deformation 198
Figure 7.51: Increased area reduction of the workpiece leading to increased distortion of a tracking line located along the diameter of the workpiece 199
Figure 7.52: Lower levels of effective strain in the centre of a form rolled workpiece where tangential deformation is low 200
Figure 7.53: Tangential deformation across the entire diameter of the workpiece at a large area reduction 200
Figure 7.54: Shear strain rate within a workpiece during form rolling 201
Figure 7.55: Tensile hydrostatic and maximum principal stress in a From Rolled part with a wide groove 203
Figure 7.56: Tensile hydrostatic and maximum principal stress in a From Rolled part with a narrow groove 204
Figure 7.57: The stress distributions in the radial, tangential and axial directions for an increasing area reduction when using the ground die set with a narrow round 205
Figure 7.58: The stress distributions in the x, y and z directions for an increasing area reduction when using the milled die set with a wide flat 206
Figure 7.59: Variation of stress distribution within the workpiece as a function of die geometry and cross sectional area reduction. 208
Figure 7.60: Indentation deformation mechanism 209
Figure 7.61: Spreading and stretching deformation mechanism 210
Figure 7.62: Velocity components of the rotating workpiece 212
Figure 7.63: Workpiece lips due to the workpiece sliding along the stationary die 213
Figure 7.64: The increase in the length of the stationary die/workpiece contact area due to the slippage of the workpiece along the stationary die 214
Figure 7.65: The waveform after one workpiece rotation 214
Figure 7.66: The waveform after one and a half rotations 215
Figure 7.67: The waveform after two and a half rotations 215

Figure 7.64: The increase in the length of the stationary die/workpiece contact area due to the slippage of the workpiece along the stationary die. ..... **Error! Bookmark not defined.**
Figure 7.65: The waveform after one workpiece rotation .. **Error! Bookmark not defined.**
Figure 7.66: The waveform after one and a half rotations.. **Error! Bookmark not defined.**
Figure 7.67: The waveform after two and a half rotations . **Error! Bookmark not defined.**
Figure 7.68: The bending of the workpiece due to the mismatch in the size of the waveforms ..... **Error! Bookmark not defined.**
Figure 7.69: The plane on which the workpiece bends when one waveform becomes much larger then the other. ..... **Error! Bookmark not defined.**
Figure 7.70: The conditions that lead to one-die rolling in the knifing zone..... **Error! Bookmark not defined.**
Figure 7.71: The die geometries that lead to one-die rolling in the knifing zone..... **Error! Bookmark not defined.**
Figure 7.72: Determining the increase in feature width over half a rotation..... **Error! Bookmark not defined.**
Figure 7.73: Incorrect starting position of the moving die that can lead to one-die rolling ..... **Error! Bookmark not defined.**
Figure 7.74: Determining error in the flat width when the starting position of the dies is set incorrectly..... **Error! Bookmark not defined.**
Figure 7.75: Circumstances leading to one-die rolling in the spreading zone..... **Error! Bookmark not defined.**
Figure 7.76: Velocity vector plot of one-die rolling process..... **Error! Bookmark not defined.**
Figure 7.77: Sections through workpiece at half rotation intervals, illustrating flow of workpiece material into groove on contact with featureless die... **Error! Bookmark not defined.**
Figure 7.78: Evidence of lips on the scarred surface of the flat die.. **Error! Bookmark not defined.**
Figure 7.79: Profile of workpiece with ironed out lips..... **Error! Bookmark not defined.**

LIST OF TABLES

Table 5.1: Experimental results produced by Lovell et al [23] 50
Table 5.2: Sign of principal stresses at workpiece centre for varying H/l ratios [46] 58
Table 5.3: Variation of recommended rolling angles 68
Table 6.1: Dimensions of Geometrically Similar Dies 98
Table 6.2: The effect of changing the number of workpiece rotations or the spreading angle on the die geometry 99
Table 6.3: Properties of D2 tool steel 106
Table 7.1(a): Accuracy of 0.45mm milled and 1mm milled dies 30° sidewalls 144
Table 7.1(b): Accuracy of 1mm milled dies with 45° and 60° sidewalls 144
Table 7.1(c): Accuracy of 2mm milled dies 145
Table 7.2: The rolling conditions that lead to part failure 175
Table 7.3: Table of stresses in workpiece for sequential and single stroke simulation 186

NOMENCLATURE

Symbol	Definition
Velocities associated with form rolling	
$V_{die,\ move}$	translational velocity of the moving die
$V_{die,\ stat}$	translational velocity of the stationary die
$V_{w,\ tang}$	tangential velocity of the workpiece
$V_{w,\ result}$	resultant velocity of the workpiece
$V_{w,\ trans}$	translational velocity of the workpiece
$V_{w,\ tang,x}$	component of the tangential workpiece velocity in the x-direction
$v_{w,s}$	small tangential workpiece velocity
$v_{w,l}$	large tangential workpiece velocity
ω_d	angular velocity of the die (Transverse Helical Rolling)
ω_w	angular velocity of the workpiece
Die and Workpiece Dimensions	
r	radius of workpiece after rolling
r_o	radius of workpiece before rolling
r_w	workpiece radius from r to r_o
d	diameter of workpiece after rolling
d_o	diameter of workpiece before rolling
ø	diameter
δ	diameter reduction, relative reduction
A_0	cross sectional area of unformed section
A	cross sectional area of formed section
ΔA	area reduction
α	sidewall angle
β	spreading angle
γ	ramp angle
f	flat width
w	groove width
$w_{sidewall}$	width of the groove sidewall

Δw	increase in the width of the groove over half a rotation
$f_{specified}$	specified width of flat
f_{actual}	actual width of flat
w_{error}	error in the die width
h	groove height
ΔR	increase in the depth of the groove over half a rotation
$l_{sidewall}$	the axial length of the workpiece sidewall
l_{formed}	the axial length of the formed part
p	die penetration into the workpiece
p_r	penetration rate
$r_{die,l}$	large die radius (Transverse Helical Rolling)
$r_{die,s}$	small die radius (Transverse Helical Rolling)
l	length of the sizing zone on the rolling die
N	rolling cycles
λ	the shear intensity in the workpiece
λ_c	shear intensity accumulated per cycle
λ_{cr}	critical shear intensity
$start_{error}$	error in the starting point of the moving die
d_z	substitute diameter
l_z	substitute sizing distance

Material Properties

E	Young's modulus
G	shear modulus
ν	Poisson's ratio
k	shear yield strength

Forces and stresses

W	axial force in reduced section
m	friction factor
σ_x	radial stress or stress in the x-direction
σ_y	axial stress or stress in the y-direction

σ_z	tangential stress or stress in the z-direction
σ_1	first principal stress
σ_2	second principal stress
σ_3	third principal stress
σ_c	mean normal contact pressure
σ_y	yield stress
ε	equivalent strain
$\dot{\varepsilon}$	equivalent strain rate
σ	equivalent stress
P_x	tangential (Rolling) force
P_y	axial force
P_x	radial force
q_m	mean contact pressure

Miniaturisation and the 'size effect'

λ	scaling factor or length scale
d_{grain}	grain diameter
g_{avg}	average number of grains in a workpiece plane
s_{area}	surface area of workpiece to be deformed
g_{area}	maximum surface area of a grain
g_{tot}	total number of surface grains in the region to be deformed by the groove
σ_f	flow stress of the micro-scale material
α_i	proportion of internal grains
α_{FS}	proportion of surface grains
$\sigma_{f,i}$	flow stress of internal grains (polycrystals)
$\sigma_{f,FS}$	flow stress of free surface grains (single crystals)
σ_{ij}	stress tensor
σ'_{ij}	stress deviator
$\dot{\varepsilon}_{ij}$	strain rate
χ	force scale
τ	time scale

Finite Element Analysis

DEFORM	Design Environment for FORMing
2D	two dimensional
3D	three dimensional
FEA	Finite Element Analysis
bcc	boundary contact conditions
AMG	Automatic Mesh Generation
RSE	Rigid Super Element
GUI	Graphical User Interface
σ^*	the maximum principal stress
$\bar{\sigma}$	the effective stress
$\bar{\varepsilon}$	the effective strain
C	Compressive stress
T	Tensile stress
x	radial or x direction
y	tangential or y direction
z	axial or z direction
W_p	total plastic work
F_F	friction force
m	friction factor

Other

π	pi
EDM	Electro Discharge Machining
CWR	Cross Wedge Rolling
WRR	Wedge Rolls Rolling
ε	non-dimensional deformation coefficient

CHAPTER 1

INTRODUCTION

CHAPTER 1

INTRODUCTION

There has been a continual trend towards miniaturisation in recent years driven by an increasing consumer demand for smaller products. Mobile phones exemplify the increasing sales of these small scale electronics products. During the five year period ending in 2003 annual sales of handsets tripled to over half a billion units [1]. These electronic devices require mechanical parts to function and, equally important, to hold them together and thus there is a need for small fasteners. These fasteners are considered micro when they have at least two dimensions in the submillimetre range. A range of micro-parts relative to the size of a coin is shown in Figure 1.1. Other industries using micro-parts include the watch, biomedical, dental and automotive industries.

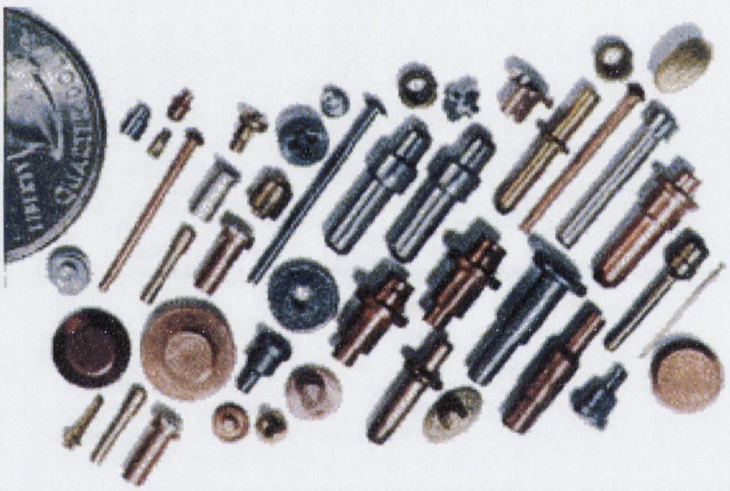

Figure 1.1: Photograph showing a range of micro-parts [2]

This research aims to produce micro-parts using the form rolling process. Form rolling is a cold forming operation that produces geometrical features on axisymmetrical components. This is achieved by rotating a cylindrical metal blank between a pair of flat dies containing the required feature geometry. It is a modern derivative of the well established thread rolling process and both of these processes have several advantages over machining such as high production rates, improved material properties and high material utilisation. These advantages have established thread rolling as the premier method of threaded fastener manufacture even in the submillimetre diameter range. However, form rolling cannot claim the same success. It has been said that " flat die form rolling technology is an art as well as a science"[3] and this black art aspect of form rolling die design has limited its utilisation

because it results in die designs that have to be redesigned or modified following initial rolling trials [4].

When form rolling is used to manufacture micro-parts the uncertainty surrounding the process increases because there is, currently, a lack of knowledge about the mechanical properties of micro-parts and this has resulted in a time consuming and costly empirical approach to micro-part design [5].

If the uncertainties associated with the micro-form rolling process were eliminated, it could be used to produce micro-parts that are currently machined, such as the brass pin shown in Figure 1.2. The pin could potentially be produced using the micro-form rolling process due to its axisymmetric geometry.

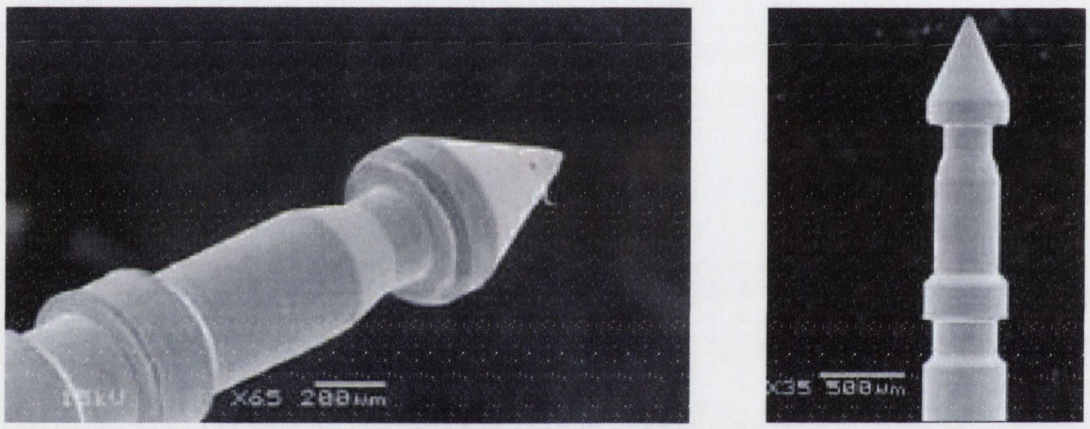

Figure 1.2: A turned brass pin, machined using a Kugler Micro Turning machine, which could potentially be produced using the micro-form rolling process [6].

To eliminate the empirical and black art aspects of micro-form rolling an accurate design process for tooling is required. However, before this can be developed the following questions must be answered:

- How can the uncertainty that is associated with form rolling die design by minimised?
- What are the limitations of the micro-form rolling process?
- How does miniaturisation affect the form rolling process?
- What effect does the die geometry and manufacturing method have on the micro-form rolling process?
- Does the choice of workpiece material have an effect on the process?
- How can a die design be tested before it is manufactured?

These questions and how they will be answered are discussed in greater detail in Chapter 2 Project Objectives.

CHAPTER 2

PROJECT OBJECTIVES

CHAPTER 2

PROJECT OBJECTIVES

As outlined in Chapter 1, a number of questions must be answered about the micro-form rolling process before it can establish itself as a rival to micro-machining. These questions are discussed in greater detail in the following chapter.

Figure 2.1 below shows how the various objectives and tasks associated with the project are connected. The Main objective is located in the centre of the diagram and is surrounded by a number of sub-objectives. Various tasks are linked to the sub-objectives and in some instances they are shared by multiple sub-objectives.

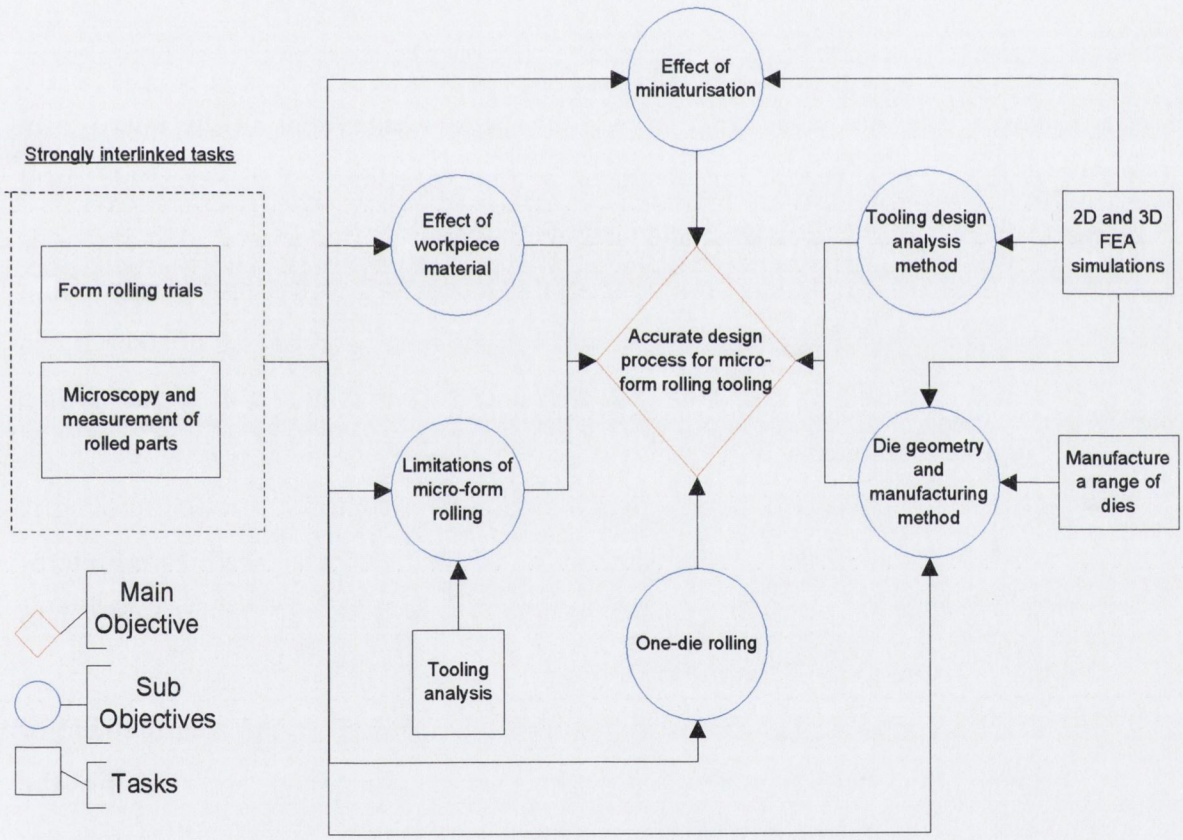

Figure 2.1: Flow chart representation of Project Objectives and Tasks

2.1 The Project Objective

- The main project objective is to remove the uncertainty associated with the micro-form rolling process and eliminate the black art aspect of die design by providing an accurate design process for micro-form rolling tooling. This will be achieved in two ways.

Firstly, a starting point for successful die design will be provided by recommending elements such as suitable die manufacturing methods and, secondly, a method for investigating a particular die design before it is manufactured will be provided by Finite Element Analysis.

The uncertainty surrounding the process can also be reduced by using Finite Element Analysis to study the predicted stresses and strains within the workpiece and develop a better understanding of the deformation experienced by the workpiece during the micro-form rolling process.

2.2 Sub-Objectives

2.2.1 Determine the Limitations of Micro-Form Rolling

- The following factors are relevant in determining the limitations of the micro-form rolling process and they are associated with the capabilities of the available form rolling machine and the geometric accuracy of the tooling:
  - There is a minimum workpiece size that can be rolled with a micro-form rolling machine which is a result of limitations in the range and finesse of setup it can achieve. These limitations will be determined by performing rolling trials with a range of workpieces.
  - Tooling Analysis will determine if the geometry of the form rolling tooling is sufficiently accurate for the manufacture of tight tolerance features on micro-form rolled components. It will also determine the most suitable method to manufacture micro-form rolling tooling.
  - There are also limitations associated with the observation and measurement of both micro-form rolling dies and workpieces. The limitations are a result of the small size and curved surfaces of micro-parts and dies. A range of microscopy and measurement techniques will be used to determine their limitations.

2.2.2 Determine the effect of Miniaturisation on the Form Rolling Process

- Trials and simulations will be undertaken, as follows, to determine the effect that miniaturisation of both the workpiece and the groove geometry has on the form rolling process:

- A wide variety of rolling trials will be performed using a range of workpiece diameters and groove geometries, followed by microscopy of the rolled parts.
- 2D and 3D FEA simulations of the form rolling process will be used to determine any changes in the deformation mechanism due to miniaturisation.

2.2.3 Determine the effect of Die Geometry and Manufacturing Method on the Micro-Form Rolling Process

- Both milling and grinding techniques will be used to manufacture a range of micro-form rolling dies to determine the die geometries and manufacturing method most suited to the micro-form rolling process. This will involve:
  - The design and manufacture of a range of dies using grinding and milling processes and determining the accuracy to which they can be manufactured.
  - Performing a series of rolling trials using these dies and determining the effect of die geometry and manufacturing method on the quality of micro-form rolled parts.
  - Performing 2D and 3D FEA to predict the effect of die geometry and manufacturing method on the deformation of a micro-form rolled parts.

2.2.4 Determine the effect of Workpiece Material on Micro-Form Rolling

- To determine the effect of workpiece material on the micro-form rolling process in terms of part quality and failure form rolling trials will be performed:
  - These trials will use both stainless steel and titanium alloy workpieces and subsequently microscopy will be performed to determine which material is more suitable to the micro-form rolling process.

2.2.5 Develop a Tooling Design Analysis Method

- The development of a method to analyse the relative performance of a micro-form rolling tool design will enable improvements to be made before it has to be manufactured.
  - A method of modelling micro-form rolling using the 2D and 3D FEA package DEFORM will be developed and validated by comparing predicted results with experimental results.

2.2.6 **Develop the One-Die Rolling Process**

- The one-die rolling process is a novel rolling process which possesses several advantages over traditional form rolling. The technique can be exploited due to the small parts and features associated with the micro-form rolling process.
    - Trials using the one-die rolling process will be performed and the resulting workpieces will be compared with those produced using traditional rolling to determine the viability of the process.

As can be seen from Figure 2.1, micro-form rolling trials will be the cornerstone of this research and they are required for almost all the sub-objectives.

CHAPTER 3

THE BASICS OF MICRO AND MACRO-FORM ROLLING

CHAPTER 3

THE BASICS OF MICRO AND MACRO-FORM ROLLING

3.1 The Basics of Micro-Forming

Micro-forming is a manufacturing process with great potential because it is the process that is most suited to producing the type of micro-parts currently required for many industries. The advantages of the process include its high production rates and the quality of the parts produced. However, uncertainty surrounding the forming process at the micro level is preventing the universal uptake of micro-forming.

Micro-forming differs from forming at larger scales and, to date, the successful determination of forming laws and analysis techniques for micro-forming processes has not been achieved. Therefore, empirical laws are crudely used to model the process. It is the use of these empirical laws in the analysis of Micro-forming that makes the design process lengthier and less reliable.

To make micro-forming a more viable manufacturing process, the mechanics of the process must be better understood as this will allow the development of forming rules and FEA simulations capable of successfully modelling the micro-form rolling process. However, to reduce forming to the micro-scale many other process challenges must be overcome. These range from problems associated with the handling and positioning of the workpieces to the design and manufacture of suitable tooling [7, 8].

3.1.1 Micro-parts

Micro Formed parts can be described as "parts or structures with at least two dimensions in the sub-millimetre range" [7]. In this research the grooves which were form rolled onto small diameter metal wire were always of a width and depth in the sub millimetre range, while the diameter of the wire was also occasionally within this range. A micro-part form rolled during this research is shown in Figure 3.1.

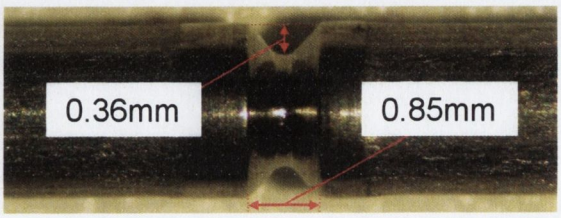

Figure 3.1: 2mm ø stainless steel micro-form rolled part

The parts form rolled during this research can, therefore, be defined as micro-parts and the process used to manufacture them can be titled 'micro-form rolling'.

3.1.2 Introduction to the 'size effect'

The 'size effect' is the change in properties of the workpiece material as its dimensions approach the micro-scale. It is a function of the proportion of surface grains to interior grains, this is due to the fact that interior grains are restrained by the grains that surround them and therefore require a greater force to deform them compared to surface grains [7]. The increasing proportion of surface grains with part miniaturisation is illustrated in Figure 3.2 below.

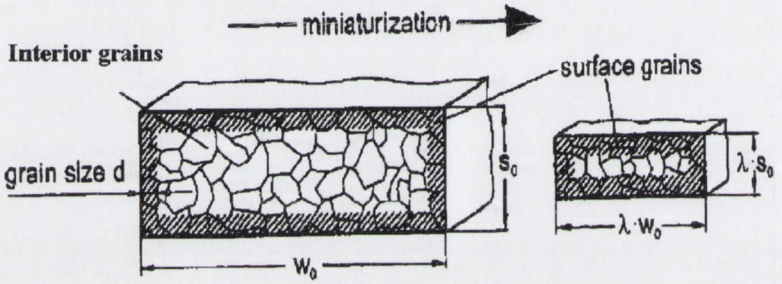

Figure 3.2: Increasing proportion of surface grains with miniaturisation [9]

Both of the parts shown in Figure 3.2 have the same grain size, d. However, the smaller part is reduced in size by a scaling factor λ which results in an increased proportion of surface grains compared with the larger part. The proportion of surface grains can also be increased by increasing the grain size.

In tensile and compression tests, the size effect manifests itself as a decrease in the flow stress of a material with a decrease in the cross sectional area of the test piece. This decrease can be quite pronounced, for example Engel et al [10] measured a 20% drop in flow stress of CuZn15 as the specimen size decreased from the macro to the micro-scale, as shown in Figure 3.3. In this figure, the flow stress for a range of scaled parts is plotted and it shows a definite trend of decreasing flow strength with part miniaturisation.

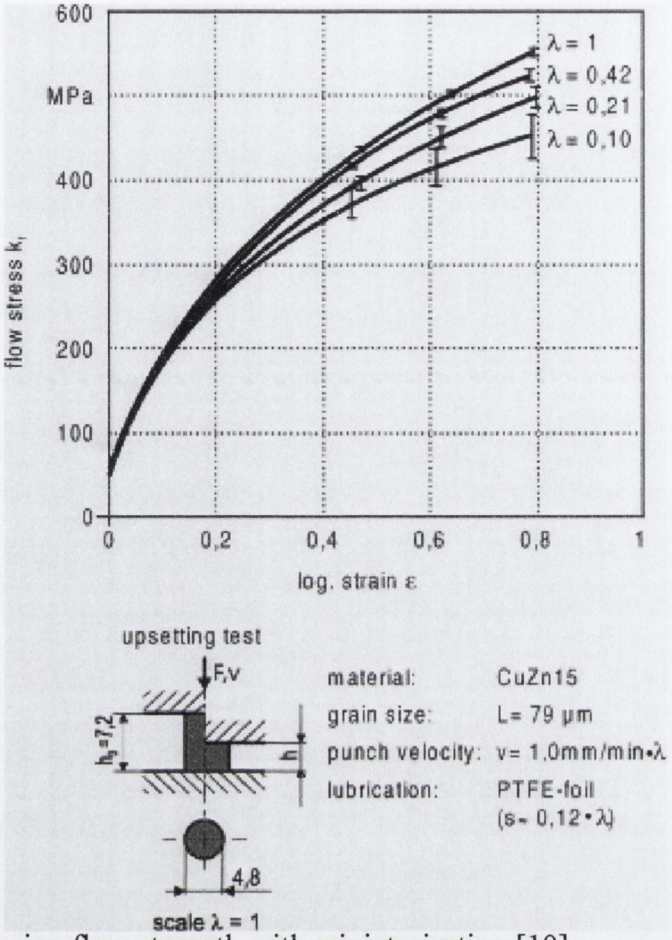

Figure 3.3: Decreasing flow strength with miniaturisation [10]

AISI 316 stainless steel, which is the primary material of interest in this research, has the same face centred cubic (fcc) crystal structure as found in CuZn15 and is, therefore, also expected to experience the size effect.

The size effect becomes pronounced when a particular threshold ratio of grain size to part size has been passed. Several authors [11, 12] predict this to be when the grain size increases to approximately one twentieth of the workpiece diameter. However, it is unknown whether other ratios can be used in predicting the presence of the size effect such as the ratio of grain diameter to feature size.

An increasing level of scatter in results is also observed with increased miniaturisation as the material properties of individual grains determine the deformation of the workpiece.

3.2 The Basics of the Form Rolling Process

This section introduces the form rolling process, explains the various types of form rolling machines in use, the forming of a part using the process, the component types the process can form and the advantages form rolling possesses over other types of manufacturing. Some of the differences that exist between traditional form rolling and micro-form rolling will also be discussed.

Form rolling has many different names and it is often referred to as Wedge Rolling, Cross Wedge Rolling (CWR) or Transverse Wedge Rolling due to the wedge shape of the die. Cross Rolling is a similar process in which the entire length of the part experiences the same diameter reduction. Other rotary forming processes, similar to form rolling, will also be briefly described in this section.

3.2.1 History of Form Rolling

Although there were some earlier developments in the form rolling process its development began in earnest in Eastern Europe in the 1960s with the production of the first commercial Cylindrical and Flat form rolling machines. The Reckroll developed by VEB Press & Shear Co., Erfurt in the German Democratic Republic was the first commercial machine to use flat dies and by the end of the 1960s it was well established having a machine in use in the UK [13, 14]. This machine had two moving dies and was used for hot rolling with the aid of an induction heater. The commercialisation of cylindrical form rolling also occurred in the early sixties in Czechoslovakia, led by Jire Holub at the Litany Automobile Works[13, 15, 16]. Initially, the field of form rolling focused on large hot rolled parts e.g., drive shafts were a common product and many machines were paired with induction heaters to heat the parts before rolling. The earliest attempts at cold form rolling small parts were in the late 70s and early 80s in the Soviet Union when Dulov and Astafiev cold rolled parts with diameters as small as 1.8mm using a cylindrical die machine. Also, at this time in the Soviet Union, flat wedge machines with only one moving die were under development [13].

3.2.2 Components Produced using the Form Rolling Process

The geometrical features formed by the form rolling process are typically simple axisymmetric features such as a groove, double groove, conical point, conical point with cavity, or radiused point. However parts with more complex features can also be formed

such as parts with knurling, screw threads, unusual threads with large height to thickness ratios and specialised parts such the locking nut shown in Figure 3.4.

Figure 3.4: Photograph of a complex form rolled part

Very often, parts are formed with a number of different features, such as threaded sections with grooves. Figure 3.5 shows a selection of form rolled parts, demonstrating the variety and complexity possible with the form rolling process.

Figure 3.5: Photograph of a selection of form rolled parts

3.2.3 Advantages of Form Rolling

The advantages of form rolling include: high productivity, material savings and increased product strength [4, 15, 16]. Material savings arise because form rolling is a near net shape manufacturing process and formed parts do not usually require any further machining. Increased product strength results from work hardening and the formation of beneficial strengthening flow lines during the forming process. The method has also been used to successfully create pre-forms for other forming operations [17]. Furthermore, the process

allows several features to be formed onto the part in a single stroke e.g. several grooves and knurled and threaded segments can be produced in one stroke of the rolling die.

3.2.4 Varieties of Form Rolling Die Configurations

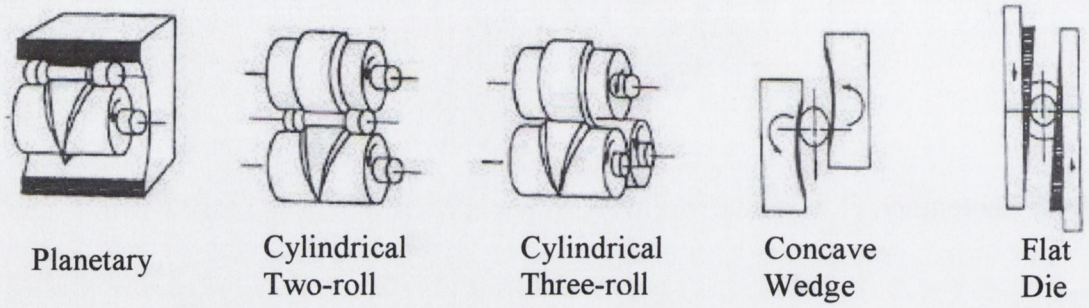

Figure 3.6: Diagrams of a variety of form rolling die configuration [13]

Figure 3.6 above shows the various die configurations that can be applied to the form rolling process. Each configuration is briefly explained below:

- **Planetary Rolling** consists of one cylindrical die and one concave die with only the cylindrical die rotating. The part experiences rotational motion around its own axis and the axis of the cylindrical die.
- **Cylindrical Form Rolling** machines come in the form of two-roll and three-roll machines with the two/three cylindrical dies all rotating in the same direction to form the part. The part experiences rotation around its own axis only.
- **Concave Wedge Rolling** consists of two concave dies that rotate eccentrically in the same direction around the stationary fastener.
- **Flat Form Rolling** machines have flat dies and the part is formed by the reciprocal motion of the dies. The part experiences rotational and translational motion if one die reciprocates and rotational movement only if both dies reciprocate.

Flat and Cylindrical form rolling die configurations are the most widely used, because the concave dies required for Planetary and Concave Wedge Rolling are difficult to manufacture and setup on their form rolling machines.

3.2.5 Micro-Form Rolling Machines

Currently only a small number of manufacturers are marketing rolling machines capable of rolling parts with diameters of less than 1mm. EWM from Germany produce the AF 3 Thread rolling Machine [18] and Sanmei from Japan produce the THI-2MR micro rolling machine [19]. Both are cold forming flat die machines. Another manufacturer, Profiroll, produces cold forming cylindrical rolling machines such as the PW 10e thread and profile rolling Machine [20].

3.2.6 The Form Rolling Process Using Flat Dies

Form rolling is a cold forming operation that produces geometrical features on axisymmetrical components, by rotating a cylindrical metal workpiece between a pair of flat dies, containing the required feature geometry. One of dies undergoes reciprocating movement and the relative motion between the dies results in workpiece rotation, illustrated in Figure 3.7.

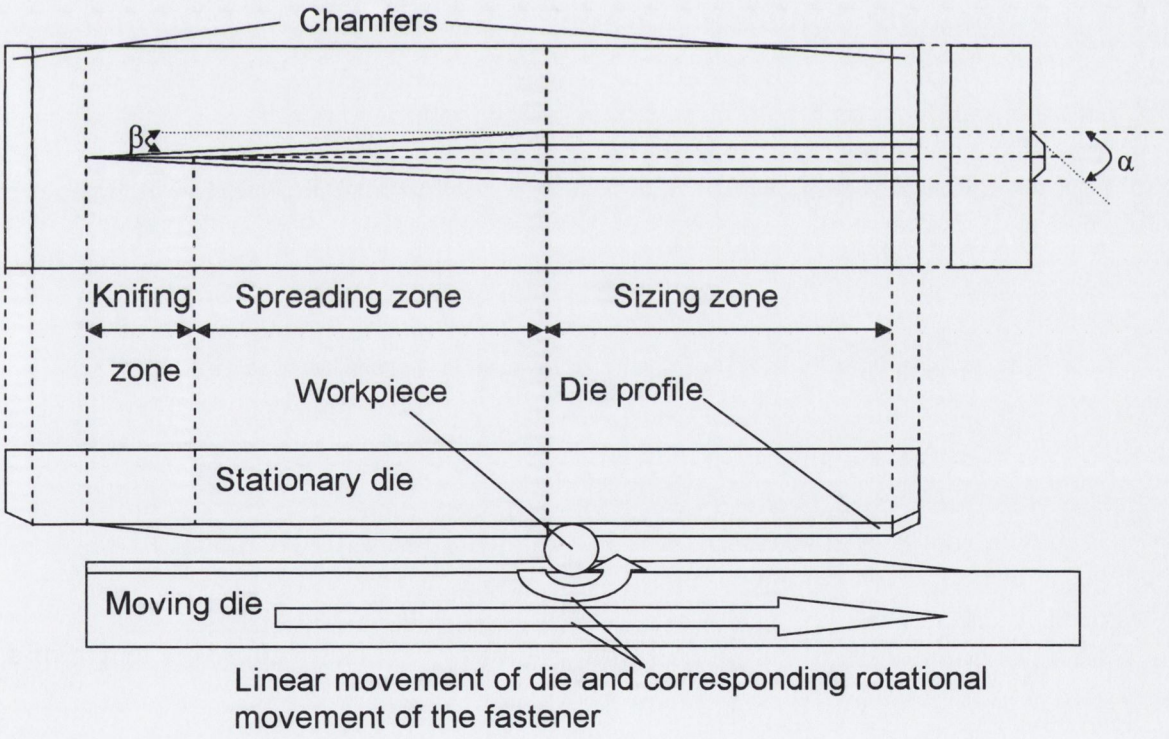

Figure 3.7: Diagram of the form rolling process and plan of a form rolling die

The form rolling tools consist of a pair of dies that have an identical set of geometric features on their surface and these features are formed onto the workpiece by plastic deformation during the rolling process. These die features generally form three distinct zones on the die, namely the knifing, spreading and sizing zones. The geometry of

the sizing zone is the same as the final desired part feature on a rolled part and, hence, this zone of the die has a constant geometry. The workpiece must usually undergo at least half a rotation in this zone to be fully formed. However, as a general design rule the part normally undergoes at least one complete rotation in the sizing zone to improve the quality of the formed part. The knifing and spreading zones involve the gradual change of the feature geometry until the final geometry of the sizing zone is achieved. The function of this gradual change in geometry is to limit the amount of metal being moved at any time, thus reducing the forces on the tooling and increasing the dimensional accuracy of the final product. In the knifing zone, the height of the die feature geometry increases from zero to the total depth of the feature being rolled, while in the spreading zone the width of the die feature is increased, as shown in Figure 3.8

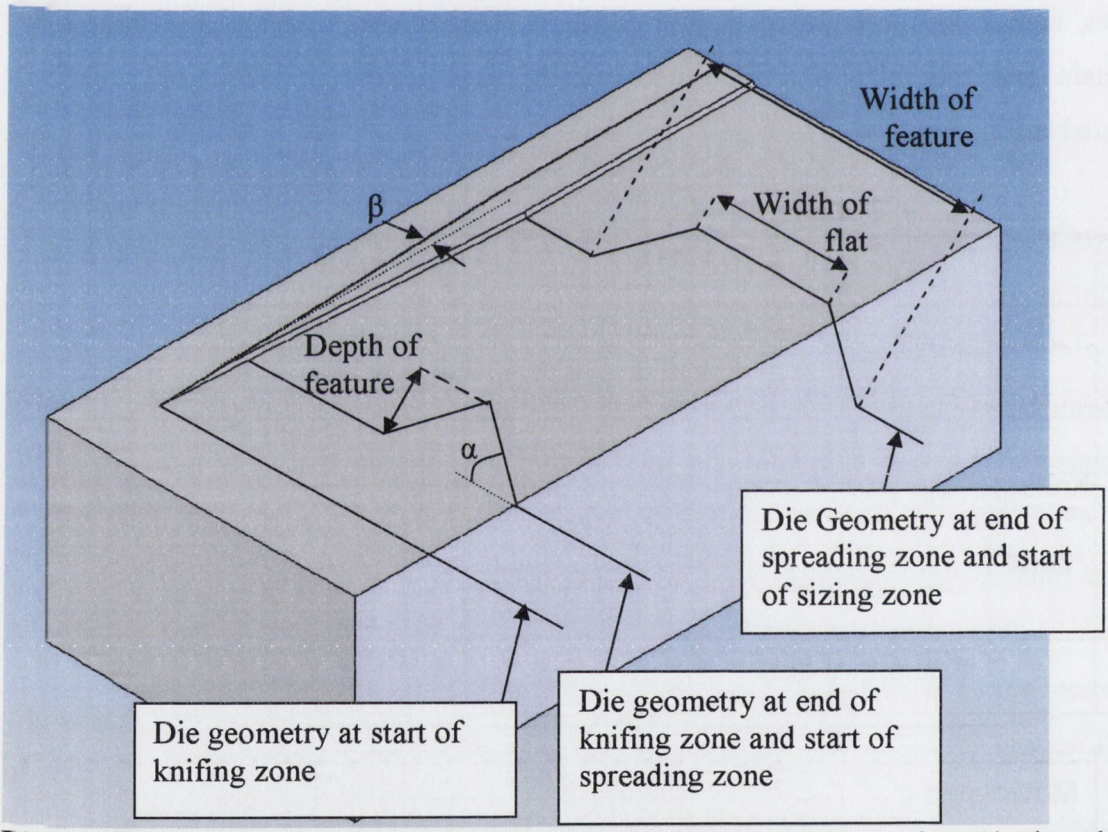

Figure 3.8: Diagram illustrating the change in the feature geometry along the length of a form rolling die

The die parameters chosen during the knifing and spreading zones are critical to the quality of final product as they will determine the magnitude of the stresses in the component and type of defects, if any, that will be produced on the rolled part [21-23]. Four major parameters are associated with the geometry of a form rolling die, namely: β,

the spreading angle, α, the sidewall angle, w, the width of the feature and h, the height of the feature.

The spreading angle, β, determines the speed at which the feature is formed on the workpiece. For small values of β, the rate of material displacement per revolution of the workpiece is small resulting in lower forces. In micro-form rolling, the ratio of die length to workpiece circumference is typically very large allowing more rotations of the workpiece and, therefore, smaller values of β than is possible for larger workpieces. The sidewall angle, α, is responsible for the draft formed on the workpiece.

The dimensions d_0 and d and other important workpiece dimensions are illustrated in Figure 3.9.

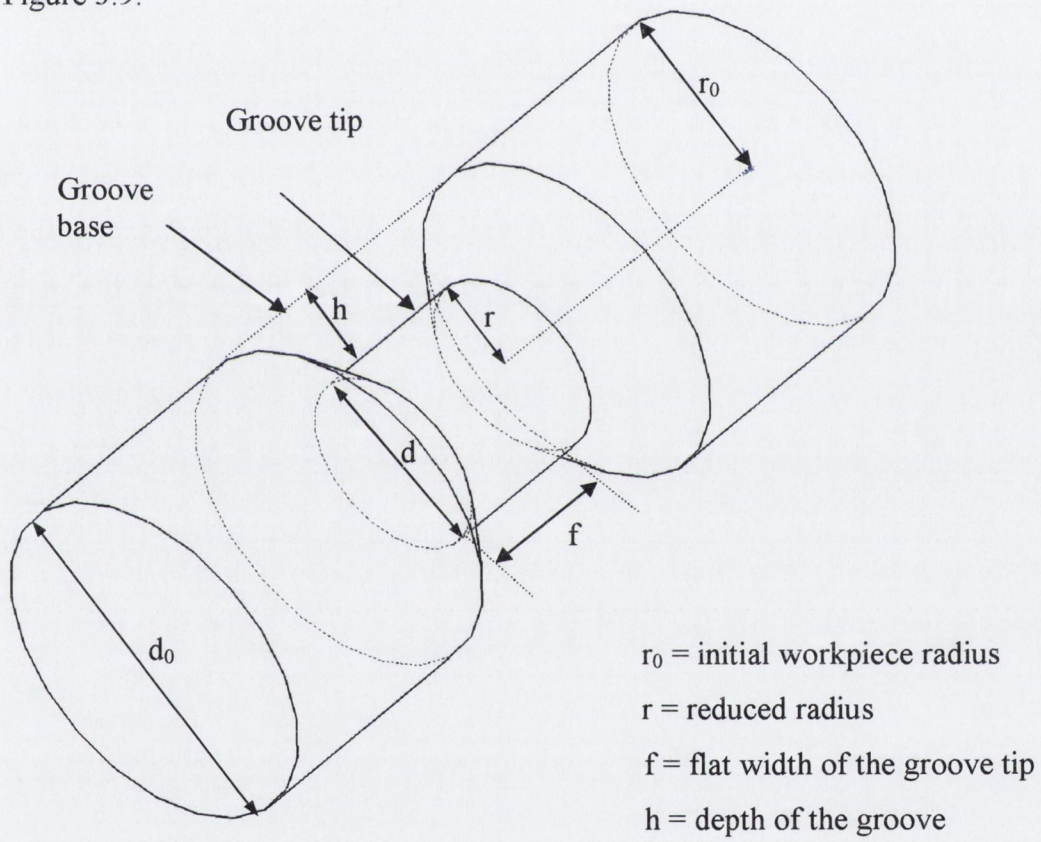

Figure 3.9: The geometry of a form rolled workpiece

Another important parameter to be considered is the amount of deformation experienced by the workpiece. This is quantified using the relative reduction, δ or the area reduction, ΔA:

$$\delta = d_0/d \tag{3.1}$$

$$\Delta A = \frac{A_0 - A}{A_0} = 1 - \left(\frac{d}{d_0}\right)^2 . \tag{3.2}$$

Where:

d_0 = initial workpiece diameter

d = reduced diameter = $d_0 - 2h$ (3.3)

A_0 = initial area = $\pi (d_0/4)^2$ (3.4)

A = reduced area= $\pi (d/4)^2$ (3.5)

It can also be seen in Figure 3.9 that the tip of the groove has a width called the flat width, f.

A second type of form rolling die was also investigated during this research and is illustrated in Figure 3.10. Like the tooling design shown in Figure 3.7, it contains a spreading angle and a sidewall angle. However, it has some significant differences. It can be seen from Figure 3.10 that this tooling has a flat from the start of the knifing zone and it does not contain a spreading zone i.e. once the groove has reached its full depth there is no further increase in the width of the flat. Due to the very small size of the groove, a sharp tip on the tooling would be very vulnerable to failure and would also prove difficult to manufacture. A flat is therefore necessary. The lack of a spreading zone on the die is a result of the process used to manufacture the tooling.

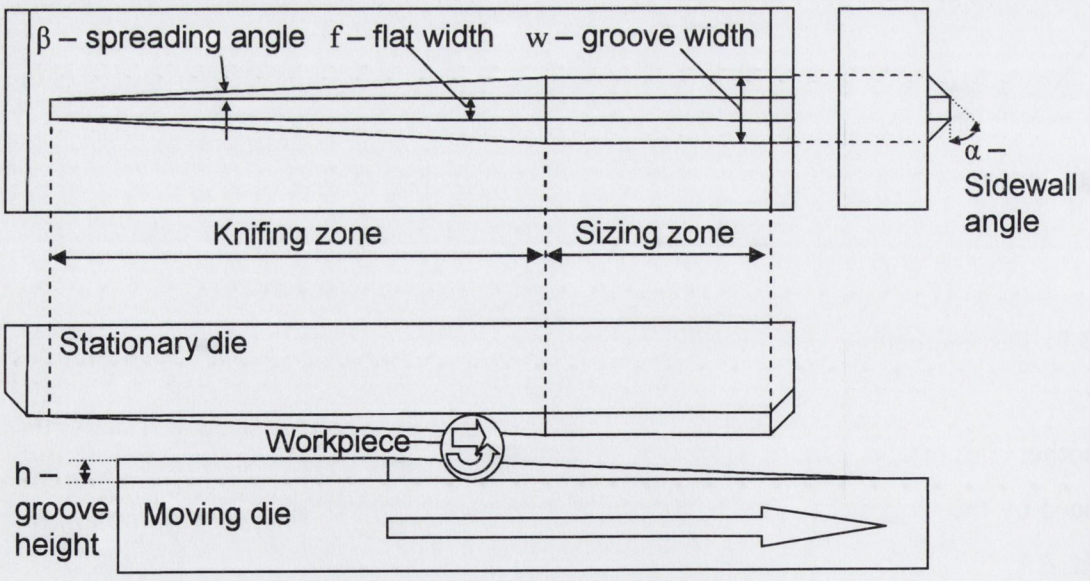

Figure 3.10: Schematic of the geometric details and nomenclature for form rolling dies

It can be seen from Figure 3.7 and 3.10 that the stationary die is shorter than the moving die and includes chamfers on both ends which help with the feeding of the workpiece into the dies at the start of the stroke and its ejection at the end of the stroke.

Traction or high friction surfaces are often provided on the tooling to ensure that adequate traction exists to prevent slip between the die and the workpiece and this surface is usually produced using Electro Discharge Machining (EDM) or grit blasting, although knurling and serrations have also been used [4, 15, 21, 24].

3.2.7 **Penetration Rate**

Another parameter of importance is the penetration rate, p_r, which is the ratio of the radius reduction per half revolution to the initial workpiece radius. The radius reduction per half revolution is used because the workpiece contacts either the moving or stationary die every half revolution. The radius reduction per half revolution is expressed as:

$$\tan\gamma\left(\frac{circumference}{2}\right) = \tan\gamma\left(\frac{\pi d}{2}\right) = \tan\gamma(\pi r) \tag{3.6}$$

Therefore:

$$p_r = \frac{\tan\gamma\,(\pi r)}{r} = \pi\tan\gamma \tag{3.7}$$

Where the ramp angle γ is a function of the sidewall angle, α and spreading angle β, see Figure 3.11, in which l is the length of the sizing zone and $w_{sidewall}$ is the width of the feature sidewall at the end of the sizing zone.

The rate of penetration is limited by the rigidity of the machine and the hardness of the metal being rolled [25]. The use of a small ramp angle, therefore, allows harder materials to be rolled and causes smaller machine deflections, thus producing more accurate parts. Increasing the penetration rate increases the contact length between the die feature and the workpiece. This is the region in which deformation occurs and, therefore, any increase in its length results in an increase in the rolling load.

Figure 3.11 also illustrates that the length of the knifing zone is dependent on α, β and h; while the length of the spreading zone is dependent on β and $w_{sidewall}$.

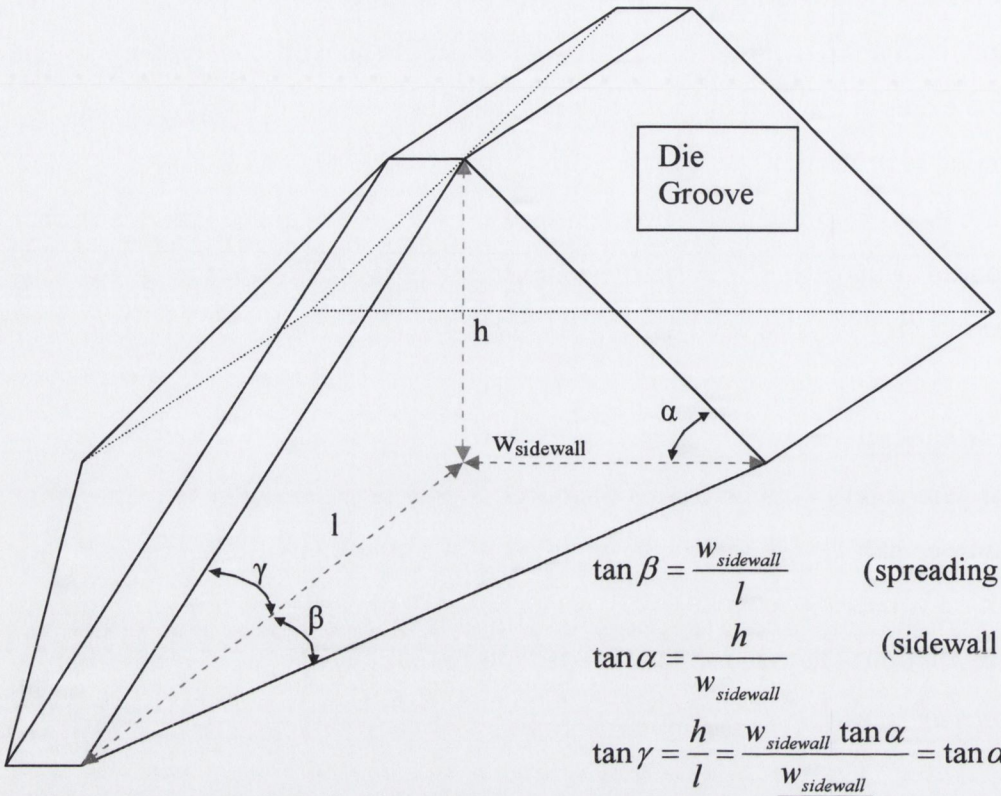

$$\tan\beta = \frac{w_{sidewall}}{l} \quad \text{(spreading angle)} \quad (3.8)$$

$$\tan\alpha = \frac{h}{w_{sidewall}} \quad \text{(sidewall angle)} \quad (3.9)$$

$$\tan\gamma = \frac{h}{l} = \frac{w_{sidewall}\tan\alpha}{\frac{w_{sidewall}}{\tan\beta}} = \tan\alpha\tan\beta \quad (3.10)$$

$$\gamma = \tan^{-1}(\tan\alpha\tan\beta) \quad \text{(ramp angle)} \quad (3.11)$$

Figure 3.11: Description of the various die angles found on a form rolling die

3.2.8 Workpiece Rotation and the Waveform

For workpiece rotation to occur the forces promoting rotation must be greater than those opposing rotation. If the forces promoting rotation are insufficient uncontrolled slippage of the workpiece occurs and the part fails through squaring i.e. forming of a part whose cross section is approaching that of a square. Slip is most likely to occur at the start of the spreading zone and is promoted by large spreading and sidewall angles, β and α respectively, low friction factors and low values of relative reduction [26].

The 'waveform' is a result of the rotational deformation mechanism associated with form rolling. It is a lump of excess workpiece material that is positioned next to the die surface as shown in Figure 3.12.

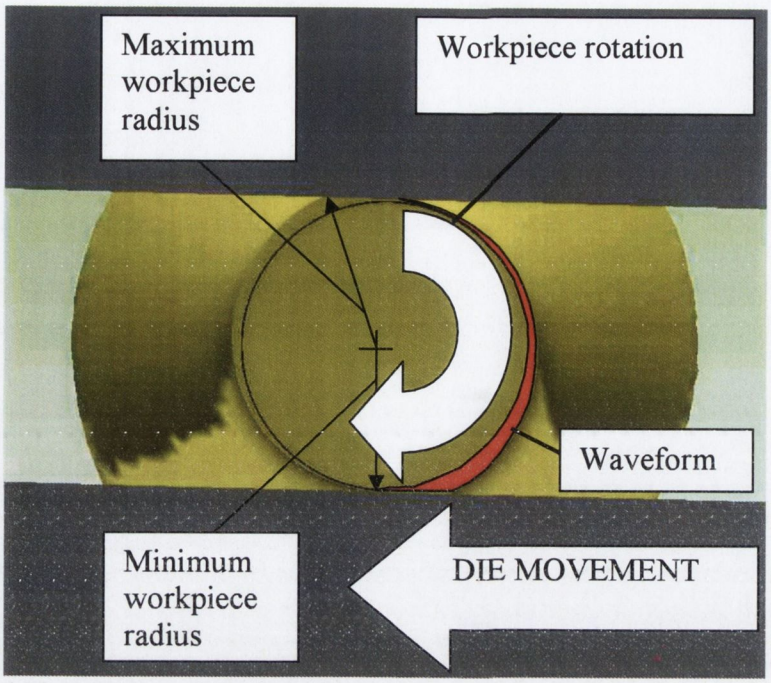

Figure 3.12: Generation of a waveform on the workpiece due to the combination of area reduction and rotation it experiences during form rolling

The waveform has the effect of increasing the contact area between the workpiece and the tool and giving the workpiece a non-circular shape. The waveform remains in contact with the tool throughout rolling and, therefore, its position on the workpiece surface changes as it rotates. This movement and its shape are the reasons why the waveform is so called. It is eventually ironed out in the sizing zone, resulting in a finished part with a circular cross section.

Figure 3.12 shows that the workpiece is not circular and actually has a range of radii ranging from a minimum, immediately after contact with the die, to a maximum immediately before contact with the die, i.e. the waveform. Figure 3.12 also shows that die/workpiece contact is largely concentrated at the waveform because, when it is ironed out, the workpiece radius is at a minimum.

The waveform grows in size when material is being added to it at a rate that cannot be ironed out; if this happens the excess material must be ironed out in the sizing zone. If the waveform becomes too large, it can hinder rotation of the workpiece and lead to uncontrolled slippage and this occurs when the forces required to deform the waveform and form a feature onto the workpiece exceed the forces available to rotate the workpiece.

3.2.9 Velocities and Torsional stresses in the Form Rolling Process

During the rolling process, several velocities are associated with the dies and the workpiece.

Moving die

The translational velocity of the moving die, $V_{die,move}$ is determined by the operational speed of the form rolling machine. The direction of $V_{die,\ move}$ defines the positive x-direction.

Stationary die

The stationary has a translational velocity, $V_{die,\ stat}$ of zero.

$$V_{die,\ stat} = 0 \tag{3.12}$$

These two die velocities and the workpiece velocities are illustrated in Figure 3.13.

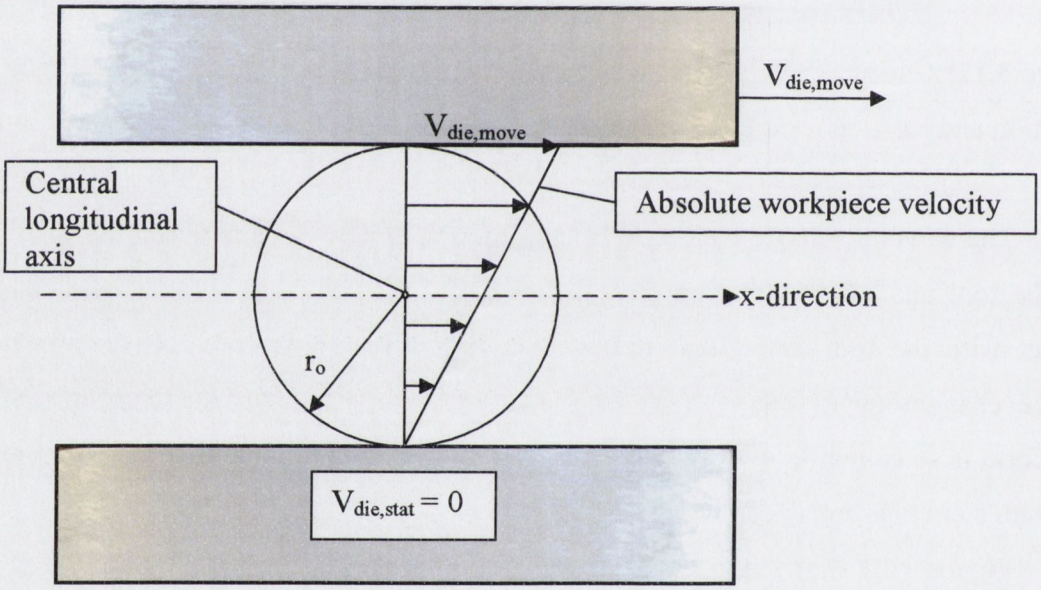

Figure 3.13: Velocities of the dies and the workpiece during the form rolling Process

Workpiece

If there is no slippage between the dies and the workpiece, the relative velocity between the workpiece and its points of contact with the dies is zero. Assuming the absolute velocity is determined relative to the stationary die, the absolute velocity of the workpiece in the x-direction increases linearly from zero at the stationary die to $V_{die,\ move}$ at the moving die as shown in Figure 3.13.

The translational velocity of the workpiece, $V_{w,\ trans}$, is the velocity of the central axis of the workpiece in the x-direction and is calculated as:

$$V_{w,\ trans} = (V_{die,\ move} + V_{die,\ stat})/2 \tag{3.13}$$

Combining equations (3.12) and (3.13) $V_{w,\,trans}$ simplifies to:

$$V_{w,\,trans} = V_{die,\,move}/2 \tag{3.14}$$

The tangential velocity of the workpiece, $V_{w,\,tang}$ is the velocity of a tangent to its surface relative to its centre. It can therefore be calculated by subtracting the translational velocity of the workpiece from its absolute velocity as illustrated in Figure 3.14.

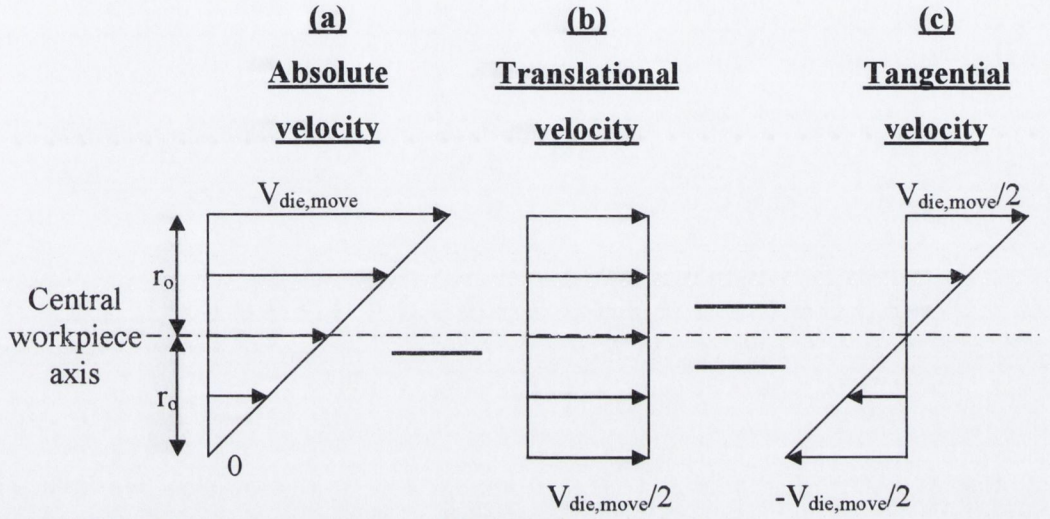

Figure 3.14: Velocity components of the rotating workpiece

The tangential workpiece velocity is, therefore, calculated as follows:

$$V_{w,\,tang} = V_{die,\,move}/2 \text{ where it contacts the moving die} \tag{3.16}$$

$$V_{w,\,tang} = -V_{die,\,move}/2 \text{ where it contacts the stationary die} \tag{3.16}$$

The angular velocity of the workpiece is the tangential velocity at the workpiece surface divided by its radius:

$$\omega_w = V_{w,\,tang} / r_o \tag{3.17}$$

Combining the above equation with equation (3.14) gives:

$$\omega_w = V_{die,\,move}/2r_o \tag{3.18}$$

Torsional stresses can arise when there are relative velocity differences between the dies and workpiece where they are in contact. This occurs in the groove region of the die where the reduced diameter of the workpiece results in a decrease in the tangential velocity of the workpiece. It also occurs because the contact between the die and the workpiece is spread over a finite length and, therefore, the tangential velocity of the workpiece, where it contacts the die is not always in the x-direction which results in a decrease of the relative workpiece velocity in the x-direction. See Figure 3.15 for conditions where this may occur.

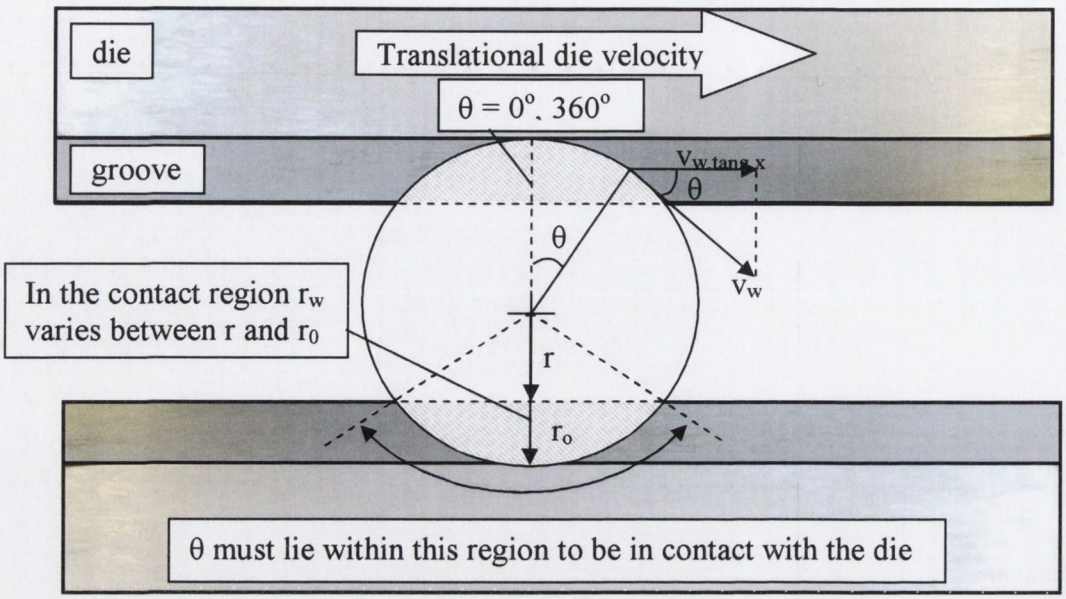

Figure 3.15: Determining the tangential velocity of the workpiece

The resultant workpiece velocity, $V_{w,\,result}$ is the total velocity of a point in the workpiece in the x-direction and if there is a difference between $V_{w,\,result}$ and the die velocity then slip and torsional stresses may arise:

$$V_{w,\,result} = V_{w,\,tang,\,x} + V_{w,\,trans} \tag{3.19}$$

Where $V_{w,\,tang,\,x}$ is the proportion of the tangential die velocity that is in the x-direction.

In Figure 3.15 θ is the angular distance between the x-direction and a tangent to the workpiece surface. Therefore:

$$V_{w,\,tang,\,x} = \cos\theta * V_{w,\,tang} \tag{3.20}$$

From Figure 3.15 it can also be seen that the workpiece radius in the groove region, r_w can vary from r to r_o. Assuming that the rotation of the workpiece is driven by the undeformed section of the workpiece the angular velocity of the workpiece will be ω_w (from equation (3.17)) and the tangential workpiece velocity is:

$$V_{w,\,tang} = r_w * \omega_w \tag{3.21}$$

Combining equations (3.18), (3.20) and (3.21) gives:

$$V_{w,\,tang,\,x} = \cos\theta * r_w * V_{die,\,move}/2r_o \tag{3.22}$$

By combining equations (3.14), (3.19) and (3.22) the resultant workpiece velocity simplifies to:

$$V_{w,\,result} = \cos\theta * r_w * V_{die,\,move}/2r_o + V_{die,\,move}/2 \tag{3.23}$$

From these equations it can be seen that the velocities of the workpiece and the dies are equal when r_w is set to r_o and $\theta = 0$ or 180 degrees. However, for all other values of r_w and θ the die will have a larger velocity then the workpiece and the die will, therefore, attempt to pull the slow moving region of the workpiece in the direction of die movement resulting in torsional effects in the workpiece.

3.2.10 Form Rolling Like Processes

- Ball spinning [27]– This process is used to reduce the diameter of thin walled tubes. The tubular workpiece has its diameter reduced by a series of balls that are in contact with it while simultaneously spinning around it. The radius at which these balls spin can be adjusted enabling the production of a part with various diameters.
- Skew rolling [28] and Helical rolling [29]– are other names for Transverse Helical rolling, which is discussed in more detail in Chapter 5.

3.2.11 Advantages/Disadvantages of Micro-Form Rolling

The small size of the workpieces used in micro-form rolling results in a process that has certain advantages and disadvantages compared with macro-form rolling.

Advantages

- The parts produced are small so that transportation costs and raw material costs associated with them on a piece by piece basis are very small.
- The main advantage of rolling smaller diameter parts is that many more workpiece rotations can be achieved for a given die length. This allows the use of a smaller spreading angle thereby reducing the deformation per rotation and, therefore, the machine forces and die stresses, resulting in less die wear and requiring a less rigid machine.
- The increase in number of rotations as the part diameter is reduced can be quite dramatic. For example the EWM AF3 machine used in this project has a stationary die length of 58mm and parts with diameters ranging from 0.5mm to 3.0mm have been rolled, resulting in 36 and 6 revolutions respectively:

Die length required for one rotation = $d * \pi$ = circumference (3.24)

For 0.5mm diameter part = $0.5 * \pi = 1.57$mm

For 3.0mm diameter part = $3.0 * \pi = 9.42$mm

Number of rotations possible on a die = die length / part circumference

For 0.5mm diameter part = 58 / 1.57 = 36.94 rotations

For 3.0mm diameter part = 58 / 9.42 = 6.157 rotations

Each die must accommodate a number of set features and these features require some of the available rotations. Two rotations are required for the sizing zone, ½ a rotation is required for feeding the workpiece into the dies and ½ a rotation for ejecting the workpiece from the dies. When these required rotations are accounted for, a 0.5mm diameter workpiece has 8.5 times the number of rotations of a 3.0mm diameter workpiece.

- The greater the number of rotations the greater the number of features that may be rolled onto the part, where the features are positioned one after the other along the die length. In this case, each feature is formed serially onto the workpiece. For example, in the case of the 0.5mm workpiece having 8.5 times the number of rotations of a 3.0mm workpiece, means that potentially 8 times as many features can be rolled onto the workpiece. Although each feature would require a sizing zone, the die length does not increase because the sizing zone can be overlapped with the knifing zone of the next feature, as very little deformation is occurring during this stage.
- Micro-form rolling, unlike other micro-forming processes, usually has one significantly large workpiece dimension, the length of the workpiece, and this makes material handling easier.
- For a given sidewall angle, the ramp angle is proportional to the spreading angle and because the ramp angle is largely responsible for the deflections experienced by the rolling machine, the use of a small spreading angle results in smaller deflections.

Disadvantages

- The danger of the creating internal voids, resulting from low cycle fatigue, due to the large number of workpiece rotations being used to form roll small diameter parts.
- Due to the small size of the features being rolled, even very small machine deflections can lead to significant geometrical errors e.g. when rolling 0.45mm wire machine deflections in the range 10μm can lead to errors of over 10% in feature dimensions. Therefore, a highly rigid machine is required which leads to increased costs. If very high tolerances are required, it may also be necessary to measure machine deflections to ensure they fall within acceptable levels. This monitoring will increase costs as provision of monitoring equipment will be necessary.

- The small size of the workpiece also results in a more difficult machine setup. A machine in which adjustments can be made accurately and repeatedly and one in which there are very fine levels of adjustment is required e.g. the use of micrometer adjusters in the die gap setup on the AF3 form rolling machine.
- The machining of dies and other machine parts which are part specific such as feed fingers must be produced to a very accurate level of dimensional tolerance.

3.2.12 One-Die Rolling

The use of a very small spreading angle, β, when rolling small diameter parts allowed the investigation of the novel 'one-die rolling' technique. This technique increases the versatility and improves the cost effectiveness of the form rolling process. One-die rolling differs from regular rolling because it uses only one die with a feature. This die is referred to as the wedge die and is responsible for forming the groove onto the workpiece. The featureless die is referred to as the flat die. The die setup used in one-die rolling is illustrated in Figure 3.16.

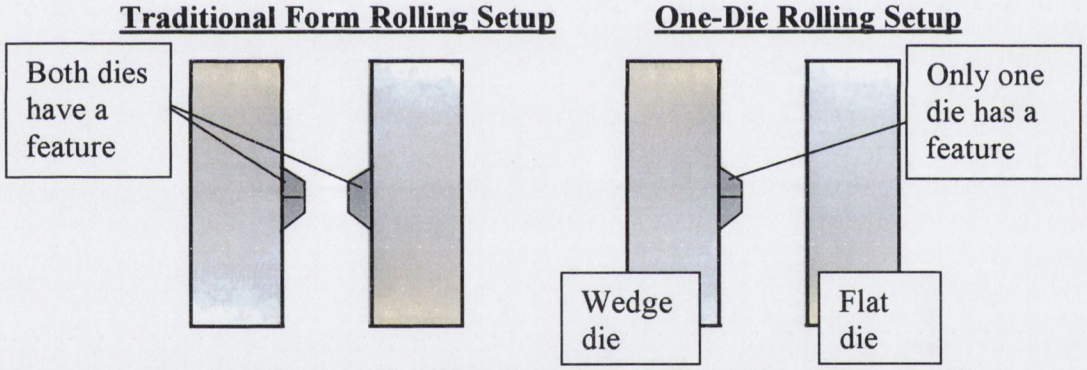

Figure 3.16: Die setup for one-die rolling compared with traditional form rolling

When form rolling is performed using dies that have a small spreading angle the rate of deformation is low. This is important when considering the rotation of the workpiece in one-die rolling. In rolling the workpiece will slip along the surface of one of the dies if this requires less energy then the rotation and resulting deformation of the workpiece. The tendency for the workpiece to slip increases in one-die rolling, because only one die is deforming the workpiece and an imbalance in contact forces exists between the workpiece and the two dies. The frictional forces that exist between the workpiece and the flat die are now the only forces preventing the workpiece slipping along its surface while the wedge die has both frictional forces and the knifing of the die into the workpiece preventing slip

on its surface. However, because the rate of workpiece deformation is low the imbalance between the forces does not become sufficiently large to result in the uncontrolled slip of the workpiece. The flat die can have an EDM traction surface applied to it to increase the friction force between it and the workpiece, thereby, encouraging rotation of the workpiece

The use of only one wedge die leads to obvious savings as it halves both material and machining die costs. Using only one wedge die also eases machine setup as the heights and the starting positions of the dies do not have to be matched.

During an extensive literature review on the form rolling process the author found no literature on one-die rolling. It would, therefore, be worthwhile to establish the viability of this method due to the advantages associated with it.

CHAPTER 4

METAL FORMING AND THE FINITE ELEMENT METHOD

CHAPTER 4

METAL FORMING AND THE FINITE ELEMENT METHOD

4.1 Overview of DEFORM software

DEFORM (Design Environment for FORMing) was the simulation program used to model the form rolling process. Both 2D and 3D Finite Element Analysis (FEA) of the form rolling process was performed. DEFORM had previously been used to model both thread and macro-form rolling processes [30-33].

DEFORM is operated using a Graphical User Interface, GUI. The GUI allows predefined options to be selected from menus. Three stages are involved in using the program, pre-processing, simulating and post-processing.

The problem is defined using the pre-processor; this involves defining geometries, materials, Boundary Contact Conditions (BCC), etc. Geometries are commonly created in graphics programs and imported into the DEFORM pre-processor. A major stage in the pre-processing of a problem is defining the mesh which will represent the workpiece. The mesh breaks the workpiece into thousands of elements. However if the mesh contains too many elements, the simulation will take too long to solve, on the other hand if the mesh is too coarse due to a lack of elements, the solution will be inaccurate. DEFORM contains tools which allow the mesh to be concentrated in areas of interest, resulting in a mesh with fewer elements but having sufficient accuracy, these tools are discussed in greater detail later.

After fully defining the problem in the pre-processor, it is solved by the simulator or solver. Both DEFORM 2D and 3D contain Automatic Mesh Generation (AMG) capabilities. AMG creates a new workpiece mesh when specific limits, such as the strain in the workpiece have been exceeded and the new mesh is defined by inputs set by the user in the pre-processor.

The post-processor allows the results of the FEA simulation to be analysed and it contains many analysis tools. The stresses or strains within the workpiece or tool can be displayed graphically, as can displacements, velocities, strain rates and other state variables. Other analysis tools include point tracking, flow nets, state variables between two points and graphing of the process load. Point tracking and the state variables between two points allow the displacements and other state variables of interest to be monitored in

points of interest. The die load required to deform the workpiece can also be plotted. The flow net covers a plane of the workpiece with a particular pattern and as the workpiece is deformed so is the pattern. The distortion of the pattern highlights regions that experience large deformations.

4.2 Modelling of a Form Rolling Process using DEFORM

DEFORM uses the von Mises yield criteria in conjunction with the Prandtl-Reuss flow rule and isotropic hardening to simulate Elasto-plastic material behaviour. In the case of incremental forming conditions, DEFORM uses a Lagrangian solver.

4.2.1 Von Mises Yield Criteria

Yield criteria predict the onset of plastic deformation in a body by relating the stress system within it to a material property. In the von Mises yield criteria, the stress system is represented by a symmetrical quadratic condition and the material property is the yield strength of the material obtained from a tensile test.

$$\sigma_y = \sqrt{(\sigma_{11}-\sigma_{22})^2+(\sigma_{22}-\sigma_{33})^2+(\sigma_{33}-\sigma_{11})+6(\tau_{12}^2+\tau_{23}^2+\tau_{31}^2)} \qquad (4.1)$$

The formula indicates the onset of yielding if the right hand side equals the yield strength of the material on the left hand side.

4.2.2 Prandtl-Reuss Flow Rule

The Prandtl-Reuss Flow rule defines material flow for an Elasto-plastic Material and its strain increment is the sum of both the elastic and the plastic strain increments. It uses the Reuss assumption that in plastic flow the strain increment is related to the deviatoric stress causing distortion rather that the total stress as in elastic deformation.

$$d\varepsilon'_{ij} = (d\varepsilon_{ij})_p + (d\varepsilon_{ij})_E = \sigma'_{ij}d\lambda + \frac{d\sigma'_{ij}}{2G} \qquad (4.2)$$

$$d\varepsilon_{ii} = (d\varepsilon_{ii})_p + (d\varepsilon_{ii})_E = 0 + \frac{1-2\nu}{E}d\sigma_{ij} \qquad (4.3)$$

4.2.3 Isotropic Hardening

Work hardening occurs when metals are subjected to cold forming and their yield strength increases. The level of hardening is proportional to the total plastic work. When an isotropic material model yields plastically, the yield strain in all directions is the same.

$$\bar{\sigma} = F(W_p) \tag{4.4}$$

Where $\bar{\sigma} = \sigma_y$ and is known as either the effective, equivalent or flow stress.

W_p is the total plastic work

4.2.4 Contact Conditions

For bulk metal forming simulations, DEFORM recommends the use of the constant shear model of friction, in which the frictional force, F_F is proportional to the shear yield strength of the material, k.

$$F_F = m \cdot k \tag{4.5}$$

Where: m is the friction factor, for form rolling simulations a friction factor of 1 is recommended.

4.3 Creating a Meshed Object in DEFORM

The resolution of a mesh in DEFORM is called the mesh density and a high mesh density implies small mesh elements. The mesh density can be controlled in a coarse fashion by adjusting the total number of elements in an object. However, the mesh density in a specific region of the workpiece can, also, be controlled using five weighing factors whose level of influence is set in the pre-processor. Four of these weighing factors - the workpiece surface curvature, strain distribution, strain rate distribution and temperature distribution - are dependent on the condition of the workpiece. The fifth weighing factor is the 'mesh density window' which is used to select regions of the workpiece where a finer mesh is required. Mesh windows are particularly useful for form rolling because the majority of the deformation is confined to a small volume of the workpiece, as shown in Figure 4.1.

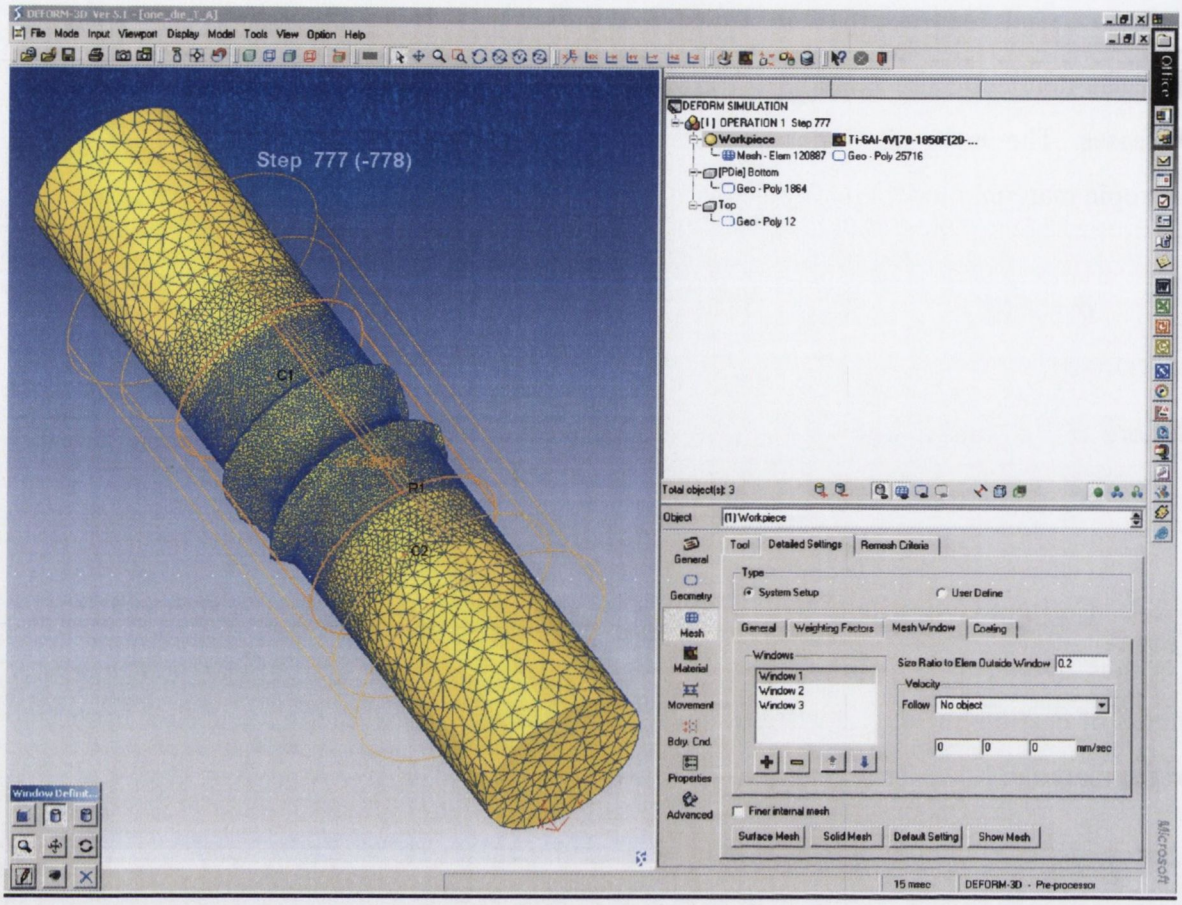

Figure 4.1: Mesh concentrated in the region of deformation using three mesh density windows

4.4 State variables in DERORM FEA package

At each time increment, the DEFORM software calculates a range of 'state variables' that describe the deformation being experienced by a workpiece. These variables include stresses, strains, strain rates velocities and displacements and they are examined in the post-processor of DEFORM to analyse the deformation process. Where applicable, the FEA package can represent the state variables using Cartesian or cylindrical co-ordinate systems. The state variables and methods of graphically representing these variables are described in the following section.

4.4.1 Graphical Representation of the State Variables

The post-processor provides several methods of displaying the state variables on the workpiece and the most useful of these are described below:

- A line contour plot represents the state variable as a series of graduated lines on the workpiece surface. An example of a line contour plot is shown in Figure 4.2(a)
- In a shade contour plot the magnitude of the state variable is displayed as a colour on the workpiece surface. An example of a shade contour plot is shown in Figure 4.2(b)
- A MinMax plot shows only the minimum and maximum values of the chosen state variable and their location in the workpiece. An example of a MinMax plot is shown in Figure 4.2(c).
- In a vector plot the colour of the vector represents the magnitude of the state variable and its orientation represents the direction in which the state variable is working. An example of a vector plot is shown in Figure 4.2(d)

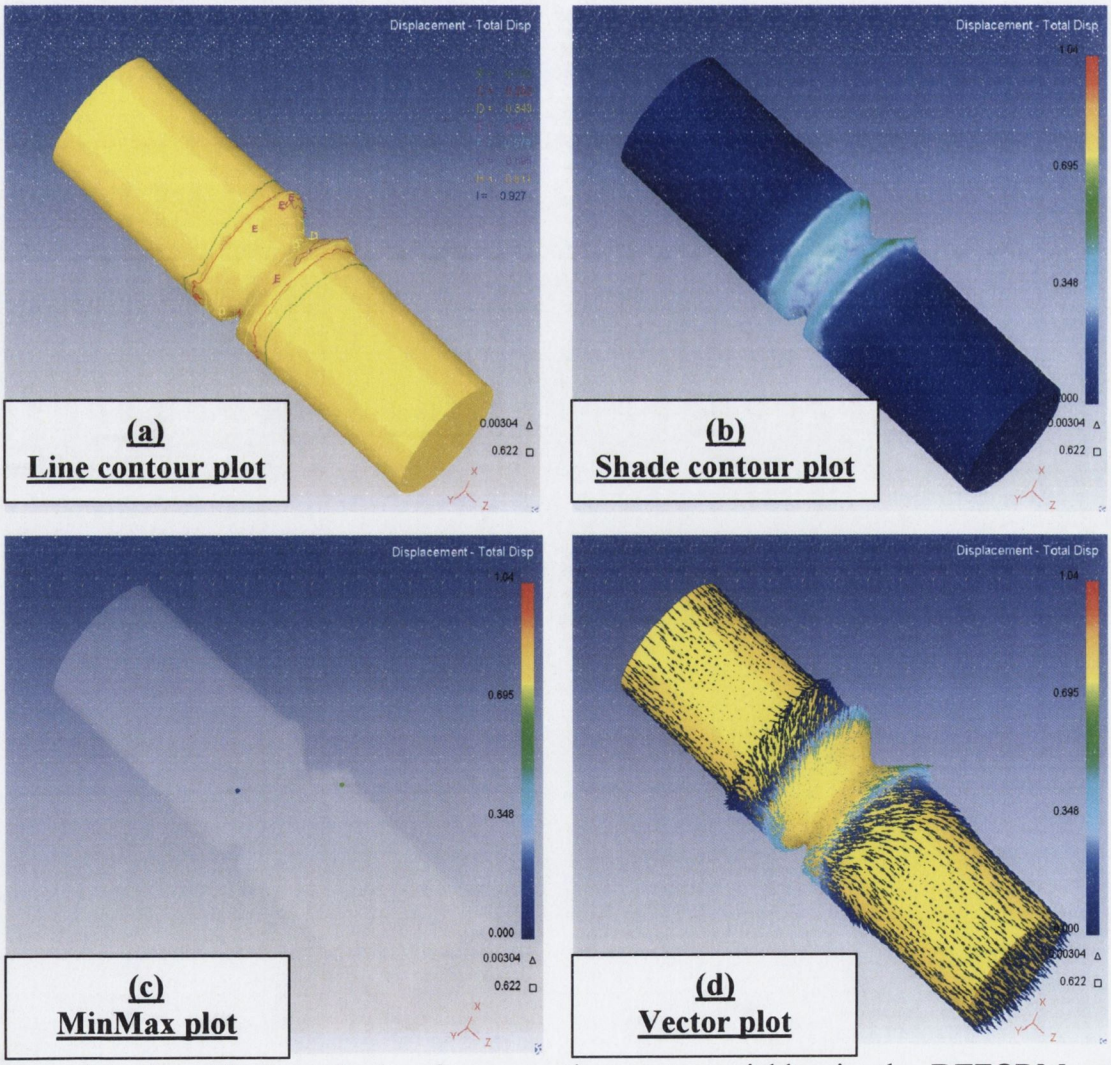

Figure 4.2: Graphical methods of representing state variables in the DEFORM post-processor

4.4.2 Definition of State Variables

- The total velocity and displacement experienced by workpiece nodes can be measured in one of two ways. If Cartesian co-ordinates are used, the components of the state variable working in the x, y and z directions can be determined; if cylindrical co-ordinates are used, the components in the radial, axial and tangential directions can be determined.
- The stresses within the workpiece can be described in several ways:
    - Directions- as in the case of velocities and displacements the magnitude of the stresses acting in a variety of directions can be determined.
    - Effective stress– as determined by the von Mises criteria. Plastic flow will ensue when it exceeds the yield strength of the workpiece.
    - Hydrostatic stress
    - Principal stresses- three principal stresses acting in three orthogonal directions are ranked in accordance to their algebraic values, the maximum principal stress having the largest value, the minimum principal stress the smallest value and the intermediate principal stress having a value that is between the minimum and the maximum. They act in directions in which the shear stress is zero.
    - Shear stresses can also be determined for the workpiece.
- The strains and strain rates within a workpiece can be described using the same methods as those used to describe the stresses.

CHAPTER 5

LITERATURE REVIEW

CHAPTER 5

LITERATURE REVIEW

This chapter consists of a review of the literature available on the main subjects of interest in this thesis namely the form rolling process and micro-forming. Subjects such as the failure of rolled parts and the size effect, a phenomenon that distinguishes micro forming from forming at larger scales, are also discussed. The FEA of both micro-forming and form rolling are also covered.

5.1 Form Rolling

Authors who have investigated the form rolling process can be divided into two groups; those who investigated the process empirically to determine the conditions that result in successful rolling and those who have tried to examine the mechanics of the process.

Those who investigated the mechanics of the process were typically the Russian pioneers of the process who during the 1960s examined the process using inventive experimental methods. Most of the Russian research involved rolling parts that had been modified so that they would in someway record the deformation parts underwent. Analysis of these deformed parts was then used to gain an understanding of the mechanics of the process. It should be noted that not all of this research was exclusively on form rolling and it included similar rotary forming processes, such as Transverse Helical Rolling.

The authors who investigated the process empirically had different ideas on what constituted successful rolling. Some were concerned with the occurrence of internal defects while others were concerned with interfacial slip (i.e. the slip between the die and the workpiece). These authors investigated the process by performing rolling trials with a series of dies having a range of sidewall angles, spreading angles and diameter reductions. They recorded the combinations that resulted in successful rolling and often created empirical relations to reflect their results. Some of the authors also tried to link experimental results with FEA and other analytical techniques.

5.1.1 Mechanics of the process

In 1964, Nefedov et al [29] published a paper in which they explained the nature of metal deformation during hot Transverse Helical Rolling. This process is similar to a Cross Wedge Rolling (CWR) process with a three die machine but in this case the forming face

of the die is replaced with a rotating cone to prevent the torsional effects associated with form rolling, see Figure 5.1.

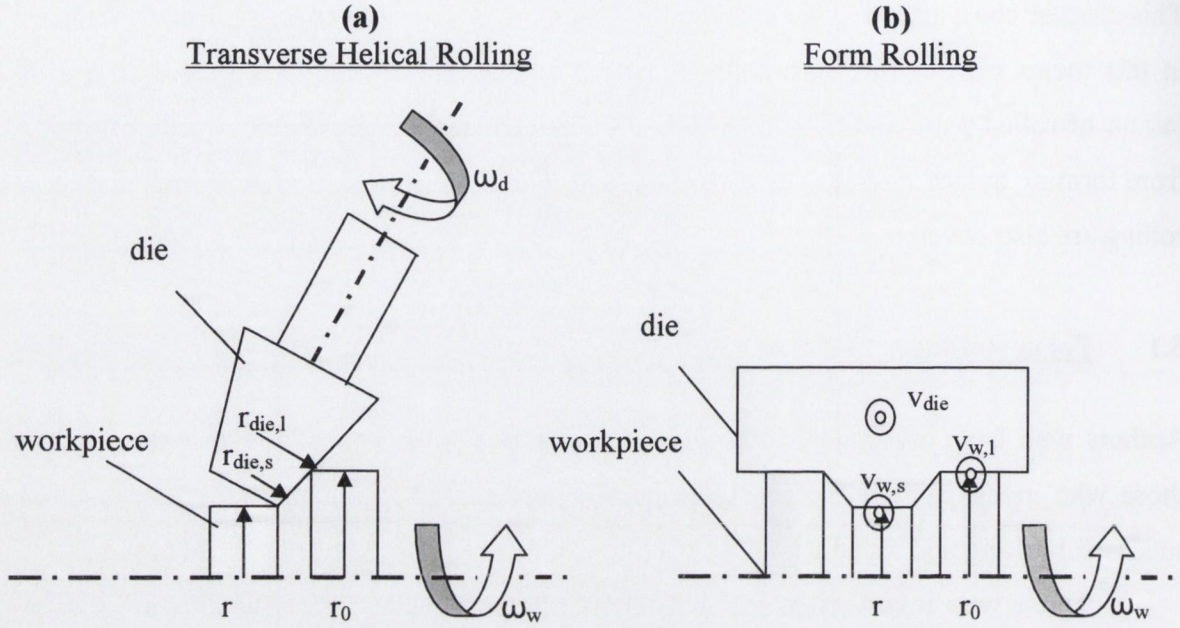

Figure 5.1: A comparison of form rolling and Transverse Helical Rolling

In form rolling the die has a constant velocity, V_{die} however the tangential velocity of the rotating workpiece, v_w, varies depending on its radius:

$$v_w = \omega_w * r_w \qquad (5.1)$$

Where: ω_w = the rotational velocity of the workpiece = $v_{die} * r_0$

r_w is the radius of the workpiece in the sidewall region and it varies from r to r_0

Figure 5.1 shows the large tangential workpiece velocity, $v_{w,l}$ in the undeformed section of the workpiece and the small tangential workpiece velocity, $v_{w,s}$ in the deformed section of the workpiece. The resulting velocity variation between the die and the workpiece results in twisting of the workpiece and corresponding torsional stresses. In Transverse Helical Rolling the use of the rotating cone shaped die results in a die whose tangential velocity at a given point on its surface is dependent on its radius at that point. The tangential velocities of both the workpiece and die can, therefore, be balanced producing a process that is free of torsional effects. Figure 5.1 shows that the undeformed section of the workpiece, which has the largest tangential workpiece velocity, is deformed by the widest part of the die cone, which will also have a large tangential velocity.

Nefedov determined the presence of four distinct regions within the zone of deformation as shown in Figure 5.2.

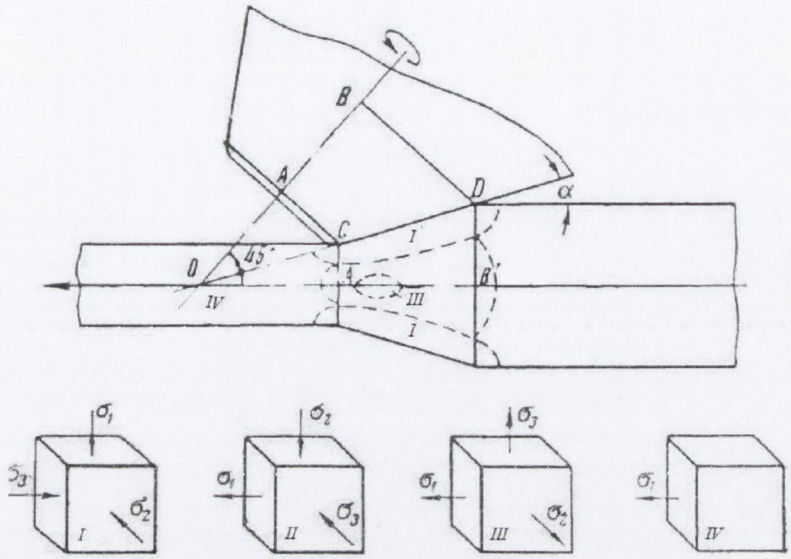

Zones of stress systems in the deformation zone of transverse helical rolling (arrows indicate the direction of the motion of the blank and the rotation of the rolls; explanation in text)

Figure 5.2: Regions of stress in Transverse Helical Rolled workpiece[29]

Region I is the region of 'difficult compression' in which the material experiences compression from all three sides. σ_1 is determined by the pressure between the workpiece and the die while σ_2 and σ_3 are a result of the frictional forces and the effect of the workpiece outside the zone of deformation (i.e. the metal is being forced to flow axially but is being restricted by the material yet to be deformed).

Region II is the 'region of tension' with one tensile and two compressive stresses. The penetration of the die into the workpiece is still resulting in compressive stresses. However the axial flow of the material in region I is pulling the material in region II with it resulting in axial tensile stresses.

Region III is the 'region of tensile stresses on all sides' with the material being subject to tensile stresses in three directions. If one of these tensile stresses exceeds the brittle strength of the material, hollows may form.

Region IV is the region of the 'linear stress system' in which the formed workpiece is subject to uni-axial tension.

To study the deformation mechanism, workpieces into which M12 bolts were screwed, were rolled to different reduction ratios. After rolling, longitudinal and transversal sections were taken and the pitch of the thread was measured. Radial

deformation was only found in region I with its magnitude increasing towards the surface. Tangential deformation is also only found in region I and its magnitude is dependent on the reduction ratio. The surfaces of the workpieces in Figure 5.3 have experienced a large amount of tangential deformation.

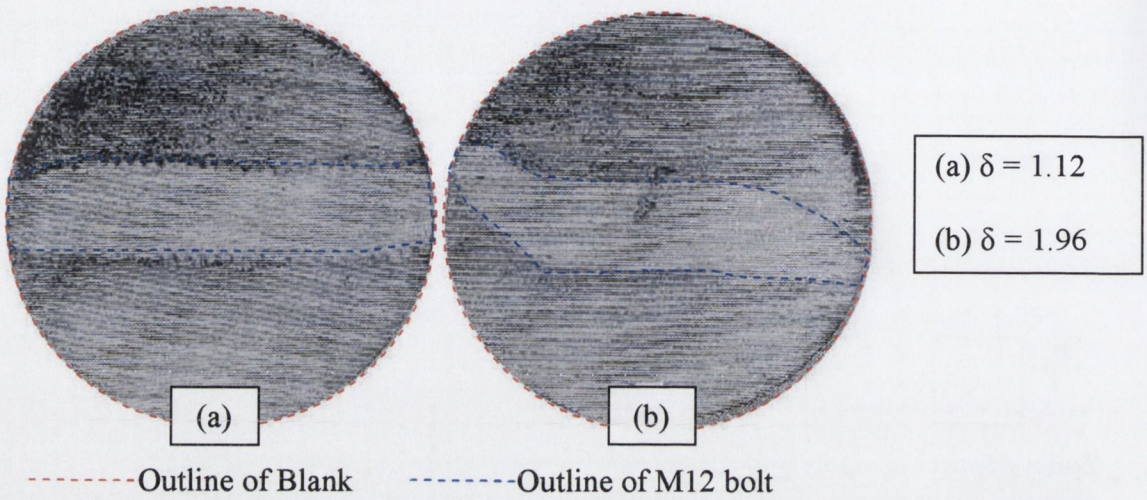

Figure 5.3: Transverse cross section of workpieces, into which M12 bolts were screwed before rolling [29]

Teterin [34] investigated the effects of axial and transverse tensile stresses on the mechanism of axial rupture in hot Cross Rolling. This was achieved through the rolling of composite and constrained workpieces, in which the workpieces experienced diameter reduction.

Composite workpieces consisted of a thin cylindrical billet welded around its circumference to two other wider billets of the same diameter, see Figure 5.4. This setup resulted in the central billet being free from axial effects. However, the axial region of this billet still experienced extensive plastic deformation and rupture during rolling. This failure indicates the existence of significant transverse stresses in the axial region of the workpiece. The internal failure develops at low levels of area reduction, ΔA, and affects the entire axial length of the workpiece at an area reduction of only 12%.

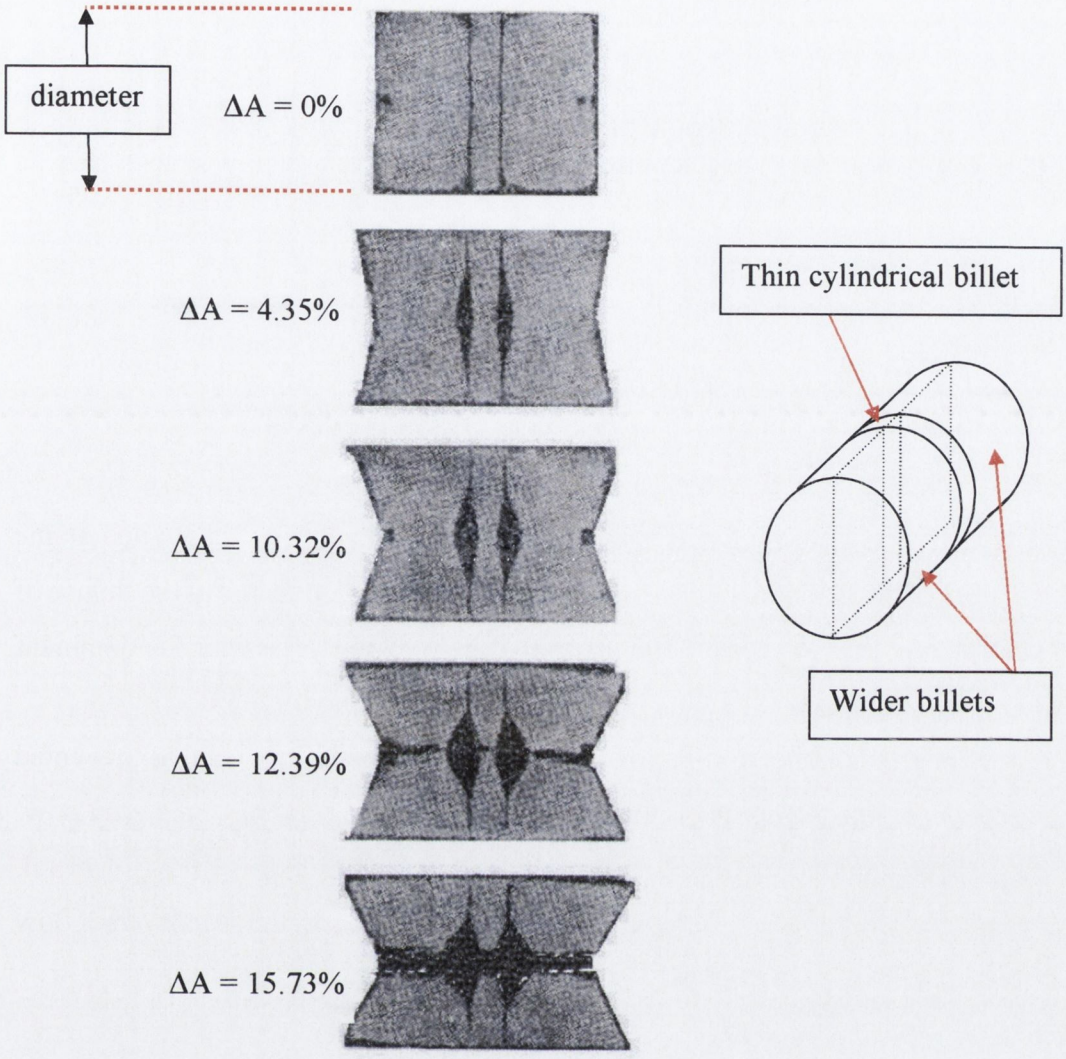

Figure 5.4: Longitudinal sections of composite workpieces showing the development of axial rupture with increasing area reduction [34]

The rolling of short billets allows larger diameter reductions before failure, which is a result of lower transverse tensile stresses. Short billets allow a larger proportion of the material to flow axially compared with longer parts as there is a smaller frictional force restricting axial flow, and this reduces the transverse flow of material.

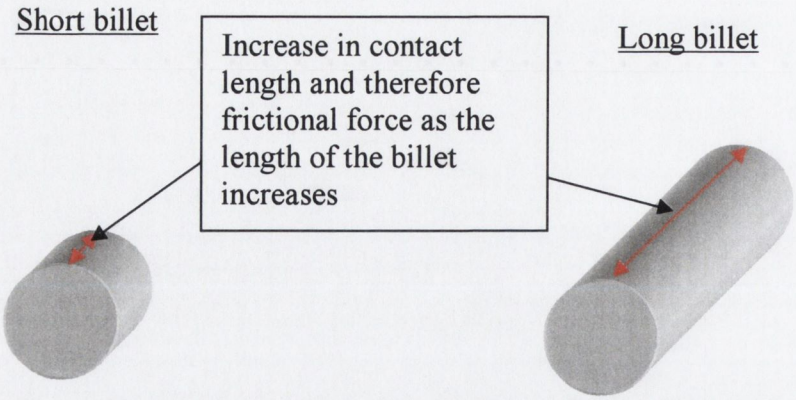

Figure 5.5: Increased frictional force when the billet length is increased

Solid workpieces with the same length as the composite workpieces failed at the same reduction ratio, indicating that axial flow was not the dominant factor in the failure of these solid workpieces, thus supporting the claim that transverse stresses are the dominant factor contributing to failure.

In constrained workpiece rolling, the workpiece was rolled by dies that prevented axial flow of the workpiece and therefore increased the amount of transverse material flow, see Figure 5.6. These workpieces in which there was increased transverse flow of metal, failed at lower reduction levels, thereby, supporting the theory that transverse flow encourages part failure.

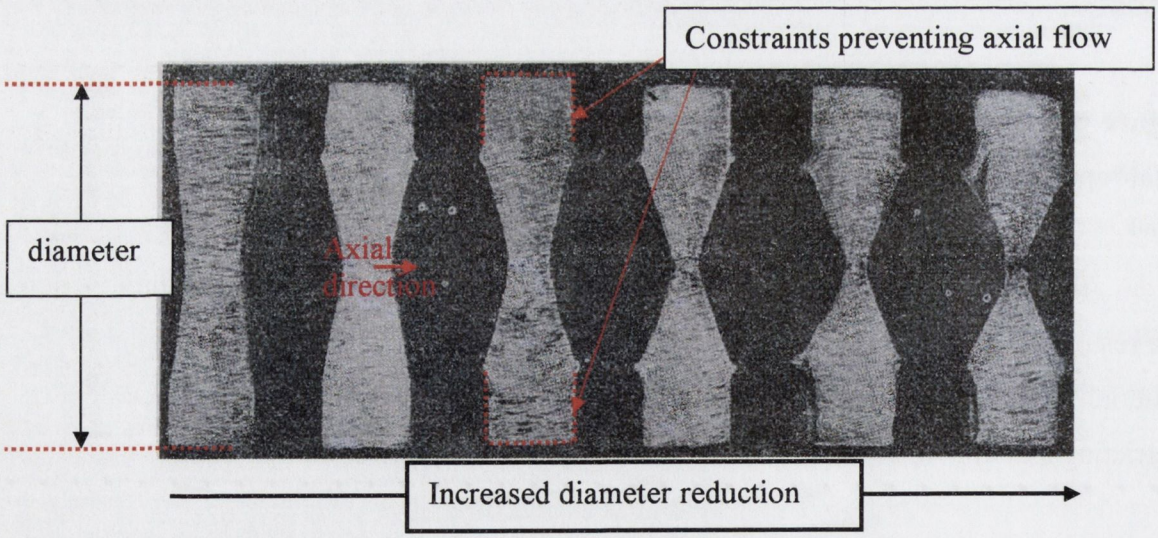

Figure 5.6: Radial sections of constrained workpieces showing the development of axial rupture with increased diameter reduction[34]

In micrographs of rolled parts, a fine grain structure was present at the periphery and the centre of the part and a coarser grain structure existed between the centre and the

periphery. This indicates the presence of the intensive plastic deformation in the centre and as the axial flow was shown not to be a factor in failure these fine grains must be a result of transverse stresses

The parts rolled during this thesis were long and only a small proportion of the workpiece was reduced which meant that there was a large amount of the workpiece resisting the axial flow of material, which would increase the transverse flow and the likelihood of failure.

Kazanskaya et al [35] examined the process by rolling workpieces with dowels positioned perpendicularly through their central axis. After rolling, the workpieces were sectioned axially or transversally. From these tests, the following conclusions were drawn:

1. When the axial sections were examined, cavities were observed around the dowels indicating the presence of tensile stresses which pulled the workpiece material away from the dowels. These stresses were at a maximum in the centre of the workpiece.
2. The shape of the cavities indicated they were deformed by axial tensile stresses.
3. The size of the cavities increased with increased die penetration, indicating the tensile stresses also increased.
4. When transverse sections were taken, no cavities were observed.
5. Distortion and flattening of the dowel at the periphery of the workpieces was due to the penetration of the die into the workpiece.

5.1.2 **Empirical Analysis of the process**

The authors who analysed form rolling based on empirical observations provided a lot of data on the process and the die geometries that resulted in successful rolling. Their work is discussed in the following paragraphs.

Lovell et al [23] rolled workpieces to increasing area reductions with a number of die sets with differing geometries. The workpieces were then examined for the presence of internal failures and the results of these tests are presented in Table 5.1.

ΔA(%)	β(°)	α(°)		
		15	20	30
27	3	no void	no void	no void
	5	void	void	no void
	7	void	void	no void
35	3	no void	no void	no void
	5	void	void	no void
	7	void	void	no void
37	3	no void	no void	no void
	5	void	void	no void
	7	void	void	no void

Table 5.1: Experimental results produced by Lovell et al [23]

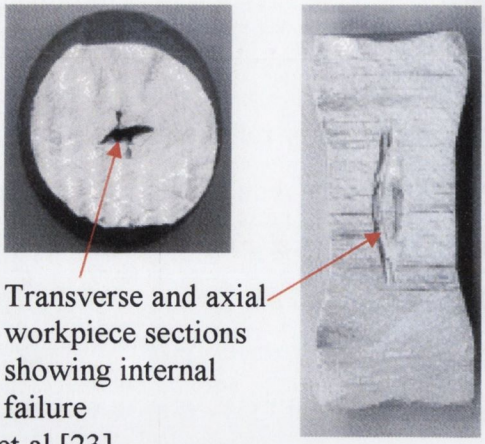

Transverse and axial workpiece sections showing internal failure

The size of the voids was also recorded and they indicated an increasing void size for larger spreading angles and smaller sidewall angles. From these experimental results they defined a non-dimensional deformation coefficient, ε

$$\varepsilon = \frac{2l_{sidewall}}{d - d_0} \frac{f}{l_{formed} - f} \frac{A_0 - A}{A_0} \tag{5.2}$$

where: $l_{sidewall}$ = the axial length of the sidewall

l_{formed} = the axial length of the formed part

It was concluded that if the value of ε exceeds 0.6 then an internal void is likely to form in the rolled part. However it is not known whether this value of 0.6 will hold for other billet materials or die geometries.

In 1998, Lovell et al [36] published a paper containing FEA of the form rolling process and by comparing the FEA with experimental results they determined that FEA was a suitable analysis tool. For example, Lovell et al determined that the FEA and experimental strain values differed by only six percent on average. Lovell et al also drew a number of conclusions from a series of FEA models they ran:

- The first principal stress at the centre of the workpiece was almost always tensile, which is a suspected cause of failure
- The first principal stress at the centre of the workpiece increases rapidly in the tool knifing zone

- The first principal stress at mid-radius points experienced a cyclic stress state, varying between tensile and compressive stress with rotation, low cycle fatigue through the Mannesmann effect could, therefore, be a problem.
- Increasing area reduction increases the magnitude of the stress and strain.
- As the sidewall angle is increased in the range from 20° to 35° the first principal stress in the workpiece centre increases. However, when the sidewall angle increases above 35°, the tool is sharp and there is little plastic stress and deformation in the centre of the billet.
- The mid-radius principal stress is sinusoidal varying between tensile and compressive stress for sidewall angles between 20° and 35°. However, angles larger that this result in the stress always being tensile (although it remains sinusoidal).

In 2000, Lovell et al [37] published a further paper in which they analysed a Cross Rolling process, using FEA simulations. A total of 14 different rolling combinations were examined by varying the sidewall angle, area reduction and friction coefficient paying particular attention to the stress state in the centre of the workpiece which is the likely position of workpiece failure. The conclusions drawn from their simulations were as follows:

- For almost all rolling conditions, the first principal stress in the centre of the workpiece was tensile. This tensile stress increased rapidly in magnitude during the knifing zone. The authors noted that the maximum stress criterion predicts the development of cracks in the workpiece if the first principal stress exceeds the ultimate tensile strength of the material and, therefore, concluded that crack development is due to the high tensile stresses in the centre of the workpiece which correlates well with other authors reasoning.
- Up to a value of 0.3 changing the friction coefficient had a significant effect on the state variables, however, above this value, the friction coefficient had less effect on the results and they remain similar to those obtained when a friction coefficient of 0.3 is used.
- 40° is the critical sidewall angle and below this value, the principal stress in the workpiece centre increases with increasing sidewall angle (20-35°). However, when the sidewall angle is increased from 35° to 40° the principal stress drops

dramatically. The authors consider a sidewall angle of 40° to be very sharp, and this angle results in very little deformation in the workpiece centre.

- Increased area reduction results in an increase in the magnitude of the stress and strains in the workpiece.

Lovell et al [36, 38-40] also did significant work investigating interfacial slip in form rolling processes. However, that work is not considered relevant to this thesis and will not be discussed further.

A major limitation of the recent research carried on the form rolling process (1990 onwards) is that it focuses on hot forming in which the workpiece is heated above its recrystallisation temperature. These authors typically carried out their experimental rolling trials with lead, which can be hot worked at room temperature and is not a commonly used engineering material. **However the research for this thesis focused on the cold forming of engineering materials, e.g. stainless steel and titanium alloy.**

Pater et al

Pater and his colleagues have produced a series of papers on the analysis of form rolling. In 1996, Pater et al [41] published a paper that used analytical methods to determine the mean contact pressure between the tool and the workpiece, q_m. Pater assumed that the mean unit pressure is equal to the pressure in a rod extrusion process in which the rod is reduced to the rolled diameter, d from a substitute diameter, d_z that is a proportion of the blank diameter, d_0 as shown in Figure 5.7.

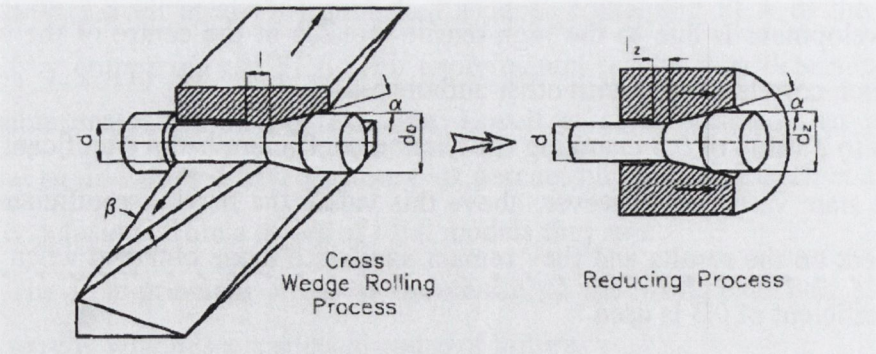

Figure 5.7: Analysing form rolling as a wedge reducing process

Pater proceeded to devise expressions for the pressure ratio q_m/σ_0 based on an energy method and an upper bound method.

The Energy method:

$$\frac{q_m}{\sigma_0} = \frac{2}{\sin\alpha \cdot \left(\delta_z^2 - 1\right)} \cdot \left(\ln \delta_z + \frac{2}{\sqrt{3}} \cdot m_k \cdot \frac{l_z}{d} \right) + \frac{m}{\sqrt{3} \cdot \cos\alpha \cdot \sin 2\alpha} \cdot \frac{\delta_z^2 + 1}{\delta_z^2} \qquad (5.3)$$

The upper bound method:

$$\frac{q_m}{\sigma_0} = \frac{1}{\delta_z^2 - 1} \cdot \frac{2}{\sqrt{3}} \left[\left(\frac{f(\alpha)}{\sin^2 \alpha} + m \cdot \cot\alpha \right) \ln \delta_z + \frac{2\alpha - \sin 2\alpha}{2\sin^2 \alpha} + 2m_k \frac{l_z}{d} \right] \qquad (5.4)$$

Where: substitute reduction $\delta_z = \frac{d_z}{d}$ (5.5)

substitute sizing distance l_z = half of the rolling pitch divided by the relative reduction of a portion

$$= \frac{\pi r_0 \lambda \tan\beta}{2\delta} \qquad (5.6)$$

$$\lambda = \left(2.587 - 1.557 \cdot \delta^{0.3528}\right) \cdot (0.00355 \cdot \alpha + 0.927) \cdot \beta^{0.0568} \qquad (5.7)$$

Friction factor for the sizing zone m_k

Different methods for calculating d_z were used with the above formulae. Comparison with experimental results gave the optimum method below:

$$d_z = d + \Delta r \qquad (5.8)$$

$$Where: \Delta r = \frac{d_0 - d}{2} \qquad (5.9)$$

The experimental and theoretical results compare quite favourably, with the upper-bound method tending to overestimate the pressure and the energy method tending to underestimate it.

A serious limitation of the equations discussed above is that they do not take account of the work hardening of the material and the experimental results used to validate them was carried out using lead, which does not work harden. Therefore, they are more suited to the analysis of hot forming. However the forming carried out for this thesis was performed at room temperature and the materials work harden considerably.

In 1998 and 1999 Pater [42, 43] published papers that detailed an analytical method to analyse the rolling process, titled the 'applied model of the CWR process'. This method allowed several rolling parameters such as forces and contact area to be determined. It

worked by converting the workpiece into a series of discs and analysing each of these discs individually using a plane strain assumption.

In 2000 [44] Pater et al compared experimental results with those determined by analytical methods.

In 2003 [21] they focused on using the applied model of the CWR process to create plots of α and β which highlighted combinations of α and β that produced successful rolling. Using this method they also investigated the effect of the sidewall shape on the process.

5.1.3 **Failures associated with Form Rolling**

To begin this section on the failures associated with form rolling a paper by Fu and Dean will be discussed [13]. In it they noted ten different mechanisms that may cause internal failure:

1. Tensile stresses

Tensile stresses result from the normal pressure between the rolling tools

2. Accumulative tensile stress

The tensile stresses in the centre of the workpiece increase as the number of cycles increases and can result in central defects

3. Repeated compression leading to supplementary tension

Assuming a plane deformation model, repeated compression of the workpiece creates a supplementary tensile stress that causes a central cavity

4. Secondary shear tensile stress and shear strain induced repeatedly

The increase in cavity size with an increasing number of workpiece rotations has been attributed to the central part of the workpiece being repeatedly exposed to secondary tensile stress and shear strain.

5. Stress and strain reversals

Stress and strain reversals in the working zone of the workpiece may result in part failure.

6. Intersecting velocity discontinuities

From slip line field analysis a pair of interesting velocity discontinuities can be observed in the centre of the workpiece, which may result in the formation of a central cavity.

7. Inhomogeneous deformation

As a result of the alternating tensile and compressive stresses (Bauschinger effect) in the workpiece, inhomogeneous deformation exists which may result in failure in the centre of the workpiece.

8. Exceeding the maximum permissible deformation

Under monotonic loading, if a material experiences deformation beyond a limiting value (i.e. the critical shear intensity value) then micro-fracture will ensue. With successive load cycles this micro-fracture will develop into a macro-fracture.

9. Torsionally induced shear stresses

Torsion arises in the workpiece due to the different tangential velocities on the workpiece depending on its radius of contact with a moving die with a constant tangential velocity. Shear stresses result from the torsional effects present in the workpiece and if they exceed the yield stress of the material, the workpiece will fail.

10. Inclusions

Large inclusions in the centre of a workpiece are likely to cause part failure

Surmising these ten mechanisms, they concluded that there were four different causes for the development of internal failure

(i) Accumulation of micro-fracture due to the cyclic nature of the process
(ii) Torsion between different portions of the diameter
(iii) Large workpiece inclusions
(iv) Alternating compressive and tensile stress and shear stress in centre of the workpiece as in the Mannesmann effect

Johnson and Mamalis [45] published a paper in 1977 on the defects arising in metal working processes, including the Cross Rolling process. They noted that many authors subscribed to the theories of tensile stresses or shear stresses causing axial failure, as discussed elsewhere in the literature review. Kneading was also suggested as a cause of internal failure. Kneading arises from excess material being trapped in the central region of the workpiece.

An interesting observation can be made on this work which is that it appears that the deformation mechanics of form rolling may actually change with increased die penetration, due to the changing H/l ratio, where H is the thickness of the workpiece and l is the width of the tool deforming it, see Figure 5.8.

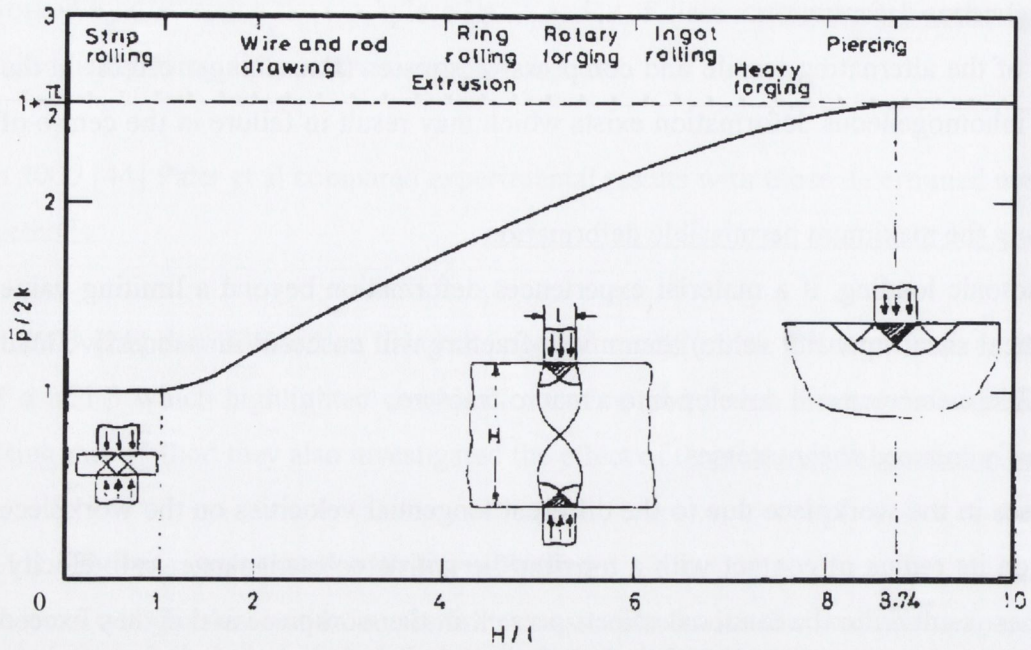

Figure 5.8: Relation between plane strain indentation pressure and H/l for a block of thickness H indented by flat rigid indenters of width l [45].

For example, when rolling a 1mm diameter wire to a final diameter of 0.28mm with a die with a 0.36mm flat, the H/l ratio decreases from 2.777 to 0.777 during the process, Figure 5.8 indicates that the process has changed from being similar to wire and rod drawing to strip rolling. Other dies geometries result in very large H/l ratios which indicate a piercing like process. Some of the internal failures associated with these different forming processes will now be discussed:

Strip Rolling:

- Failures are typically a result of 'secondary' tensile stresses
- The reduction in area achievable in a tensile test is directly related to the levels of reduction possible before cracking occurs. The stainless steel wire used in this research typically achieved a 33% area reduction before failure.
- Alligatoring or crocodiling is a failure in which the workpiece splits along its centre with the top and bottom sections following the rotation of their respective rolls (see Figure 5.9(a)). A problem arises when the H/l ratio is between 1.4 and 1.7; resulting in a residual tension in the workpiece that is equal to the yield stress of the material (see Figure 5.9(b)), this is caused by a greater elongation of the workpiece in the centre compared to the surface, see Figure 5.9(c).

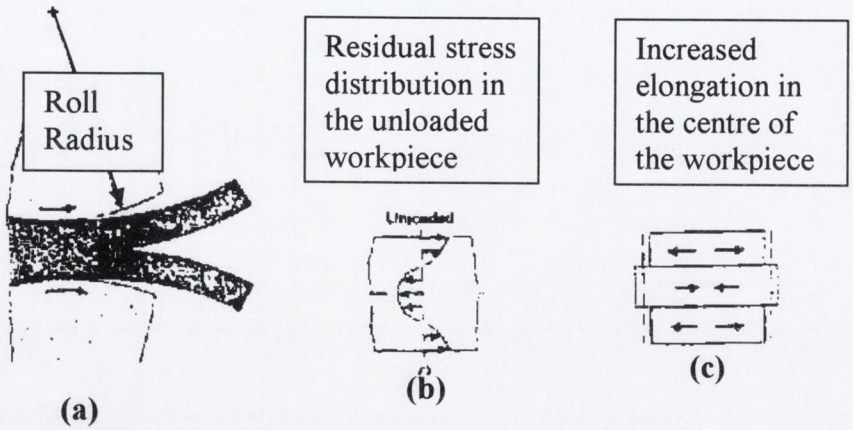

Figure 5.9: Alligatoring or crocodiling failure [45]

Wire and Rod Drawing:

Repeated internal cup and cone (chevron failure), see Figure 5.10.

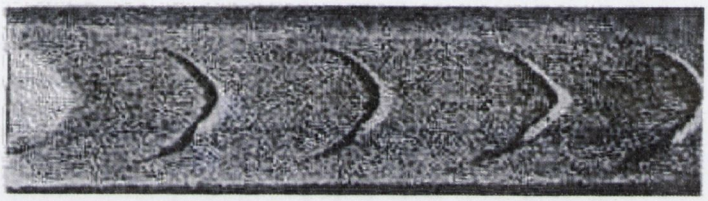

Figure 5.10: Chevron failure in drawn wire [45]

In wire and rod drawing material flow occurs in only one direction and the point of the chevron failure points in the direction of material flow. However, in form rolling material flow in both the positive and negative axial directions occurs (i.e. the groove forces material equally in both directions). Therefore if an internal failure was to occur in a form rolled part it would have a different shape. The length of the groove in form rolling is also much smaller than length of the workpiece in a drawing process so there would be only one failure in a form rolled workpiece compared with the multiple failures found in a drawn workpiece.

FEA analysis of the process also indicates a change in deformation mechanism with increased die penetration, as the H/l ratio decreases. Figure 5.8 also predicts lower forging loads for lower H/l values; this is evident in the FEA simulations as a decreasing forging load with increasing penetration, beyond a certain penetration.

In 1979 Thompson and Hawkyard [46] published a review on crack formation in transverse rolling concentrating mainly on slip line fields to validate their claims. The slip

line field analysis of the process is based on a transverse section of the workpiece as shown in Figure 5.11.

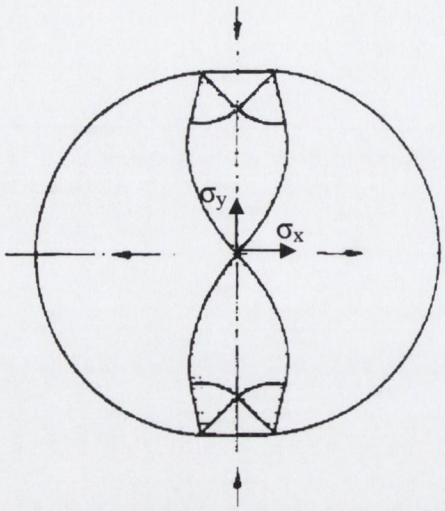

Figure 5.11: Slip line field of transverse rolling section [46]

Thompson and Hawkyard's observations are outlined below:

- Discontinuities: crack formation is most likely to occur in the centre of the workpiece because from observation of the slip line field this is where the velocity discontinuities are located.
- As a radial line is rotated through one complete rotation it travels through two compressive and two tensile stress zones. This fluctuating stress could result in low cycle fatigue and void formation.
- With increased die penetration into the workpiece the ratio of contact width to workpiece height increases and the stress state in the centre of the workpiece changes from having a triaxially tensile stress state to having a tensile stress in only one direction, see Table 5.2.

H/l limits	σ_x	σ_y	σ_z
8.7 < H/l	Local plasticity under dies. No through penetration.		
4.8 < H/l < 8.7	+	+	+
1.9 < H/l < 4.8	+	-	+
1.0 < H/l < 1.9	+	-	-
H/l < 1.0	This slip line field not applicable		

Table 5.2: Sign of principal stresses at workpiece centre for varying H/l ratios [46]

However, it can be seen from Figure 5.12 below that the H/l values required to achieve a singularly tensile stress state are very unrealistic because the workpiece would have to conform to a geometry that would be very difficult to roll. Therefore, the stresses in the centre of the workpiece are likely to remain tensile in two or three directions.

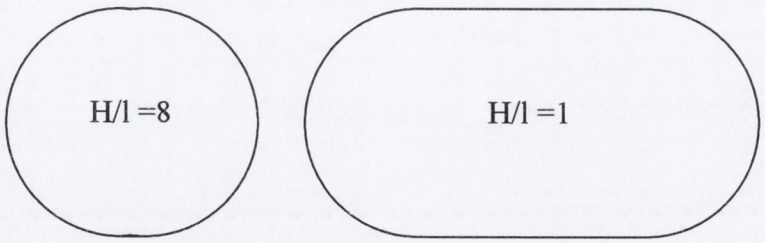

Figure 5.12: Workpieces at different levels of H/l.

An interesting observation, based on an examination of the contact forces, was the identification of the possible development of a kneading effect during rolling.

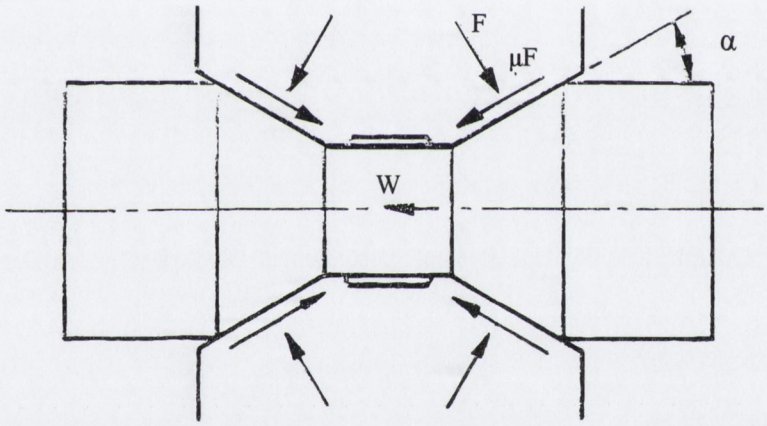

Figure 5.13: Simplified contact forces between tool and workpiece [46]

By balancing the workpiece forces illustrated in Figure 5.13 Thompson and Hawkyard determined the force in the central portion of the workpiece, W, to be:

$$W = F.Sin\alpha - \mu.F.\cos\beta \qquad (5.10)$$

Therefore, for certain combinations of friction and sidewall angle, it is possible that material could be forced into the central region resulting in a kneading effect in which the trapped material is repeatedly compressed and stretched. They felt this could contribute to the development of internal failure. However the difference between rolling subject to this 'kneading effect' and regular rolling, in which the gradual diameter reduction of the workpiece subjects it to these fluctuating forces, was not explained.

In 2002 Li et al [23] developed a theory for the development and growth of internal voids in form rolling, which they categorise as an example of the Mannesmann effect. This is the weakening of the central part of the workpiece due to its rotation and diameter reduction and it results in the formation of axial voids. They theorise that low cycle fatigue may also be a factor in the development of internal voids; due to cyclic loading of the workpiece in compression (perpendicular to the die face) and tension (parallel to the die face) as it rotates. Parts that develop large voids have already developed small inclusions by the end of the knifing zone. Axial deformation in the stretching zone then opens up these inclusions. Tensile and shear stresses can also lead to the coalescence of voids.

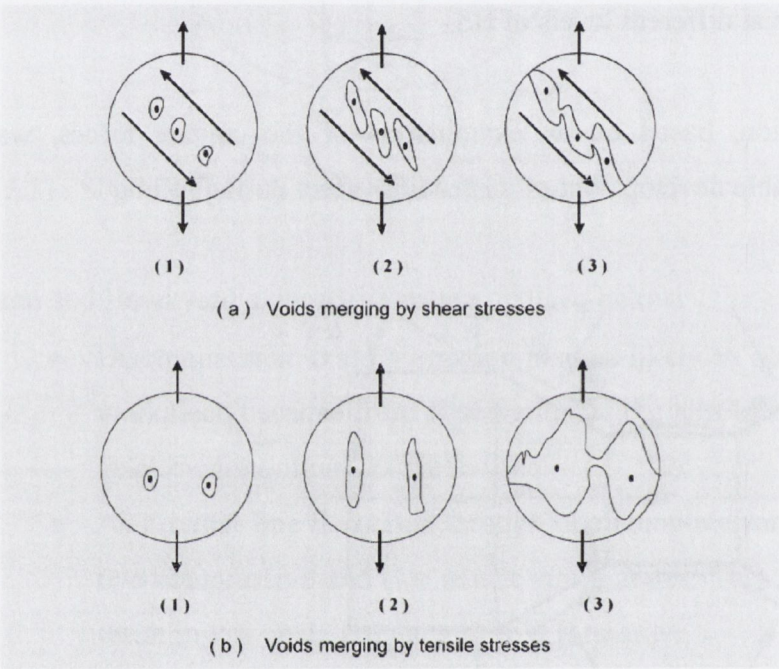

Figure 5.14: Void development [23]

In Figure 5.14(a), the growth mechanism is due to shear stresses which are at 45^0 to the tensile stress direction. The voids are thus turned to this direction and elongated until they merge creating larger voids.

In Figure 5.14(b), the voids are elongated due to tensile stresses and when the distance between two voids becomes comparable to their lengths, they can merge through micro-scale necking.

The authors surmise that "large tensile stresses initiate the opening of voids and local shear determines the level of aggregation and the size of the voids in the workpiece".

In specimens at the end of the knifing zone, the authors noticed the presence of small voids in the path of the large void's 'crack' tips (see Figure 5.15(a)) this indicates

that void initiation is the result of hydrostatic tension within the central region of the workpiece. Fully rolled specimens lacked these smaller voids indicating they had merged to form one large void. When longitudinal and transverse cross sections of the workpiece are examined, the non uniformity of the voids is evident, see Figure 5.15(b, c).

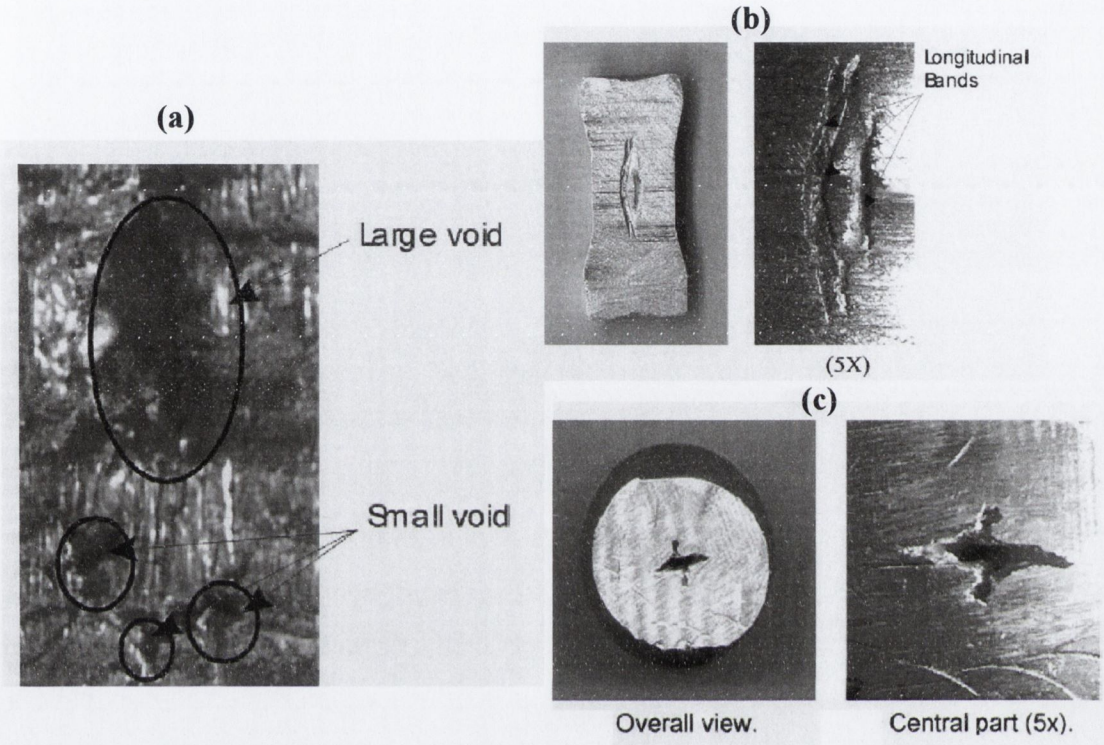

Figure 5.15: Failures within a form rolled part [23]

The cruciform shape of the failure evident in the transverse section of the workpiece shown in Figure 5.15(c) is a result of the maximum and second principal stresses being tensile. The major crack A opens in a direction normal to the maximum principal stress while the minor crack B opens in a direction normal to the second principal stress, see Figure 5.16.

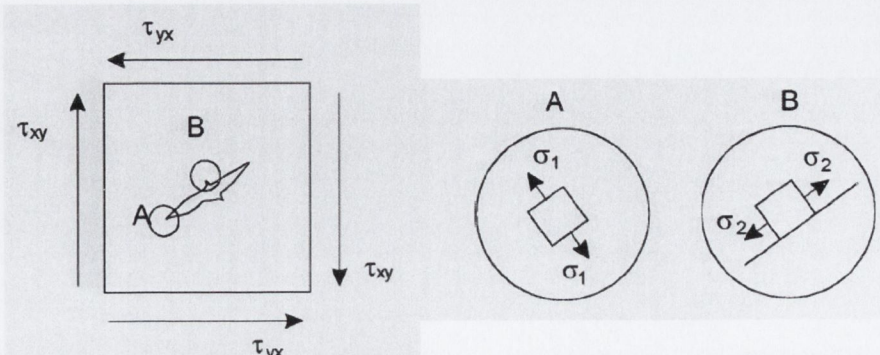

Figure 5.16: Internal stresses generated in a workpiece during form rolling [23]

5.1.4 **Lap Formation during the Form Rolling process**

The literature discusses two different types of lap formation. The lap formations observed depend on the type of die geometry used. If a spreading zone is present on the rolling die then helical laps are created on the workpiece. A die with a wide flat creates axial laps on the workpiece. These two different lap types will now be discussed in greater detail:

Axial Laps: Tsuchikawa et al [47] produced a rather unique paper in which the effects that the rolling process had on the surface of a rolled part were examined. The authors observed a variety of surface fracture/roughening modes depending on both the workpiece material and the rolling conditions. The rolling process they used was different to that used by other researchers in three regards: firstly as illustrated in Figure 5.17 the tooling they used had a sidewall angle of 90^0, whereas most other researchers used angles of approximately 45^0; secondly they were performing rolling as a cold-forming process, while most other researchers considered the process as hot rolling; and thirdly the rolling machine they used differed to those used by other researchers. The Toyoda form rolling machine they used is most similar to a traditional two roll machine and instead of having dies that have a knifing zone which increases the depth of penetration, the dies have a constant feature depth and penetration into the workpiece is controlled by reducing the gap between the dies, see Figure 5.17.

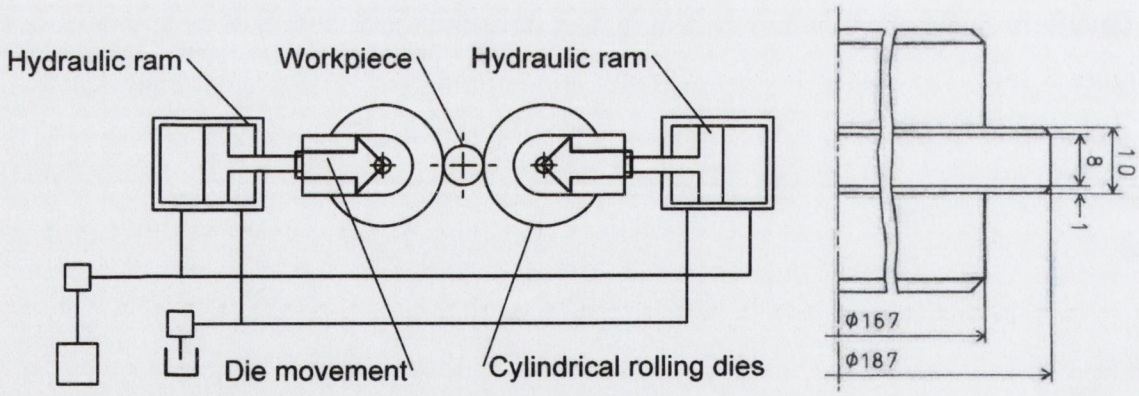

Figure 5.17: Schematic of Toyoda form rolling machine and die [47]

As regards steels two different types of surface roughening were observed:

1. Small 'fish-skin' roughening is the formation of fish scale like creases on the workpiece surface which come off as fine flakes, see Figure 5.18. This feature has very

small dimensions and is likely to be associated with the inhomogeneity of the workpiece (i.e. the plastic anisotropy of individual grains). As the workpiece is deformed, 'irregular corrugation' is expected to develop in the waveform due to anisotropy of the grains. As these corrugations are flattened out during rolling, they result in the formation of the small fish-skin. The problem becomes more pronounced with increased forming rate, diameter reduction and grain size.

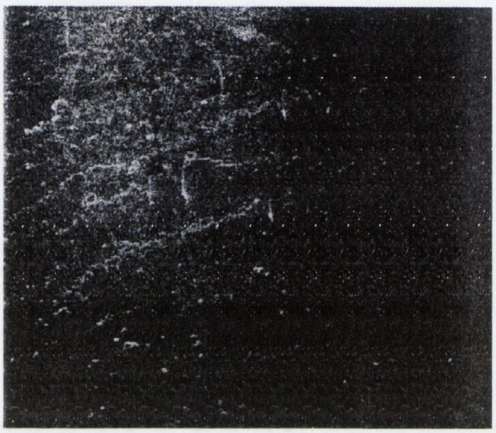

Figure 5.18: Small 'fish-skin' or axial lap on a form rolled part[47]

It is suspected that small fish-skin roughening becomes more pronounced as the part size is miniaturised, due to the increasing ratio of grain size/workpiece diameter.

2. Large fish –skin roughening (i.e. laps) is the formation of creases in the axial direction across the entire groove width, see Figure 5.19.

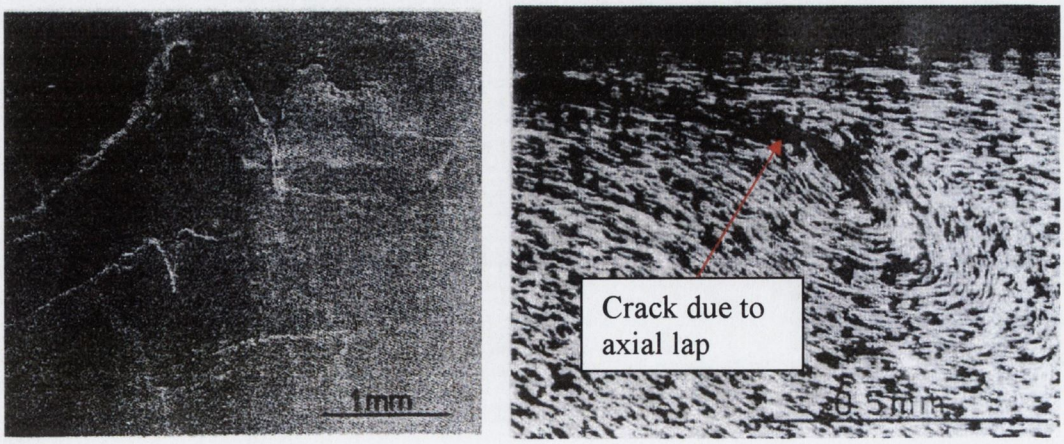

Figure 5.19: Large 'fish-skin' or axial lap and associated surface crack on a form rolled part [47]

Large fish skin roughening results from the folding over of material in the waveform found between the die and the workpiece. It appears suddenly in the workpiece once a threshold diameter reduction has been passed and quickly reaches its maximum scale. The forming limit of the workpiece in regard to the formation of these large fish skins increases with increased forming rates. The large fish-skin is considered to be the more important of surface roughening types as regards workpiece quality because it is visible with the human eye and it leaves large cracks in the workpiece surface, see Figure 5.19.

The aluminium alloy they tested developed small fish-scale roughening that grew with continued rolling to a scale that was visible to the eye. Brass suffered from a different and more extreme type of roughening in which a thick portion of the surface separated from the workpiece due to a fracture induced by shear stresses near the surface of the workpiece. As for the steel samples the forming limit increased for both brass and aluminium with increased forming rates.

Helical laps: As discussed in a paper by Fu and Dean [13], several authors have observed helical laps and they are a result of the increasing flat width in the spreading zone of the die folding workpiece material back into the groove as shown in Figure 5.20.

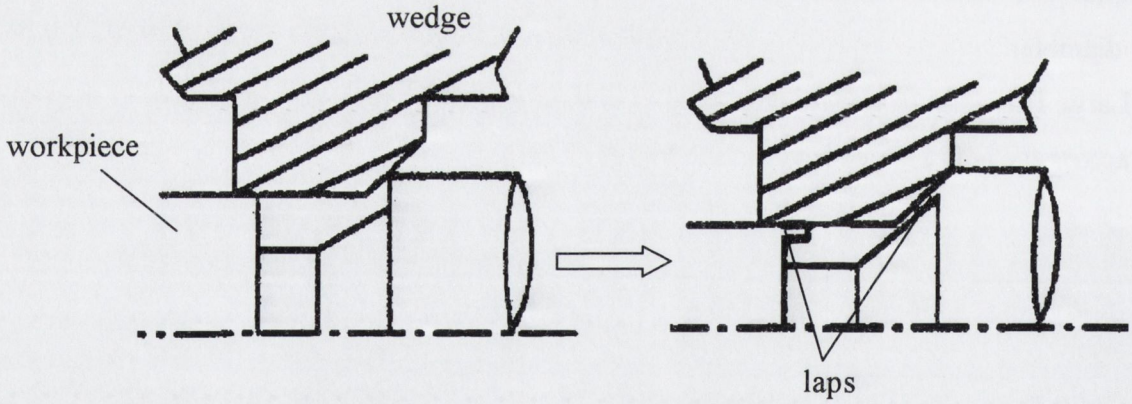

Figure 5.20: The creation of helical laps as workpiece material is enfolded into the groove [13]

More evidence of the creation of helical laps by the folding of material into the workpiece groove was discovered by Eyres [32] using the FEA package DEFORM 3D. By examining the workpiece velocity using vector plots, he clearly observed that some workpiece material was flowing back into the groove as shown in Figure 5.21.

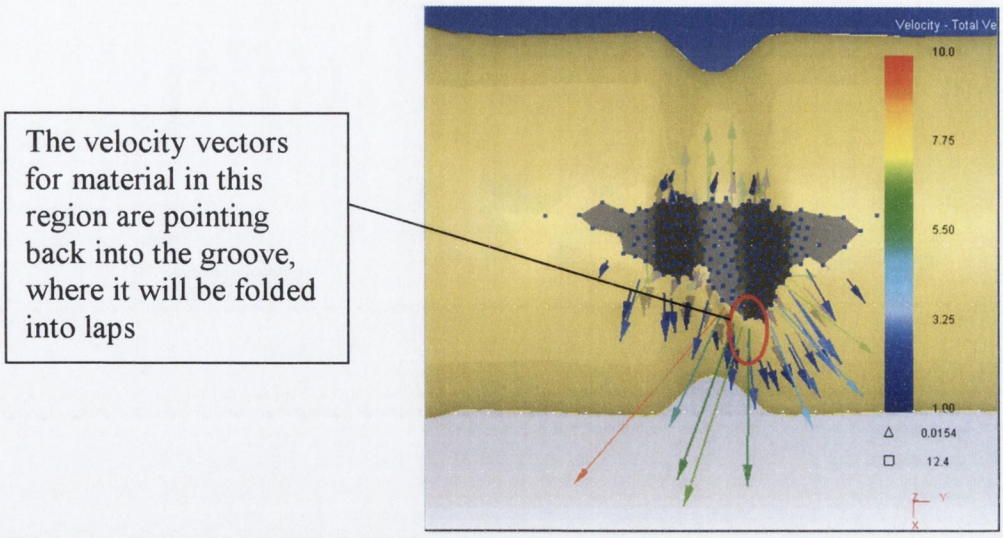

Figure 5.21: Velocity vector plot illustrating the flow of workpiece material into the groove which creates helical laps [32]

Eyres also observed laps in the axial cross section of a form rolled part see Figure 5.22. The number of laps on the workpiece is equal to twice the number of rotations experienced by the workpiece in the spreading zone as a lap is created on each die/workpiece contact. The distance between each of the laps is equal to the increase in the groove width during one rotation of the workpiece, which is a function of the workpiece circumference and the spreading angle of the die.

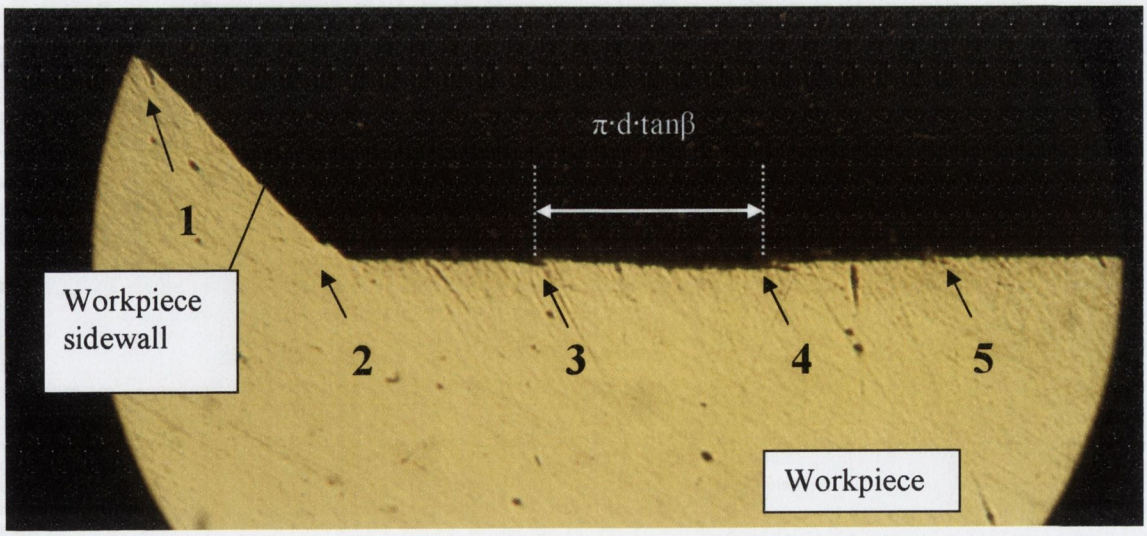

Figure 5.22: A series of laps evident in the cross section of a workpiece: (x100) [32]

The laps described above are termed helical laps as they create a helical pattern on the workpiece surface, see Figure 5.23.

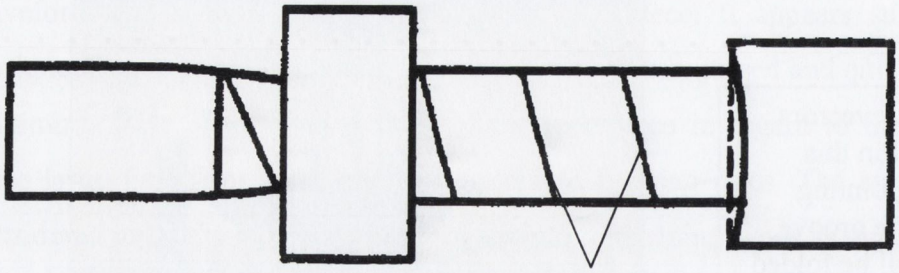

Figure 5.23: Diagram of helical laps on a form rolled part [13]

5.1.5 **Tool Design**

Dies may only represent a small cost relative to that of the form rolling machine, however, they are crucial in determining the quality of parts produced and the lead time required for part production. The effectiveness of the die design and the process used in their manufacture affects the entire form rolling process. Die tryout is still an important and expensive factor, especially in the form rolling industry for which die setup is notoriously difficult. Form rolling dies often need to be modified or redesigned after initial testing. With these issues in mind having the basis for a good initial die deign is critically important.

There have been a number of investigations of the form rolling process to determine pertinent die parameters for the manufacture of defect free parts; the main die parameters examined in these investigations have been the spreading angle, β and the sidewall angle, α. The recommended values for these parameters and methods for determining them are discussed below.

In 1979, Thompson and Hawkyard [46] recommended values of α of between 25° and 40°, while recommending an angle of around 10° for β.

In 1984, Ishii *et al* [48] recommended angles of between 5° and 8° for β while advising for angles between 20 and 30 ° for α.

To prevent necking at the core of the billet and to limit excessive twisting Fu and Dean [13] suggested that the relationship between α and β should be as follows:

$$\tan\alpha \cdot \tan\beta \leq 0.08 \qquad (5.11)$$

To prevent inner cracks occurring in the billet, Koizumi *et al* [13] suggested that the relationship between α and β should be as follows:

$$0.04 \leq \tan\alpha \cdot \tan\beta \qquad (5.12)$$

Later, in 1979, Hayama [13] developed the following relationship to prevent internal defects:

$$1.93\beta^{-.925} \geq 0.15+.0038\alpha \geq M\cdot\beta^{-.325} \tag{5.13}$$

Where M is a constant material parameter between 0.35 and 0.4 and α and β are expressed in degrees.

Summing up, according to literature, to form roll defect free parts, β should be in the region of 5° and α should be in the region of 30° and the following relationship should be followed:

$$0.04 \leq \tan\alpha\cdot\tan\beta \leq 0.08 \tag{5.14}$$

Pater et al [22] published a paper in 1999 in which they summarised the formula found in the literature relating to tool design that would lead to a stable process. They also added several formula of their own, and these are presented below.

Andrejew et al [22] determined a limiting condition for the possible occurrence of laps in form rolled parts as follows:

$$\delta \geq 1+\pi\tan\alpha\cdot\tan\beta \tag{5.15}$$

To prevent necking the following formula devised by Tsukamoto et al and Hayama [22] should be used

$$\frac{\sqrt{2\tan\alpha\tan\beta}}{\pi}\left(1+\sqrt{\frac{1}{\delta}}\right)(\delta-1)\leq 0.2 \tag{5.16}$$

$$\delta \leq \frac{1}{2}\left(2+\pi\tan\alpha\tan\beta+\frac{\sqrt{\frac{3\pi}{2\tan^3\alpha\tan\beta}}}{\xi}\right) \tag{5.17}$$

where ξ is the load coefficient

While these formulae remove a certain amount of doubt from the design of form rolling tooling, their suitability for application on a micro-form rolling process has yet to be tested. The scope of the formulae is also quite limited as they are only applicable to the form rolling of grooves; however, other features are often required on form rolled parts such as radiused or pointed ends. The formulae also require the forming of a draft on the rolled groove which is not always desirable and adds to the lack of versatility of the formulae. It is intended that the design methodology resulting from this research will be versatile enough to design form rolling tooling for a greater variety of workpiece features, and will, therefore, contribute to the optimisation of the tool design process.

A major problem associated with the die angles recommended in the literature is that they vary greatly from author to author which indicates that the angles they determined were specific to the material, scale, and even machine that they used. A table of recommended angles is given below.

Author	Material	Rolling Machine	Hot/Cold Forming	Spreading angle, β	Sidewall angle, α	Max area reduction
Guifu et al [49]	steel	3 Roll	Hot	Max 19°42`	Max 22°	30-50%
Ishii et al [48]	steel	2 Roll	Hot	5-8°	20-30°	75%
Mockel et al [50]	steel	Flat	Hot	5-15°	15-45°	n/a
Thompson [46]	steel	n/a	Hot	10°	25-40°	50%
Koizumi et al [13]	n/a	n/a	n/a	5-12°	n/a	n/a
Kusiak et al [51]	steel	n/a	n/a	3-15°	15-45°	n/a
Tsukamoto [52]	steel	2 Roll	Hot	5-8°	20-30°	n/a
Holub [15]	n/a	n/a	Hot	5-30°	15-30°	n/a

Table 5.3: Variation of recommended rolling angles

Other points on tool design

Shoulder radius - The effect of the shoulder radius on the quality of the rolled part was investigated by Glab et al [53].

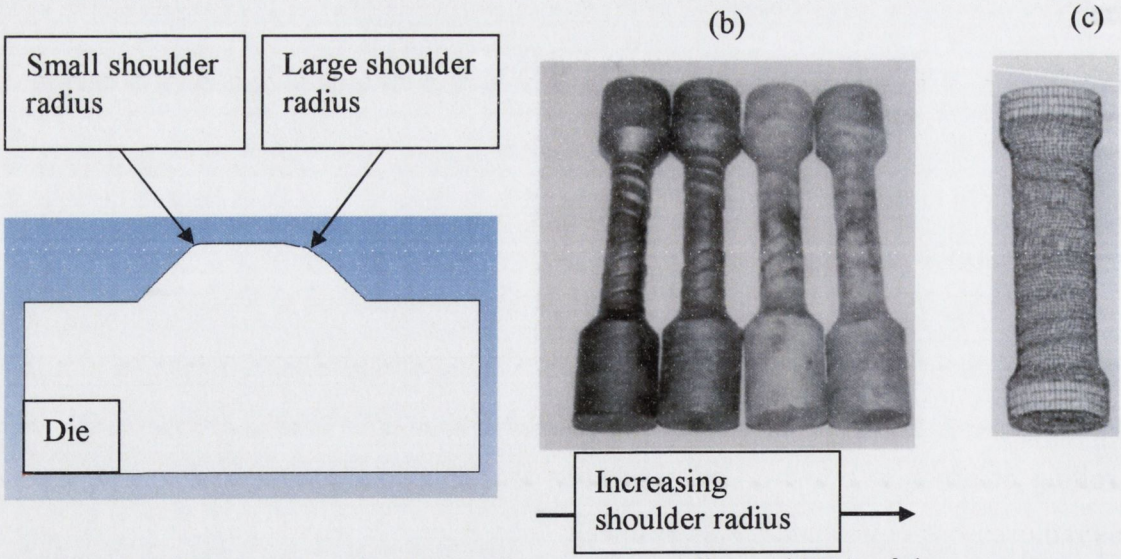

Figure 5.24: Effect of the shoulder radius on part quality and FEA of the process

The shoulder radius is between the sidewall and the die flat. Increasing the shoulder angle improves the surface quality of the rolled part, by reducing the magnitude of the helical laps. However, it reduces the effective sidewall angle.

As large a radius as possible should be put on all corners of rolled grooves [54]. However the application of relatively small corner radii on micro-form rolling dies is obviously much more difficult and in many cases simply not feasible.

Rolling two parts from one blank- To balance the axial forces when rolling asymmetrical parts, two parts can be rolled simultaneously using a single blank as illustrated in Figure 5.25 below [55].

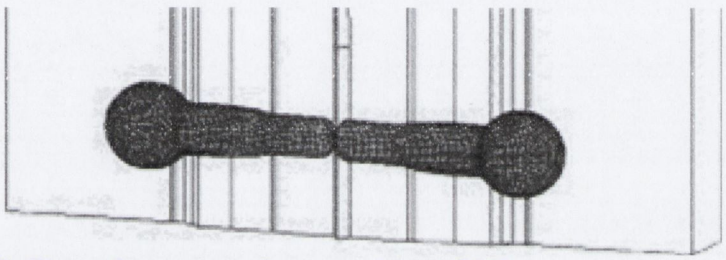

Figure 5.25: Rolling of two parts from one blank [55]

Double Rolling- If all the features on a part cannot be formed in one stroke then the part can be rolled twice to achieve the necessary features [4, 24].

Simultaneous versus Progressive Rolling- In simultaneous rolling several grooves are formed onto the part at the same time. However, if the grooves are of differing depths, then they must be formed one at a time to prevent the twisting and slippage that would occur due the differing workpiece radii and, therefore, peripheral velocities. The die is designed so that that as one groove is being completed the next groove begins.

Also, if a deep or wide groove is being formed it must be formed independently of any other features because the material from the groove will be displaced axially resulting in an elongation of the part and this material must be accommodated before other features can be applied [4].

In 2006, Pater et al [56] published a paper in which the benefits of using only one wedge die were espoused. The authors developed a modified version of the flat die rolling technique in which one of the wedge tools was replaced with a pair of shaped rollers and they dubbed the process the Wedge-Rolls Rolling method (WRR). This WRR process is illustrated in Figure 5.26. The need for only one wedge tool has savings associated with both machining and raw material costs. In the case of micro-form rolling the raw material

savings may not be substantial due to the small size of the dies however micro-tooling requires very precise machining on which substantial savings can be made if only one tool is required.

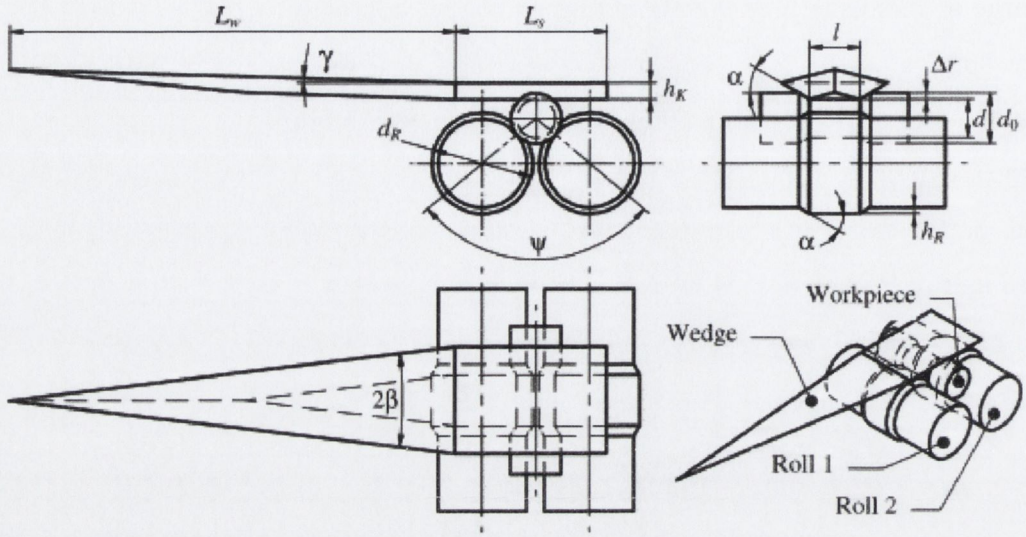

Figure 5.26: Schematic of Wedge Rolls Rolling [56]

If a technique requiring only one wedge tool could be developed for micro-form rolling it would create a more economically attractive process and result in its more widespread uptake. The one-die rolling process which used only one wedge tool is described in Chapter 3.

5.2 The Forming and Machining of Micro-Parts

This section details unique aspects of micro-manufacture that differentiate it from manufacturing at larger scales. Micro-milling and micro-forming manufacturing processes were used during this research and they were both subject to the effects of miniaturisation. In micro-forming, both the strength of the workpiece and the magnitude of interfacial friction are dependent on the diameter of the workpiece. Micro-machining is subject to different miniaturisation effects due to the decreased stiffness and sharpness of the miniaturised cutting tool.

5.2.1 The 'Size Effect' in Micro-Forming

Several attempts have been made to explain the differences associated with forming at a micro-scale and at larger scales. These differences centre around the so called 'size effects'. The size effect relates to the observation that as a materials size is reduced its

mechanical behaviour also changes, an example of this effect is illustrated in Figure 5.27 where the variation of flow stress with specimen size is clearly visible. In the figure λ represents the scaling factor used in the experiments, therefore, the diameter = 4.8mm x λ, so the test pieces range in diameter from 0.48 to 4.8mm.

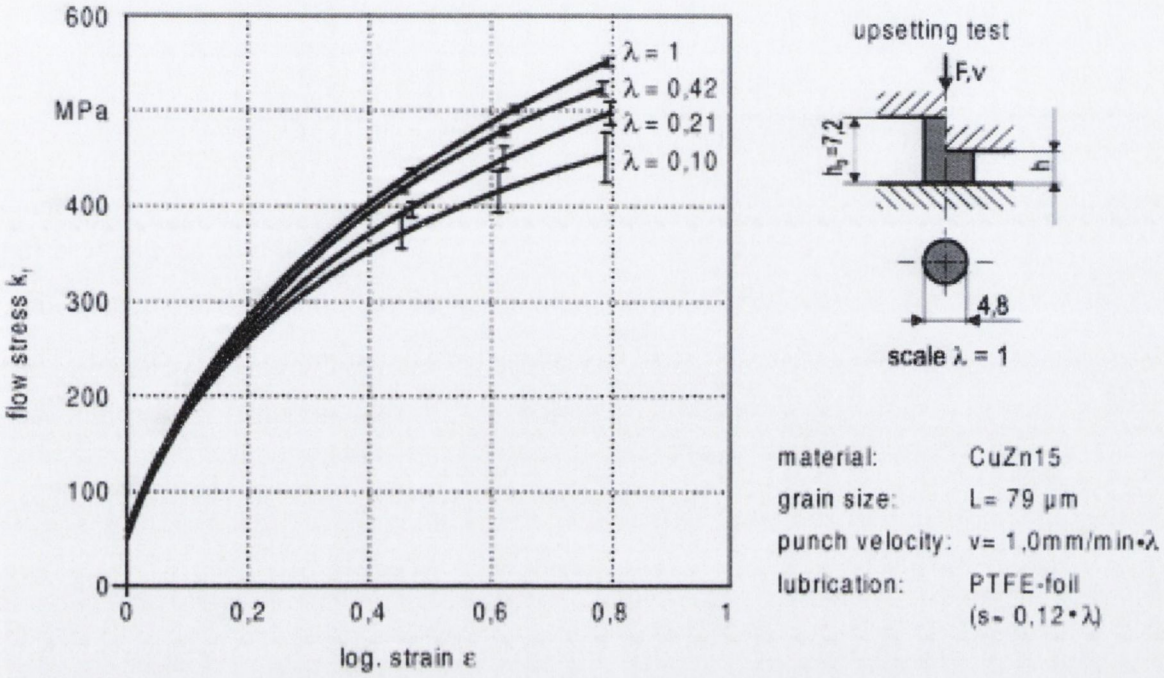

Figure 5.27: Graph showing varying material flow stress with test specimen size [10]

As early as 1961 Armstrong [57] observed that the size of a specimen could affect its strength (i.e. that for a given grain size a smaller specimen tended to exhibit a lower flow stress) he termed this the 'specimen size' effect. He also noted that this effect was most pronounced when there was only a relatively small number of grains across the specimen thickness, his chosen number being twenty. He suggested that the 'size effect' was due to the orientation dependence of crystal plastic flow and, therefore, dependent on grain orientation. He noted that the effect was independent of grain size, and that if the number of grains and the grain orientation was kept constant for various specimen sizes, the flow stress also remained constant.

In 1979, Miyazaki *et al* [12, 58] identified a change in the physical properties of a material with a change in size of the specimen tested. The authors determined through tensile tests, on specimens ranging from 0.13 to 2mm in diameter, that a material's flow stress was not only related to its grain size, but was also affected by the specimen's diameter. Therefore, the flow stress is dependent on the ratio of D/d, where D is the diameter of the specimen and d is the size of an average grain. Decreasing the D/d ratio, by

decreasing D or increasing d, results in a decrease in the flow stress of a material. The effect of d on the flow stress can be explained by the well known Hall-Petch equation:

$$\sigma_y = \sigma_0 + \frac{k}{\sqrt{d_{grain}}} \tag{5.18}$$

Where σ_y = yield strength

d_{grain} = the mean grain size

k and σ_0 are constants

The result of this effect can be seen in Figure 5.28 which shows an increase in material strength with decreasing grain size. The shape of the curve to the right of the critical grain size d_c, follows the form of the Hall-Petch equation as stated above. The critical grain size is the grain size that gives the highest material strength, at this point the grain size is comparable to the distance between dislocations.

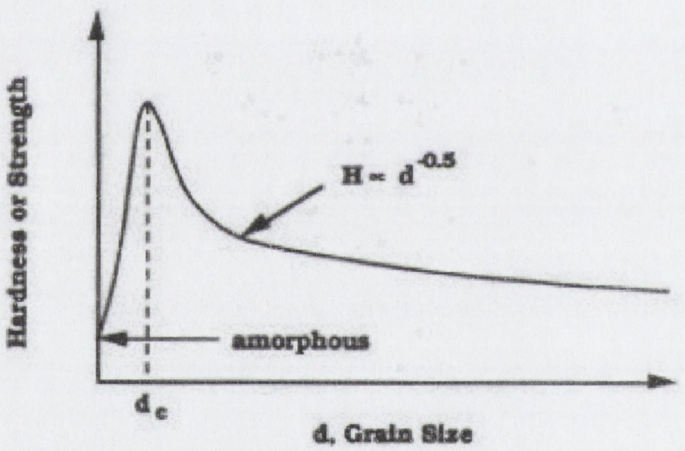

Figure 5.28: Graph demonstrating the Hall-Petch effect [59]

The increase in flow stress with decreasing grain size predicted by the Hall-Petch equation is a result of the increasing area of grain boundaries in the specimen which act as restrictions to the movement of dislocations, thus increasing the flow stress.

However, the effect of varying D on the flow stress requires a different explanation, the authors concluded that the effect of changing the specimen diameter, D on the flow stress was a result of the change in the volume fraction of grains in the surface region of the specimen. The surface grains require less force to deform because they are less constrained to deformation compared to the internal grains which are surrounded and constrained by other grains.

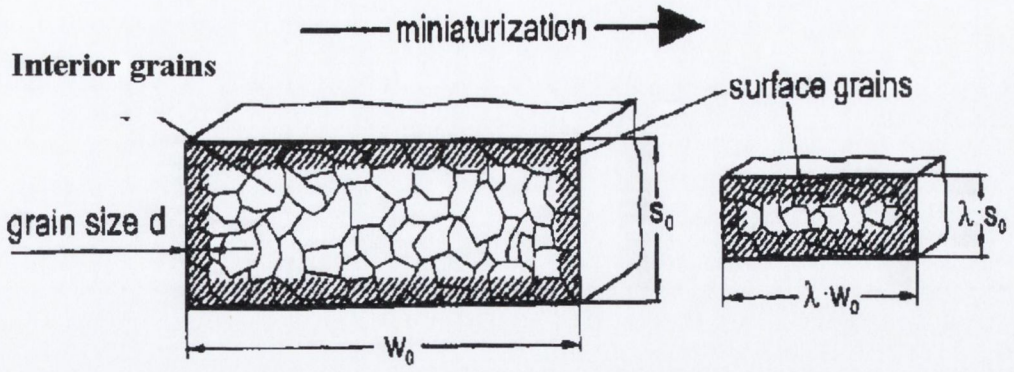

Figure 5.29: Increasing proportion of surface grains with miniaturisation [9]

The authors also determined the critical values of D/d at which the size effect became apparent for a particular grain size; this was also determined for plate specimens resulting in values of T/d, where T is the plate thickness. The critical ratio of T/d was typically half that of the critical ratio of D/d, which supports the authors volume fraction theory because, for a given volume, a plate will have a greater volume of surface grains than a rod, meaning a plate is more susceptible to the size effect. The effect they measured was large with a difference in flow stress of over $100MN/m^2$ (300 versus $200MN/ m^2$) being measured at larger strains.

In 1994, Geiger *et al* [5] published a paper which again pointed to the magnitude of the 'size effect' being determined by the volume fraction of surface grains in a specimen, stating that the dislocation movement in free surface grains is less constrained than it is in internal grains. The results by these authors indicated that the 'size effect' could have a major effect on material properties. In one example, they showed that a material's flow stress was halved by reducing the specimen size from 2 to 0.5mm.

Over the following years, Geiger et al published various papers detailing their expanding understanding of the size effect. For example, in 1995 [60], they published a paper indicating that the power law that defines the relationship of flow stress at constant temperature to the strain rate holds for smaller specimens. In the same paper, they also devised a helpful description of the size effect problem, they stated that "the size effect can roughly be characterised by the relation of macro geometry of the billet to microstructure, surface topography and state of lubrication in the tool-workpiece interface."

In 1997 [9] they proposed a method of determining the flow stress of a given material. This method requires the proportion of internal and surface grains to be

determined, this can be done using the average gain size. The internal grains are assumed to have the flow stress of the polycrystalline material, while the surface grains are assumed to have the flow stress of a single crystal material, which has a lower flow stress than a polycrystalline material. The flow stress for this composite is then modelled as:

$$\sigma_f \approx \alpha_i * \sigma_{f,i} + \alpha_{FS} * \sigma_{f,FS} \tag{5.19}$$

Where: σ_f = flow stress of the micro-scale material

α_i = proportion of internal grains

α_{FS} = proportion of surface grains

$\sigma_{f,i}$ = flow stress of internal grains (poly-crystals)

$\sigma_{f,FS}$ = flow stress of free surface grains (single crystals)

Teisler *et al* [61], members of the same research group, discussed the application of similarity theory to the field of micro-forming. Similarity theory is used to model a process at a different scale than the one at which it actually occurs.

To minimise the size effect, a large D/d ratio should be used and because the workpiece diameters used in this research are small, a fine grained workpiece was required. Below a D/d ratio of twenty, the size effect is observable. The minimum workpiece diameter used in this research was 0.45mm, therefore, to achieve a ratio of over twenty a grain diameter of less than 0.0225mm was required. The material used in the research for this thesis had a grain diameter of 0.005mm and therefore the workpieces had a D/d ratio sufficiently large to prevent the size effect.

The effect of miniaturisation on the friction coefficient has also been examined. It has been observed to increase when performing lubricated micro-forming, but remain unchanged when performing unlubricated micro-forming compared to forming at larger scales [10, 61]. Because traction between the workpiece and the dies is essential to rotate the workpiece in form rolling, it is an unlubricated forming process and, therefore, no change in the friction factor is expected with miniaturisation. The decreasing friction coefficient with miniaturisation when lubrication is used can be explained in terms of closed and open lubricant pockets. Lubricant pockets are cavities on the boundary between the die and the workpiece that trap lubricant and thereby decrease the coefficient of friction. However if these cavities are located on the edge of a workpiece they will be unable to trap lubricant and are termed open lubricant pockets. The size of the lubricant pockets is independent of the size of the workpiece and, therefore, with miniaturisation an

increasing proportion of the lubricant pockets will be open pockets, as shown in Figure 5.30. As the proportion of open pockets increases so does the friction coefficient.

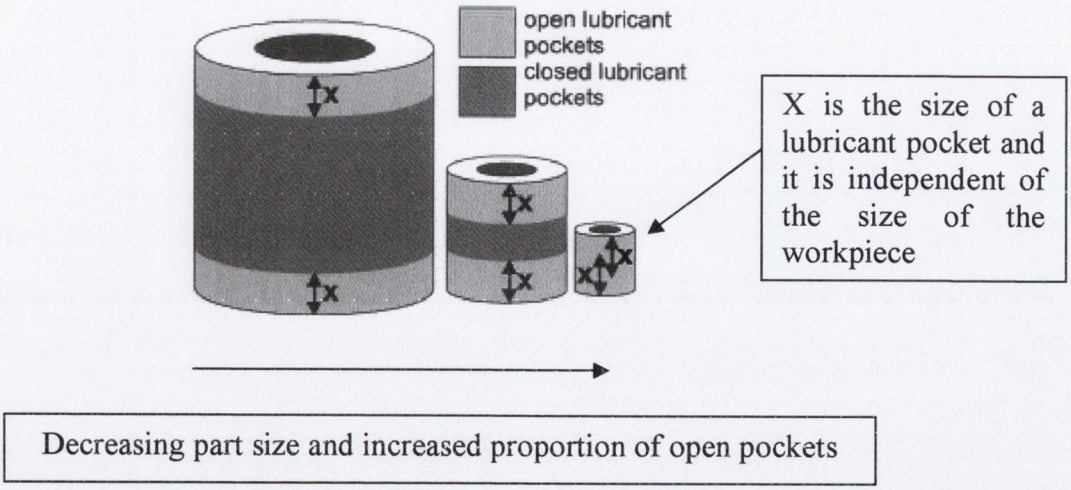

Figure 5.30: Increasing proportion of open lubricant pockets with miniaturisation which increases the friction coefficient [10]

All the research on the size effect discussed above deals with workpieces that have very large free surfaces which are not in contact with a die. As discussed earlier, these grains are less constrained when being deformed compared to internal grains and, therefore, have a lower yield stress. In forming processes with large free surfaces, there is a decrease in process forces with miniaturisation. However when the workpiece is deformed in the form rolling process it is in contact with the die surface and the grains are therefore more constrained. Micro extrusion is a process in which the surface grains are constrained, and research on the process has shown an increase in the process load with miniaturisation [7]. The increasing load with miniaturisation is due to the increasing friction coefficient as extrusion is a lubricated process.

5.2.2 The Size Effect in the Machining of Micro-Forming Tooling

The dies required for micro-form rolling required the machining of micro-scaled geometries onto their surface: Bissacco [62] noted several 'size-effects' associated with this micro-milling:

1. The material removal geometry changes with miniaturisation. There is a minimum cutting edge radius of 1-4μm that can be produced on a cutting tool. This is independent of the diameter of the cutting tool, therefore, relative blunting of cutting edge occurs with miniaturisation, see Figure 5.31.

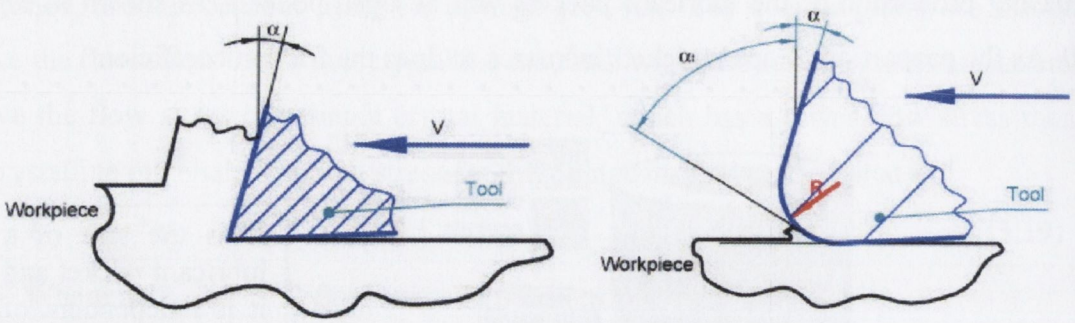

Figure 5.31: Blunting of cutting edge radius with miniaturisation of an end mill cutter [62]

The relative bluntness of the cutting edge radius results in an increase in the cutting forces and, if the ratio of cutting edge radius to chip thickness exceeds a critical value, a ploughing action is expected to dominate. This problem tends to worsen with tool wear as the bluntness of the tool increases.

2. The process is subject to higher tool deflections – because as the process is miniaturised there is a relative increase in the cutting forces and a relative decrease in the stiffness of the tool (due to issues associated with manufacturing the cutting tools, a large proportion of their length has a small diameter)
3. Tool breakage becomes more common for the same reasons that cause increased tool deflection.
4. Tool wear increases
5. Burr formation can lead to major difficulties as their removal becomes more problematic with miniaturisation

A size-effect associated with the tool material arises if the dimensions of the tool and the workpiece are miniaturised but the grain size of the die material remains unchanged. This can result in the forming chip being confined to a single grain compared to macro-milling in which the chip is several grains in thickness. When this occurs, the stresses applied to the tool are dependent on the orientation of individual grains which results in high frequency fluctuation of the cutting forces. This size effect can be minimised by choosing a tool material with high homogeneity, small grain size and well distributed carbides.

The quality of machined dies tends to suffer with miniaturisation because:

- The ploughing action that is associated with micro-milling can result in a series of burr like lines appearing on the workpiece surface that increase the surface roughness, see Figure 5.32.

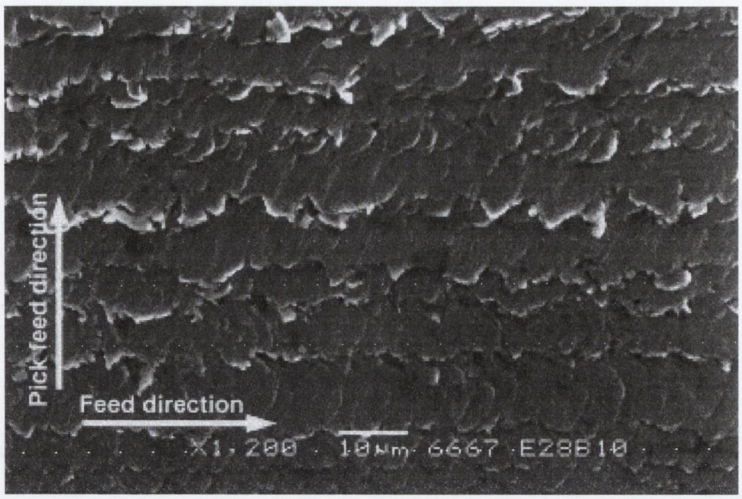

Figure 5.32: Burr like surface of micro-milled component [62]

- Part accuracy in the x and y directions decreases due to increased tool deflections. Accuracy in the z direction is determined by the accuracy with which the milling machine can control the axial depth of cut.
- The ploughing action forces a large amount of material to bulge on free surfaces increasing the relative height of top burrs.

Bissacco recommends decreasing the ratio of cutting edge radius to chip thickness, currently it is not possible to reduce the cutting edge radius so to improve this ratio the feed per tooth must be increased. However, while this improves the surface quality and reduces the burr size, it also results in an increase in tool forces.

5.3 Theory of Similarity

To demonstrate the existence of the size effect, it is necessary to be able to compare the results of experiments performed at different scales. The theory of similarity states that this is possible once the experiments are geometrically scaled. Therefore, the results of scaled experiments should be the same in terms of workpiece deformation, stresses and strains etc. and any differences can be attributed to the miniaturisation of the process and the size effect.

In their paper "Production of micro-parts –size effects in bulk metal forming, similarity theory-", Geiger et al [9] determined that, if thermal effects are ignored, similarity is achievable if the dimensions and the velocities are scaled. Because form rolling is a cold forming process carried out at room temperature, ignoring the thermal effects should be sufficiently accurate.

The constitutive equations relate the stress tensor, σ_{ij}, the stress deviator, σ'_{ij} and the strain rate, $\dot{\varepsilon}_{ij}$ for the micro and the macro scale. They are fixed by the fundamental scales, which are the length scale, λ, the force scale, χ and the time scale, τ. In the constitutive equations below the micro-scale is represented by the subscript m while the macro-scale is represented by the subscript M:

$$\sigma_{ij,m} = \frac{\chi}{\lambda^2}\sigma_{ij,M} \tag{5.20}$$

$$\sigma'_{ij,m} = \frac{\chi}{\lambda^2}\sigma'_{ij,M} \tag{5.21}$$

$$\dot{\varepsilon}_{ij,m} = \frac{1}{\tau}\dot{\varepsilon}_{ij,M} \tag{5.22}$$

Scaled tests can now be designed by assuming that a material's flow stress at the micro and the macro level are the same, $\sigma_{ij,m}$ and $\sigma_{ij,M}$ respectively. Tests will produce results that are scaled versions of each other provided $\sigma_{ij,m}$ and $\sigma_{ij,M}$ are the same, however, if the results differ it will indicate that $\sigma_{ij,m}$ and $\sigma_{ij,M}$ are not the same and that a material size effect is present. From the constitutive equations for $\sigma_{ij,m}$ to equal $\sigma_{ij,M}$ χ must be equal to λ^2 and for $\dot{\varepsilon}_{ij,m}$ to equal $\dot{\varepsilon}_{ij,M}$ τ must equal 1.

For dynamic similarity the velocities, v must also be scaled according to the formula:

$$v_m = \frac{\lambda}{\tau} v_M \tag{5.23}$$

As the time scale, τ has been set as 1 the relationship for the scaling of the velocities reduces to:

$$v_m = \lambda v_M \tag{5.24}$$

For example if the diameter of a part is to be reduced by 50% (i.e. $\lambda = 0.5$) and the process is to be scaled to maintain similarity, then $\chi = \lambda^2 = .25$ and $v_m = 0.5 v_M$.

5.4 The FEA of Form Rolling and Micro-Forming

Several different approaches have been presented in the literature to model the form rolling process. The methods used and the results achieved will be discussed in the following section. The FEA of micro-forming is also quite diverse, with some authors attempting to incorporate the size effect while other authors ignore it, both methods will be covered in the following section.

5.4.1 The Application of FEA in the Analysis of Form Rolling

Some factors associated with the form rolling process make it a difficult process to simulate using FEA [26, 63], the setup of the simulation can require extensive tweaking and the simulation times can be very long. These problems seem to have dissuaded FEA research of the process and, consequently, limited the number of research papers on the topic.

Problems that must be addressed:

1. Due to the complex 3D stress state within the workpiece a 3D simulation is required to fully understand the deformation mechanism. 3D simulations are more complicated than 2D simulations which are sufficient for less complicated processes.
2. A rotating workpiece in a FEA simulation tends to experience a volume loss due to repeated projections of nodes due to tangential velocities. Modelling rotation also tends to increase simulation times.
3. The process involves only localised deformation so a large percentage of the workpiece undergoes no deformation; however, the unformed region still requires a mesh which increases the total number of workpiece elements and consequently the simulation times.
4. The long die stroke length, relative to the workpiece circumference, results in the deformation being carried out over a long die stroke increasing simulation times.
5. There are also problems associated with contact conditions: for the workpiece to rotate, the mesh must be sufficiently dense and the correct values of friction factor and overlap between the workpiece and the die must be used or there will not be sufficient traction to rotate the workpiece.

Thread rolling is a more widespread manufacturing process than form rolling and because they are broadly similar, both being rotary forming processes, it was viewed as an

appropriate starting point for an investigation of form rolling. 2D analysis of the thread rolling process, as a plane strain FEA problem, has been available for some years and this methodology has been applied to form rolling [30, 31, 64]. However, 3D FEA is viewed as being more useful to the analysis of form rolling than 2D FEA, so this section will focus on the 3D FEA of form rolling. In terms of the 3D FEA of form rolling, a number of research groups have modelled the process in recent years.

Fang *et al* [33], in 2002, performed 3D analysis of the two-Roll Cross Wedge Rolling process, using the FEM program DEFORM-3D. Their main aim was to develop an understanding of the mechanics of the process, in order to help explain a common failure mechanism in the form rolling process namely the development of central cracks. They found evidence to help explain the development of such cracks; the fact that the compressive hydrostatic stress, which can help prevent material failure, is lowest at the centre of the workpiece while in the same region there is also a region of tensile stress, which can contribute to crack growth, see Figure 5.33. The authors also monitored the Rolling Wedge Torque (i.e. the torque necessary to drive the rolling die) during the process, and found that it experiences a constant rate of increase during the knifing zone, remains constant during the stretching zone and decreases during the sizing zone.

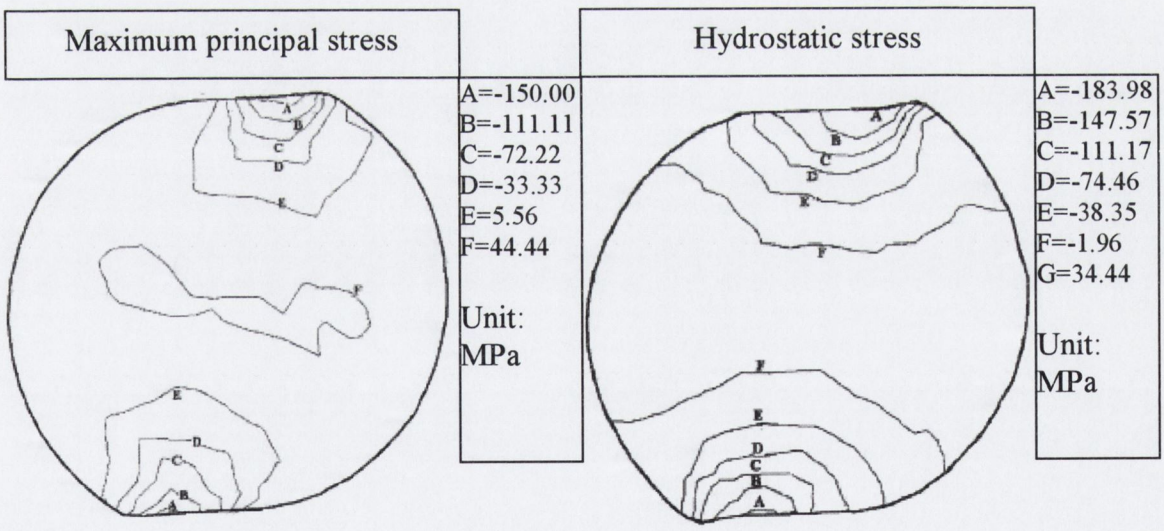

Figure 5.33: Maximum principal and Hydrostatic stress in form rolled workpiece [33]

Researchers as the Fraunhofer-Institut für Werkzeugmaschinen und Umformtechnik IWU, Chemnitz [65] modelled the form rolling process for flat dies using the LS-DYNA3D program. A video of their FE model rolling a groove is available on the referenced website. However, no other information about the process is available.

In 2005 and 2006 Pater et al published papers [55]and [26] in which they used 3D FEA to model the form rolling process. The 2005 paper used the 3D FEA package MSC.SuperForm 2004 to model the form rolling of ball pins. The authors demonstrated that 3D FEA was a suitable means of modelling the form rolling process through a series of Figures that showed the development of workpiece shape and die forces and the stresses and strains within the workpiece.

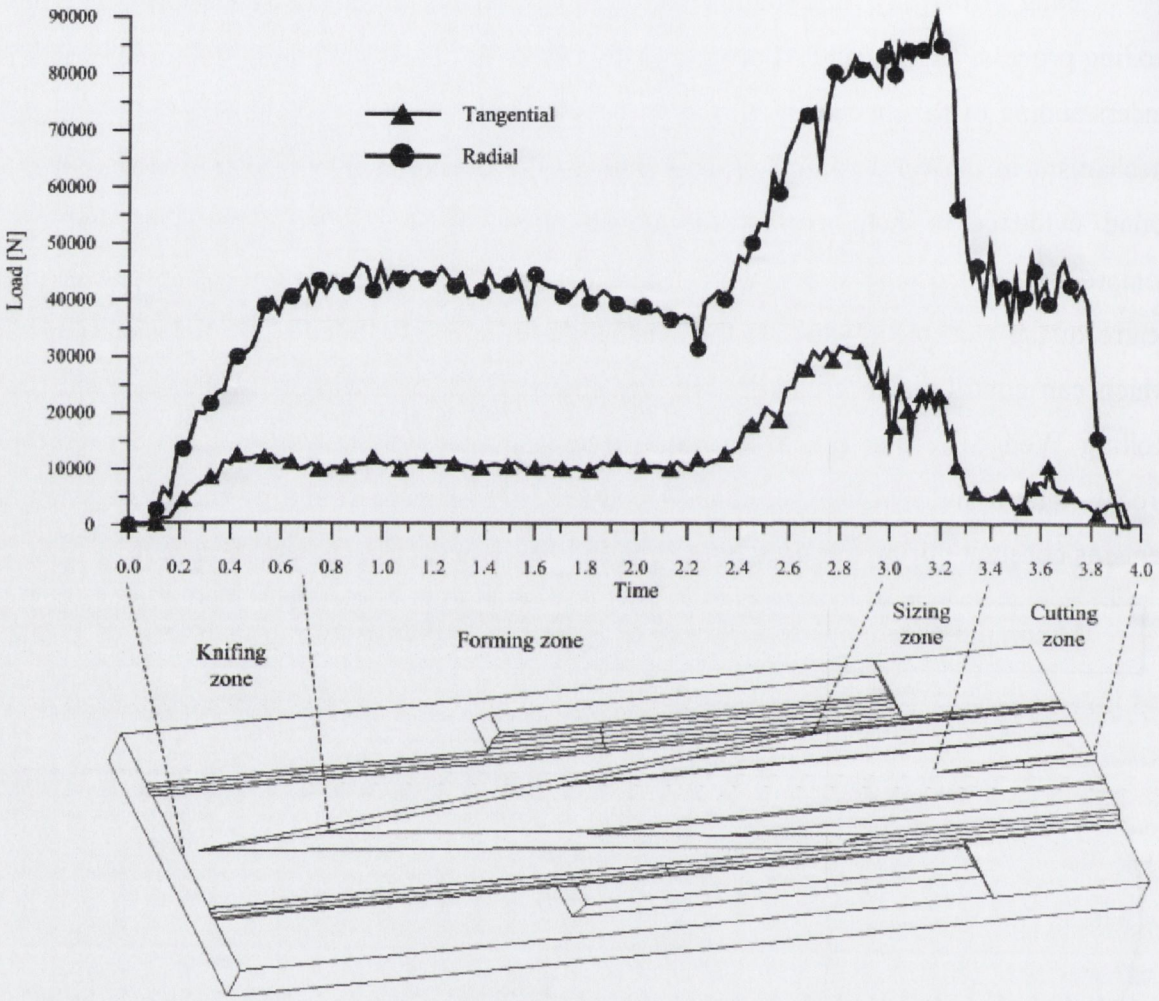

Figure 5.34: Load distribution during form rolling[55]

Figure 5.34 shows the variation of the tangential and radial loads present in a form rolling process. Qualitatively, the changes to both loads are very similar. However, the radial load is significantly larger than the tangential load. Both loads increase in the knifing zone and remain constant during the initial part of the forming zone before they experience another increase due to the interference of guides that restrict the axial flow of the workpiece and form the ball shape of the component, the loads then drop off in the sizing zone. Figure 5.35 shows the development of the workpiece shape during the form rolling

process and demonstrates that it is possible to model the rolling of quite complex geometries using 3D FEA.

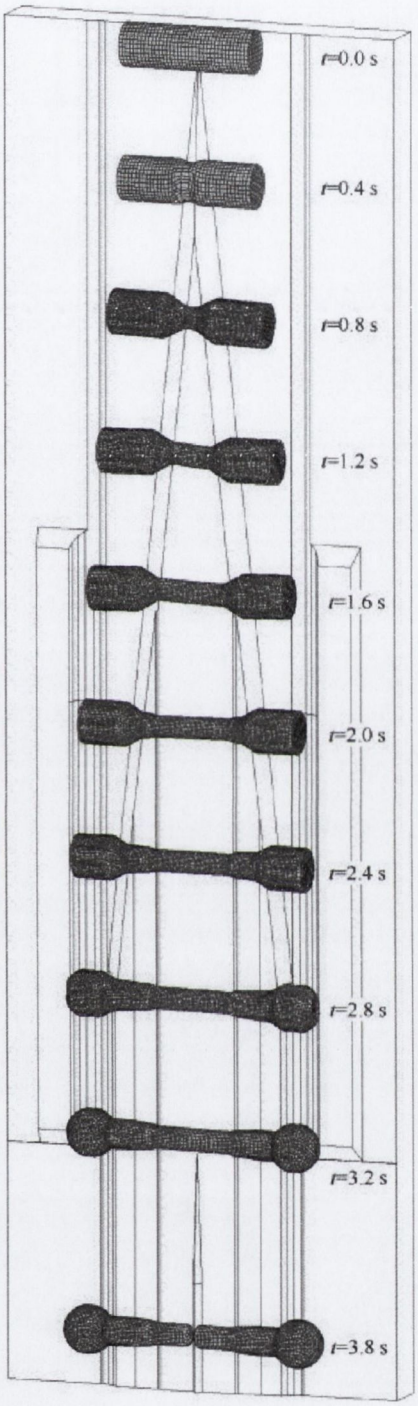

Figure 5.35: Shape development of a workpiece during form rolling [55]

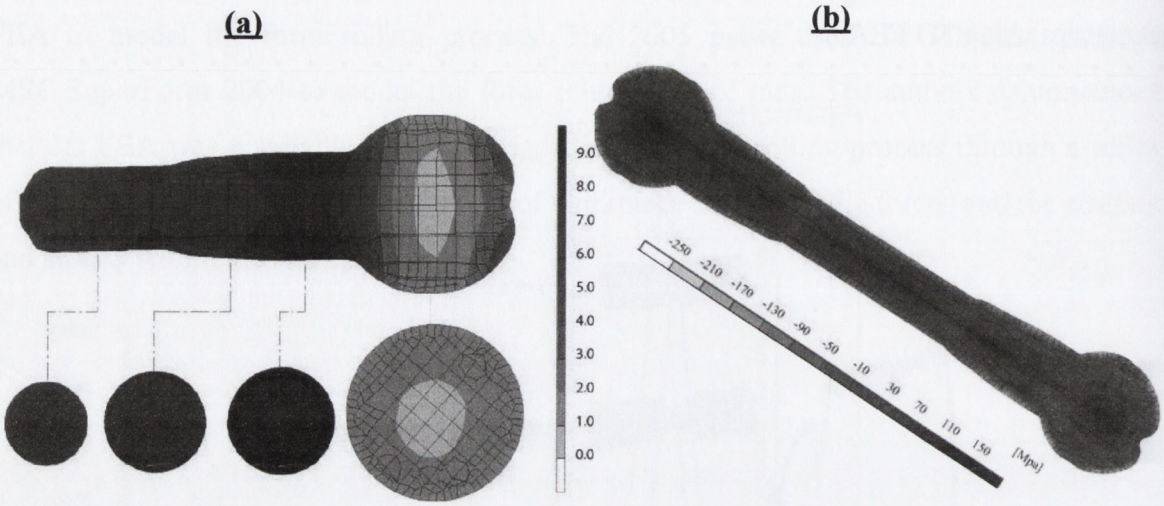

Figure 5.36: Effective strain and mean stress distributions within the form rolled ball pin [55]

Figure 5.36 (a) shows the effective strain distribution within the workpiece, it shows the large strains present in a form rolled part and also the 'laminar distribution of strain' that is typical of such parts, where the strains are distributed in layers that reduce in value towards the centre of the workpiece.

Figure 5.36(b) shows the mean stress distribution within the workpiece. It can be seen that mean stresses with the largest positive values are found along the central axis of the workpiece. As has been mentioned earlier, the likelihood of part failure increases as the value of mean stress increases. The mean stress plot therefore confirms the theory that internal failure during the form rolling process is most likely to occur in the central (medium) layers of the workpiece.

In this paper Pater also recommends using a friction factor, m of 1 for modelling the form rolling process.

In his 2006 paper on the Finite Element Analysis of Cross Wedge Rolling Pater examined the rolling process using 3D FEA to investigate, stress and strain distributions within the workpiece, rolling loads and part failure. The FEA package used was MARC/AutoForge. The FEA results were compared with experimental results obtained through the rolling of lead workpieces. An outline of the forming process, showing the development of workpiece shape can be seen in Figure 5.37.

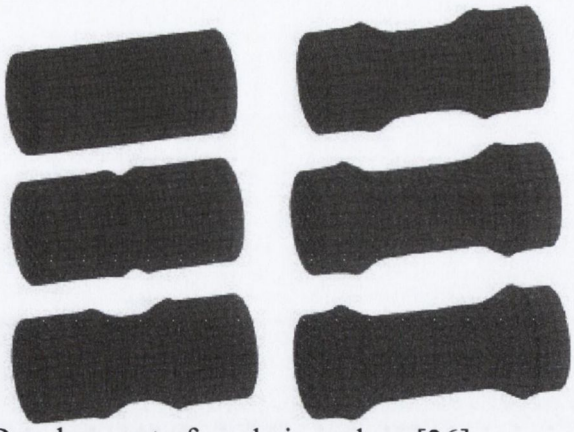

Figure 5.37: Development of workpiece shape[26]

The FEA forces and workpiece rotational velocities were validated by comparison with experimental results see Figure 5.38; there is a close similarity between the two sets of results thereby justifying the authors claim that FEA can be used as a reliable means of modelling a form rolling process.

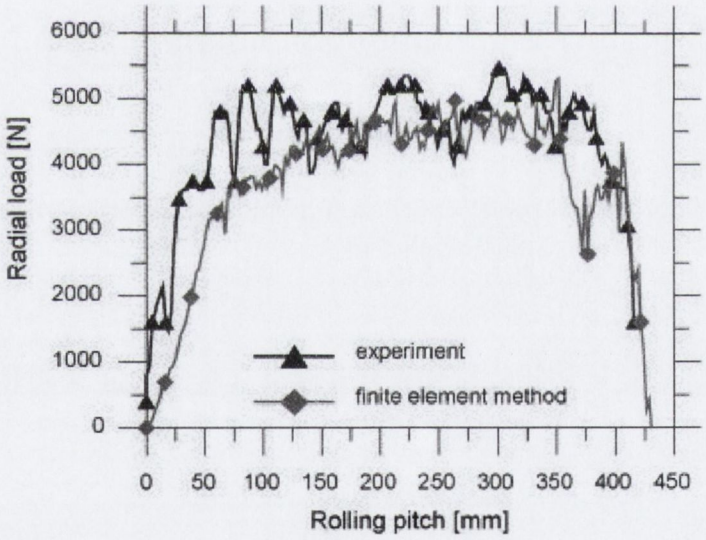

Figure 5.38: Comparison of loads from both experimental and FE analysis of the process $\alpha = 30°$, $\beta = 5°$, $d_0 = 22$ mm, $d = 14$ mm, $m = 1.0$, v=0.1 m/s, billet material—commercial pure lead [26]

As in his 2005 paper [55], Pater observes a laminar strain distribution within the rolled part with the maximum strain values located at the workpiece surface. Examining the hydrostatic stress in the workpiece, Pater observed that the regions of the workpiece that were in contact with the die were under compression, while the free surfaces

experienced tensile stresses and are connected through the central portion of the workpiece.

He also observed that the FEA predicted both necking and slip during the rolling process. Necking was predicted in the workpiece when a die with large sidewall and spreading angles was used to induce large relative reductions, see Figure 5.39(a). Slip is likely with the use of a die having large sidewall and spreading angles, low friction factors and small values of relative reduction. Slip leads to ovalization of the workpiece and the largest strain values are present in the workpiece sidewall where it contacts the die, see Figure 5.39(b).

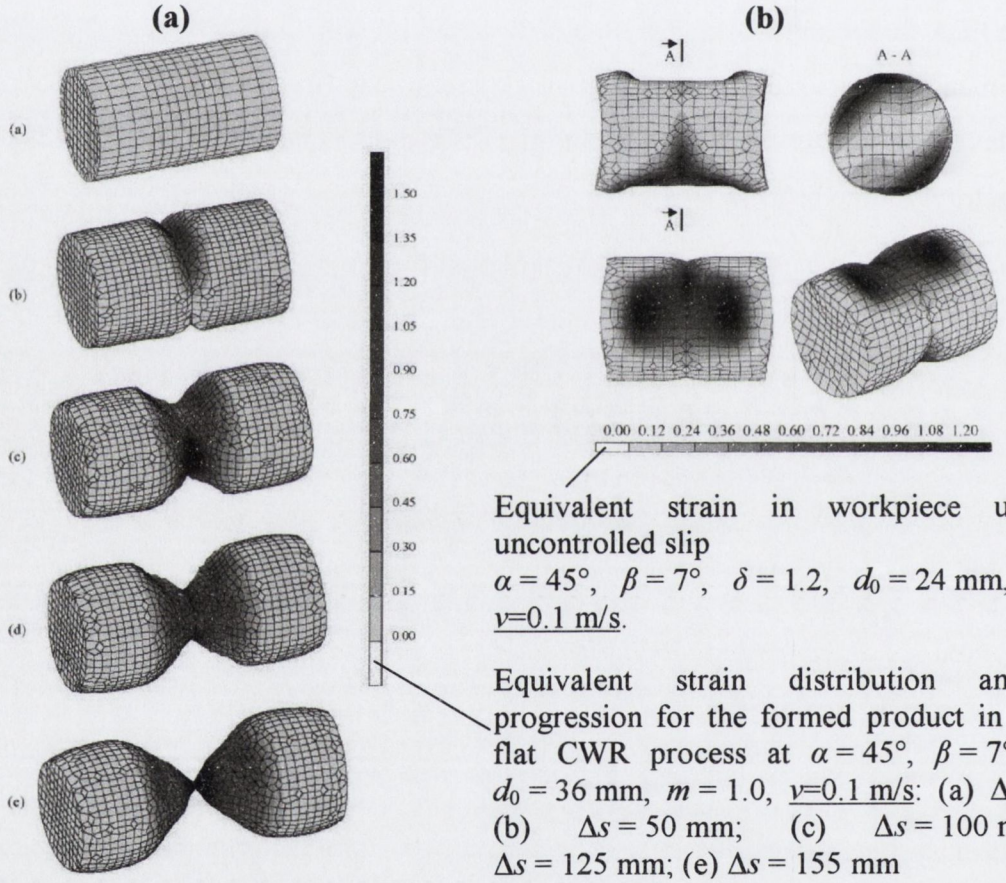

Equivalent strain in workpiece undergoing uncontrolled slip
$\alpha = 45°$, $\beta = 7°$, $\delta = 1.2$, $d_0 = 24$ mm, $m = 0.5$, v=0.1 m/s.

Equivalent strain distribution and shape progression for the formed product in course of flat CWR process at $\alpha = 45°$, $\beta = 7°$, $\delta = 1.8$, $d_0 = 36$ mm, $m = 1.0$, v=0.1 m/s: (a) $\Delta s = 0$ mm; (b) $\Delta s = 50$ mm; (c) $\Delta s = 100$ mm; (d) $\Delta s = 125$ mm; (e) $\Delta s = 155$ mm

Figure 5.39: Necking and slip of the workpiece [26]

As discussed earlier, several authors also used FEA in an empirical fashion to determine which combinations of die geometries resulted in successful rolling.

In 2002, Fang et al [33] used DEFORM 3D to perform Rigid Plastic analysis of the Cross Wedge Rolling process using cylindrical dies. They used a plastic workpiece with 14000 elements, and to minimise the number of elements, heavily concentrated the elements in the region of deformation and used a ½ symmetry models, in which only half

the workpiece was used taking advantage of the symmetry around the centre of the die, see Figure 5.40.

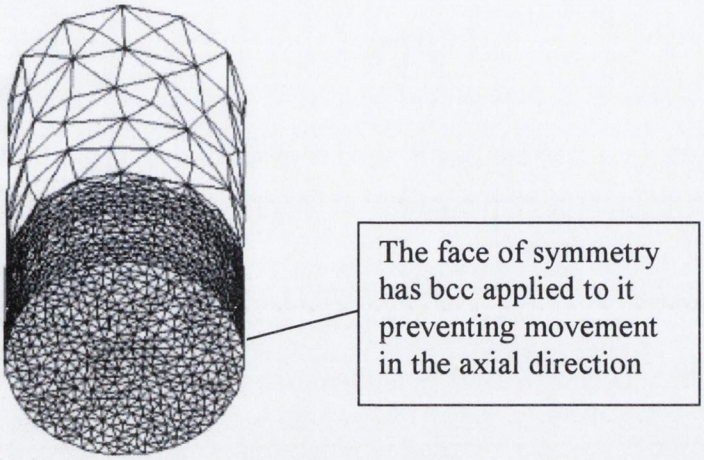

Figure 5.40: ½ symmetry model used in the 3D FEA package DEFORM

Apart from reducing the number of workpiece elements and thereby improving the simulation times the use of the ½ symmetry also helps improve the stability of the simulation by restraining the workpiece from unwanted movement.

Another advantage of using this method is that it increases the mesh density in the centre of the workpiece, see Figure 5.41

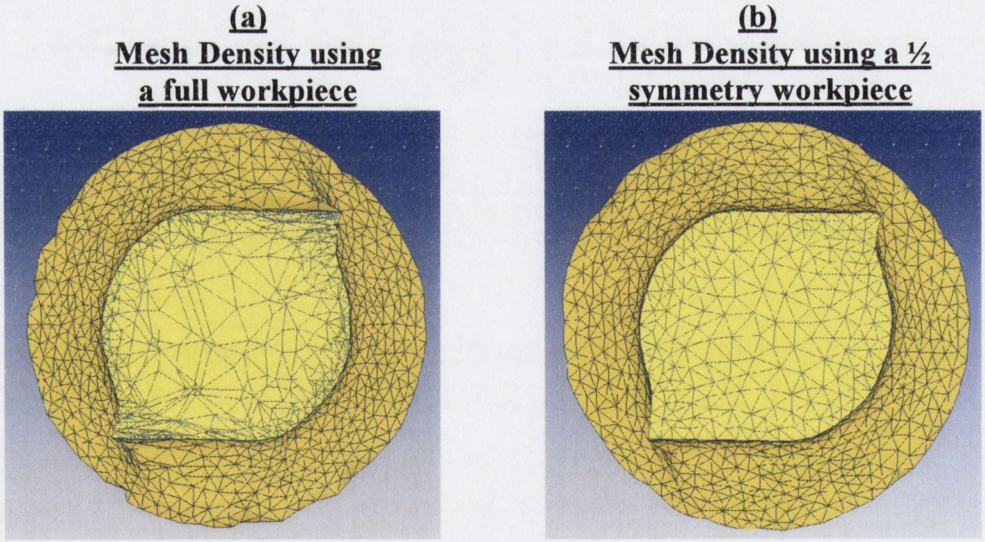

Figure 5.41: Improvement of mesh density resulting from the use of the ½ symmetry model

Although the mesh density can be improved in the workpiece by selecting a finer internal mesh option in the pre-processor this severely reduces the simulation time.

In 1998, Dong *et al* [36] used the ANSYS/LS-DYNA package to model the form rolling process. However, they have concentrated on the knifing and guiding zones. The aim of their model was the characterisation of friction and slip in these zones. The FEA results compared well with experimental results for interfacial slip. In 2000 and 2001, Dong et al [38, 39] released further papers analysing friction and slip conditions utilising the same FEA model. In 2000 the same authors produced a paper [37] in which they described how they used the same model to analyse the stresses in the workpiece during form rolling in an attempt to understand the failure mechanisms associated with the process. The major limitation with this research was that it focussed on only a small section of the form rolling process, a section where the amount of deformation experienced by the workpiece is small.

At the 2004 IMC, Eyres *et al* [32] presented their work on the 3D analysis of the form rolling process, with flat dies. Their model was used to predict the flow of material during the process. They also observed the presence of tensile stresses which could aid crack propagation, and the increase in magnitude of tensile stress with groove depth.

FEA has been shown to be a useful tool in the analysis of the form rolling process in terms of understanding the deformation mechanism and determining certain operational parameters.

5.4.2 The Application of FEA to Micro-Forming

There have been a number of attempts to model micro-forming processes using FEA, and these methods were based on obtaining the micro-properties of the workpiece material and then using these in the FEA in place of the materials macro-properties.

In 1989, Ampere Tseng [66] discussed how 2D FEA was used to design an improved set of tools for the production of a micro-part. The part was manufactured by stamping and had dimensions of 0.25 x 0.6 x 12mm. Tensile tests were first carried out on strips of the workpiece material, type 305 stainless steel, to determine its mechanical properties. The thickness of the strip tested was the same as that used in the stamping process (.254 to .508mm). The stamping process was then modelled using the experimentally determined material properties in FEA and the predicted geometries were compared with the geometries on stamped parts, the results verified that the FEA was capable of representing the process. He then designed a number of dies and modelled their performance and the resulting workpiece geometry using FEA. The die design that

predicted the best parts in the FEA, were then manufactured and used in place of the original dies. The new dies produced stamped parts as predicted by the FEA. This research showed that FEA could be used to successfully model a micro-forming process and that it could be used to improve the overall tooling design for the process.

In 1994 Messner *et al* [67] produced a size dependent FE model that was used for modelling the compression of micro-cylinders; the method was verified by comparing the FEA results with experimental upsetting tests. The material's properties were determined by performing compression tests on cylinders ranging in diameter from 0.5mm to 4.8mm, and this data was then inputted into the FEA program. To perform the FEA simulation, the corresponding size dependent flow stress data was used. The FEA results for the compression of cylinders compared well with the experimental data and over the specimen size range the calculated load did not vary from the experimental load by more than 5%. This method was successful in modelling the upsetting of cylinders. However, it was never tested for more complicated forming operations and so remains an unproven technique for the modelling of micro-forming processes.

Another interesting point that must be considered when discussing the FEA of micro-forming, is the variability in shape of the formed parts due to the heterogeneity of metals at small scales. Geibdorfer [68] created workpieces for his 2D FEA simulations that contained random grain shaped objects using a grain generating program. As expected, he observed that the shape of the formed part was affected by the grain size. However, even when the grain size was kept constant the shape of the formed part depended on the grain structure created by the grain generating program. Because both the experimental and finite element analysis of the process used workpieces that had a random grain structure, they could not be expected to conform. This obviously leads to difficulties in verifying the accuracy of the FEA. The author of this thesis predicts that it limits the use of grain based 2D FEA simulations. The limitation arises because, although in the plane that is being modelled in the FEA simulation there are only a few surface grains, when the entire circumference of the workpiece is considered there are actually a significant number of surface grains around the periphery, see Figure 5.42.

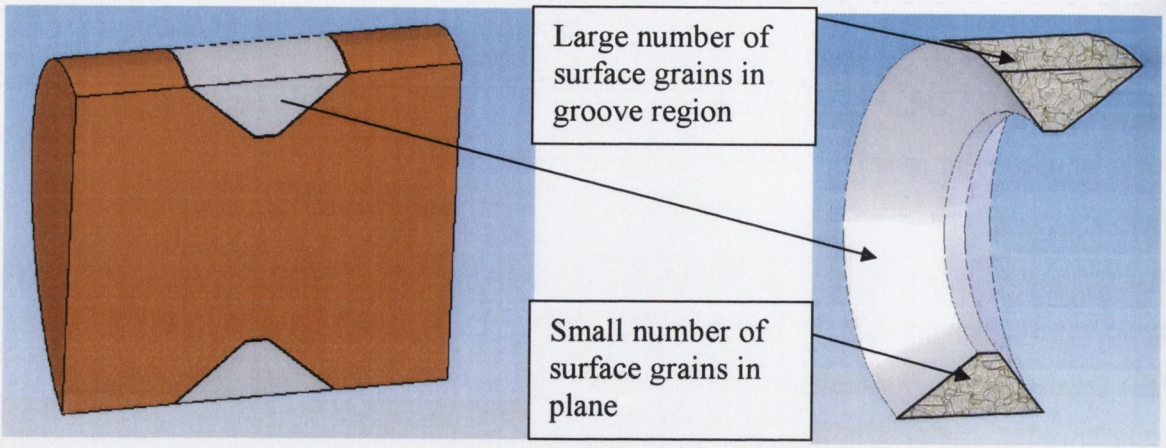

Figure 5.42: The volume of workpiece material displaced during the form rolling of a groove and number of workpiece grains contained in this volume of material

Average number of surface grains in a workpiece plane, g_{avg}

$$g_{avg} = \frac{w}{d_{grain}} \tag{5.25}$$

Surface area of workpiece to be deformed by the dies, s_{area}

$$s_{area} = \pi d_0 w \tag{5.26}$$

Maximum surface area of a grain, g_{area}

$$g_{area} = \frac{\pi d_{grain}^2}{4} \tag{5.27}$$

The total number of surface grains in the region to be deformed by the groove, g_{tot}

$$g_{tot} = \frac{s_{area}}{g_{area}} = \frac{4 d_0 w}{d_{grain}^2} \tag{5.28}$$

The formula indicates that the total number of surface grains increases in direct proportion to the groove width and the workpiece diameter and decreases as the grain size is increased. This formula implies that even if the grain size is large relative to the workpiece diameter there will still be a significant number of surface grains deformed by the dies, for example if the average grain diameter is 1/40 of the workpiece diameter then:

$$g_{tot} = \frac{4 * 0.5 * 0.1}{.025^2} = 320$$

Where: $w = 0.1\text{mm}$

$d = 0.5\text{mm}$

$d_{grain} = 0.05\text{mm}$

Therefore, there are in fact a large number of surface grains that must be deformed and this will increase the homogeneity of the formed part.

The papers discussed in this section provide a material model for the FEA of micro-forming, namely to model a workpiece with the flow stress data determined by compression tests on a specimen of similar size. This material model has been determined from parts in which the entire area of the part is deformed, thus limiting the size effect to the scale of the specimen. However, during the micro-form rolling process the workpiece will be deformed by a geometric feature which is of a smaller scale than its diameter (see Figure 5.43) and it is yet to be determined whether the material representation described above will be appropriate for modelling the process.

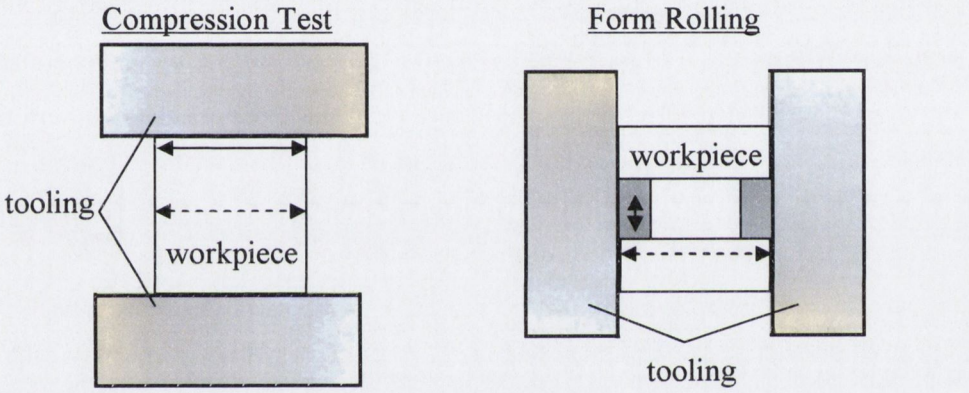

Figure 5.43: Comparison of workpiece scale to deformation scale

5.5 Fracture and Damage Criteria

5.5.1 Fracture Surfaces

The fracture surface of a part that experiences ductile failures is very rough and is comprised of a series of dimples or craters. The craters are a remnant of spherical pores that coalesce and result in part failure. Ductile fracture can result from excessive tensile or shear stresses in the part and some degree of plastic deformation is usually evident in the failed part.

5.5.2 Damage Criteria

The surface failures that effect Form-Rolled parts such as lapping and necking appear as such in FEA simulations and are, therefore, easily identifiable. However, the prediction of internal failures is less straight-forward. Damage algorithms can be used for this task; these algorithms are a function of the stress state within the workpiece and many such damage algorithms exist. However, in this research, the Cockcroft & Latham and the Normalised Cockcroft & Latham algorithm were used:

$$\text{Damage as predicted by the Normalised Cockcroft \& Latham} = \int^{\bar{\varepsilon}} \frac{\sigma^*}{\bar{\sigma}} d\bar{\varepsilon} \quad (5.29)$$

$$\text{Damage as predicted by the Cockcroft \& Latham algorithm} = \int^{\bar{\varepsilon}} \sigma^* d\bar{\varepsilon} \quad (5.30)$$

Where: σ^* = the maximum principal tensile stress

$\bar{\sigma}$ = the effective stress

$\bar{\varepsilon}$ = the effective strain

If the values of damage calculated by this algorithm exceed a 'critical value' then failure of the part is likely to ensue. The critical damage value is determined by comparing experimental and FEA results for the same experiment. The damage value in the FEA simulation at the time and location that failure occurs in the experiment is considered to be the critical damage value. This damage value can then be used in the FEA of similar processes to predict part failure without the necessity of undertaking experimental trials.

The theoretical basis of the Cockcroft and Latham [69] formulae is that there is a material property named the 'true' ductility and, if it is exceeded, then failure will occur. The equations show that it is dependent on both the stresses and strains experienced by the workpiece which make it a function of the total plastic work done per unit volume and therefore independent of deformation type.

Kim et al [70] compared the Cockcroft & Latham damage algorithm with several other algorithms in respect to the prediction of ductile failure in cold forming. They concluded that it had several advantages over the other algorithms as outlined below:

1. It is integrated into the DEFORM FEA package.
2. The only material property required is the flow curve, which can be obtained from the FEA package, unlike other algorithms which require specific properties.
3. It was amongst the most accurate algorithms for predicting the ductile fracture of workpieces in processes such as forward extrusion.

Because of these advantages, they concluded it could be used in conjunction with FEA to predict and eliminate ductile fracture in cold forming. However, it must be noted that it failed to predict the location of internal cracks in certain processes where cracks were a result of severe deformation resulting from compressive stress.

They also noted that the critical damage values increased after the material had been heat treated; that the values obtained from tensile tests are larger than those obtained from compression tests; and they used the values obtained from compression tests in their simulations.

CHAPTER 6

WORK PROGRAMME

CHAPTER 6

WORK PROGRAMME

6.1. Die Design

A major difficulty encountered during this research was the manufacture of suitable tooling and, as a result, the experimental portion of this research does not contain as great a variety of die geometries as those discussed in the theoretical and FEA section of the thesis. However, the micro form-rolling trials carried out with the available dies has demonstrated that useful results could be obtained.

The problems associated with manufacturing suitable tooling included issues of geometrical accuracy; the selection of a die material capable of withstanding the large stresses associated with the process; and the selection of a suitable traction surface to prevent slip between the rotating workpiece and reciprocating tooling. These problems are dealt with in more detail in the following section.

6.1.1 Dies to Investigate the size effect

It was necessary to design a series of die sets that would enable the size effect to be investigated. The theory of similarity dictates that if appropriate scaling factors are applied it is possible to accurately scale a forming process [9]. Therefore, scaled form rolling trials were performed, ranging from the macro to the micro-scale. According to the theory of similarity, the stresses and strain in the scaled trials should be the same and, therefore, any variation was attributed directly to the miniaturisation of the process.

The form rolling trials were undertaken using geometrically similar tooling sets; this tooling consists of a groove shape that was constant for all the tooling sets but which was scaled to the diameter of the wire being rolled. The forming and spreading angles must, therefore, be the same for each set of tooling. The groove geometry used was a symmetrical truncated triangle. A small spreading angle was used to allow for a very gradual displacement of material. The tooling was manufactured using the techniques discussed in the following sections; the dimensions of the scaled tooling are presented in Table 6.1, while its geometry is shown in Figure 6.1.

Wire diameter [mm]	% reduction in cross sectional area	Feature height, h [mm]	Width of flat, f [mm]	Spreading angle, β [degrees]	Sidewall angle, α [degrees]	Ramp angle, γ [degrees]
0.45	59	0.0825	0.0275	0.8	45	0.8
1	59	0.18	0.06	0.8	45	0.8
2	59	0.36	0.12	0.8	45	0.8

Table 6.1: Dimensions of Geometrically Similar Dies

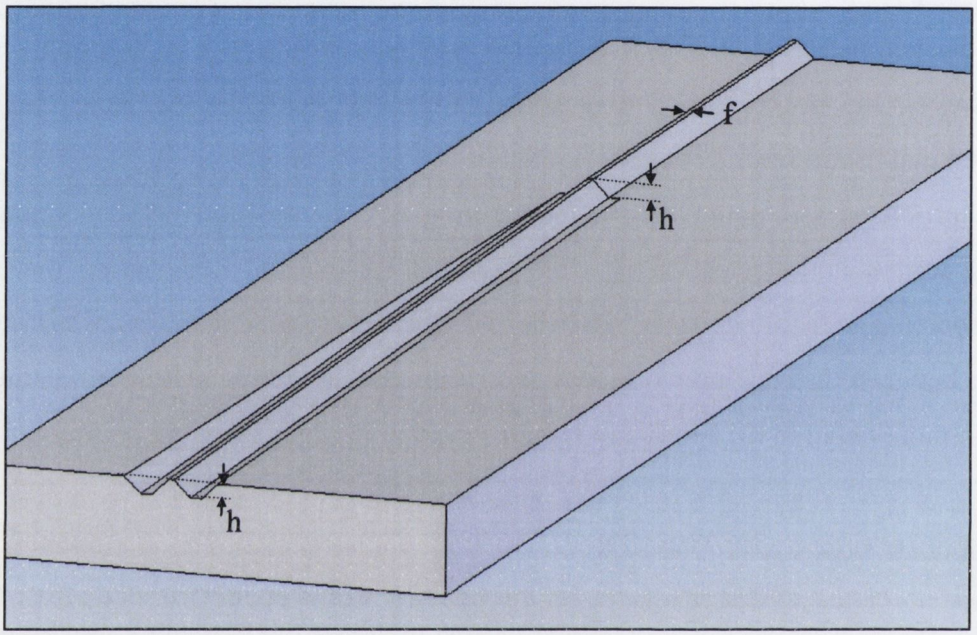

Figure 6.1: Geometrically scaled form rolling tooling

6.1.2 Dies to Investigate the Effect of Die Geometry

The sidewall angle is one of the most critical parameters in form rolling, therefore, a series of dies to investigate the effect of this angle were designed. These die sets were designed to roll one millimetre diameter wire and they all had the same feature height, however, unlike the other die sets which had a sidewall angle of forty five degrees these die sets had a sidewall angle of thirty or sixty degrees. Due to the interrelationships between the sidewall angle, feature height, spreading angle and the number of workpiece rotations, changing one affects the others. The number of workpiece rotations is the number of revolutions the workpiece will undergo in the knifing zone of the die. By keeping the feature height the same while changing the sidewall angle either the number of workpiece rotations or the spreading angle must change, these are constant at 4.1 and 0.8°

respectively for the other die sets. The die geometries that would result if either the spreading angle or the number of workpiece rotations were changed are listed in Table 6.2.

	Changing the no. of workpiece rotations	Changing the spreading angle
sidewall angle, α	30°	30°
spreading angle, β	1.33°	0.8°
no. of rotations	4.1	7.1
sidewall angle, α	45°	45°
spreading angle, β	0.8°	0.8°
no. of rotations	4.1	4.1
sidewall angle, α	60°	60°
spreading angle, β	0.47°	0.8°
no. of rotations	4.1	2.36

Table 6.2: The effect of changing the number of workpiece rotations or the spreading angle on the die geometry

From Table 6.2 it is clear that if the spreading angle was kept at 0.8° the difference in the number of workpiece rotations would become quite significant, with some die geometries requiring three times as many rotations as others. Therefore, it was decided to keep the number of workpiece rotations constant while varying the spreading angle of the die.

6.2 Die Manufacture

The basic die block dimensions are set by the design of the rolling machine and for the EWM AF3 they are set to a depth of 19.9mm (excluding the forming feature), a width of 31.9mm and a length of 57.8mm for a stationary die and 65.8mm for a moving die. During the course of this research the features on the die sets were produced using either a grinding or a milling process, a brief overview of these two methods will now be given.

6.2.1 Milled Die Manufacture

Figure 6.2 details the steps involved in the manufacture of a milled die set.

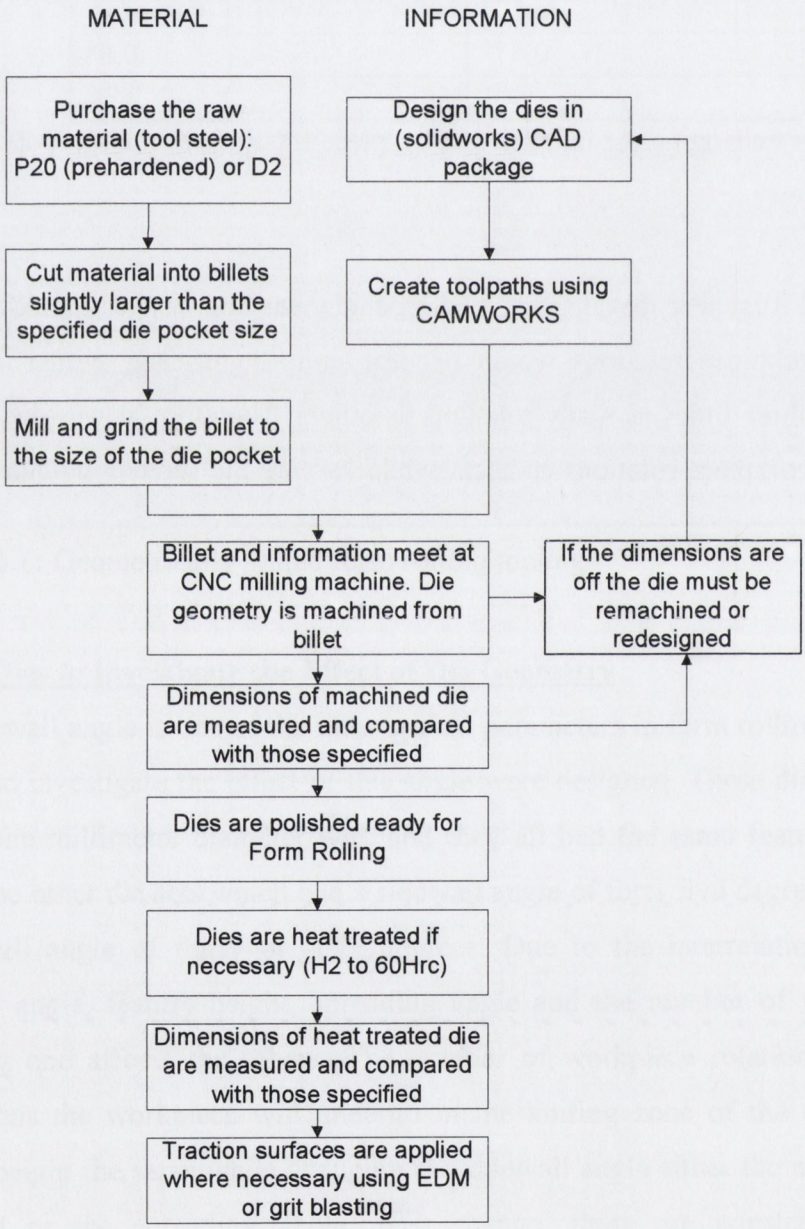

Figure 6.2: Flow chart of die manufacture by machining

Figure 6.2 shows that the material and die information initially flow on separate paths in the flow chart and these paths merge at the CNC milling stage of the process.

All the milled dies were machined in the workshop of the Department of Mechanical and Manufacturing Engineering in Trinity College Dublin. The milling machine used was a 3-axis CNC Bridgeport and the cutting tools used were Holex solid carbide slot drills. The CAD and CAM package used were SolidWorks and CAMworks respectively. The creation of the toolpaths and machine code by CAMworks is discussed below:

1. A solid model of the die was opened in CAMworks
2. The position of the origin and the directions of the axes were set in CAMworks, the origin was located at the bottom left hand corner of the die, see Figure 6.3(a)
3. A 3 axis feature consisting of a roughing and finishing cut was created in the CAM package. A 3 axis feature was used due to the 3D shape of the groove feature being machined onto the die. The roughing cut allowed a large amount of material to be removed from the die relatively quickly, but only produced a rough outline of the die feature. While the more precise but slower finishing cut machined the final die geometry.
    a. The roughing cut used a 4mm diameter cutter and operated using a 0.1mm slice cut on the x-y plane, which means the cutter took cuts up and down the length of the die in the x direction and each cut moved the axis of the cutter 0.1mm in the y direction.
    b. The finishing cut used a 1mm diameter cutter and operated using a 0.01mm or 0.02mm slice cut on the x-y plane. The smaller cut size for the finishing cut improved the accuracy of the finishing cut.
4. The CAM package then created the tool paths, see Figure 6.3(a).
5. The effectiveness of the toolpaths was checked using a visualisation of the die after machining created by CAMworks (see Figure 6.3(b-d)) and, if necessary, modifications of the toolpaths were made.
6. CAMworks generated Heidenhaim HH2500 machine code which controlled the Bridgeport during the machining of the dies.
7. The machine code was uploaded to the Bridgeport.

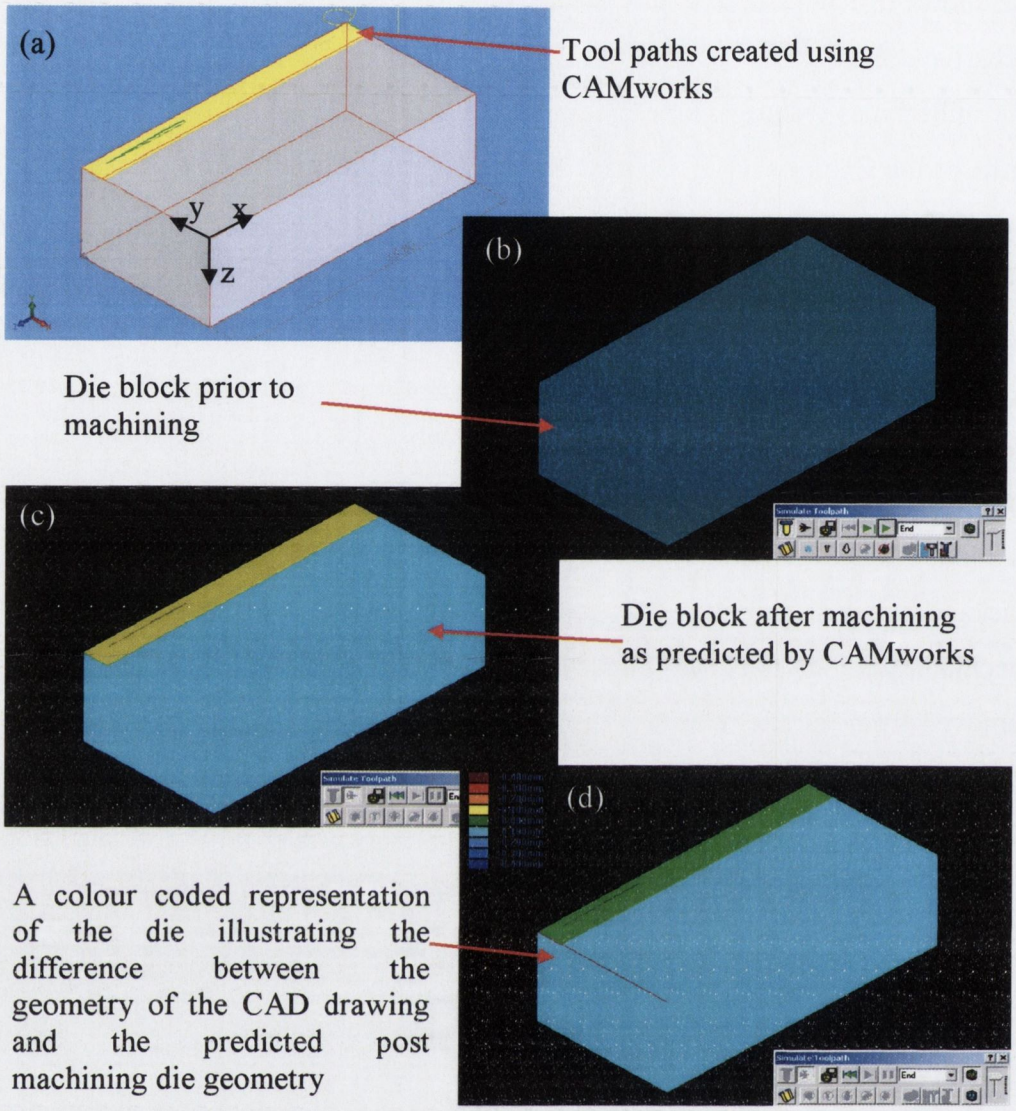

Figure 6.3(a-d): The generation and checking of toolpaths for the finishing cut on a 1mm moving die with a 30° sidewall

As illustrated by Figure 6.3(a-d), the toolpaths and subsequent machining are restricted to the region around the groove to reduce the machining time.

Figure 6.4 shows a finished die 2mm die. The difference in the colour of the dies between the photos is a result of the heat treatment process.

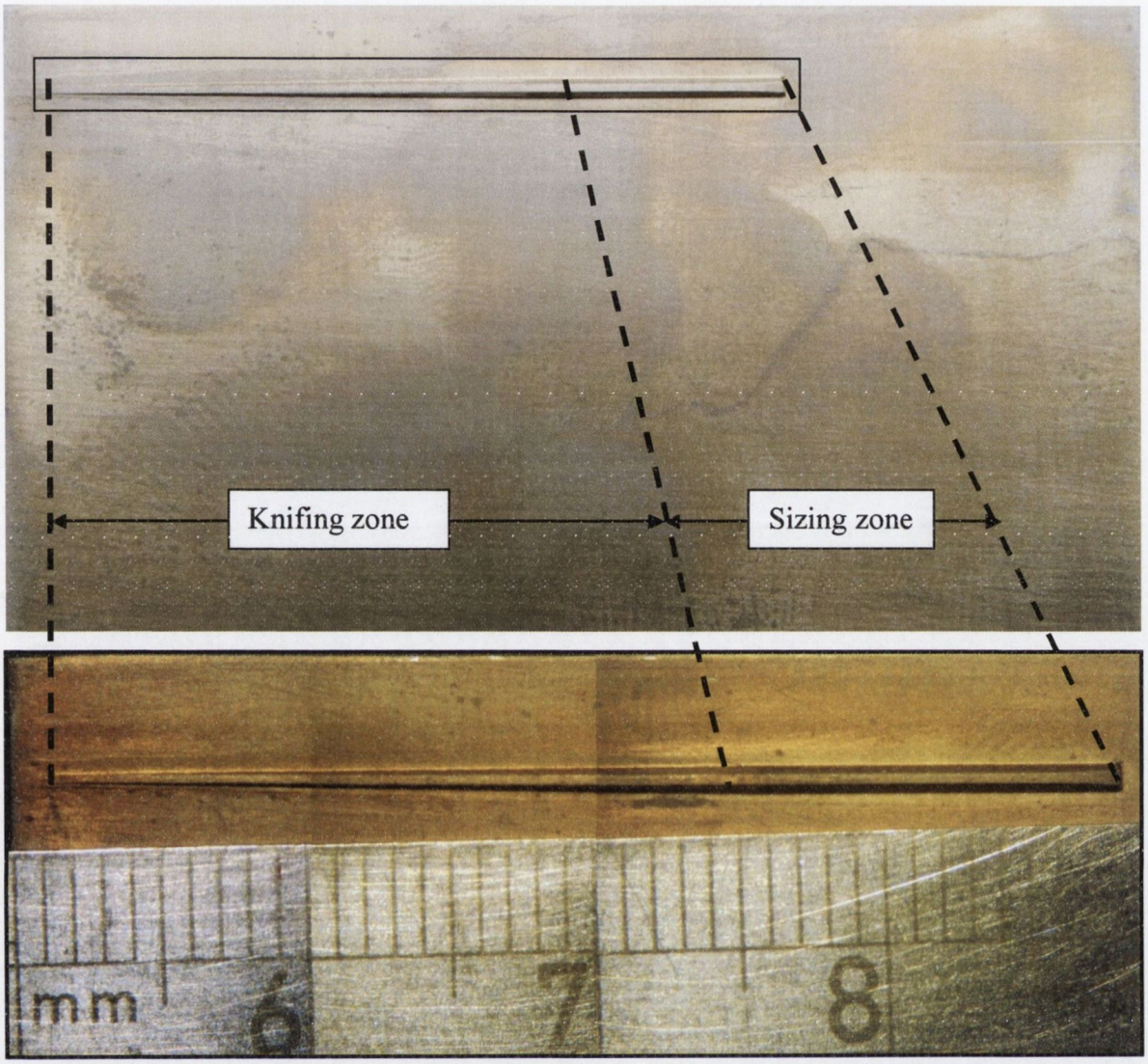

Figure 6.4: Photographs of a 2mm machined die

6.2.2 **Ground Die Manufacture**

The manufacture of a rolling die using a grinding process involves five steps carried out using two grinding machines. The first machine produces a cylinder known as a crush roll which has the same surface profile as the feature to be ground onto the die. The second machine uses the crush roll to dress a grinding wheel which then grinds the required feature geometry onto the die:

Grinding the crush roll, see Figure 6.5

1. A metal plate known as the crush plate is machined to have the same feature geometry as the die set being manufactured.

2. This crush plate is then used to dress a grinding wheel. The profile of the grinding wheel is now the inverse of the required die geometry.
3. The grinding wheel then grinds the geometry of the die onto the crush roll.

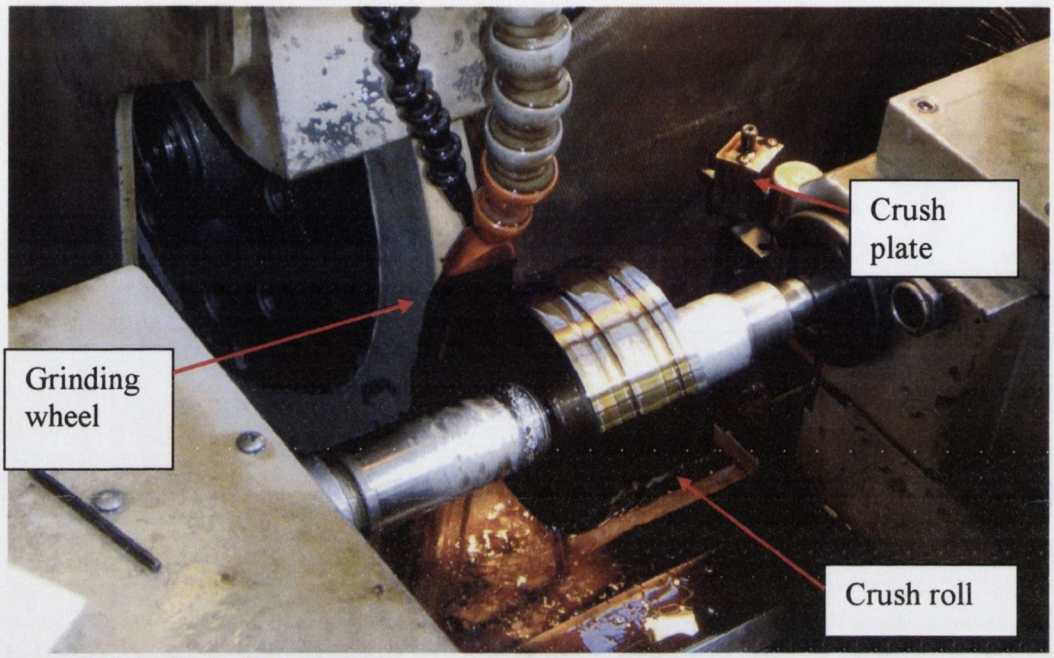

Figure 6.5: Grinding of crush roll

Grinding the die, see Figure 6.6

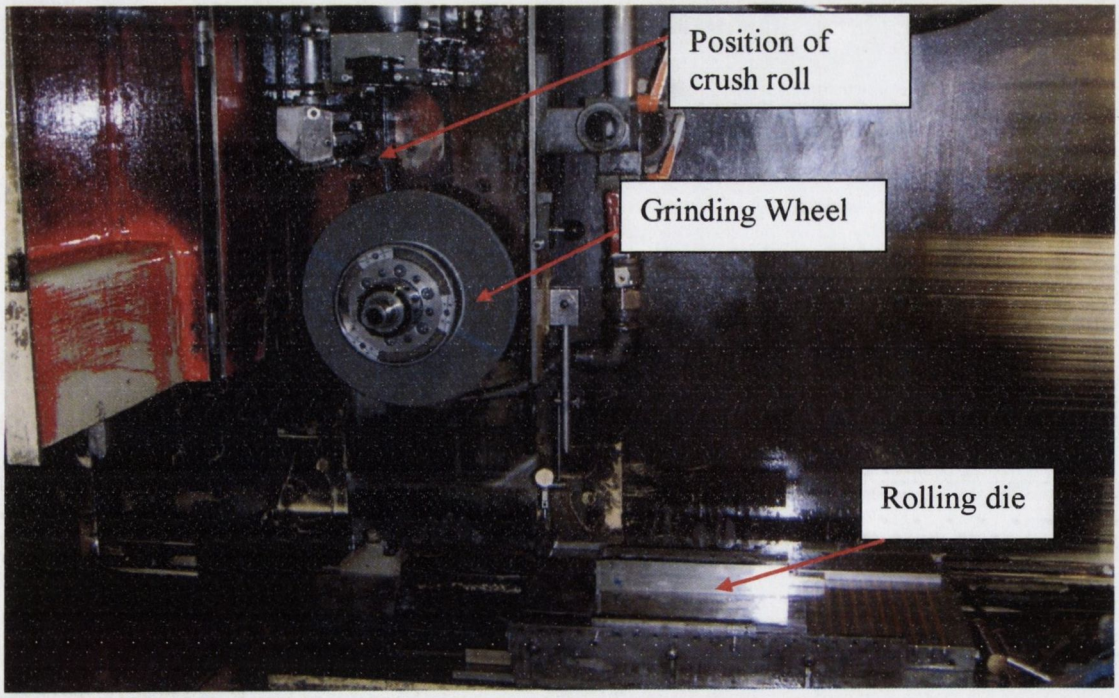

Figure 6.6: Grinding machine used to manufacture form rolling dies

4. The crush roll is used to dress the grinding wheel that will produce the die. The grinding wheel has a profile that is the inverse of the die geometry.
5. The rolling die is then ground using grinding wheel.

The crush roll is made even though it requires two extra steps because it is hard wearing and once it has been made it can be used to dress many other grinding wheels.

The rolling die is held in place on the base of the machine using a magnetic clamp. The crush roll is placed in contact with the grinding wheel and as the grinding wheel is rotated the crush roll is forced onto its surface crushing the feature onto it.

The grinding wheel is then used to grind the form onto the rolling die; the relative horizontal and vertical movement of the grinding wheel determines the ramp and spreading angles of the die see Figure 6.7.

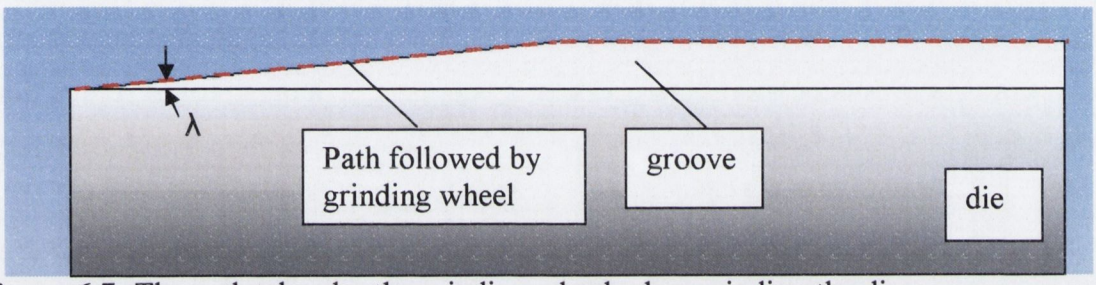

Figure 6.7: The path taken by the grinding wheel when grinding the die

Due to the geometry of the grinding wheel the dies have trenches on either side of the groove, see Figure 6.8.

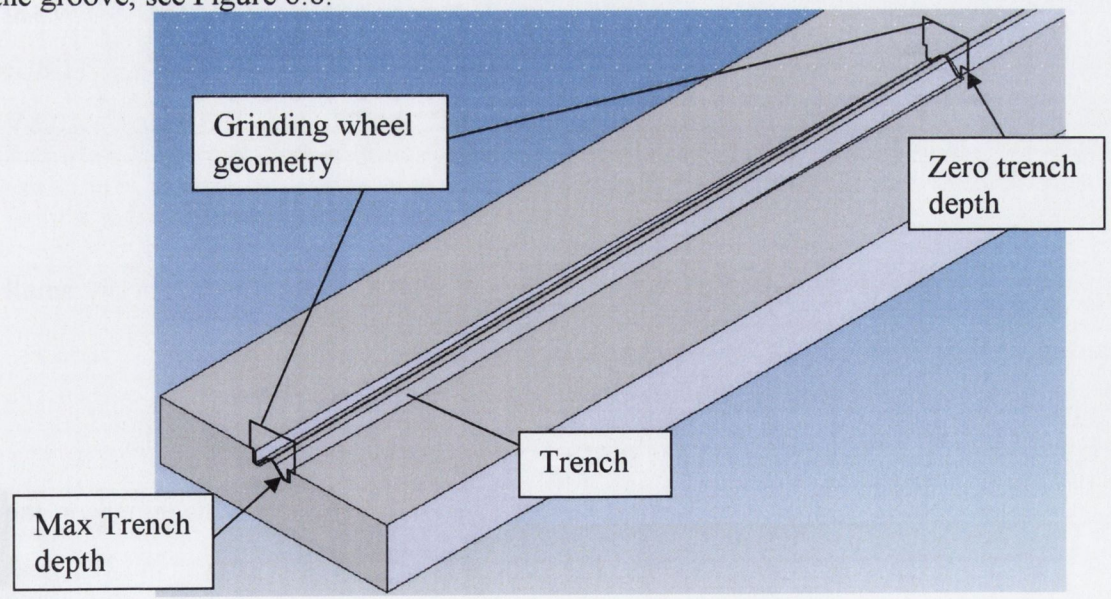

Figure 6.8: Trenches in the die as a result of the grinding process

At the start of the knifing zone, the tip of the groove has to be level with the die surface, therefore, the entire groove geometry has to be ground below the top surface of the die as shown in Figure 6.8. During the knifing zone, the tip of the groove gradually rises above the die surface until by the end of the knifing zone the entire feature is above the die surface.

6.2.3 **Die Material**

Four different die materials are recommended for the manufacture of thread rolling dies [71] A2, D2 M1 and M2. D2, M1 or M2 are recommended when rolling alloys of higher hardness. A2 or D2 are recommended when high tolerances i.e. low distortions during heat treatment are required. D2 has approximately 0.05% average distortion. In this project, the workpiece was either stainless steel or titanium and the accuracy of the die feature was also a major consideration, therefore, D2 provided the best combination of properties. However, a disadvantage associated with D2 is that it is very hard to grind after heat treating to improve the dimensional accuracy because this can lead to grinding cracks.
The relevant properties of AISI D2 are given below [72]:

Hardness [HRC]	Compressive Yield [MPa]	Elastic Modulus at Room Temperature [MPa]	Grain size [ASTM]	Nominal grain Ø [μm]	Composition
60	2150	210000	5	65	1.55C 0.3Si 0.4Mn 11.8Cr 0.8Mo 0.8V

Table 6.3: Properties of D2 tool steel

The tool life increases as the parts diameter is reduced, which is significant as only small diameter parts were rolled during this research.

6.2.4 **Heat Treatment of Micro-Form Rolling Dies**

The heat treatment was performed after the required geometry had been machined on the D2 dies. A hardness of 60 HRC was specified for the entire tool surface and the heat treatment was performed in a vacuum furnace, after treatment hardness tests were carried out to ensure the requisite hardness had been achieved.

After hardening, SEM photograph were taken along the entire length of the die feature on several dies and there was no evidence of micro-cracks or deviation in geometry resulting from heat treatment.

6.3 Form Rolling Trials

Form rolling trials were performed using the available dies in combination with different wire diameters and workpiece materials. These tests allowed the relationship of feature size to diameter, miniaturisation and different materials to be investigated. The effects of miniaturisation were determined by performing geometrically scaled trials (i.e. the feature size is matched to the parts diameter). The influence of feature size with respect to workpiece diameter was determined by rolling a diameter with a number of different sized grooves. The stability of the rolling process for all die/workpiece combinations was also monitored; this encompasses the development of internal failures, gross failure of the part and squaring (slipping) of the part.

6.3.1 The EWM AF3 Micro Thread / Form Roller

1. The form rolling machine used for rolling trials was an E.W. MENN AF3 form rolling machine, see Figure 6.9.

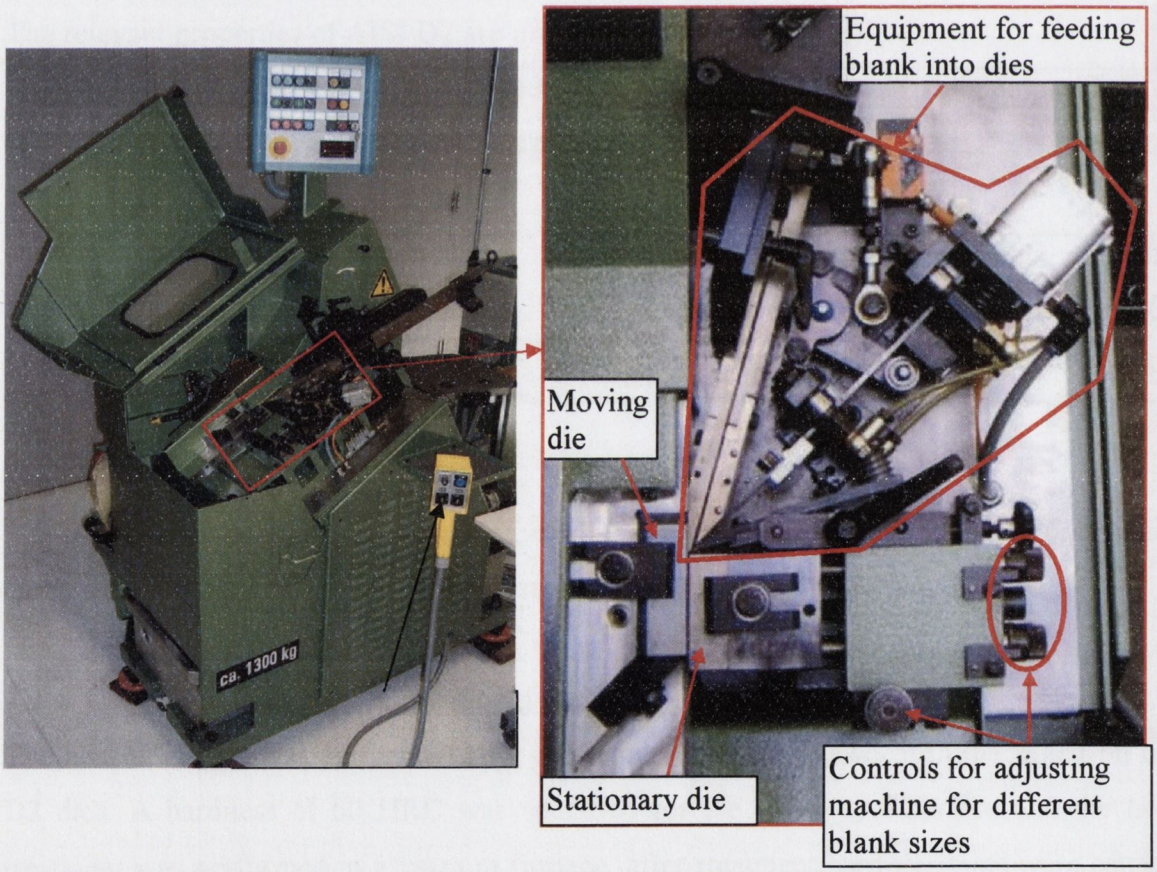

Figure 6.9: Working area and overview of EWM AF3 form roller

This machine has been specifically designed for the thread and form rolling of small parts. The machine has several advantages compared to other machines when rolling micro parts:

1 It has micrometer controls for setting the die gap

2 It has an infinitely variable manual speed controller

AF3 Adjustments

It is worth explaining the setup procedure used when installing a new set of dies, to help understand the decision made in designing the dies.

When adjusting a form rolling machine for a new set of tooling there are three main machine parameters that must be set. These are the die gap, the height of the stationary die and the starting position of the moving die; they are set by positioning one die relative to the other as described in Figure 6.10.

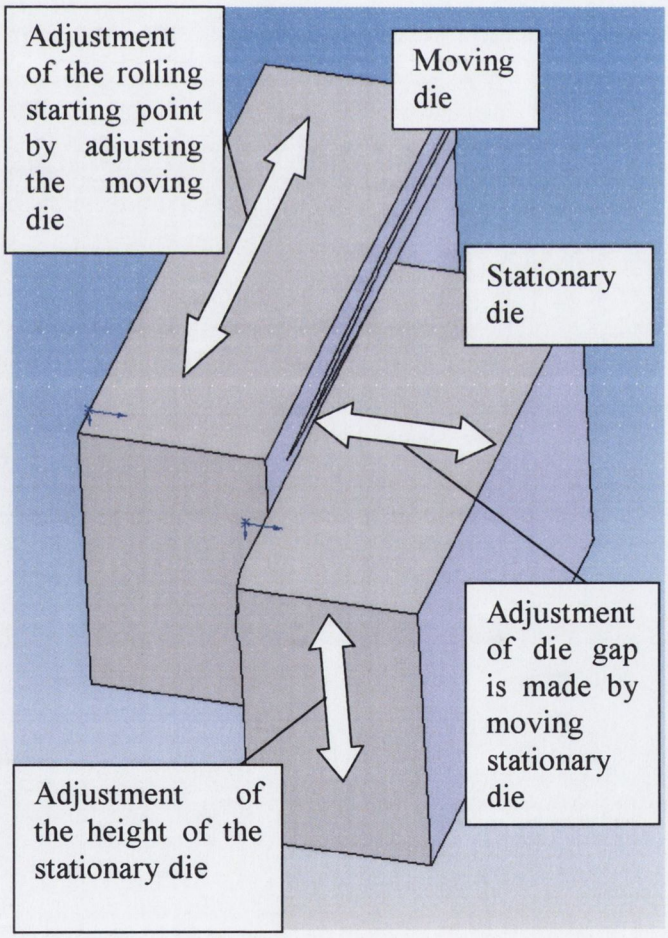

Figure 6.10: Form rolling machine adjustments

Die gap

The die gap is the distance between the forming faces of the stationary die and the moving die. The die gap is adjusted by moving the stationary die either towards or away from the moving die. The die gap is approximately equal to the workpiece diameter being rolled. However, it must be set slightly less than the wire diameter to provide the correct level of force on the workpiece. If the gap is too large, the force generated will be too small and the dies will not have sufficient traction on the workpiece to rotate it. However, if the die gap is too small, slippage will occur as rotation of the workpiece would result in large workpiece deformation.

Starting position of the moving die

Finally the starting position of the moving must be adjusted. When the workpiece starts rolling the distance from the workpiece to the start of the grooving feature on the stationary and the moving dies must be the same, otherwise the deformation induced by each die will be different resulting in unbalanced forces which can result in slippage, see Figure 6.11.

d1 = the distance from the workpiece to the grooving feature on the stationary die

d2 = the distance from the workpiece to the grooving feature on the moving die

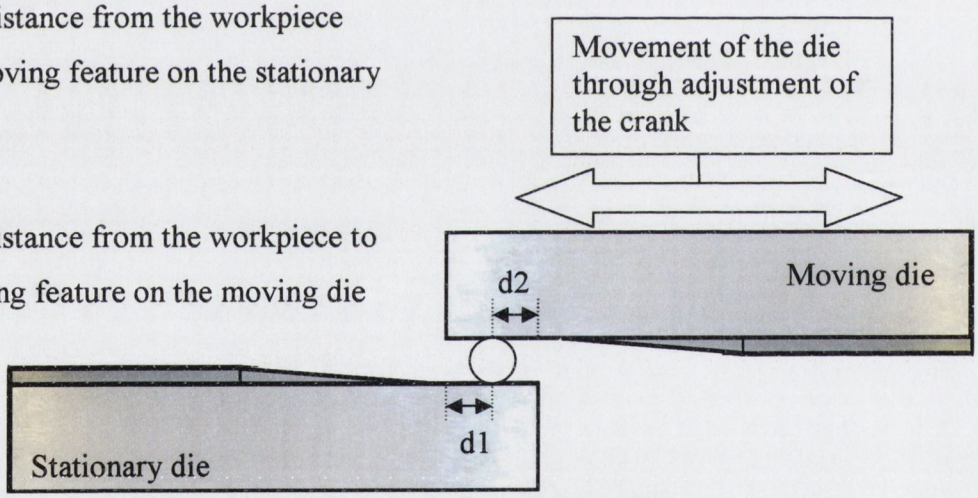

Figure 6.11: Adjusting the starting position of the moving die

A form rolling setup sheet, see Appendix, was devised for a number of reasons:

1. To ensure that all the necessary setup steps for the machine were carried out in the correct order
2. To record the machine setups that resulted in successful rolling
3. To record any noteworthy occurrences

Stationary die height

Adjustment of the height of the stationary die is necessary to ensure that the features on the moving and stationary die are aligned to the same height relative each other, see Figure 6.12. If the die features are not in line, the feature rolled on the workpiece will be wider than specified and twisting and, therefore, slippage of the workpiece may also result due to unbalanced rolling forces

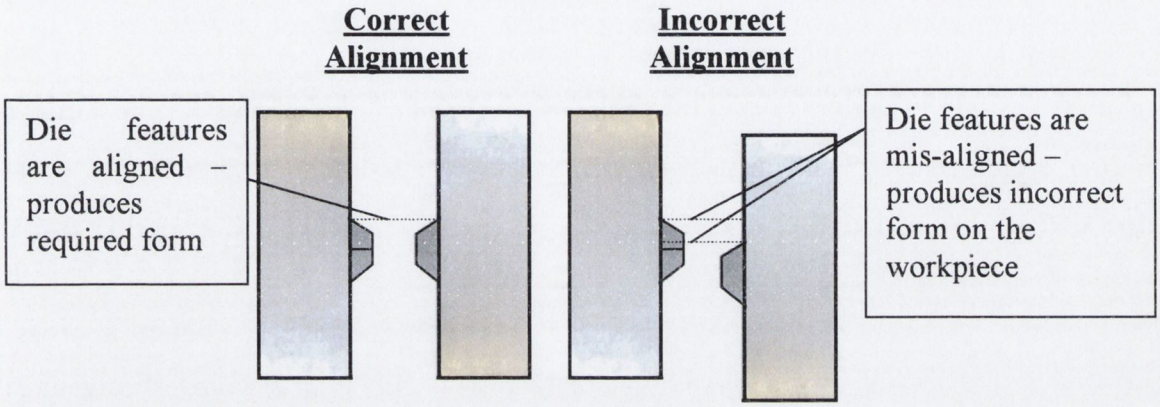

Figure 6.12: Adjusting the height of the stationary die

6.3.2 Blued Dies

To investigate the contact region between the die and the workpiece, a technique known as 'bluing' was used. This process involves performing rolling trials with dies that have been coloured blue using a permanent marker. During the rolling trials regions of the dies that were in contact with the workpiece had the bluing removed, thereby allowing the actual die/workpiece contact regions to be identified, see Figure 6.13.

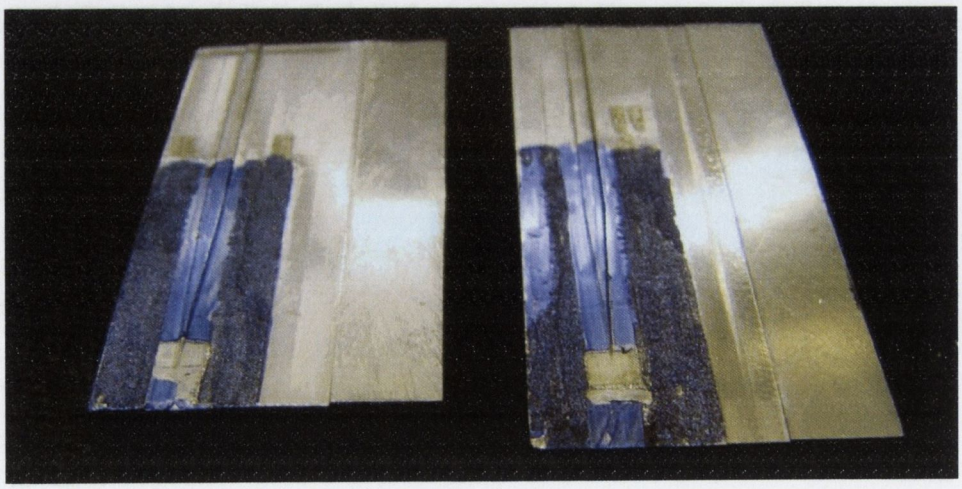

Figure 6.13: Blued dies used to illustrate die/workpiece contact

Workpieces rolled with the dies shown in Figure 6.13 were known to have experienced slippage from an early stage in the rolling stroke. To investigate the cause of this problem, the dies were blued and the workpiece was rolled a small distance and then removed. It can be seen from Figure 6.13 that the bluing was not removed from the traction surfaces, indicating that they are not contacting the workpiece and, therefore, they cannot be providing sufficient traction to rotate the workpiece, resulting in slippage.

6.3.3 **Form Rolling Trials**

To gain as much information as possible on the micro-form rolling process a wide variety of rolling trials were performed. Six different die sets were used in the trials and they were named after the manufacturing process used to make them, the diameter of wire they were designed to roll and their sidewall angle, see Figure 6.14.

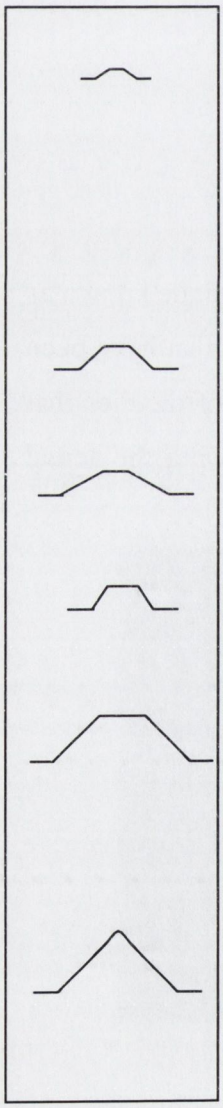

0.45mm milled: This set of dies was designed to induce a cross sectional area reduction of 60% in 0.45mm ø wire. The feature geometry is that of a truncated triangle with a sidewall angle of 45°. They were milled from D2 tool steel.

1mm milled: This set of dies was designed to induce a cross sectional area reduction of 60% in 1mm diameter wire. The feature geometry is that of a truncated triangle with a sidewall angle of 45°. They were milled from D2 tool steel.

1mm milled 30°: This die set is the same as the previous set but with a sidewall angle of 30°.

1mm milled 60°: This die set is the same as the previous set but with a sidewall angle of 60°.

2mm milled: This set of dies was designed to induce a cross sectional area reduction of 60% in 2mm diameter wire and has a sidewall angle of 45°. They were milled from D2 tool steel.

2mm ground: Again this set of dies was designed to induce a sectional area reduction of 60% in 2mm diameter wire. However it was manufactured using a grinding process and its geometry is that of a triangle with a rounded point with a sidewall angle of 45°. It was manufactured from D2 tool steel

Figure 6.14: Geometries of the die sets used in this research

The workpieces rolled were either AISI 316 stainless steel (FE-Cr18-Ni10-Mo3), with diameters of 0.45, 1, 2 and 3mm or ASTM Grade 5 titanium (Ti-6Al-4V), with a diameter of 1mm.

6.3.4 **Workpiece Materials**

When choosing materials to micro-form roll, the primary concern was the production of parts that would meet an industrial need. Therefore 316 and Ti6Al4V were chosen as they are used in the medical, aerospace and automotive industries where material properties and the geometric accuracy of the part are considered very important. These materials have impressive properties in regards to strength, biocompatibility and corrosion resistance and the form rolling process produces parts with good material properties.

Another important consideration was the suitability of the material to the form rolling process e.g. some metal products such as gray iron castings cannot be rolled due to their low ductility which causes them to fracture rather than conform to the shape of the die [25].

6.3.5 **One-Die Rolling Trials**

Trials using the one-die rolling process were also performed to prove its viability. This derivative of the form rolling process which uses only one wedge die and therefore has cost advantages associated with it was discussed in more detail in Chapter 3.

6.4 Investigation of Form Rolled Parts

The parts produced in the rolling trials were examined using both an optical microscope and an optical stereomicroscope to search for any defects that may have resulted from the form rolling of the workpiece. These included burrs, flakes, laps and internal defects. A stereo microscope provides a greater depth of field than a regular microscope and is, therefore, ideal for observing the contoured surface of a form rolled workpiece. However, its maximum level of magnification is relatively low and so when large magnifications were required a traditional microscope had to be used.

To determine the presence, location and magnitude of internal defects the samples rolled with each die/workpiece combination were mounted, sectioned and polished to reveal their internal cross section. Both axial (see Figure 6.15(a)) and radial (see Figure 6.15(b)) cross sections were investigated and this was necessary because the internal failures were not all of a uniform geometry and, therefore, to develop a proper sense of their three dimensional shape orthogonal sections were required.

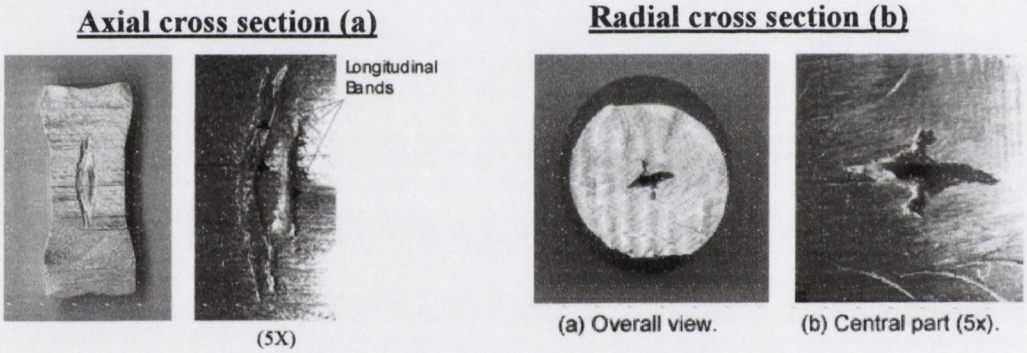

Figure 6.15: Sectioned form rolled workpieces showing internal failures[23]

6.4.1 Mounting of the Rolled Specimen

The specimens were mounted using a hot mounting technique. The specimen was positioned in the mounting press with some black epoxy mounting resin (METPREP EPO-MOUNT) in a powdered state. Through the application of pressure and heat by the mounting press the resin was cured to a solid encasing the specimen.

6.4.2 Polishing of the Mounted Specimen

The mounted specimens were ground and polished using a Jean Wirtz phoenix 4000 automated polishing machine. This machine allowed the control of the pressure being

exerted on the specimens, the rpm and direction of rotation of both the spinner (which holds the specimens) and the polishing wheel. The process involves three distinct stages

1. Grinding – this was performed using a coarse three hundred and twenty grit silica paper. It was performed to grind the specimen to the area of interest. For example, if the central axis of the workpiece is to be investigated then one half of the workpiece must be ground away.

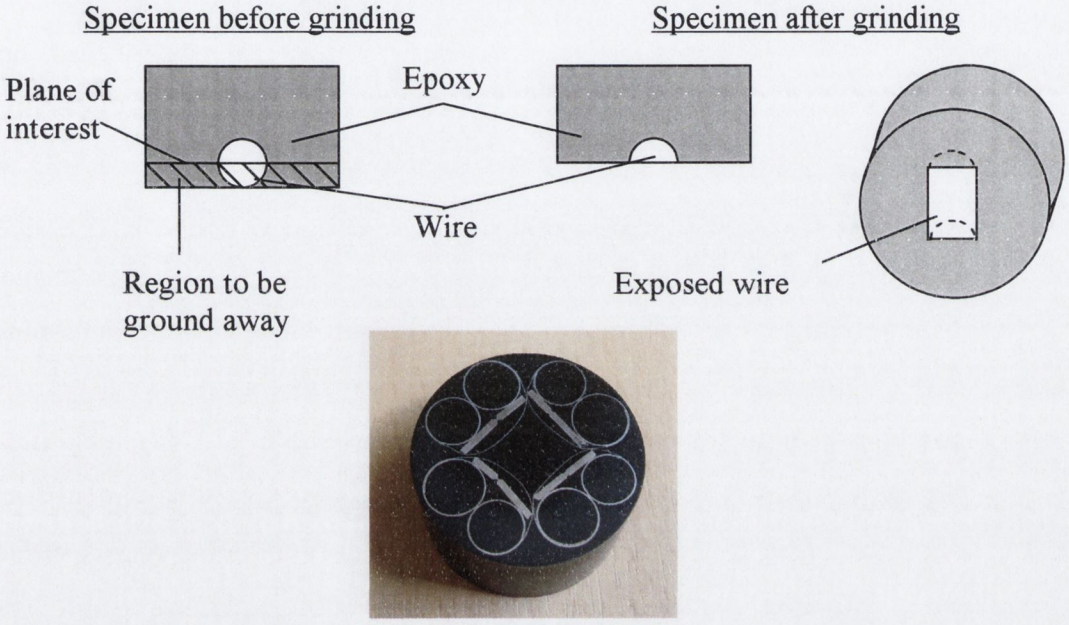

Figure 6.16: Grinding of mounted From Rolled parts

2. Fine Grinding – performs two functions. Firstly it grinds away workpiece material at a lower material removal rate thus reducing the risk of over grinding the workpiece. As grinding is an abrasive process it results in a scratched workpiece surface with the size of the scratches proportional to the grit size of the silica paper used. The second function of fine grinding is to reduce the size of the scratches on the workpiece surface to make polishing easier.
3. Polishing – is performed using a diamond pastes with aggregates ranging from 6 down to 1μm. Polishing is necessary if the microstructure of the specimen is to be investigated, as it produces a workpiece surface that appears free of scratches even at high magnification under a laboratory microscope. If polishing is not performed the scratches dominate the surface and the microstructure cannot be determined. Polishing is not always necessary (e.g. if the presence of internal failure is being investigated then it is not required).

6.4.3 Etching the Specimen

Etching was required when the grain structure of the specimen was to be investigated and it was only performed on mounted and polished specimens. When the presence of voids or other failures was being investigated, it was not necessary to etch the specimens as such defects were generally clearly visible on the polished surface.

6.4.4 Microscopy of Micro-Form Rolled Parts and Micro-Form Rolling dies

Initially, rolled parts were investigated using both optical microscopy and optical stereomicroscopy. The microscope used was a Leica DMLM which could provide fifty to a thousand times magnifications. The optical stereomicroscope used was a Leica S6D which could provide six to forty three times magnification. Both microscopes were used in conjunction with a digital camera which produced photographs of the magnified images.

Mounted specimens were examined using the optical microscope to determine the average grain size of the workpiece and the presence of internal failure

Although the stereomicroscope did not provide the same the level of magnification as the microscope, it was used to investigate the unmounted workpiece specimens because it had a greater depth of field, which was important when examining the curved surface of a form rolled part. However, in many cases, it was still not sufficiently powerful to observe the surface of form rolled parts and a Scanning Electron Microscope (SEM) was, therefore, used. The SEM has several advantages over optical microscopes when examining micro-form rolled parts:

- A SEM has a very large depth of field and the contoured surface of the form rolled part could, therefore, be clearly seen.
- An SEM can also provide much greater magnification then an optical microscope and although this was not exploited during this research it is an obvious advantage in the analysis of micro-form rolled parts.

The combined result of these advantages is that photographs taken with a SEM are far superior to those taken with an optical microscope as illustrated in Figure 6.17.

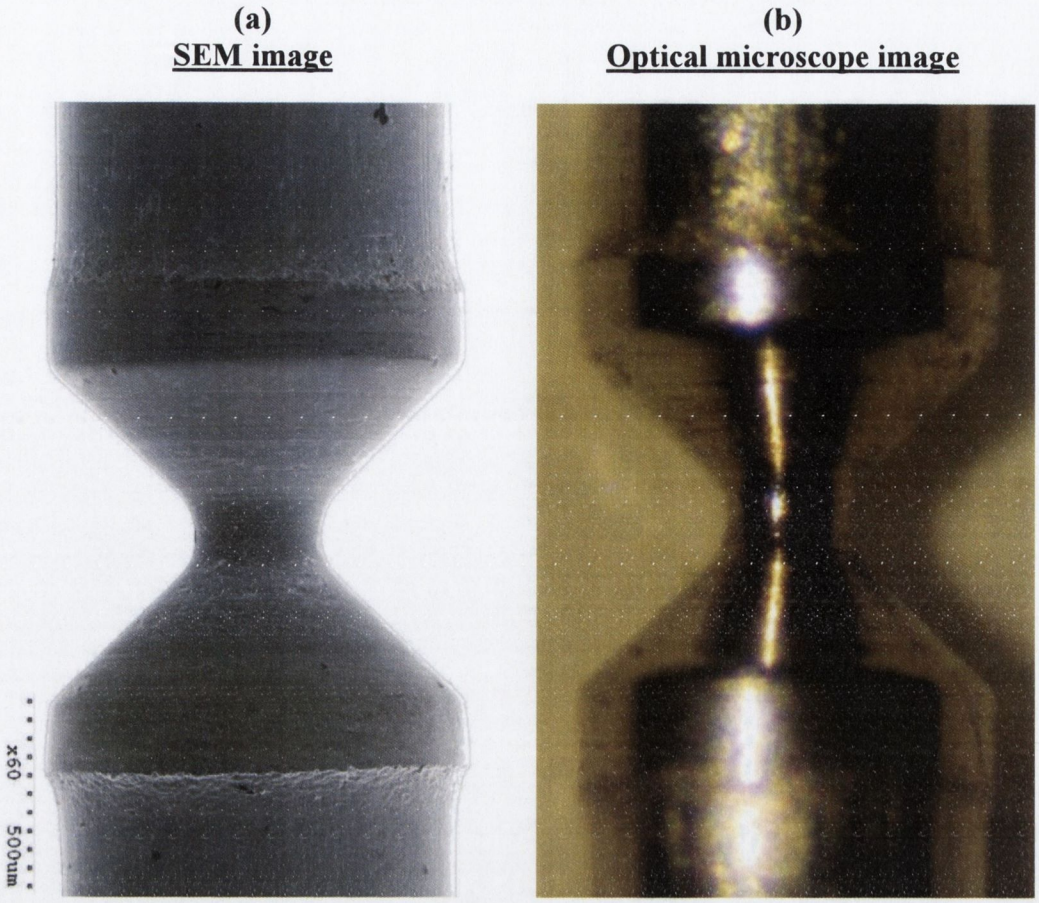

Figure 6.17: Photographs of a micro-form rolled part obtained using a Scanning Electron Microscope (SEM) and an optical microscope. 1mm ø Stainless steel part rolled with the 2mm ground die set to an area reduction of 92%

All of the workpiece in the SEM image is in focus. However, due to an insufficient depth of field some of the optical microscope image is out of focus. The superior quality SEM images were, therefore, used to analyse the surface quality of micro-form rolled parts.

6.5 Determining Accuracy and Dimensions of the Die Sets

The dimensions of all the die sets were measured and were compared with the specified design dimensions to determine the accuracy with which they were machined. The measured dimensions were also used to draw dies in graphics packages so that FEA simulations using the actual die geometries could be performed, thereby, allowing more accurate comparisons with the experimental results to be made. The dimensions on the x – y plane were measured using a Mitutoyo MT300 tool makers microscope, while dimensions in the z direction were measured using a micrometer, see Figure 6.18 for representation of the x, y and z axis in relation to the die.

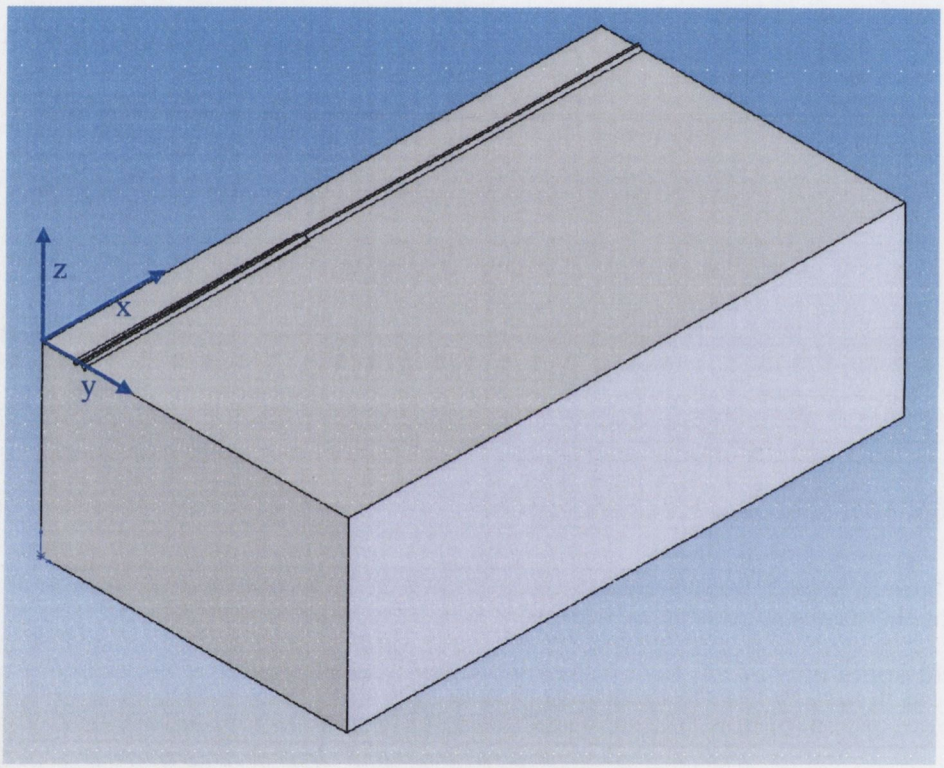

Figure 6.18: x, y and z axis relative to die

The die geometry can also be determined by taking measurements from SEM images of the die. Each SEM image has a graduated scale and by relating the length of this scale to the length of the die feature its dimensions can be measured. This was accomplished using the imaging software, ImageJ.

6.6 FEA of Form Rolling Process

6.6.1 2D Simulation Methods

To create a 2D simulation of the form rolling process a number of simplifications in the representation of the workpiece and tool segments were necessary. These simplifications are shown in Figure 6.19.

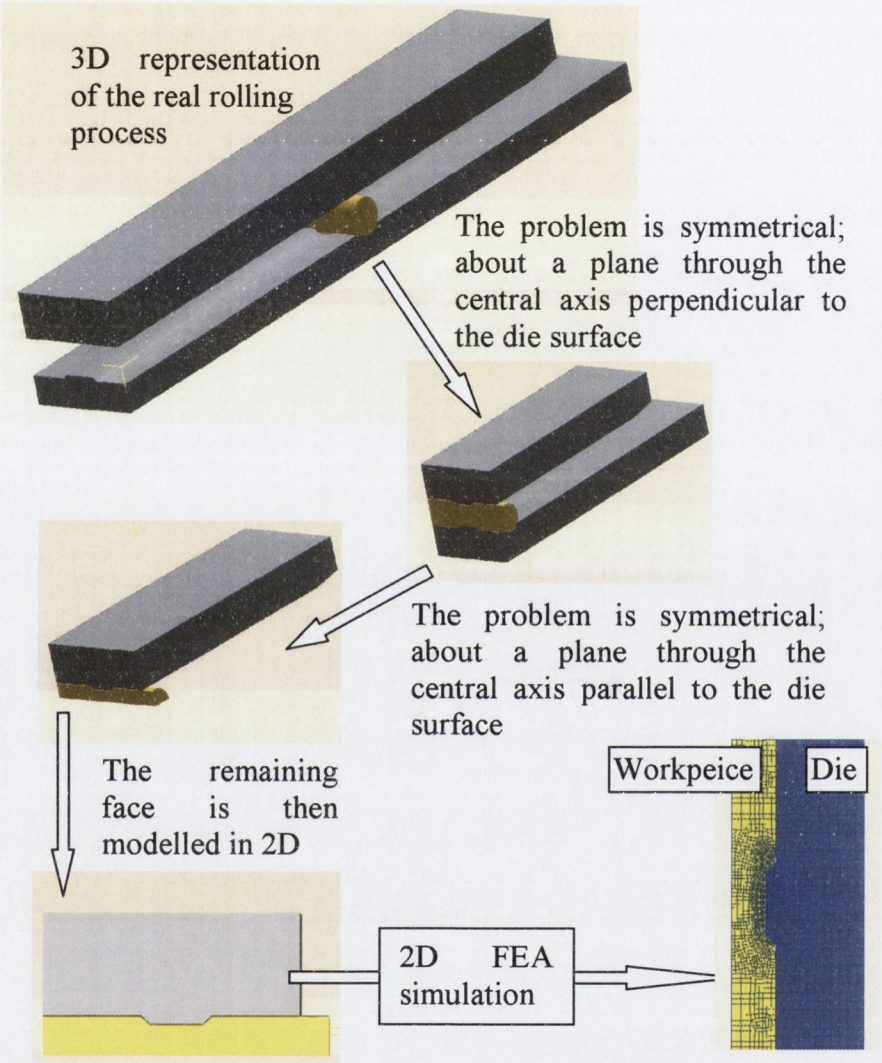

Figure 6.19: Converting the 3D form rolling process into a 2D simulation

Now that the process has been simplified to 2D it must modelled using either a plane strain or an axisymmetrical assumption. Both of these assumptions have limitations associated with them. When a plane strain assumption is used, the predicted area reduction in the workpiece, for a given die penetration, is less then in the actual form rolling process. This results in an underestimation of the strains in the workpiece and it arises because a plain strain assumption assumes cubic workpiece geometry when in reality it is cylindrical.

However, when an axisymmetric assumption is used the predicted strains in the workpiece are more accurate but the die stresses cannot be calculated. This is because an axisymmetric assumption requires a ring shaped die whose radius shrinks to deform the workpiece. Therefore, if accurate workpiece strains and stresses are required an axisymmetric simulation is recommended while a plane strain simulations is recommended for determining the die stresses.

In 2D FEA the form rolling process is usually modelled by deforming the workpiece progressively with a series of changing die profiles in a sequential fashion to represent the formation of the desired feature. The methodology of this method is explained in the following section. To determine the metal flow during the form rolling process the deformation of a plane located through the central longitudinal axis of the workpiece was examined; this can be simplified to half a plane as it is a symmetrical problem, see Figure 6.20

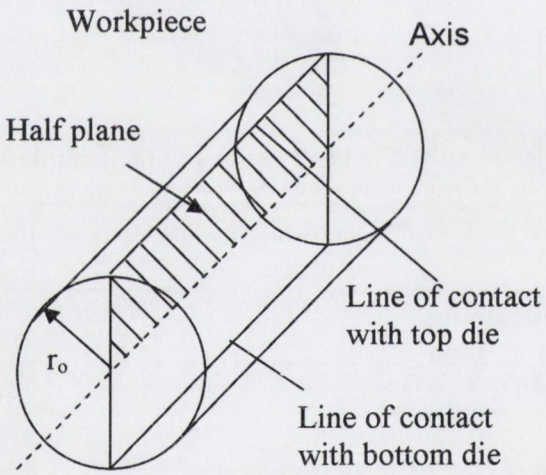

Figure 6.20: 2D simplification of 3D process

As the half plane rotates through 360°, it will contact the top die once and the bottom die once, therefore it contacts a die every half rotation. Each time this plane contacts a die, it is encountering a new die profile and is deformed from its old shape to the current shape of the die. A profile of the die is taken every πr_o along its length, where r_o is the workpiece radius, see Figure 6.21. πr_o is half the circumference of the workpiece or the distance travelled by the die during half a workpiece rotation.

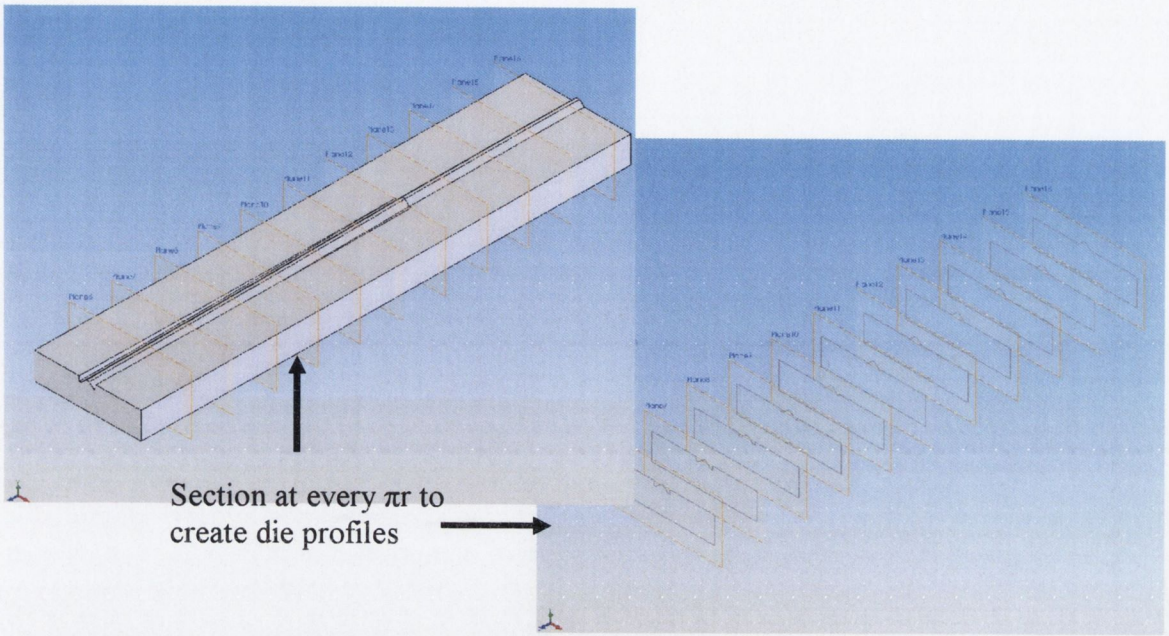

Figure 6.21: Sectioning the die to create die profiles to be used in 2D FEA simulations

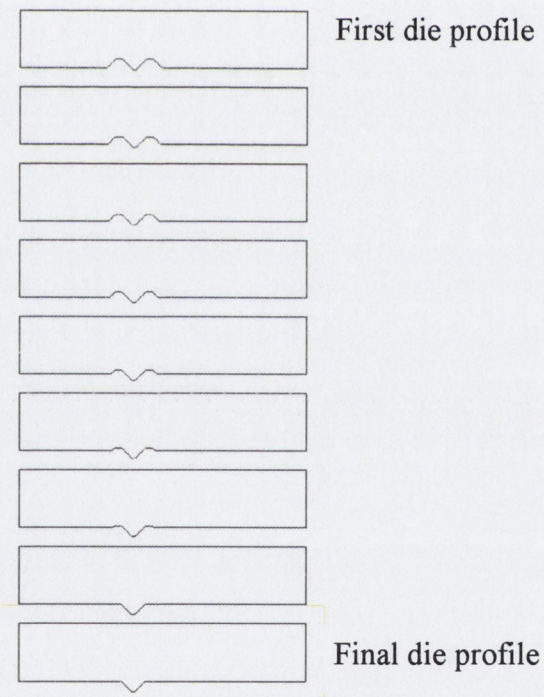

Figure 6.22: Die Profiles used in 2D FEA simulations

An example of a typical set of die profiles produced can be seen in Figure 6.22 above. Each of these profiles is then impressed upon the workpiece, so that it is gradually deformed to the desired shape, see Figure 6.23. The 2D simulation of the form rolling process can therefore be viewed as a sequential forging process, with the plane of interest

being deformed by a series of 2D die sections. This provides a simple method of modelling the process in 2D FEA [47].

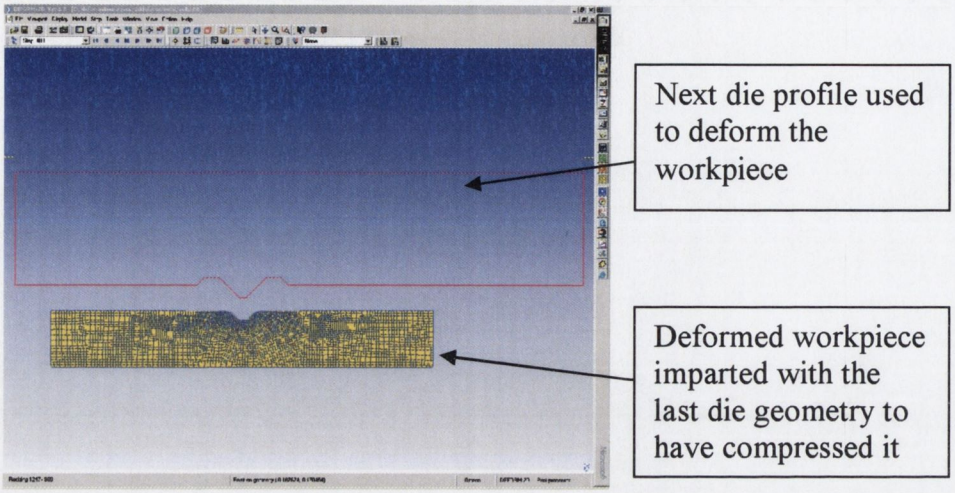

Figure 6.23: Image of 2D FEA form rolling simulation

The DEFORM package can represent an object such as the workpiece or the die as Rigid, Elastic, Plastic or Elasto-plastic. This enables a number of useful workpiece/die material behaviour combinations to be modelled.

1. Using a Rigid Object to represent the die and a Plastic Object to represent the workpiece results in fast processing times. Unfortunately, no information on the die stresses is produced and the predicted results for the workpiece stresses is less accurate than that provided by other material representations.
2. Using an Elastic Object to represent the die and a Plastic Object to represent the workpiece results in slower processing times than for a rigid die and plastic workpiece combination, but it is still relatively fast. Results are now provided for the die stresses, however, the information on the workpiece stresses is still less accurate than that provided by more realistic material models.
3. Using an Elastic Object to represent the die and an Elasto-plastic Object to represent the workpiece increases the processing times. However, this combination does provide better information on the workpiece stresses because, now, the residual stresses retained in the workpiece, following rolling, can be determined.
4. Using an Elasto-plastic Object to represent the die and an Elasto-plastic Object to represent the workpiece results in the slowest processing times. However, this combination provides the best results for the prediction of workpiece stresses and die stresses because the residual stresses are retained in both the workpiece and the

die. However, in industry, the die should not experience any plastic deformation so the use of an Elasto-plastic model to represent its behaviour is somewhat excessive - all that is required is to check that the die stresses do not exceed the yield stress of the die material.

6.6.2 3D Simulation Methods

Two different methods for investigating the process in 3D have been used. In the first method the dies rotate around a stationary workpiece while in the second method the fastener is rotated by the movement of one die relative to the other. Although the second method is obviously the most realistic approach as it more accurately represents the movements of the tooling of an actual machine, it was not initially possible to model the process in this fashion due to slippage between the workpiece and dies preventing the rotation of the workpiece. Furthermore, the rotating dies method also has the benefit of being less computationally intensive, allowing quicker simulation times for faster lead times.

In the rotational die modelling method, each die is given a translational velocity equal to half that of the die velocity in the actual process and, in addition, it is given a rotational velocity equal to that of the workpiece in the actual process, see Figure 6.24.

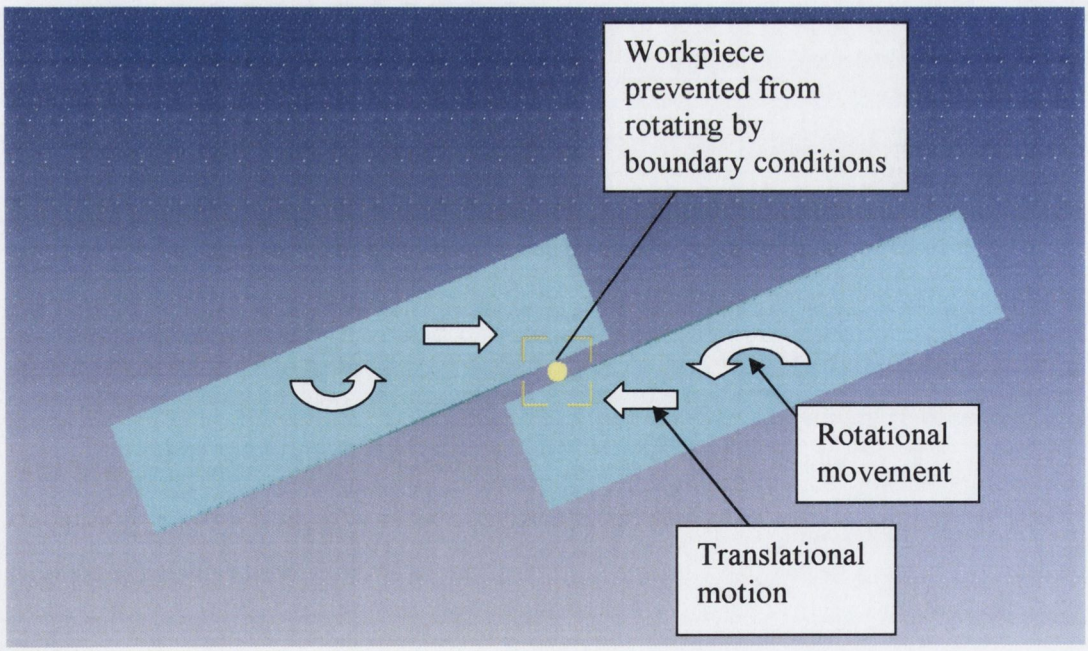

Figure 6.24: Images of 3D FEA with rotating dies

The rotational die method models the form rolling process by producing the same relative velocities between the dies and the workpiece as found in an actual rolling process, although this is done with somewhat unconventional die/workpiece movement.

A problem with this method is that it cannot be used to model interfacial slip as the movement of the fastener relative to the workpiece is provided by the problem definition rather than frictional interaction between the die and workpiece.

The developers of the DEFORM software produced an additional tool which allowed for the rotation of the workpiece without slippage and volume change. This enabled the process to be modelled with one stationary die and one moving die thereby inducing rotation of the workpiece in an identical manner to that of an actual process, see Figure 6.25.

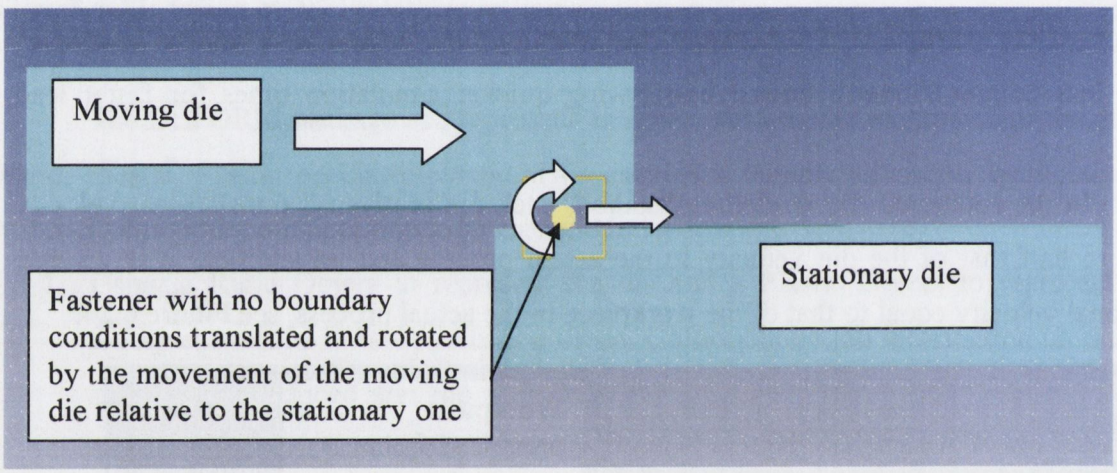

Figure 6.25: Images of 3D FEA with translating die

Despite these developments a number of problems still exist with this method. Firstly, it cannot be run with an Elasto-plastic workpiece (whereas the rotational die method can). However, time constraints would have prevented the use of a full Elasto-plastic 3D FEA model. And secondly choosing suitable contact conditions is difficult.

For the workpiece to rotate the contact condition between the workpiece and the dies, which is controlled by the friction factor and the initial compression of the workpiece, must be carefully specified. The initial compression of the workpiece is achieved by moving both dies radially into the workpiece and it is performed to increase the contact surface between the die and the workpiece and, therefore, improve traction and the prospects of rotation. To determine which values of friction factor and initial compression produced the most satisfactory results a large number of combinations were trialled. It was found that irrespective of the initial workpiece compression a high friction factor of one

was required; this is supported by Pater [55] who also recommended a value of one when performing 3D FEA of the form rolling process. The initial compression that produced workpiece rotation were typically between one and two percent of the workpiece radius.

This translating die method with a rotating workpiece meshes the workpiece using Rigid Super Elements (RSEs). The FEA solver considers the RSEs to be plastic unless the strain rate they are experiencing falls below a cut-off level set by the user in which case they are considered to be rigid. The workpiece is more likely to rotate without slippage when a high cut-off value is used and a large proportion of the RSEs are rigid, these conditions also improve the simulation times. However, if the cut-off value is too high the simulation results will be inaccurate because regions of the workpiece in which deformation is occurring will be considered to be rigid. Therefore, choosing a suitable strain rate cut-off value is very important and it proved to be problematic when simulating the micro-form rolling process. The majority of the deformation and, therefore, the high strain rates, are confined to the die/workpiece contact region while the strain rates in the centre of the workpiece are very low; however, knowledge of the stress state in the centre of the workpiece is important due to the process's propensity for developing internal failures. When the strain rate cut-off value was too high, the stresses in the centre of the workpiece were predicted to be compressive when they should have been tensile. It subsequently transpired that the strain rate cut–off value that could accurately predict the stresses in the workpiece centre, resulted in a workpiece that had insufficient rigid RSEs to rotate the workpiece. Therefore, RSEs, with a strain rate value of 0.1, and translating dies were used to predict the condition under which rolling would occur while the rotating dies method, which does not require RSEs, was used to predict the stresses and strains within the workpiece.

A range of form rolled pars using the 3D FEA package DEFORM are shown in Figure 6.26.

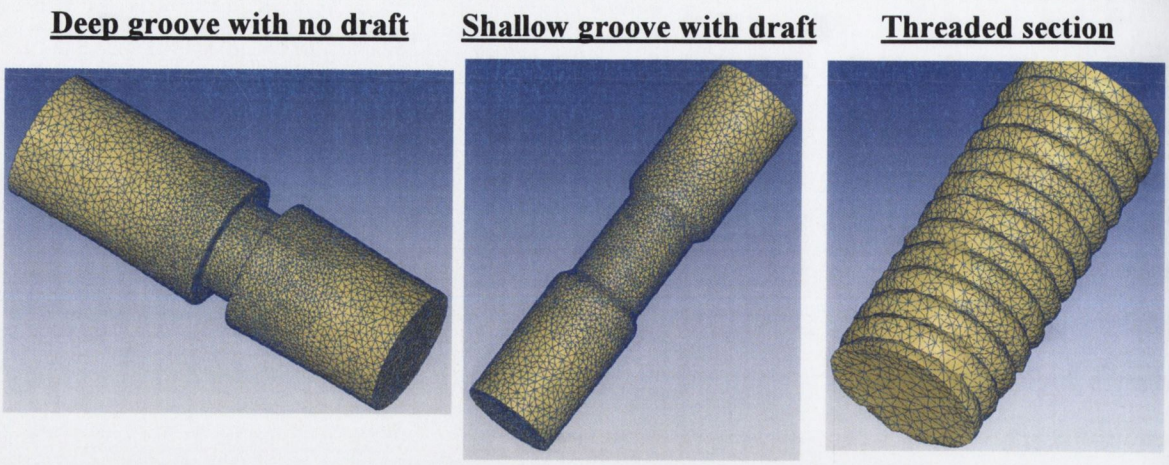

Figure 6.26: Pictures of parts modelled using 3D FEA with translating die

None of the fasteners illustrated have heads and this was done purposely to reduce the number of elements needed and because the stresses in the head of the part are not generally of interest. Also, most of the workpieces rolled during this research had no heads as they were cut from spools of wire.

A limitation of the 3D FEA used in this research is that it doesn't account for the Bauschinger effect, which results in a decrease in the compressive strength of a material after it has been strained to yielding in tension. The Bauschinger effect could affect the form rolling process because the workpiece undergoes cyclical stresses that alternate between tension and compression, however it will not be predicted by the FEA.

6.6.3 Stress Regions

To aid the understanding of the deformation mechanism being experienced by the workpiece, stress region plots were created. In these plots, the letters C and T indicate compressive and tensile stresses respectively, while x (radial), y (axial) and z (tangential) represent the directions of these stresses. The workpiece is divided into different regions depending on the combinations of x, y and z stresses, as Nefedov [29] did when modelling a Transverse Helical Rolling process. However, there is no function in DEFORM 2D for producing these plots so they were, therefore, produced manually using the following steps:

1. Individual stress plots were produced for the x, y and z directions, and these plots show the boundaries between tensile and compressive regions within the workpiece see Figure 6.27.

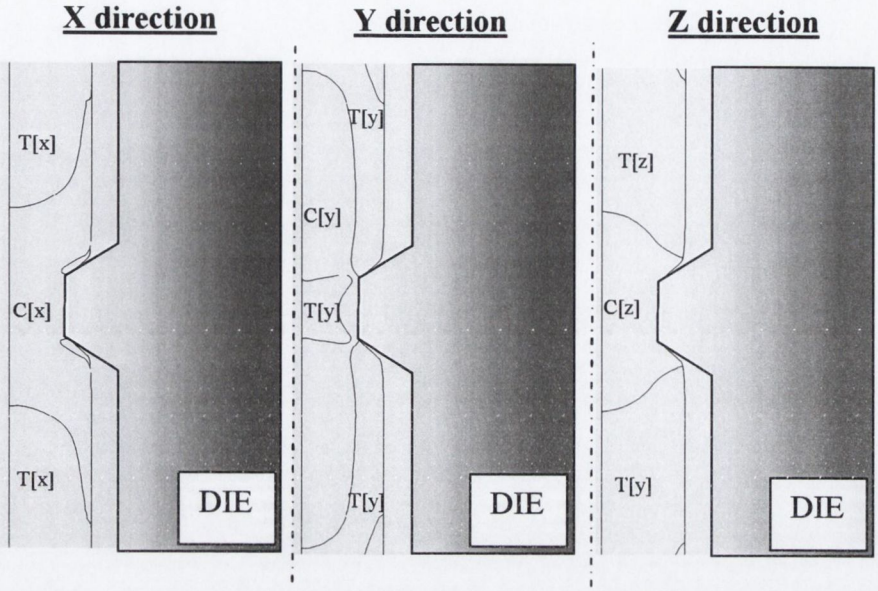

Figure 6.27: Plots of boundaries between tensile and compressive regions

2. These plots are then superimposed upon each other using a graphics package and C, T, x, y and z are used to distinguish the different stress regions, see Figure 6.28.

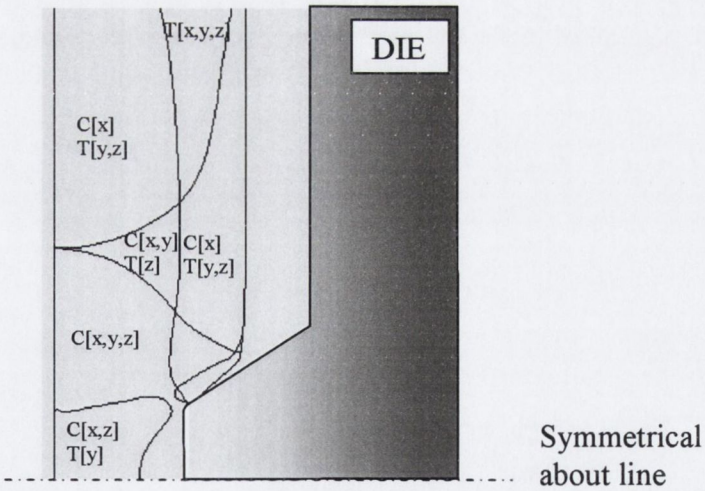

Figure 6.28: Stress Regions within a form rolled workpiece

6.6.4 **Damage Plots**

To aid the visualisation of the damage experienced by a workpiece during form rolling, damage plots were created. Each damage plot (see Figure 6.29), shows the changing level of damage along a series of tracking points in the workpiece as it is deformed by a die, see Figure 6.29. The 'relative distance to the surface' indicates the

distance of a point from the workpiece surface, i.e. a value of 0 is at the surface while a value of 1 is in the centre of the workpiece.

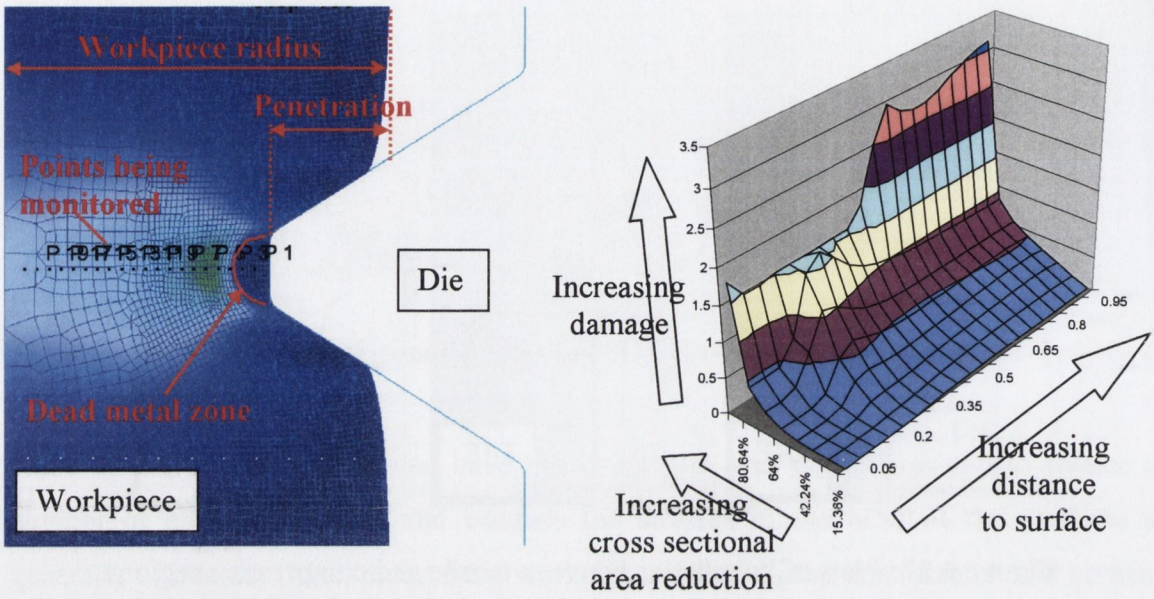

Figure 6.29: FEA of micro form-rolling damage

6.7 Successful Die Design

The design of dies that successfully rolled parts without interfacial slippage and excessive die wear is described in the following section.

6.7.1 Traction Surface

The provision of a suitable traction surface is critical to successful form rolling but many problems exist when designing and applying a traction surface to the surface of a die.

1. Choosing an appropriate surface roughness

When a workpiece is rolled, it takes the shape of the feature on the die and, likewise, if the die has a traction surface it is also impressed onto the workpiece, resulting in a rough surface close to the rolled feature, see Figure 6.30. The traction surface is applied to the die surface in the knifing zone until the force required to form the workpiece is sufficient to rotate it without the aid of a traction surface. After this point the part is rolled on a smooth die surface which can iron out the rough workpiece surface created by the traction surface. However, the surface quality of the workpiece can be permanently affected if the rough workpiece surface created by the traction surface is too rough to be ironed out.

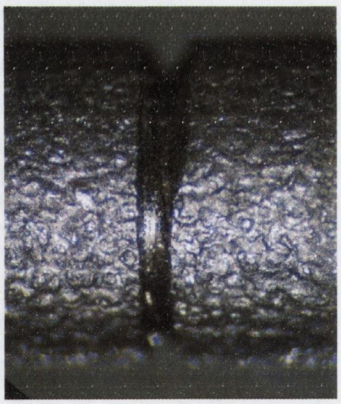

Figure 6.30: Roughened surface on the workpiece due to the EDM finish on the tooling

In this research the workpiece being form rolled, is actually relatively rough and the surface quality generally improves with rolling. This is evident in Figure 6.31 which shows a 2mm diameter stainless steel workpiece that was rolled with a die that had a traction surface with a Ra value of 0.69. While the rolled region of the workpiece has a Ra of approximately 0.2, the unrolled region has a Ra value twice that, see Figure 6.31

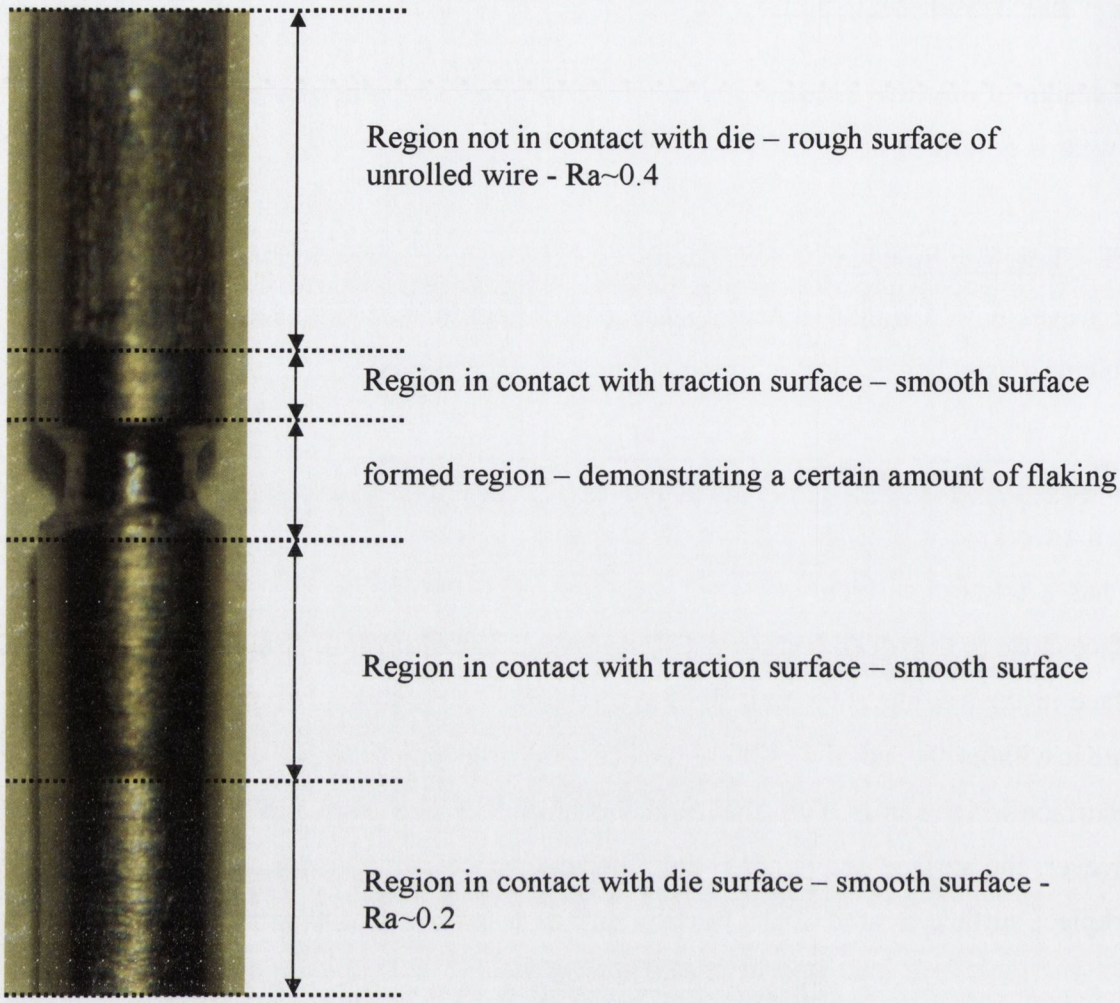

Figure 6.31: Improvement of surface quality with rolling

However, when the smallest die feature, a 0.07mm deep groove, was rolled onto the 0.45mm diameter wire then excessive roughness of the traction surface became problematic. For example, when this die and wire combination was used for one-die rolling with a flat die that had a traction surface created using 60 grit shot blasting, the workpiece deformation caused by the traction surface was comparable in scale to the groove geometry being formed on the workpiece as illustrated in Figure 6.32(a). This problem improved significantly when the traction surface was created using 120 grit, see Figure 6.32(b).

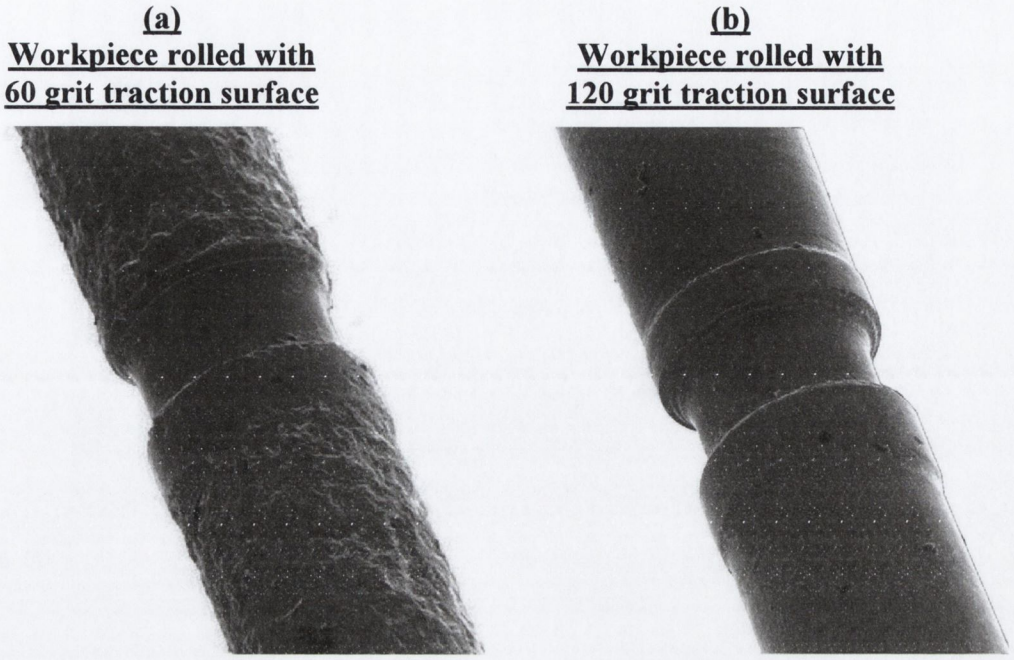

Figure 6.32 The scale of deformation on 0.45mm diameter wire due to traction surfaces created using 60 grit and 120 grit shot blasting

Therefore, although it is important to have a traction surface that is sufficiently rough to rotate the workpiece, if it is too rough it will adversely affect the surface quality of the workpiece.

2. Designing and applying a suitable traction surface

The selection of the optimum method for applying a suitable traction surface to the die proved difficult and during this research five different methods were investigated:

1. An EDM traction surface was applied in-house directly to the die surface. However, a number of problems were experienced with this method
    a. The surface roughness generated on the die was too high, with a Ra value of five micrometers
    b. Because EDM is a material removal process, the traction surface was below the areas of the die that were not subject to EDM. This meant that the workpiece was not in contact with the traction surface. This problem is illustrated in Figure 6.33 which shows blued dies in which no bluing is removed from the traction surface indicated a lack of die/workpiece contact.

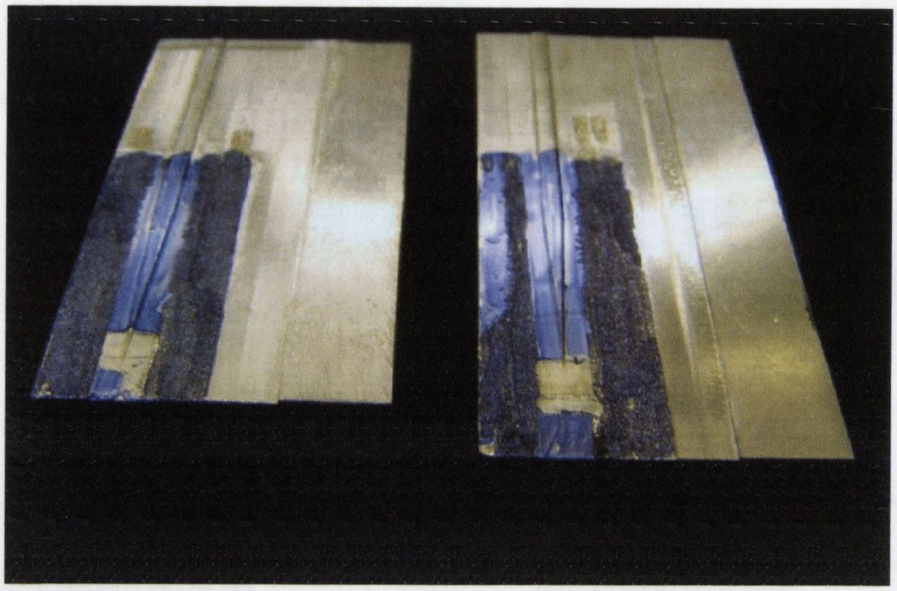

Figure 6.33: Blued dies demonstrating a lack of contact between the workpiece and the traction surfaces of the dies

c. The tool used to EDM the die surface was smaller than the required traction surface and therefore the tool had to be repositioned and plunged into the die several times resulting in an uneven surface.

2. To prevent the EDM traction surface being below the areas of the die that were not subject to EDM, raised surfaces on the die were used for the traction regions as shown in Figure 6.34.

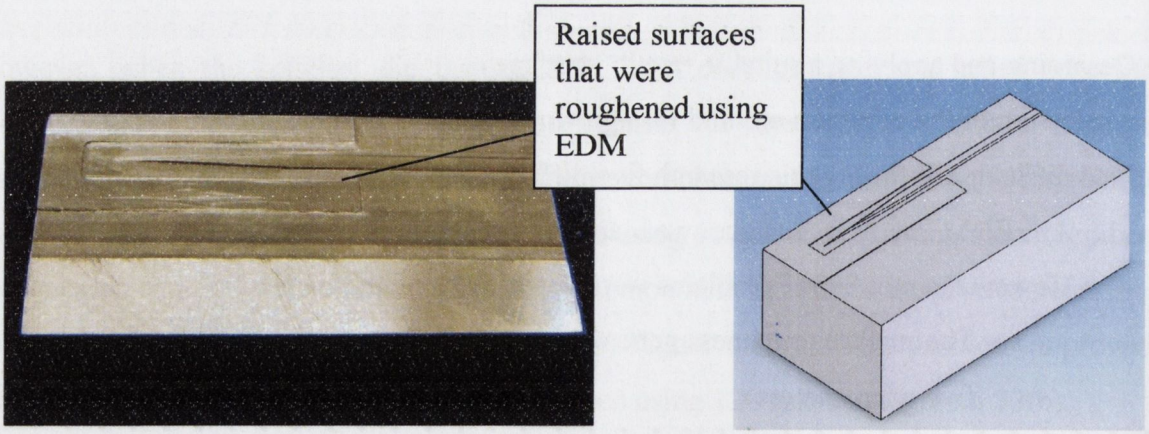

Figure 6.34: Photograph of a die with a raised area for the application of the EDM traction surface

However, the problems of an excessively rough and uneven traction surface still remained. A problem also arose due to the traction surface being generated on raised surfaces because once the workpiece reached the end of the traction surface

the die gap effectively increased resulting in a loss of contact between the workpiece and the die surface and therefore a drop in traction.

3. EDM surfaces were also applied in house to raised die regions using a prong shaped tool (see Figure 6.35) which allowed the entire traction surface to be applied in one plunge providing a level surface. However, the surface roughness applied to the die surface was still too high and the issue of increasing die gap at the end of the traction surface remained

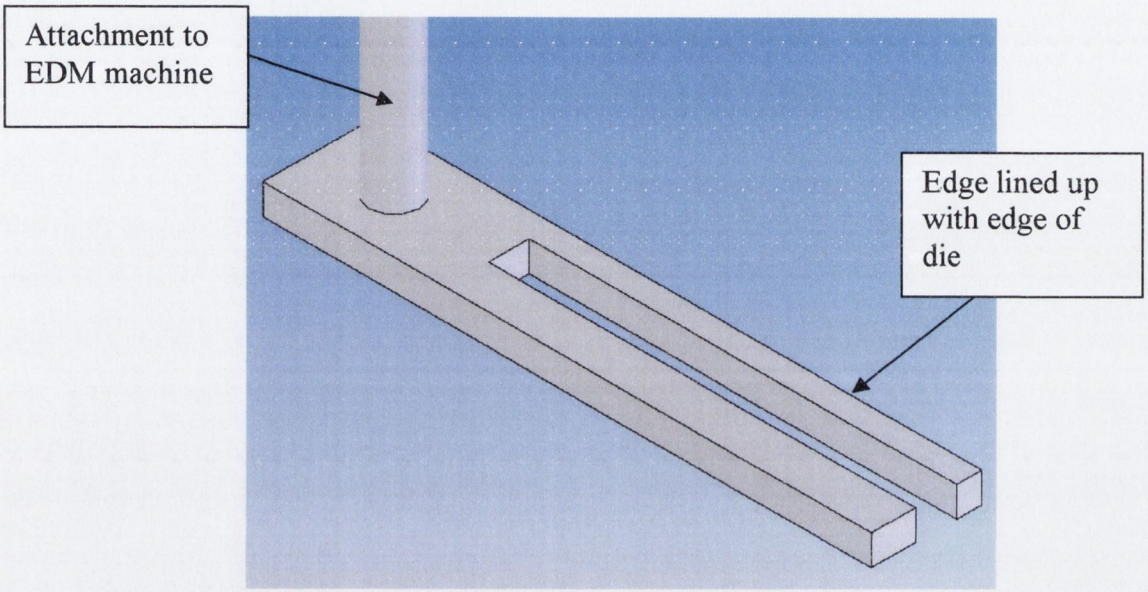

Figure 6.35: EDM prong used to selectively apply EDM traction surface to form rolling dies

4. Due to the difficulties in applying a suitable traction surface in-house, a grit blasted traction surface was trialled. Unlike EDM, grit blasting is not a material removal process and raised surfaces on the die were not required. The traction surface applied using grit blasting was also relatively smooth with a Ra of 0.69μm, see Figure 6.36. This surface worked very well for a range of dies and workpiece diameters and materials but the surface wore off after approximately one hundred workpieces had been rolled and this resulted in workpiece slippage.

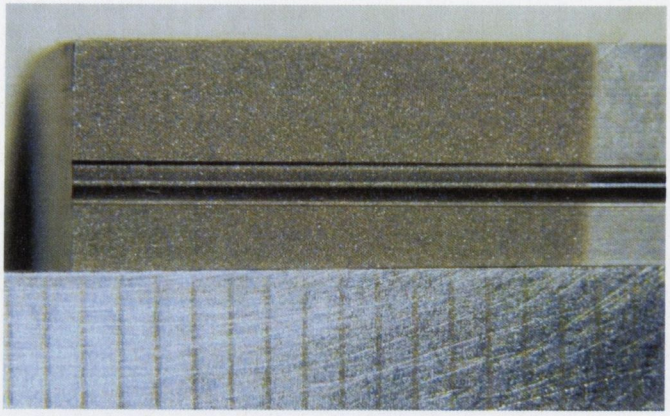

Figure 6.36: Photograph of grit blasted traction surface

5. Although the grit blasted surface was successful at rolling a variety of parts, its high rate of wear made it an impractical traction surface. Therefore, it was replaced with a smooth EDM surface with a Ra approaching that of the grit blasted surface, see Figure 6.37. Because the EDM surface was so smooth, it had a Ra of 0.85μm, there was very little material removal and raised surfaces on the die were not required. This EDM surface proved as successful at rolling parts as the grit blasted surface it was based on while being more robust and it is, therefore, deemed to be the most suitable traction surface for micro-form rolling.

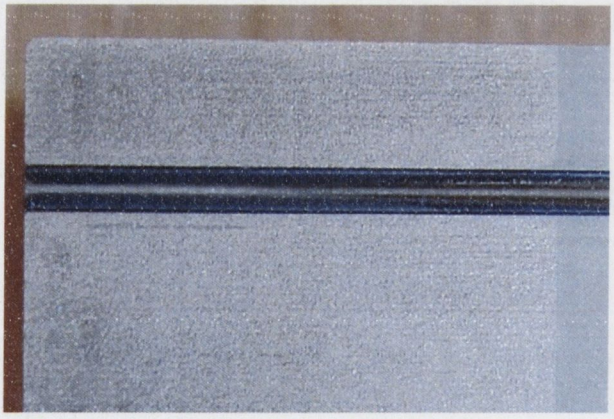

Figure 6.37: Photographs of EDM surface

The traction surface ran for over a third of the feature length (i.e. the combined length of the knifing and sizing zones). This is a relatively large proportion of the feature length to be covered in a traction surface however it was deemed necessary due to the small size of the feature being rolled.

6.7.2 **Die Material**

Two die materials were used during this project, pre-hardened P20 tool steel and D2 tool steel that was heat treated after machining. Although P20 is not regularly used for form rolling dies it has a number of advantages over D2 which made it worth investigating. Relative to D2, it is easier to machine and it does not have to be heat treated. Both of these factors should lead to improved dimensional accuracy of the finished die. The lead-time was also improved by removing the need for heat treatment. The major disadvantage of P20 relative to D2 in its hardened state of 60HRc, is its low compressive yield strength. D2 has a yield strength of approximately 2000Mpa while P20 yields at a relatively low value of 900Mpa and this proved to be insufficient for the form rolling of AISI 316 stainless steel. Dies made from P20 suffered catastrophic wear after rolling only one part, with the feature being heavily deformed by the workpiece, see Figure 6.38. For this reason, all the subsequent dies used in this project were made from D2.

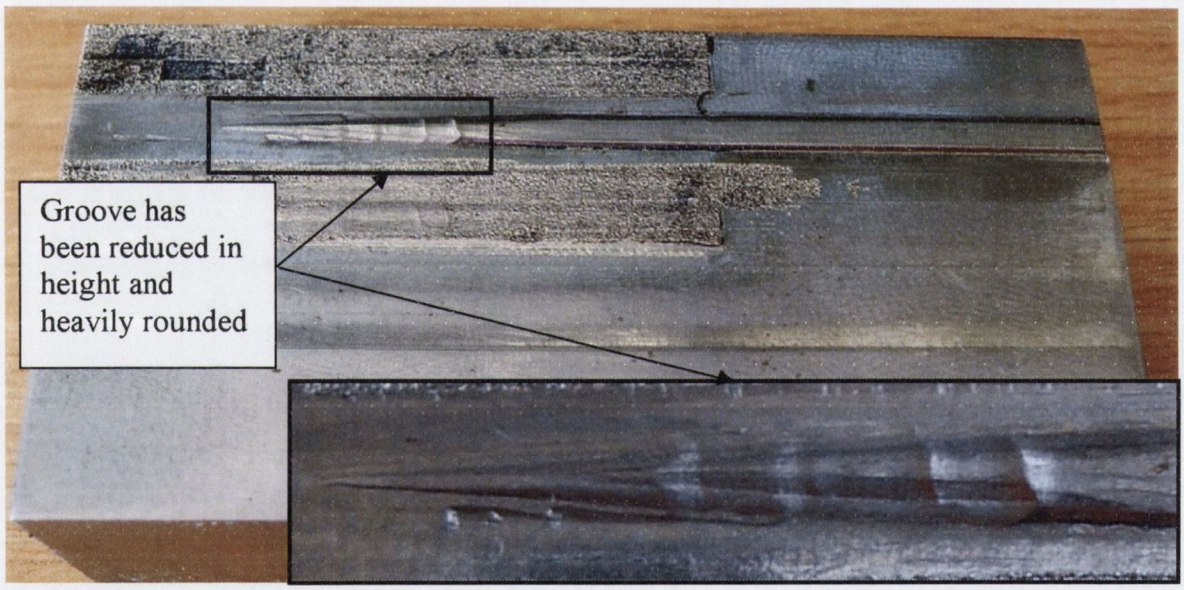

Figure 6.38: The excessive wear experienced by dies made from P20 during the form rolling of stainless steel

6.7.3 **Die Geometry**

The die geometry designed for this project was successful in rolling workpieces without interfacial slippage or the development of internal defects once the maximum area reduction was kept below a critical value of between 60 and 90%. This compares well with literature with several authors predicting the development of internal failure when area reductions exceed 50%. Most authors recommended a sidewall angle of less then 45°. The

spreading angle of 0.8° is actually considerably smaller than minimum recommended angle but it was used because of the small size of the feature being rolled and the large amount of die available due to the large size of the rolling machine compared to the workpiece.

The truncated triangle die design used in this research is significantly different from the other geometries found in literature, yet, it was still used to successfully form roll parts. The large flat on the tip of the die feature is present from the very start of the die. However using traditional die designs, this flat would be created using a spreading zone. This indicates that a wider variety of die design than is currently used can be successfully used to form roll parts.

6.7.4 Other Points on Micro-Form Rolling Die Design

When designing micro-form rolling dies, special consideration must be paid to the aspects of process that differentiate it from form rolling at larger scales. Due to the small diameters of the workpiece micro-form rolling dies have either no traction surface or a relatively smooth grit blasted or EDM surface. The lack of a traction surface can then lead to slippage of the workpiece. Slippage was prevented by positioning the starting point of the groove at the front of the stationary die, see Figure 6.39. This resulted in the workpiece being deformed from the very start of the stroke which encourages workpiece rotation.

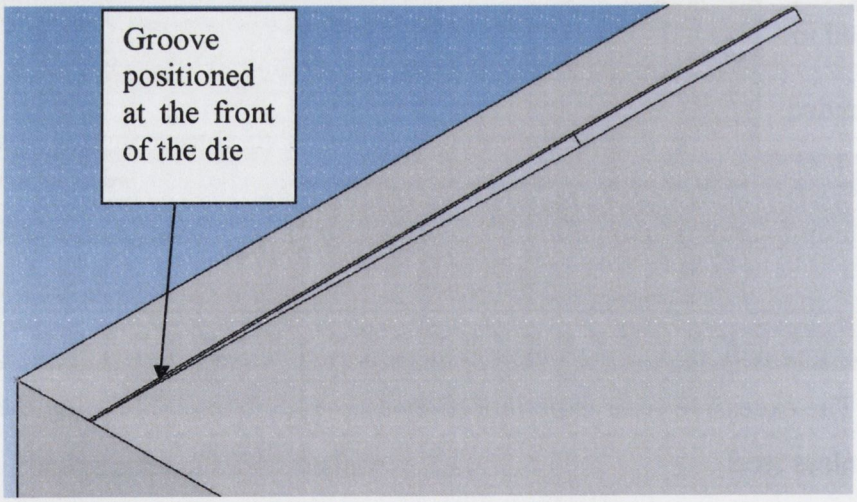

Figure 6.39: Start of groove positioned at the front of the die

For a die set to be used in a EWM AF3 form rolling machine, it has to be of a standard length and the number of workpiece rotations which can be achieved using these dies is the die length divided by the workpiece circumference. However, micro parts typically do not need the full length of the die as they have a very small circumference and can achieve a large number of rotations in a small distance. Therefore, they typically experience a

number of unnecessary additional rotations if they are rolled to the full length of the dies. Unfortunately, excessive workpiece revolutions are considered a factor in the development of internal failures due to low cycle fatigue and to reduce the number of workpiece revolutions, release pockets were ground into the dies, see Figure 6.40.

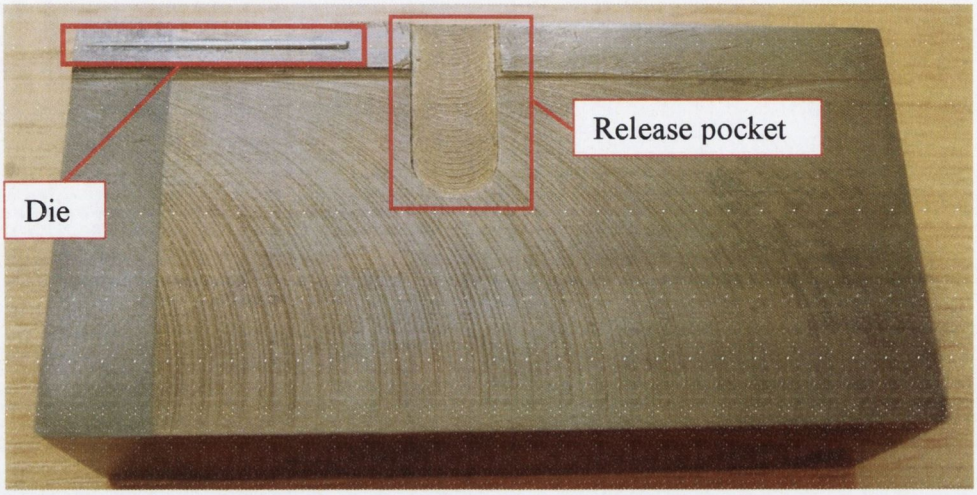

Figure 6.40: Release pocket in die to release wire after rolling

Release pockets were positioned after the die feature and when the workpiece entered the release pocket it lost contact with the dies and could be removed before the end of the rolling stroke.

6.7.5 Waste of Die Material with Miniaturisation

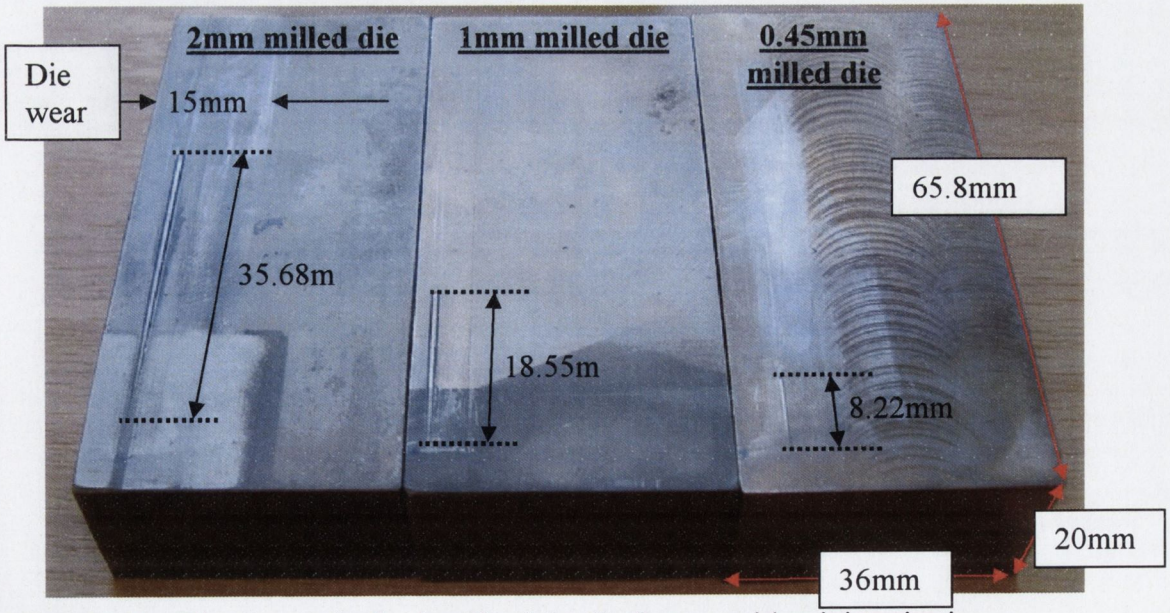

Figure 6.41: The change in the length of the die feature with miniaturisation

An unfavourable aspect of using a large rolling machine for micro-form rolling is the large size of the required die blank. For a die blank to be positioned accurately and securely in the EWM AF3 rolling machine, it has to be 20mm deep, 65.8mm long and 36mm high, as shown in Figure 6.41. However, the greatest length of wire rolled is only 15mm long, as illustrated by the wear on the dies shown in Figure 6.41, and the longest die feature is only 35.68mm long while the shortest feature is merely 8.22mm in length. Therefore, if the die size was determined by the length of the die feature and the wire being rolled rather than the depth of the rolling machine, then great savings in die material could be made. For example a die that was 8.22mm long and 15mm high would use only a twentieth of the material compared with a die with dimensions of 65.8mm long and 36mm high.

Decreasing the die size has the added benefit of reducing the amount of grinding and machining that is required to manufacture the die and, therefore, the lead time for die manufacture would also be decreased.

CHAPTER 7

RESULTS AND DISCUSSION

CHAPTER 7

RESULTS AND DISCUSSION

7.1 The size effect

7.1.1 The size effect in Micro-Form Rolling

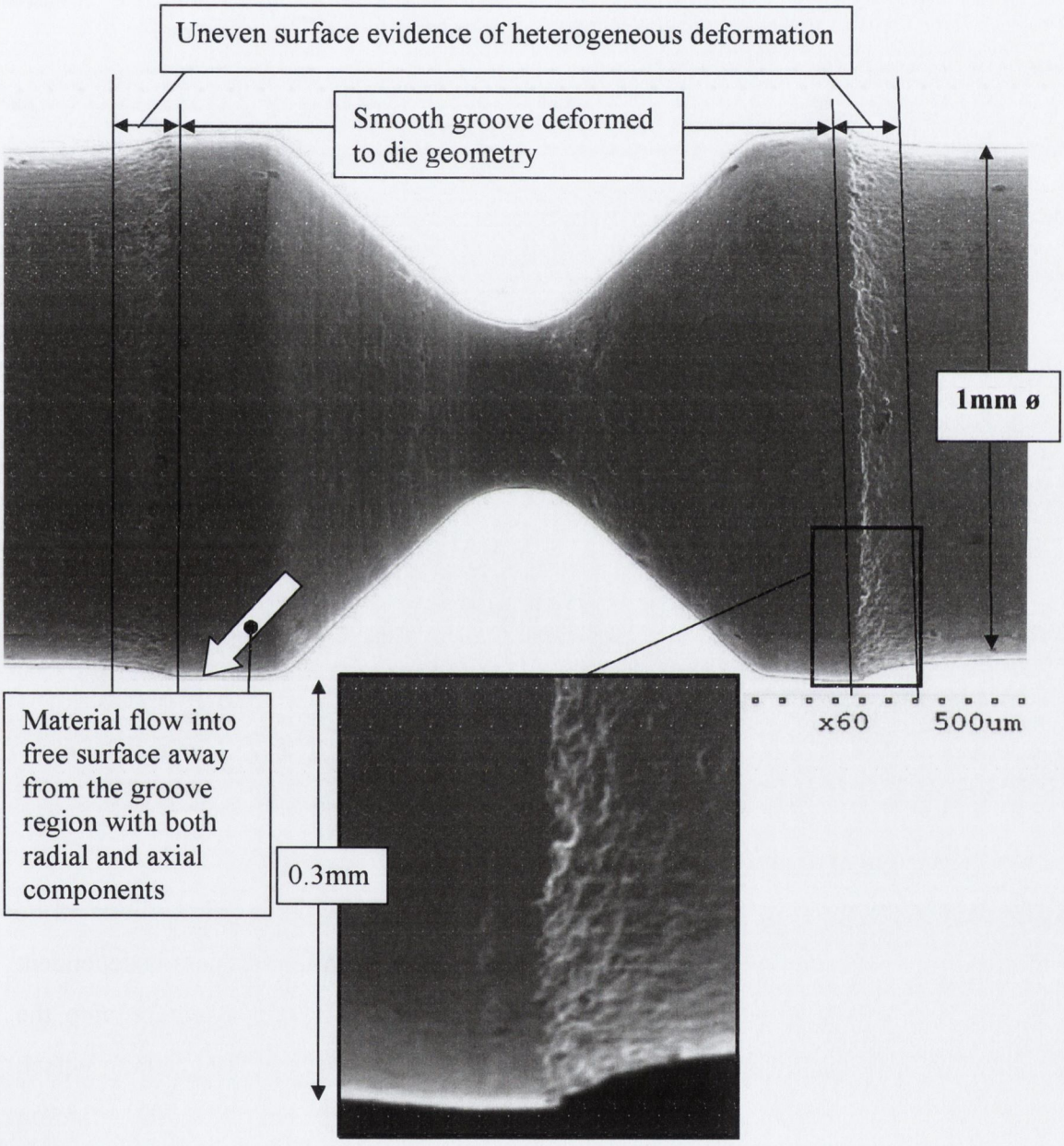

Figure 7.1: Heterogeneous deformation on the free surface of the workpiece

The micro-form rolled parts from this research project display very little evidence of the size effect. This is due to the compressive nature of the rolling process in which the die penetrates radially into the workpiece and, thereby, forces it to exactly conform to the

geometry of the die feature. However, the free surfaces of the workpiece which experienced material flow but were not in contact with the die surface were not so constrained and showed evidence of the size effect, in particular, heterogeneous material flow, see Figure 7.1.

The free surface was created during the formation of the groove when material was displaced in both the axial and radial directions as shown in Figure 7.1.

The scale of this heterogeneous deformation was much smaller than the feature being rolled and is, therefore, not generally problematic.

On larger diameter samples, heterogeneity of material flow on the free surface was not apparent. However, large 2mm diameter workpieces had rougher surfaces than the small 1mm diameter workpieces and this roughness tended to dominate the heterogeneous material flow which was small in scale, see Figure 7.2.

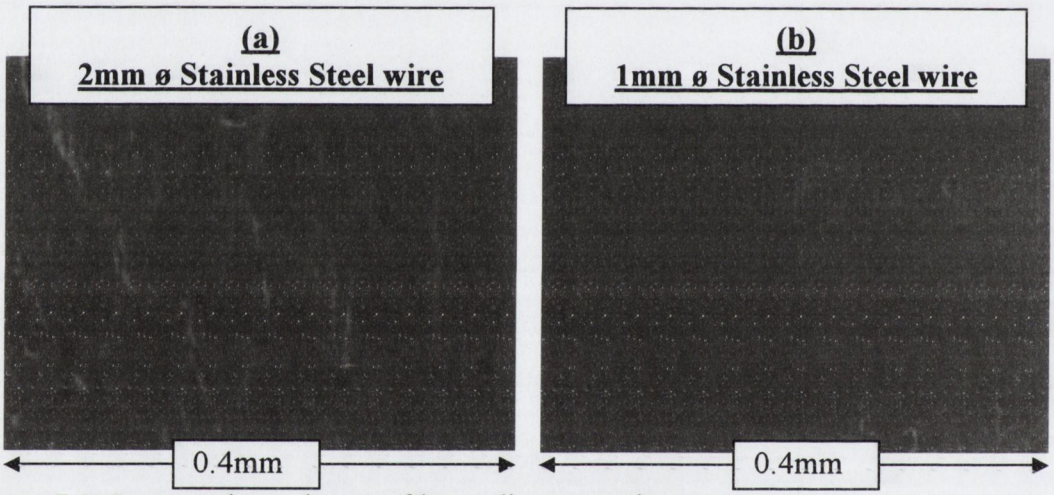

Figure 7.2: Increased roughness of large diameter wires

7.1.2 The size effect in the Grinding of Micro-Form Rolling Dies

A size effect in the grinding process used to manufacture micro-form rolling dies will be briefly discussed. The minimum feature size achievable in a grinding process is dependent on the grit size of the grinding wheel. It is impossible to machine a feature onto the grinding wheel that has dimensions which are less than the grit size of the grinding wheel. This proved to be the limiting factor when manufacturing die sets using the grinding process. The smallest dimension on the dies manufactured for this research was the flat width/top radius. The 2mm dies were the first to be manufactured using the grinding process and it proved very difficult to achieve the desired flat width which had to be redesigned to be rounded.

7.2 Limitations of Micro-Form Rolling

7.2.1 Accuracy of Milled Dies

As predicted by Bissacco [62], cutting tool deflection during the milling of the die sets had a negative effect on the accuracy of the micro-milled die-sets. The difference between the designed die geometry and the actual milled die geometry is illustrated in Figure 7.3 below. The z dimensions were largely unaffected by tool deflection and could, therefore, be machined to a higher accuracy than the dimensions on the x-y plane. The design dimensions and actual die as measured die dimensions are compared in Table 7.1 (a-c). They illustrate that the majority of the dimensions are quite close to the design dimensions, except for the flat width and the width of the base, which are located on the x-y plane. In general, the machined flat width and the base width were in the range of 0.2mm wider than those specified in the machining program. These errors are large in magnitude and tend to increase as the feature size is decreased, due to the constant magnitude of the error.

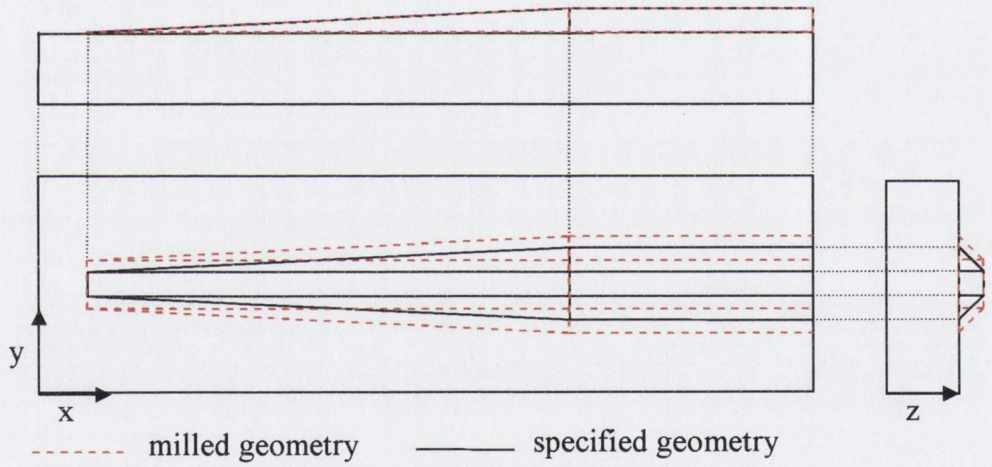

Figure 7.3: Accuracy of Machining – problems due to machining tolerances

Because these widths are actually the function of two cuts (one on either side of the feature), the tool deflection can be approximated to 0.1mm. The net result of the tool deflections is a groove as specified but for an increase in the flat width. Because the deflection is constant, the relative machining errors tend to increase as the feature size is decreased. For example, considering the die sets with a 45° sidewall angle the maximum error in the flat width is 645% for a 0.45mm mach. die, 255% for a 1mm mach. die and 215% for a 2mm mach. die.

Name	0.45mm milled die set with a 45° sidewall angle			0.45mm milled die set with a 45° sidewall angle			1mm milled die set with a 30° sidewall angle			1mm milled die set with a 30° sidewall angle		
Feature	groove			groove			groove			groove		
move/stat	moving			stationary			moving			stationary		
Material	D2			D2			D2			D2		
	design	actual	% error	design	actual	% error	design	actual	% error	design	actual	% error
feature positioning	5.00	4.93	-1.32	5.00	4.95	-1.06	2.03	1.88	-7.39	2.03	1.95	-3.94
	4.00	4.55	13.85	0.00	0.05	n/a	4.00	4.25	6.13	0.00	1.00	n/a
feature height	0.0825	0.07	-15.15	0.08	0.07	-15.66	0.18	0.17	-5.56	0.18	0.18	0.00
lengths												
ramp zone	5.91	5.96	0.85	5.91	5.91*	n/a	12.89	12.78	-0.88	12.89	12.70	-1.47
sizing zone	2.83	2.26	-20.21	2.83	2.83*	n/a	5.85	6.06	3.59	5.85	5.85*	n/a
overall length	8.62	8.22	-4.66	8.62	8.47	-1.71	18.74	18.84	0.54	18.74	18.74*	n/a
feature width												
flat in ramp zone	0.03	0.17	521.82	0.03	0.14	390.91	0.10	0.27	167.00	0.10	0.23	128.00
flat in sizing zone	0.03	0.21	645.45	0.03	0.13	372.73	0.10	0.31	214.00	0.10	0.32	216.00
width of base	0.19	0.43	123.90	0.19	0.28	44.94	0.72	0.96	33.61	0.72	0.88	22.36
Angles												
α	45.00	40.86	-9.20	45.00	78.39	74.19	30.00	33.16	10.54	30.00	42.41	41.36
β	0.80	1.06	32.13	0.80	0.73	-9.13	1.39	1.46	4.75	1.39	1.26	-9.14

Table 7.1(a): Accuracy of 0.45mm milled and 1mm milled dies 30° sidewalls

Name	1mm milled die set with a 45° sidewall angle			1mm milled die set with a 45° sidewall angle			1mm milled die set with a 60° sidewall angle			1mm milled die set with a 60° sidewall angle		
Feature	groove			groove			groove			groove		
move/stat	moving			stationary			moving			stationary		
Material	D2			D2			D2			D2		
	design	actual	% error	design	actual	% error	design	actual	% error	design	actual	% error
feature positioning	1.89	1.81	-4.07	1.89	1.42	-24.71	1.820	1.729	-5.0	1.82	1.843	1.26
	4.00	4.02	0.40	0.00	0.00	n/a	4.000	4.794	19.9	0	0	n/a
feature height	0.18	0.18	0.00	0.18	0.17	-5.56	0.180	0.170	-5.6	0.18	0.17	-5.56
lengths												
ramp zone	12.89	12.60	-2.27	12.89	12.50	-3.03	12.890	12.242	-5.0	12.89	12.3	-4.58
sizing zone	5.85	5.96	1.81	5.85	5.89	0.75	5.850	6.236	6.6	5.85	6.832	16.79
overall length	18.74	18.55	-1.00	18.74	18.39	-1.85	18.740	18.478	-1.4	18.74	19.13	2.09
feature width												
flat in ramp zone	0.06	0.21	245.00	0.06	0.21	255.00	0.100	0.162	62.0	0.1	0.117	17.00
flat in sizing zone	0.06	0.21	248.33	0.06	0.17	176.67	0.100	0.181	81.0	0.1	0.163	63.00
width of base	0.42	0.59	39.52	0.42	0.48	14.29	0.310	0.426	37.4	0.31	0.45	45.16
Angles												
α	45.00	46.26	2.80	45.00	45.89	1.97	60.000	54.224	-9.6	60	49.83	-16.95
β	0.80	0.78	-2.30	0.80	0.76	-5.47	0.460	0.573	24.6	0.46	0.668	45.22

Table 7.1(b): Accuracy of 1mm milled dies with 45° and 60° sidewalls

Name	2mm milled die set with a 45° sidewall angle			2mm milled die set with a 45° sidewall angle		
Feature	groove			groove		
move/stat	moving			stationary		
Material	D2			D2		
	design	actual	% error	design	actual	% error
feature positioning	4.36	4.30	-1.49	4.36	4.07	-6.61
	4.00	4.35	8.73	0.00	2.08	0.00
feature height	0.36	0.30	-16.67	0.36	0.33	-8.33
lengths						
ramp zone	25.78	25.39	-1.51	25.78	22.92	-11.08
sizing zone	12.57	10.29	-18.18	12.57	13.38	6.42
overall length	38.33	35.68	-6.92	38.33	36.30	-5.29
feature width						
flat in ramp zone	0.12	0.34	180.83	0.12	0.33	176.67
flat in sizing zone	0.12	0.38	215.00	0.12	0.38	214.17
width of base	0.84	1.03	22.26	0.84	0.96	14.64
Angles						
α	45.00	45.43	0.96	45.00	49.66	10.37
β	0.80	0.68	-15.59	0.80	0.70	-12.21

Table 7.1(c): Accuracy of 2mm milled dies

Although the width of the die features was significantly larger than specified, it was beneficial because it allowed the effect of wide flats on the form rolling process to be investigated and compared to the narrow flats found on the ground dies. It was subsequently found that a workpiece rolled with a die set which had a wide flat, experienced significantly different deformation compared to a workpiece rolled with a die set which had a narrow flat. This is discussed in greater detail later in this chapter. The percentage error for the feature positioning was also quite large on some of the dies. However, this was not a critical tolerance because inaccuracies in the feature positioning could be accounted for when the dies were setup on the form rolling machine.

A set of 1mm milled 45° sidewall dies was also milled from P20 prehardened tool steel. These dies lacked the requisite strength to be used for form rolling and the suffered catastrophic wear after rolling one sample. However, the errors of the flats on this die set was approximately 80% or one third of the error associated with dies milled from D2. Therefore, if the accuracy of the process is to be improved, softer materials could be rolled with dies milled form P20.

Cutting tool breakage, as predicted by Bissacco [62], was also an issue when small diameter cutters were used; 0.5mm cutters proved to be too fragile and several would have been required to machine one die. Therefore the smallest cutters used were 1mm in diameter and these proved to be much more resilient.

With increasing miniaturisation, it became much more difficult to monitor the process because the features being milled and the cuts being made were so small that it was very difficult to determine if the milling was proceeding as planned. Issues that could affect the process were incorrect CNC programs or inaccurate zeroing of the die. It was only when the milling process was finished that the die could be examined under a microscope and the success of machining could be determined decisively. This could have a significant effect on the lead time because machining a die, typically, took ten hours, so re-running the program would cost a working day.

Measuring the dimensions of the dies also proved to be quite troublesome for two reasons. Firstly, the length of the groove feature is actually very long and the flat width and groove width tended to vary slightly over the length of the feature. It was difficult, therefore, to make a definitive measurement of the features width. Secondly, due to the small size of the features, even a small mistake during measurement can result in a large relative error in the measured dimension.

7.2.2 **Limitations Associated with Machine Adjustability**

The setup of the form rolling machine becomes more difficult as the resolution of the adjustment being made and the size of the feature or the diameter of the wire gets smaller. The smallest possible machine adjustment is relatively large compared to the wire diameter or feature being rolled. The three types of machine adjustment will now be discussed individually:

Die Gap - The smallest possible adjustment in the die gap is 0.02mm, which is relatively small when dealing with large diameter wires of up to 3mm or 0.67% of the 3mm wire. However, when dealing with smallest wire used in this project with a diameter of 0.45mm, the adjustment of 0.02mm represents 4.44% of the 0.45mm wire diameter.

Stationary Die Height - It is a similar story when considering the die height, which can also be raised or lowered by 0.02mm by one turn of a thumb wheel. There are no markings on this wheel so the repeatability of the adjustment is somewhat difficult. However, it is quite possible to get a resolution of 0.005mm by adjusting the wheel in quarter revolutions. This is still nearly 4% of the flat width of the 0.45mm tooling which was the smallest feature

dimension used in this research. If a smaller feature was to be used or the accuracy improved, then a modification to the machine would be necessary so that the resolution of this adjustment could be improved further. Replacing the thumb wheel with one graduated to 1/20 of a revolution would allow a repeatable resolution of 0.001mm.

Starting Point of the Moving Die – An error in the starting point of the die is a linear distance and it is, therefore, related to the workpiece through its circumference. The starting point of the moving die is adjusted in rather crude steps of 0.5mm. These adjustments are very large when it is considered that the 0.45mm wire has a circumference of only 1.414mm meaning the adjustment represents 35.36% of the wire circumference, for larger 3mm diameter wire the adjustment represents just 5.31% of the wire circumference.

The setup of a form rolling machine is an iterative process in which a workpiece is rolled and then measured under a tool-makers microscope after each adjustment of the machine to determine if any subsequent adjustments are required. Obtaining satisfactory measurements using the tool-makers microscope became more difficult with miniaturisation.

The comments above highlight that the importance and difficulty of machine setup increase with part miniaturisation. The difficulty with the die gap setup can be eased somewhat by firstly setting the die gap for a larger diameter wire and then adjusting the die gap down for the smaller diameter wire.

7.2.3 **The Limitations of Measurement Accuracy and its Effect on FEA Simulations**

Significant errors can arise if there is a difference between the die geometry used in the rolling trials and that used in FEA simulations. For example, in experimental tests internal void formation occurred when 1mm stainless steel wire was rolled with the 2mm ground dies. However the 2D FEA simulations predicted maximum damage values, and therefore the likely fracture zone at a position towards the surface of the workpiece, as shown in Figure 7.4(a).

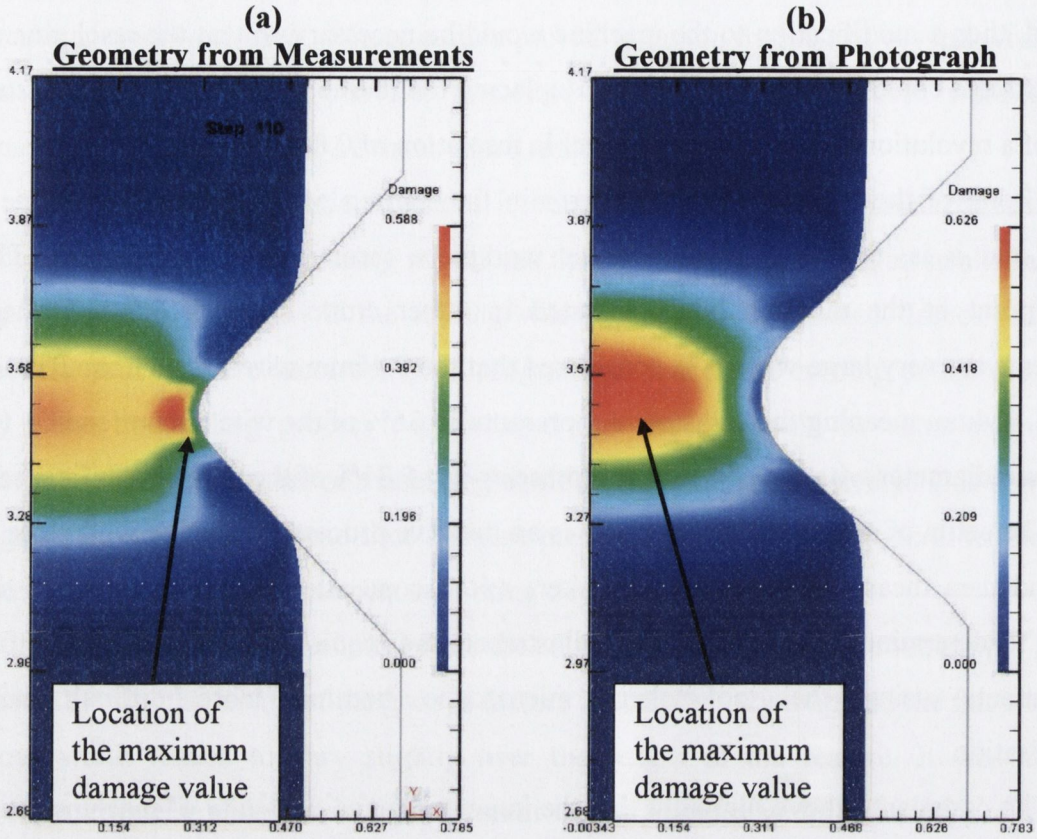

Figure 7.4: The location of the maximum damage values in the workpiece when the die geometry is created using measurements and a trace of a photograph

The incorrect location of the maximum damage values was due to errors in the geometry of the rigid object used to represent the die in 2D FEA simulations. The geometry was drawn using dimensions of the die measured using a toolmakers microscope. Although this technique proved to be sufficiently accurate for the milled die sets it was unsatisfactory for the 2mm ground die set due to their complicated curvature. Therefore, to create more realistic die geometry for the FEA simulations, it was necessary to replicate the actual geometry of the ground die set more precisely. To do this, a photograph of the die was imported into the CAD package, SolidWorks, and its geometry was traced. This geometry was then saved as a dxf file and imported into the DEFORM 2D FEA package.

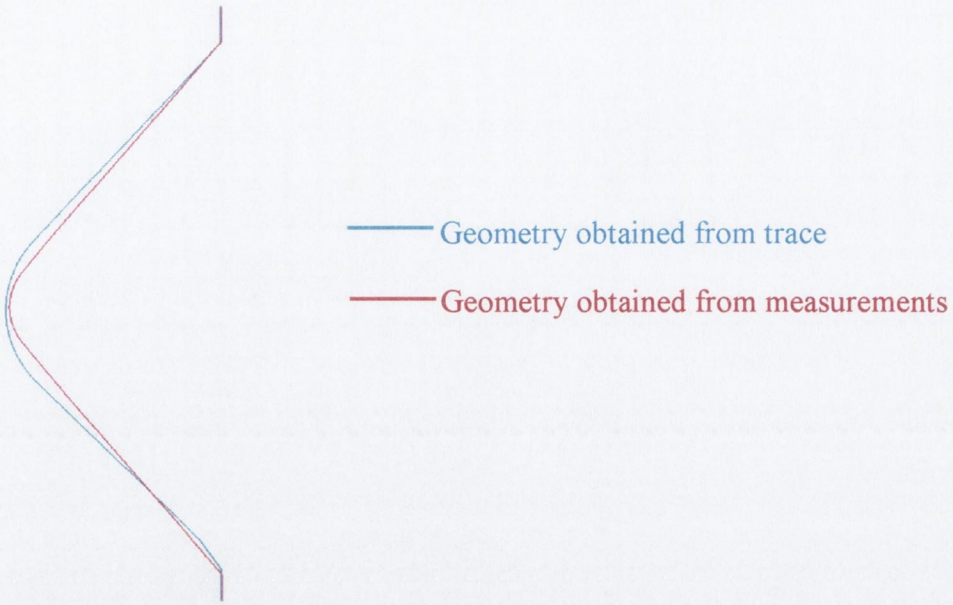

Figure 7.5: Difference in the geometries obtained from measurements and trace

Figure 7.5 illustrates that although the two geometries have the same groove widths and depths and similar sidewall angles the geometry obtained from the trace has a blunter tip, which results in significantly different damage profiles and values. Blunter die geometries tend to force the maximum damage value towards the centre of the workpiece, as shown in Figure 7.4(b). The location of the highest damage values at the centre of the workpiece corresponds well with the experimental results in which the workpiece was found to have failed along its central axis.

The results also indicate that relying on specified die dimensions may not be sufficient for the accurate FEA of the process if the scale of manufacturing errors is large, because the FEA results obtained may vary significantly depending on whether the specified or the as machined dimensions are used. Therefore, for FEA to be a useful tool, the die geometry must be machined to a high accuracy so that the machined dimensions are the same as the specified dimensions. This will allow the accurate prediction of the stress state within the deforming workpiece using the specified die dimensions, which will allow a die geometry to be investigated using FEA before it is manufactured.

7.3 The Quality of Milled Die Sets

7.3.1 Steps on the Sidewall of the Milled Die Sets

The milling process creates sidewalls that have a stepped geometry, with each step representing the width of cut used in the machining programme, see Figure 7.6.

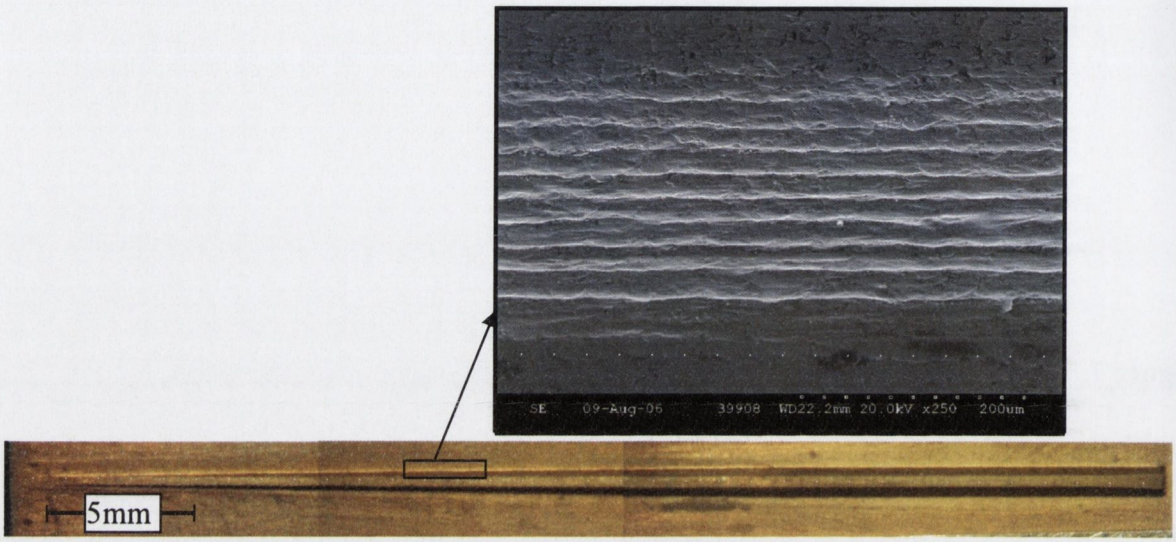

Figure 7.6: Photographs from stereo-microscope and SEM illustrating the machining lines on the die sidewalls

As Figure7.7 below shows the shape of the die improves with a reduction in cut size, however the machining time increases as the depth of cut is reduced and therefore a balance between machining time and geometric accuracy must be obtained.

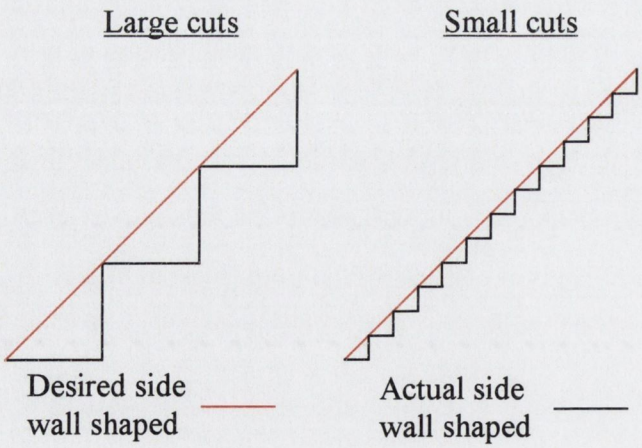

Figure 7.7: The improvement of die shape with the reduction of machining cut size

The die sets were lightly polished after machining which smoothed the sidewalls somewhat but did not completely remove their stepped geometry. Therefore, the actual geometry of

the die is not as pronounced as that shown in Figure 7.7 as the corners of the steps were blunted by polishing.

7.3.2 Burrs

After machining burrs were sometimes found running along the top corners of the die features. Typically they were removed after the dies were polished however sometimes they could not be removed. Three observations about the location and magnitude of the burrs were made:

1. They are typically more pronounced on the bottom sidewall of the die, see Figure 7.8(a)
2. They tended to be located in the knifing zone of the die rather than the sizing zone, see Figure 7.8(a-c).
3. They were more pronounced on the smaller dies, see Figure 7.8(a, d)

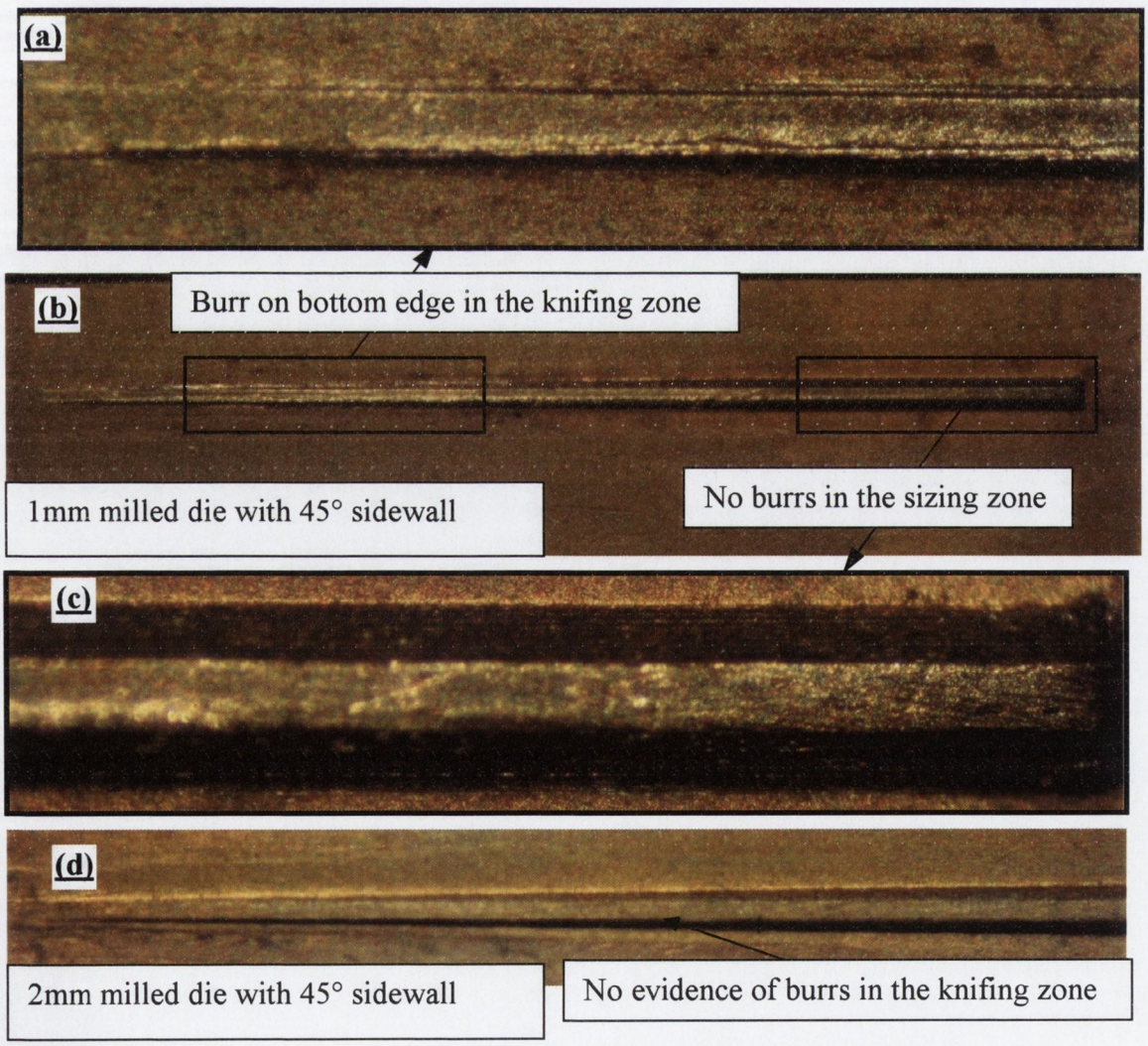

Figure 7.8: Evidence of burrs on dies – photographs from stereo-microscope

The use of a new cutter also seemed to reduce the magnitude of the burrs, this is most likely due to the effect of increased blunting of the tool due to tool wear and the ploughing of the die material as predicted by Bissacco[62].

7.4 The Quality of Micro-Form Rolled Parts

In this section all aspects of micro-form rolled part quality will be discussed and particular attention will be paid to the consequences of miniaturisation. Finally, recommendations to maximise part quality will be discussed.

7.4.1 The Surface Quality of Form Rolled Parts

The factors that affect surface quality, such as flaking and lap formation, will now be discussed. The conditions under which these phenomena arise will be determined. The effect of workpiece diameter and material on flaking and lapping will also be explained. The Japanese authors, Tsuchikawa et al [47], observed the development of two different sized axial laps:

1. Large laps that extended across the width of the flat and appeared after a critical area reduction had been achieved.
2. Small laps that gradually increased in magnitude with increased area reduction and had smaller dimensions than large laps.

Tsuchikawa et al used large diameter (38mm) steel workpieces. The dies used to roll the workpieces had proportionally large flats, similar to those used in this research, and the area reductions ranged from 45 to 66%. **The author of this thesis is not aware of any other work examining the surface of micro rolled parts or the surface of stainless steel and titanium rolled parts.**

By examining the micro parts rolled for this thesis the effect of a series of rolling variables on the surface quality of rolled parts can be determined, these include:

- workpiece diameter, as illustrated by Figure 7.9
- workpiece area reduction, as illustrated by Figure 7.10
- die manufacturing method, as illustrated by Figure 7.10
- die geometry
    - flat size, as illustrated by Figure 7.10
    - sidewall angle, as illustrated by Figure 7.12
- workpiece material, as illustrated by Figure 7.13

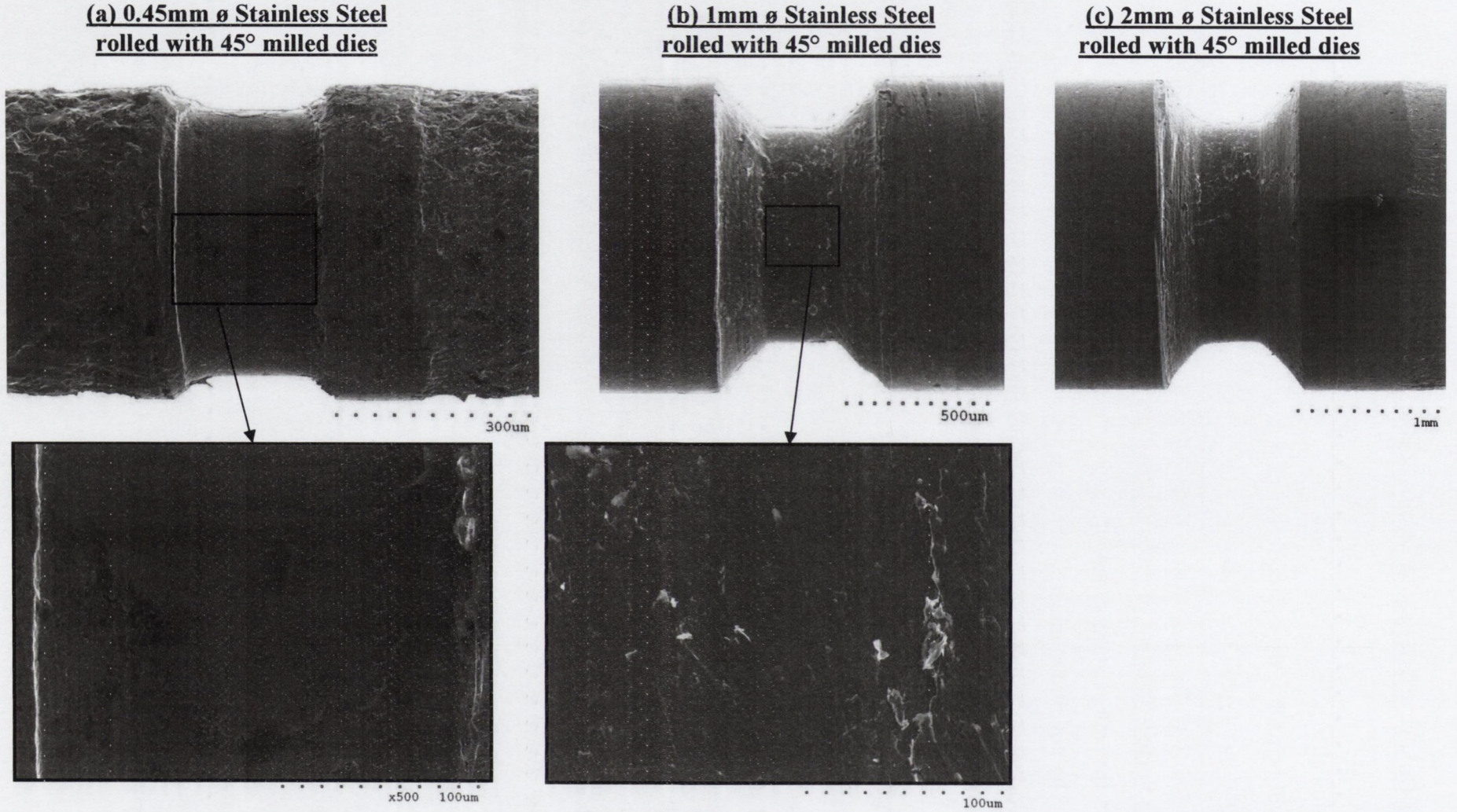

Figure 7.9: Photographs illustrating the effect of workpiece miniaturisation. The parts have diameters ranging from 0.45mm to 2mm

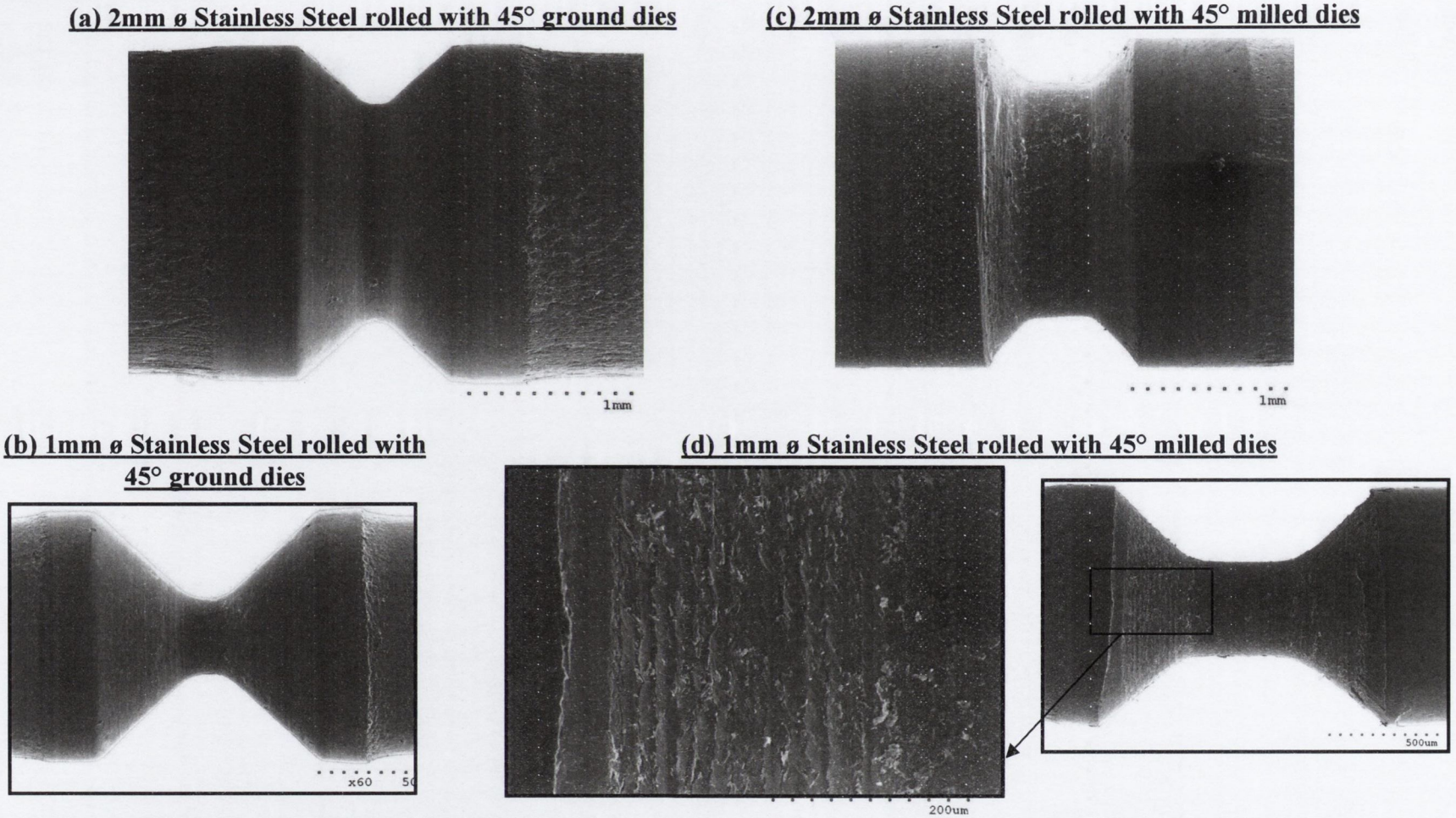

Figure 7.10: Illustrating the effect of increasing area reduction and die manufacturing method. Parts (a) and (b) were formed using ground dies while parts (c) and (d) were formed using milled dies. Parts (b) was formed using the same die set as part (a) but because of its smaller diameter it experienced a larger area reduction, similarly part (d) experienced a larger area reduction than part (c)

The parts shown in Figure 7.10 illustrate the effect of increased area reduction, the effect of a wide die flat and the effect of the die manufacturing method on the quality of the rolled part. The main effects are:

- Increased area reduction tends to reduce the surface quality of the part. The 1mm diameter part rolled with the ground die set has a rougher surface near the tip of the groove where small dimples can be seen then the 2mm diameter part rolled with the same die set which shows no evidence of this pitting.
- Parts rolled using a milled die set were inferior to those rolled using a ground die set. The milled dies were produced using flat ended cutters and to produce the angled geometry of the die sidewall the cutter had to move in a stepped pattern. The machining process therefore produced a series of lines on the sidewall of the die, see Figure 7.11(a), and these lines were transferred to the workpiece during the rolling process. These lines have a detrimental effect on the surface quality of the sidewall compared with those produced with ground dies which were free of machining lines, see Figure 7.11(b).

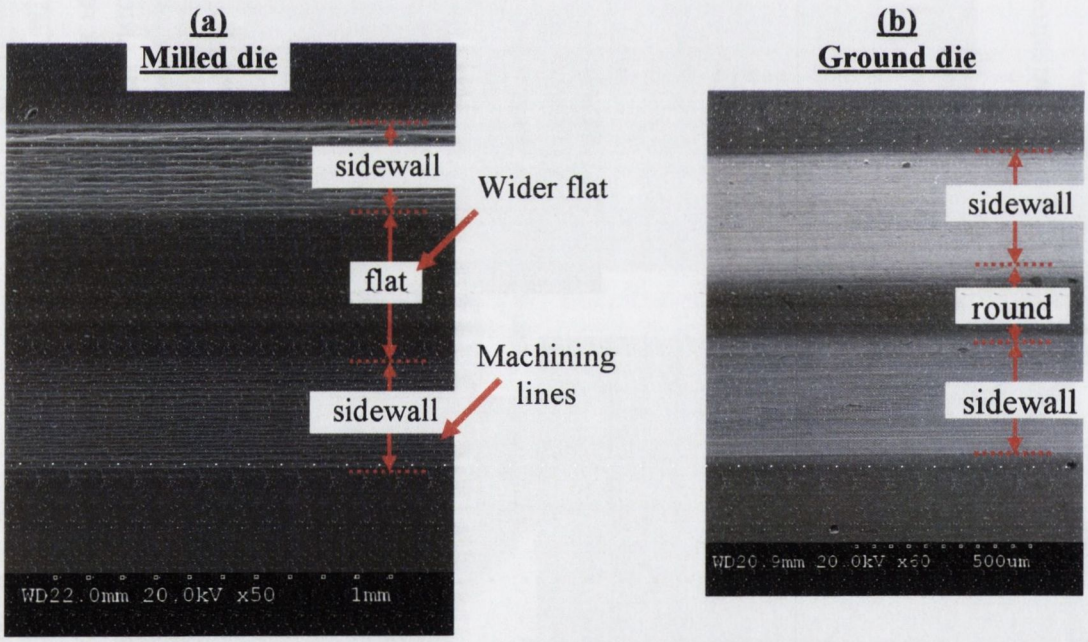

Figure 7.11: Comparison of milled and ground dies using SEM photographs

The wide flats on the top of the feature on the milled die sets had a detrimental effect on part quality compared with the narrower rounds found on the top of the feature on the ground die set. As a workpiece rotates between a die set, there is a build up of material where the workpiece contacts the die and if this material is folded back into the workpiece

an axial lap is created. Workpiece material is less likely to be folded into a lap if it can be displaced axially away from where laps are created. The narrow rounds found on the ground die set (see Figure 7.11(b)) encourage material flow in the axial direction and parts rolled using such dies are therefore free of axial laps. However, the wide flats found on the milled dies (Figure 7.11(a)) hinder the axial flow of workpiece material and encourage its tangential flow where it may create axial laps.

The improvement in the quality of form rolled parts when die features with narrow rounds are used instead of wide flats indicates that form rolling dies should be designed with the former. However, this conclusion also means that the form rolling dies should be manufactured using a grinding process because, during this research, it proved very difficult to machine the narrow die features and it would be very time consuming and difficult to machine a round onto the top of the die feature.

The results presented in Figure 7.12 show that the sidewall angle had little effect on the quality of the workpiece. All three parts (a-c) in Figure 7.12, show evidence of the imprint of the machining lines from the die sidewall onto their surface and the formation of axial laps in the flat region at the bottom of the groove. Smaller sidewall angles are recommended when large amounts of material are displaced by each workpiece revolution. However, due to the small size of the die feature and the very small spreading angle of only 0.8°, the amount of material being displaced per revolution is small and this allows larger sidewall angles to be used without a detrimental effect on the surface quality when rolling micro parts.

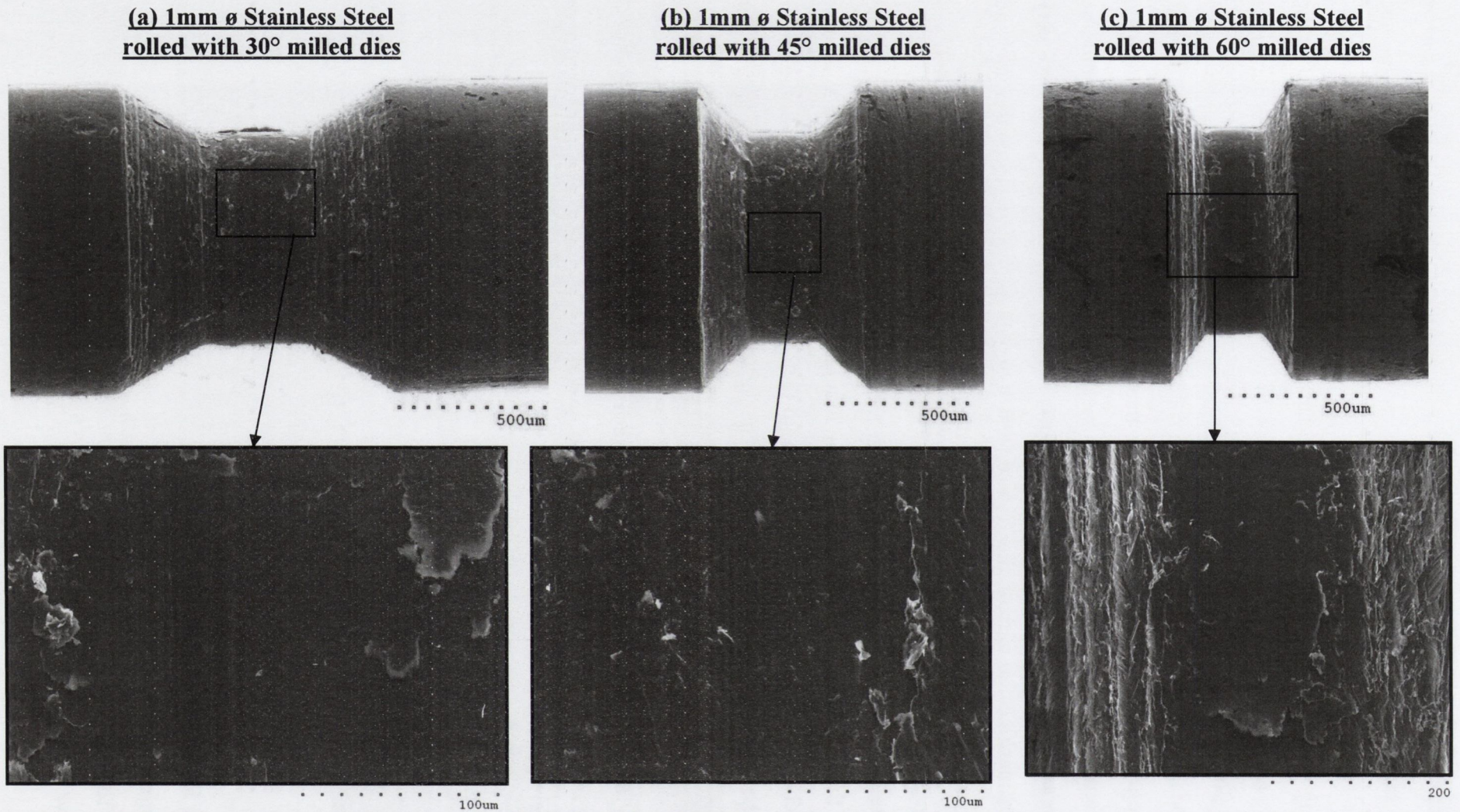

Figure 7.12: These photographs illustrate the effect of the die sidewall angle on the surface quality of the workpiece. Parts (a-c) are 1mm stainless steel workpieces that experienced a 60% area reduction however their sidewall angle varies from 30° to 60°

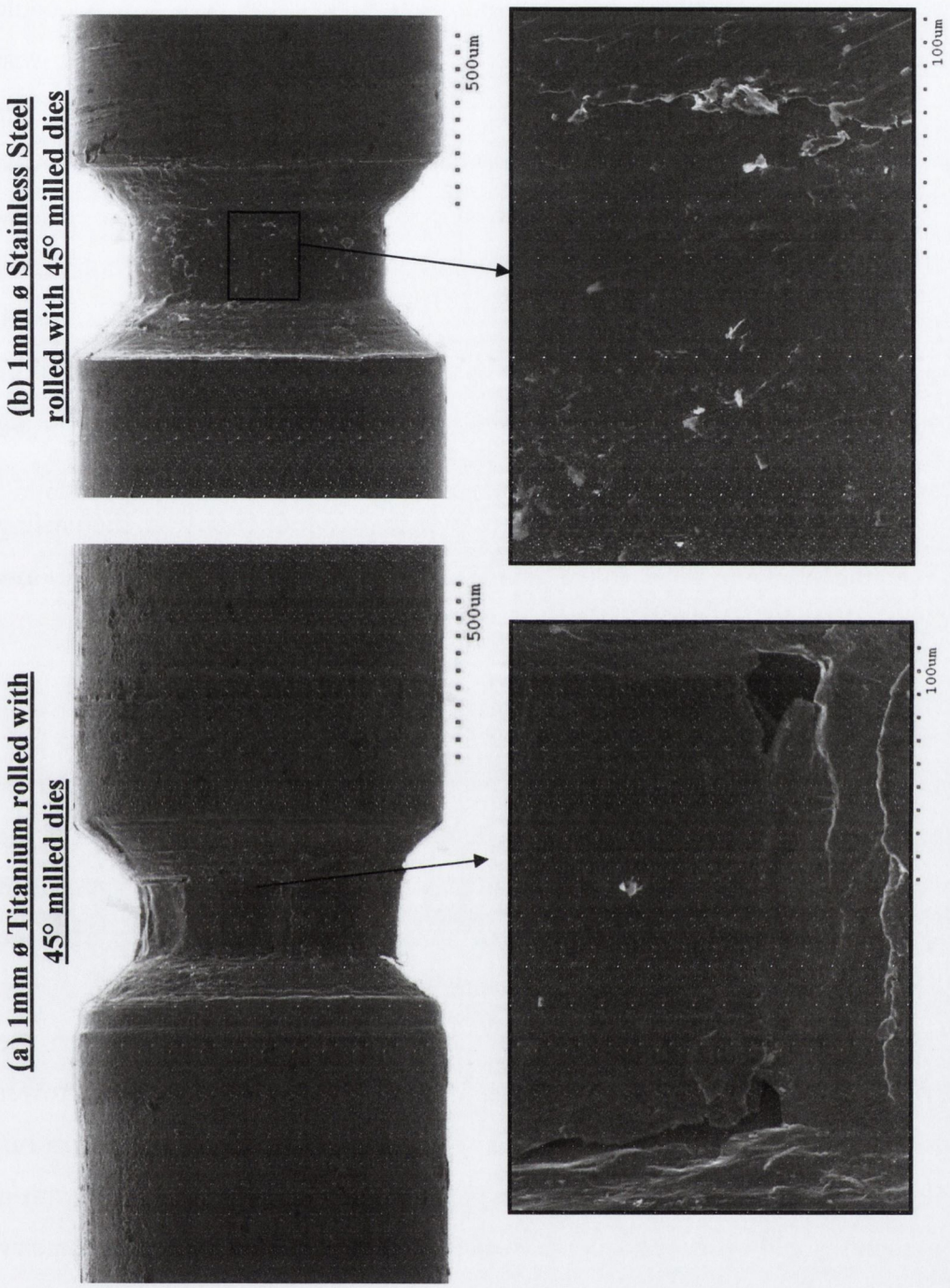

Figure 7.13: Illustratration of the effect of workpiece material on the surface quality of parts. Both (a) and (b) experienced the same area reduction and were rolled using the same die sets however the workpiece mterial varies

Parts (a) and (b) in Figure 7.13 show that the workpiece material has a significant effect on the surface quality of form rolled parts. The titanium part has a much inferior surface quality compared to that of the stainless steel part. In the groove flat region, the titanium part has suffered from a peeling process in which a thin layer of surface material has separated from the remainder of the workpiece. In Figure 7.13 the peeling layer was still attached to the workpiece, however, on many of the samples examined, the layer had detached either partially or completely leaving a surface with a series of axial ridges.

Tsuchikawa et al [47] predicted that the form rolling process resulted in the development of large shear stresses just under the workpiece surface and that these shear stresses could lead to the exfoliation of a surface layer. Authors [73, 74] that have investigated the wear properties of Ti6Al4V have found it very vulnerable dry to sliding wear, with the delamination of large surface fragments of the workpiece observed during wear trials and attributed to the low resistance of the material to plastic shearing. This is a result of Hexagonal Close Packed (HCP) structure of titanium alloys which limits the number of slip systems and the possibility of cross slip available to a deforming titanium alloy crystal. Because of this the crystal orientation within a titanium alloy workpiece is unlikely to be favourably oriented for deformation and the material will be relatively brittle [75]. During form rolling, parts experience plastic shearing due to dry sliding while a large amount of additional shearing results from the rotational nature of the process, therefore, the peeling or delamination observed on form rolled parts can be attributed to Ti6Al4V's low resistance to plastic shearing.

Some conclusions regarding surface quality can be now be made:

- When rolling with milled dies, a series of machining lines on the sidewall of the die feature were formed onto the workpiece. This defect was a direct result of the milling process used to manufacture the dies and it was not present on parts rolled with ground dies. Therefore, unless the machining lines can be removed from the milled dies, the ground dies will produce superior micro-form rolled parts.
- The die geometry had an influence on the development of axial laps on the workpiece surface. Wide flats tended to enfold material into laps unlike narrower rounds which moved material axially and, thereby, prevented lap formation. Therefore, for the production of lap free parts the use of a die geometry with a narrow round would be recommended. Because it is easier to achieve this geometry using a grinding process, it should be used in place of milling to manufacture micro-form rolling dies.
- Increasing the area reduction had a detrimental effect on the surface quality of the workpiece, as it tended to increase flaking and pitting of the workpiece surface
- The surface quality varied considerably depending on the workpiece material used. Titanium parts experienced peeling in which a layer of the workpiece in the groove

region lifted away from the workpiece. This indicates that stainless steel is a more suitable material for the micro-form rolling process.

As laps are a possible location for larger cracks to originate the production of lap free form rolled parts significantly improves their quality. The type of laps usually observed on form rolled parts are helical laps which are a result of workpiece material being folded into the workpiece groove during the spreading zone. And the number of laps on the workpiece is equal to the twice the number of workpiece rotations in the sizing zone. No laps of this kind were found on the workpieces rolled during this research because the dies had no sizing zones. However, as discussed above, axial laps were observed on parts form rolled using milled dies, the only other authors to observe such laps were Tsuchikawa et al [47]. In the rolling process used by Tsuchikawa et al, a pair of wide rotating cylinders was forced into the workpiece to reduce its diameter and the groove was formed over a large number of rotations. This process is explained in greater detail in Chapter 5. Because the milled dies used during this research had a large flat and small ramp angle, they created a wide groove which gradually increased in depth over a large number of rotations. Therefore, the deformation experienced by the workpiece is closer to that observed by Tsuchikawa et al than traditional flat die form rolling which uses two flat wedge dies whose width increases gradually over the rolling stroke. **However, the ground die set is free from both wide flats and a sizing zone and parts rolled using them were free of both helical and axial laps. They are, therefore, recommended in situations when lap free parts are required.**

7.4.2 Loss of Die-Workpiece contact on the Groove Sidewall

Under certain rolling conditions a loss of contact between the sidewall of the die and the workpiece was observed in both FEA simulations and actual form rolled parts. The result was that the groove rolled onto the workpiece was wider than that of the die used to form them, see Figure 7.14. This is problematic as it will lead to the production of incorrectly dimensioned parts, particularly, given they are micro-parts where even a small deviation from the specification can result in relatively large geometrical tolerance errors. A trend towards increasing feature width with decreasing workpiece diameter was also observed.

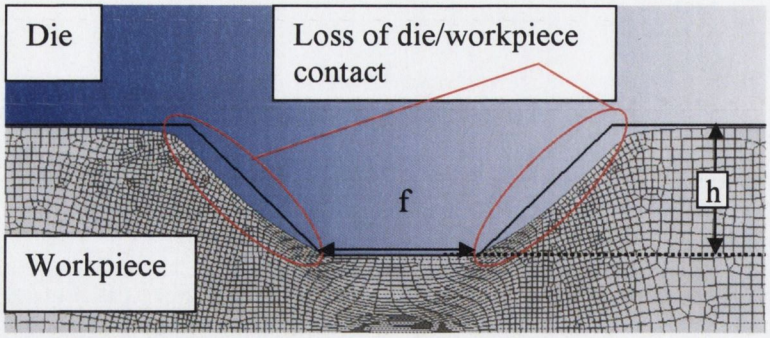

Figure 7.14: 2D FEA illustrating loss of die/workpiece contact along the sidewall

In 2D FEA this problem became more pronounced if the sidewall angle or the flat width was increased or if the workpiece diameter was reduced. The phenomenon can be explained using constant volume and axisymmetric or plane strain assumptions, depending on whether the 2D simulation was run using an axisymmetric or plane strain assumption. As the die moves radially into the workpiece by an increment x, it results in axial flow of the workpiece material which is controlled by either the relative axial movement of the die sidewall, y_{die}, or the axial elongation of the material under the flat, $y_{workpiece}$, whichever is larger.

If the flow of material is controlled by the die sidewall, then contact between the workpiece and the die is maintained and the shape of the groove formed onto the workpiece is equal to the geometry of the die feature. y_{die} is related to the to the radial die increment, x by the geometric relationship described below, see Figure 7.15.

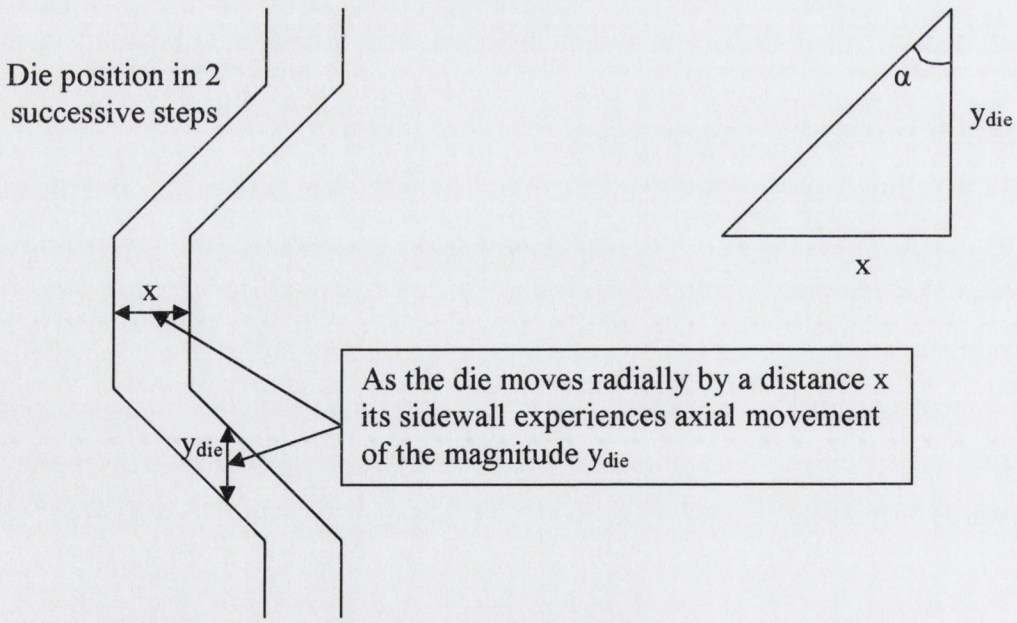

Figure 7.15: Determining y_{die} from the die geometry

From Figure 7.15 y_{die} can be found using the tan function:

$$y_{die} = \frac{x}{\tan \alpha} \tag{7.1}$$

Because α is a constant y_{die} is constant throughout the process.

If the flow is controlled by the axial elongation of the material under the flat, $y_{workpiece}$ then contact between the die and workpiece sidewalls will be lost. $y_{workpiece}$ is dependent on the reduced workpiece diameter d_1, and therefore changes throughout the process as the die penetration, p increases. The initial workpiece diameter, d_o is related to the reduced diameter and the die penetration by the following formula:

$$d_1 = d_0 - 2p \tag{7.2}$$

As the die penetrates the workpiece by a further distance x, it is assumed that the material under the die flat is extruded axially by a distance $y_{workpiece}$, and that the volume of material before and after extrusion remains the same.

In the case of an axisymmetric assumption, the volume of material before extrusion, V_1 is described by the equation below:

$$V_1 = f \cdot \pi \left(\frac{d_1}{2} \right)^2 \tag{7.3}$$

This is the volume of a cylinder with a length f and a diameter of d_1, see Figure 7.16.

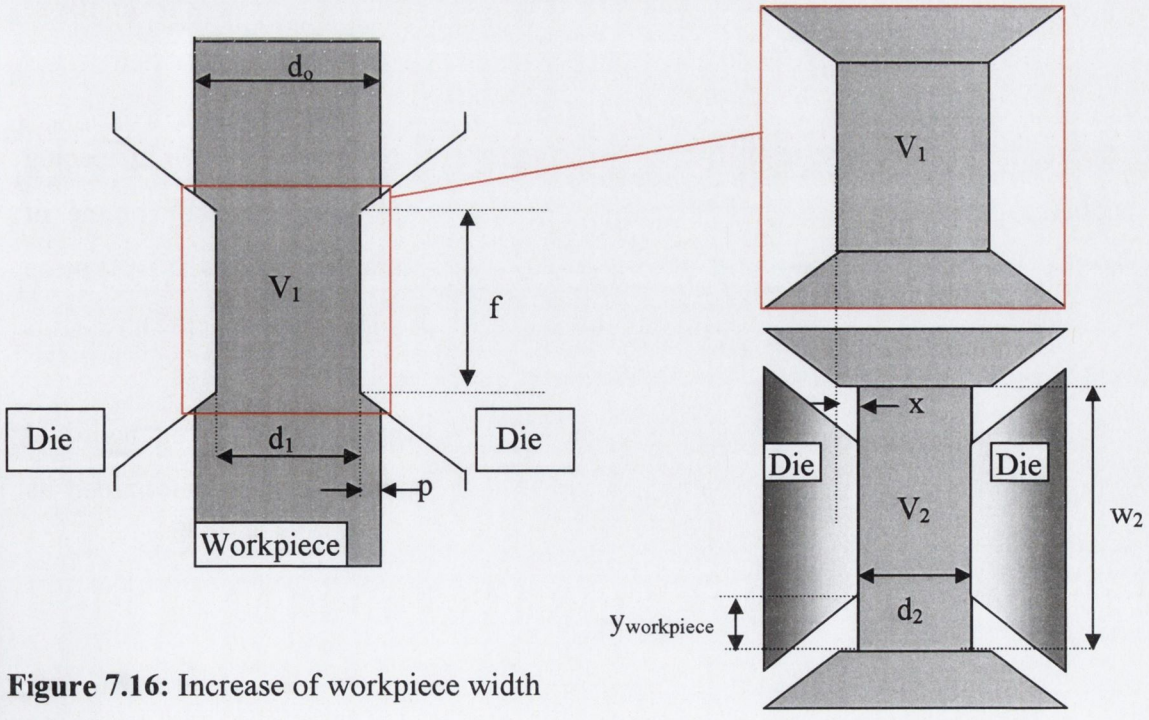

Figure 7.16: Increase of workpiece width

Now the diameter is further reduced to d_2 where:

$$d_2 = d_1 - 2x \tag{7.4}$$

Due to the constant volume assumption the volume of material after extrusion, V_2 must equal V_1, see Figure 7.16.

$$V_1 = V_2 \tag{7.5}$$

And because from equation 7.3 it is known that the diameter has decreased the length must increase to maintain this constant volume.

$$w_2 = f + 2y_{workpiece} \tag{7.6}$$

And the volume of the volume of material in the reduced diameter section, V_2 is:

$$V_2 = w_2 \cdot \pi \left(\frac{d_2}{2} \right)^2 \tag{7.7}$$

Then combining equations 7.4, 7.6 and 7.8.gives:

$$f \cdot \pi \left(\frac{d_1}{2} \right)^2 = w_2 \cdot \pi \left(\frac{d_2}{2} \right)^2 \tag{7.8}$$

This simplifies to:

$$f \cdot d_1^{\,2} = w_2 \cdot d_2^{\,2} \tag{7.9}$$

combining equations 7.4, 7.6 and 7.9 to give:

$$y_{workpiece} = \left(\frac{f \cdot d_1^{\,2}}{2} \right) \cdot \left(\frac{1}{(d_1 - 2x)^2} - \frac{1}{d_1^2} \right) \tag{7.10}$$

From this equation it can be seen that $y_{workpiece}$ increases proportionality with increasing flat width or decreasing diameter. Increasing the flat width, increases the volume of material that must be displaced and therefore $y_{workpiece}$. Although decreasing the workpiece diameter decreases the amount of material that must be displaced, it increases $y_{workpiece}$ because the relative size of x to the reduced diameter increases.

By applying an iterative process to formula 7.10, in which d_1 varies from the initial to the final workpiece diameter the finished workpiece geometry can be determined as illustrated in Figure 7.17.

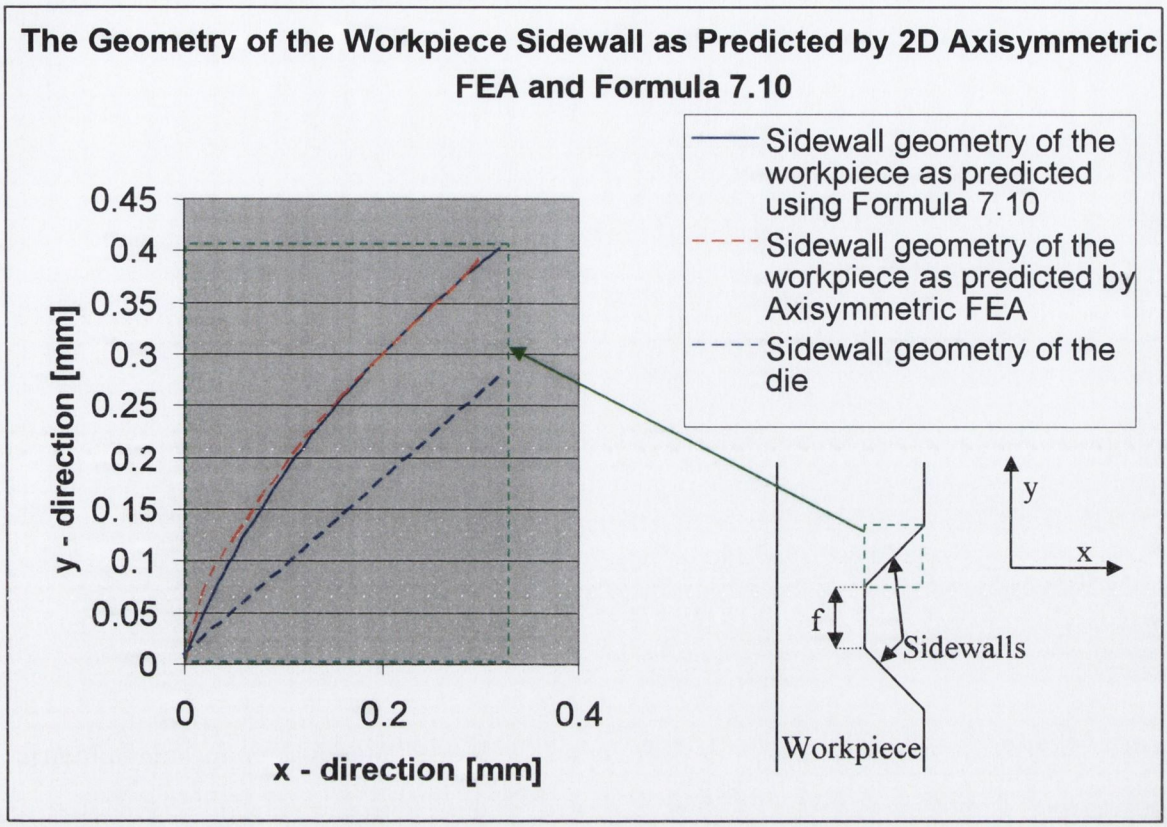

Figure 7.17: Comparison of the workpiece shape as predicted by 2D axisymmetric FEA simulation and using formula 7.10

This plot is for a 1mm stainless steel workpiece deformed by a die with a 0.36mm flat and a 50° sidewall angle. The figure also shows the geometry of the workpiece sidewall as predicted by an axisymmetric 2D FEA simulation, and it is apparent that the geometries predicted using the FEA and formula 7.10 compare favourably. It can be seen that as the area reduction increases, the difference in the slope between the die and the workpiece becomes more pronounced. Once the slope of the workpiece shape becomes smaller than the slope of the die sidewall, contact is lost. In the example illustrated above, this occurred from the very start of the process. The slope of the workpiece sidewall angle, $\alpha_{workpiece}$ is plotted in Figure 7.18. It is calculated using the formula:

$$\alpha_{workpiece} = \tan^{-1}\left(\frac{x}{y_{workpeice}}\right) \tag{7.11}$$

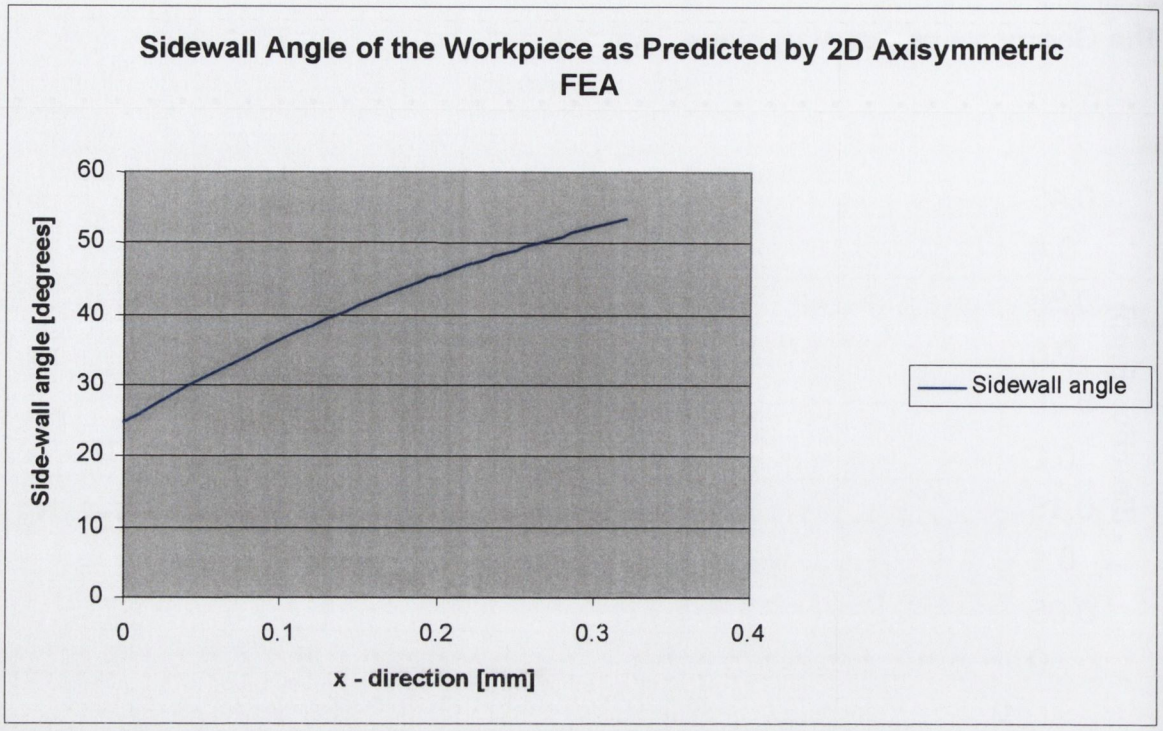

Figure 7.18: The angle of the workpiece sidewall as predicted using an axisymmetric assumption

Similar equations can be developed using a plane strain and constant volume assumptions. y_{die} remains the same as that determined above, equation 7.1.

As for the axisymmetric example if the amount of radial die penetration is increased by x, the reduced diameter becomes d_2:

$$d_2 = d_1 - 2x \tag{7.12}$$

The width of the die also increases as radial die penetration results in axial material flow:

$$w_2 = f + 2y_{workpiece} \tag{7.13}$$

The constant volume assumption produces the following relationship:

$$d_1 f = (f + 2y_{workpiece})(d_1 - 2x) \tag{7.14}$$

Solving for $y_{workpiece}$

$$y_{workpiece} = \left(\frac{f \cdot d_1}{2}\right) \cdot \left(\frac{1}{(d_1 - 2x)} - \frac{1}{d_1}\right) \tag{7.15}$$

Using a plain strain assumption results in a smaller value of $y_{workpiece}$ and therefore loss of contact occurs at a greater area reduction than for an axisymmetric assumption. This is illustrated by Figure 7.19, which predicts that no loss of contact will occur between

the die and the sidewall, in sharp contrast with the axisymmetric assumption, in Figure 7.18.

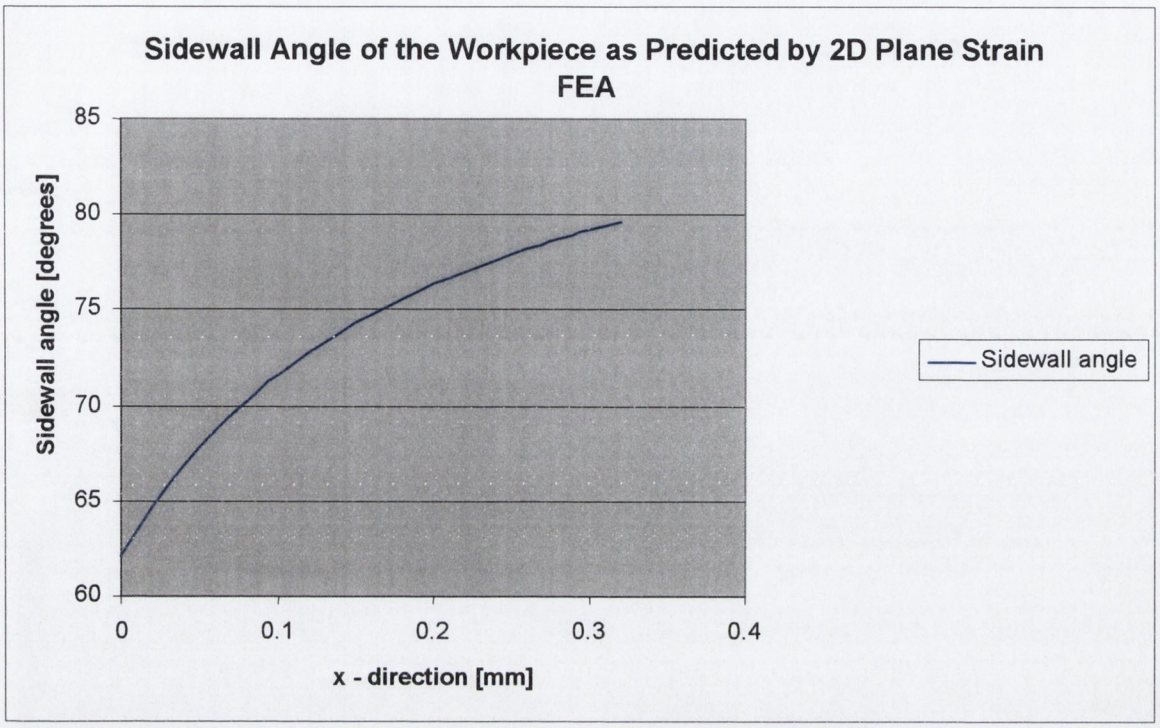

Figure 7.19: The angle of the workpiece sidewall as predicted using a plain strain assumption

In conclusion if contact between the die and workpiece is to be maintained, the maximum die flat width that can be used is dependent on both the sidewall angle of the die and the final reduced diameter of the workpiece. Therefore, the maximum flat width is directly proportional to the diameter of the wire being rolled and decreases with miniaturisation.

The effect of increasing the flat width and decreasing workpiece diameter on the loss of sidewall contact will now be discussed. Figure 7.20 shows a 1mm and a 2mm diameter workpiece that have been rolled using the 2mm ground dies that have narrow rounds. The sidewall geometry of the groove on both the large and the small diameter parts is identical this indicates that decreasing the workpiece diameter does not increase the likelihood of sidewall separation when a narrow round is used.

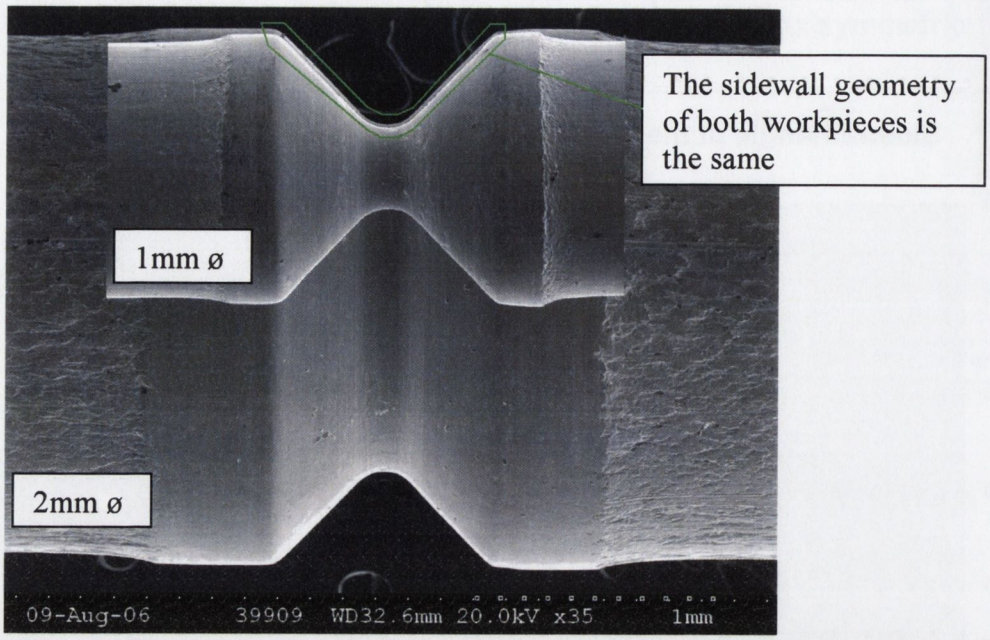

Figure 7.20: SEM photographs showing that the groove geometry is independent of workpiece diameter when a narrow flat is used

However this is not the case when a wide flat is used. Both of the workpieces shown in Figure 7.21 were rolled with the 2mm milled die set however the width of the groove increases as the diameter is reduced.

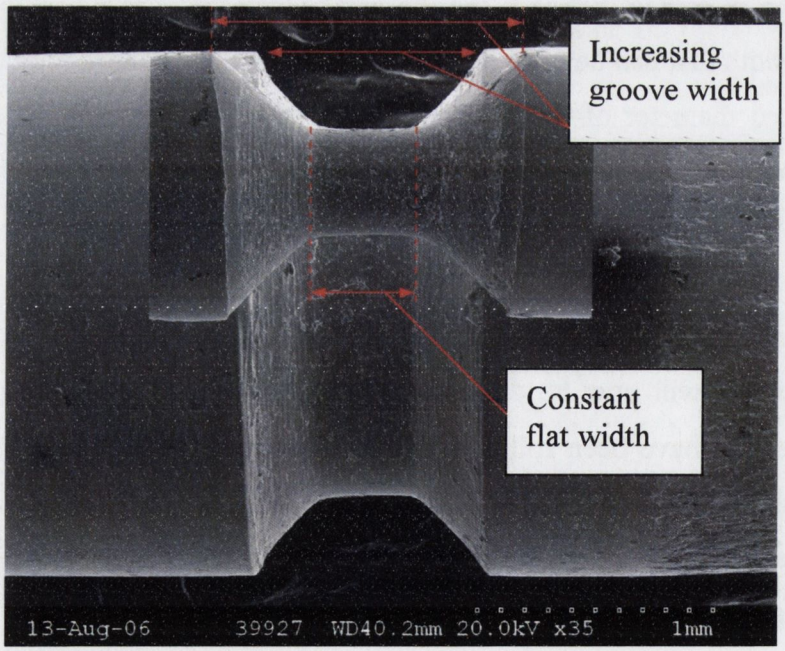

Figure 7.21: SEM photographs showing that the groove geometry changes with workpiece diameter when a wide flat is used

The flat width is the same for both of the parts shown in Fig. 7.21, however, the sidewall angle is smaller for the small diameter part, especially near the base of the groove. This is the same type of groove shape as predicted using the constant volume assumption. In conclusion from Figures 7.20 and 7.21 it has been shown that the likelihood of losing contact in the sidewall region increases as either the diameter of the part decreases or the flat width increases.

A loss of die/workpiece contact in the sidewall region was also observed in the 3D FEA simulation of 1mm diameter stainless steel workpiece being rolled with 2mm milled dies.

Figure 7.22 shows the workpiece while it is still in contact with the sidewall of the die and its geometry still conforms to that of the die.

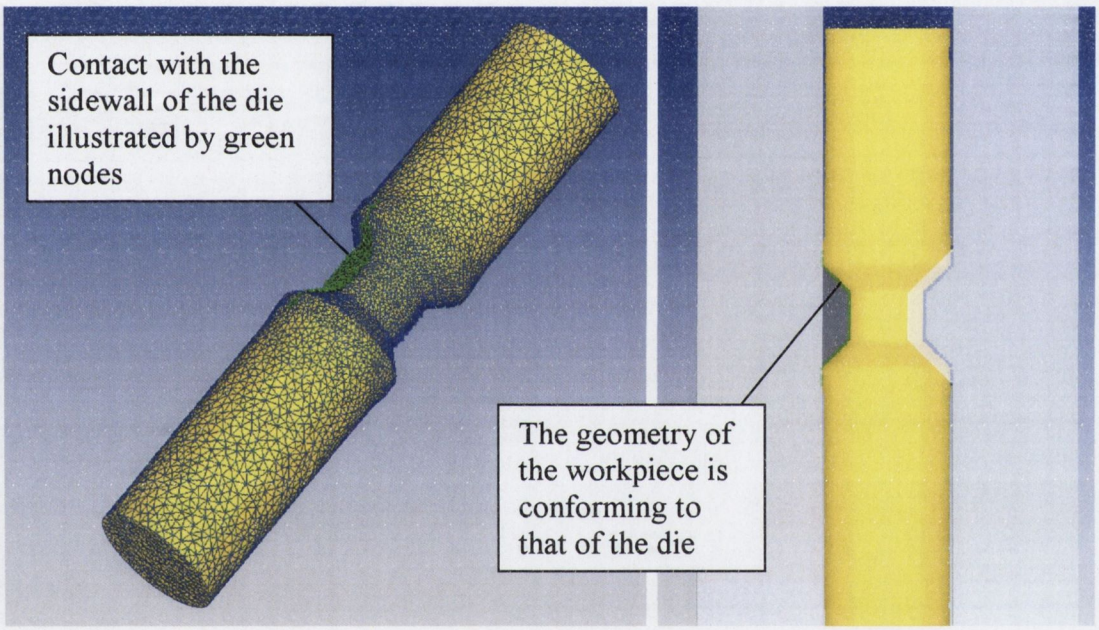

Figure 7.22: Contact conditions and the geometry of the workpiece when it is in contact with the die sidewall

With continued area reduction, the workpiece loses contact with the sidewall of the die and the geometry of the workpiece stops conforming to the die geometry. Figure 7.23 shows that the width of the workpiece groove increases and its sidewall angle decreases.

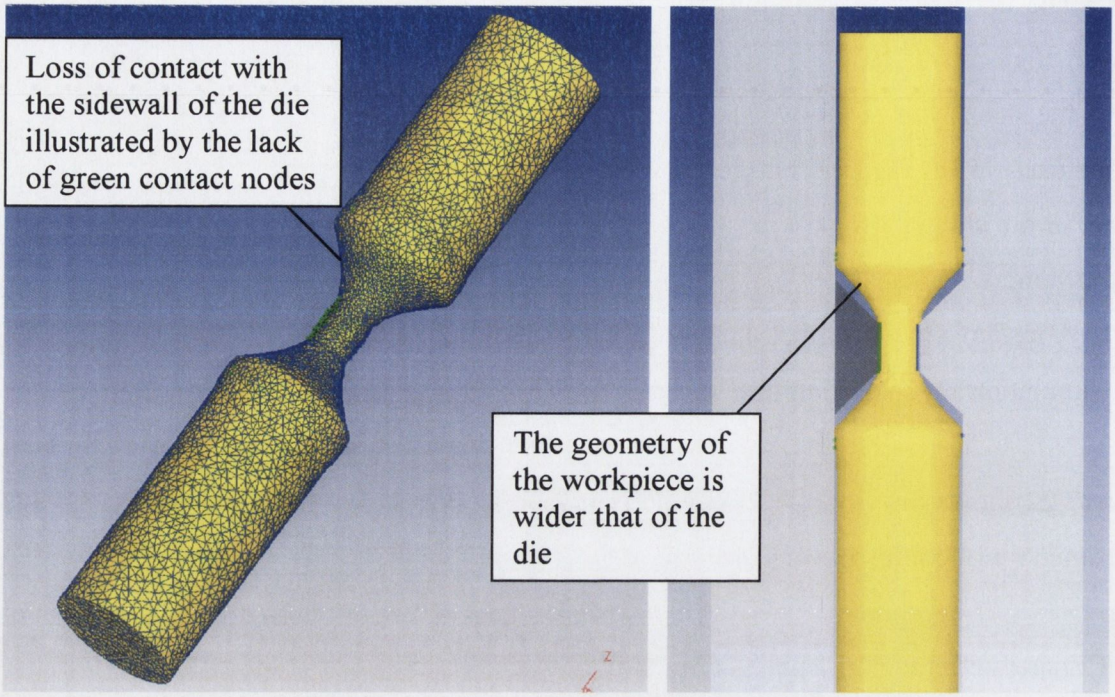

Figure 7.23: Contact conditions and the geometry of the workpiece after it losses contact with the die sidewall

Earlier, it was noted that the loss of contact with the sidewall of the die would occur if the axial velocity of the workpiece due to area reduction exceeded the axial velocity of the die sidewall and this can be confirmed by examining the axial velocities predicted by the FEA simulations. Figure 7.24 (a) and (b) show the axial velocity of the workpiece before and after it loses contact with the sidewall of the die. Figure 7.24(a) illustrates that the axial velocity before losing contact with the die sidewall is 0.015mm/s. After the workpiece loses contact with the sidewall of the die, the axial velocity increases with increasing area reduction. In Figure 7.24(b), the workpiece has experienced an area reduction of 83% and the axial velocity is 0.025mm/s. Equations 5.1 and 5.10 which analytically determine the axial displacement of the die and the workpiece respectively can be used to determine velocities by introducing a time step. Using these modified equations, the axial velocity of the die works out to be 0.0134mm/s and the axial velocity of the workpiece at and area reduction of 83% works out as 0.25mm/s. Both of these values compare well with those predicted by the FEA simulation.

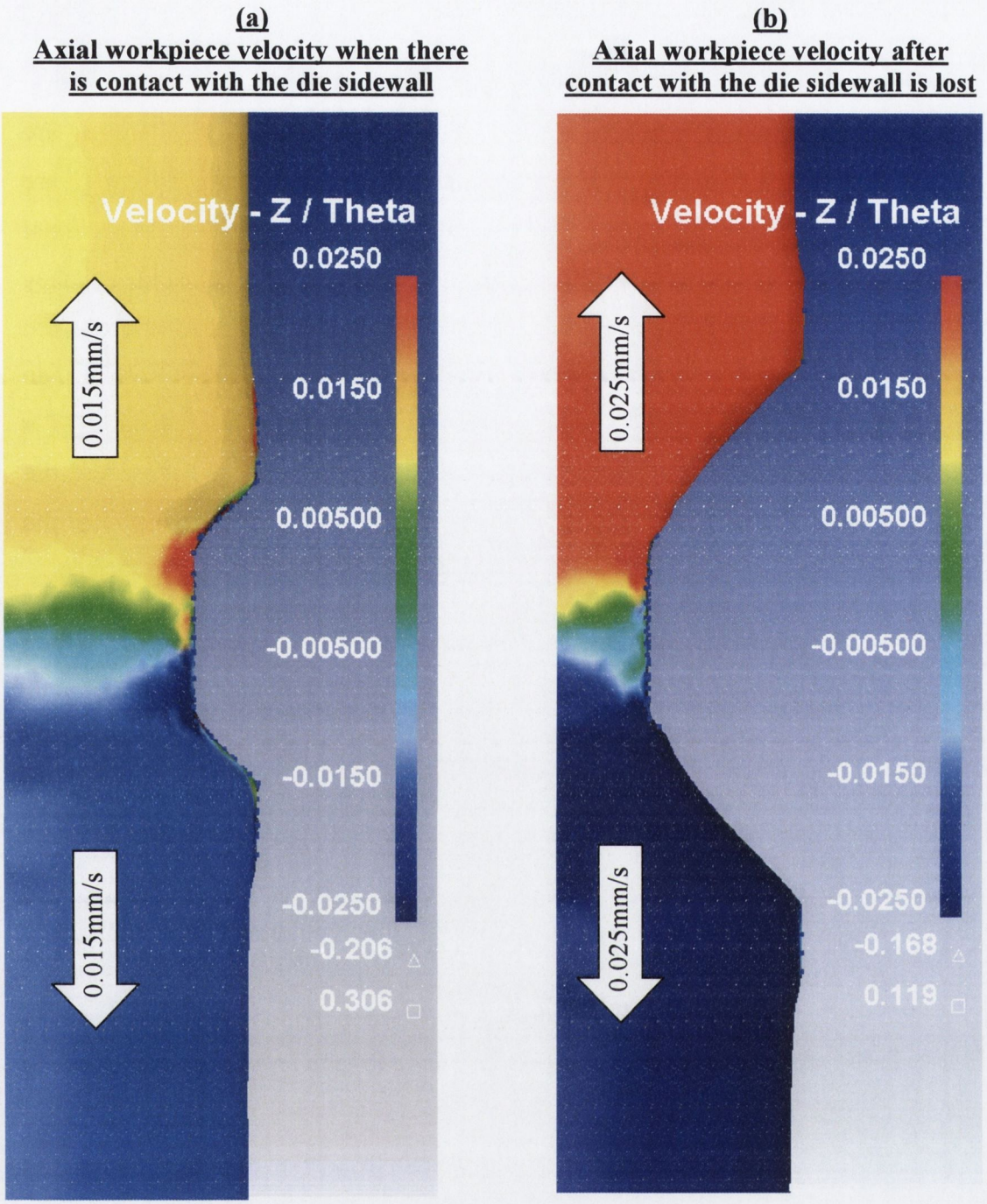

Figure 7.24: The axial velocity of the workpiece before and after it loses contact with the die sidewall

7.5 Internal Defects in Micro-Form Rolled Parts

7.5.1 Axial Workpiece Failures Located Away from the Groove

Mannesmann type cruciform failures are located along the central axis of billets and are caused by cyclical stresses that alternate between tension and compression. Failures were observed in regions of form rolled parts that had experienced only small cross sectional area reductions but which had experienced many rotations and this would indicate they were Mannesmann type failures. The regions of the workpiece in which these failures were observed were experiencing deformation more closely associated with Cross Rolling than form rolling. Cross Rolling is the forming process in which diameter reduction of a workpiece is achieved by rolling it between a pair of flat dies. Teterin [34] observed the failure of Cross Rolled parts at area reductions of only twelve percent and he attributed the failures to the development of radial tensile stresses on a plane parallel to the die surface.

1. Mannesmann Failure Originating on the End of the Workpiece

   The Mannesmann failure was located along the central longitudinal axis of the workpiece and originated on the end of the workpiece that was rolled between the dies. This region can be seen in Figure 7.25 below as the smooth region on the right.

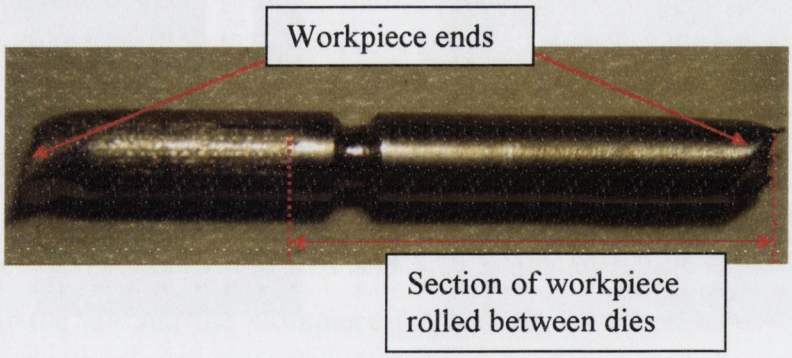

Figure 7.25: Photograph showing the proportion of the workpiece that is rolled between the dies

The workpieces used in this research were produced by cutting spools of wire to the required length using a shears. The cutting process produced rough workpiece ends as shown in figure and it was suspected that this was contributing to the failure of the workpiece. However subsequent rolling trials using workpieces that had polished ends still suffered from these failures.

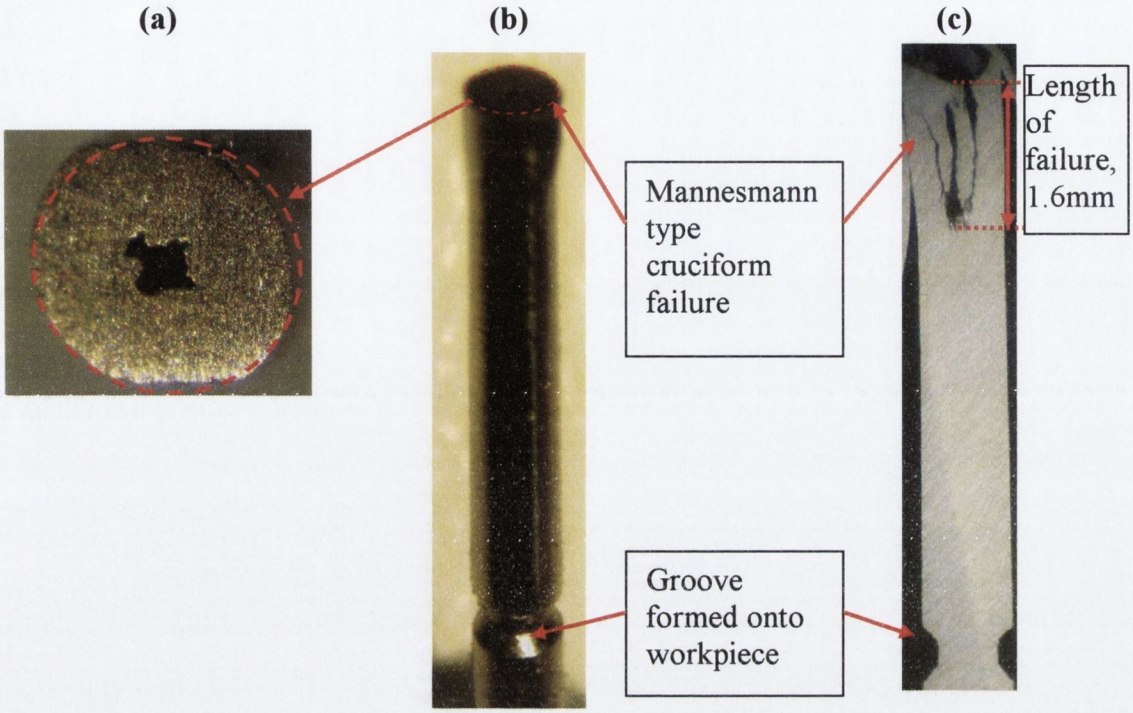

Figure 7.26: Mannesmann failure on the end of a 1mm diameter stainless steel workpiece rolled with 1mm milled dies: (a) and (b) are photographs of a transverse section while (c) is a photograph of an axial section

Figure 7.26(a) shows the cruciform shape of the failure which identifies it as a Mannesmann failure as observed by Li et al [23]. Figure 7.26(b & c) illustrate the distance between the failure located at the end of the workpiece and the location of groove. The rolled section of the workpiece tends to experience a small area reduction of between two and six percent. The small level of area reduction experienced by the workpiece and the location of the failure on the end of the workpiece indicates that it is a result of the rotational nature of the process rather than the forming of the groove. Therefore, this type of failure cannot be prevented through die design and it was subsequently observed in all the 1mm samples rolled using the milled die sets. However, it was not present when using the ground die set because the die/workpiece contact is concentrated in the region around the groove and the rest of the wire is free of the cyclical forces that cause Mannesmann failures. Therefore, preventing area reduction in the rolled wire can prevent the development of internal failures.

These failures were not present in larger diameter wires, which would have experienced fewer rotations when rolled. This observation supports the theory that

failure was a result of the cyclical stresses arising during the large number of rotations experienced by workpieces with small diameters.

The diameter of the workpiece at the location of the failure is wider than the remainder of the rolled wire by approximately 5-8%, see Figure 7.26(b & c). The increased diameter is a result of elastic recovery in the failed length of workpiece when it is released from the dies at the end of the stroke. The failure length is independent of the length of workpiece which supports the theory that the failure originates at the end of the workpiece.

At its widest point the failure in Figure 7.26(a) is 0.26mm wide while the failure in Figure 7.26(c) has a maximum width of 0.5mm.

2. Mannesmann failures located immediately outside of the groove region

This failure type was found in a 1mm wire that had fractured during the rolling stroke. The fracture was located along the central axis of the workpiece and outside the region of the groove. One end of the failure is located directly outside the groove region, see Figure 7.27.

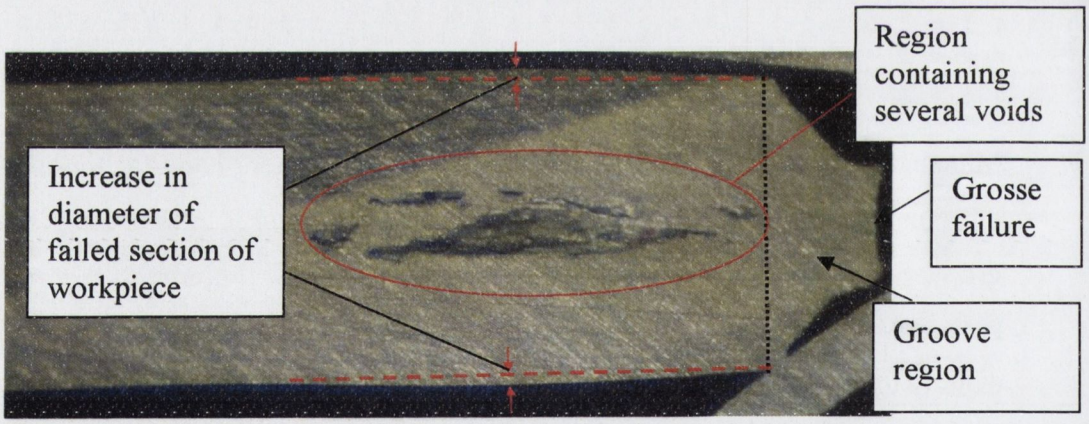

Figure 7.27: Mannesmann failure located immediately outside the groove region of a failed 1mm diameter stainless steel workpiece rolled with 2mm milled dies

It can be seen from Figure 7.27 that there are several pores which are part of a large Mannesmann failure. Perhaps the failure originated at the edge of the deformation region due to an inclusion, however this failure was only observed in one sample and so conclusive evidence as to its cause is unavailable. The failure measures 1.5mm in length and 0.25mm in width (or diameter).

As with the Mannesmann failure located on the end of the workpiece there is a diameter increase of 5% in the failed section of the workpiece.

7.5.2 Workpiece Failures Due to the Forming of the Groove

The results of the rolling trials are summarised in Table 7.3 below. Approximately ten of each die/workpiece combination was rolled. Four different die/workpiece combinations could lead to part failure and each of these combinations introduced very large reductions in the cross sectional area of over 85% in the workpieces. Two different failure methods were apparent - internal void and the double cup failures.

WORKPIECE		DIE SET								
		1mm milled			2mm milled			2mm ground		
diameter	Material	% red	Failure	Type	% red	Failure	Type	% red	Failure	Type
1mm	T	59	-	-	88	YES	Double cup	93	YES	Double cup
1mm	SS	59	NO	-	88	YES	Double cup	93	YES	Internal
2mm	SS	33	NO	-	55	NO	-	60	NO	
3mm	SS	22	NO	-	39	NO	-	43	NO	

Table 7.2: The rolling conditions that lead to part failure

Internal failures were located along the central axis of the workpiece and were elliptical in shape when the part was sectioned on a plane through the central axis of the workpiece, see Figure 7.28.

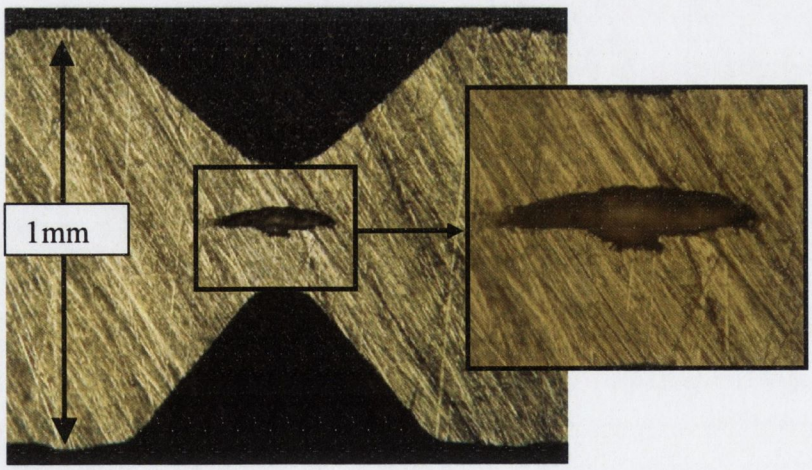

Figure 7.28: Stainless steel wire with internal failure

The location of the failure in the centre of the workpiece under the groove is not unprecedented as several authors have observed the development of failures in this

location. The 2D and 3D FEA simulations also predicted tensile maximum principal and hydrostatic stresses in the centre of the workpiece. This is significant because it is known that tensile maximum principal stresses can cause the opening of voids while they can be prevented by compressive hydrostatic stresses.

The internal failure shown in Figure 7.28 shares certain similarities with the failures found in strip rolling and wire drawing specimens that are discussed in Chapter 5. The H/l ratios for these processes are similar to those found in the form rolling process.

An example of a double cup failure is shown in Figure 7.29. The fracture surface displays the cratered uneven topography which is typical of a ductile tensile failure. This indicates that the axial tensile stresses, inherent in the rolling process due to the axial displacement of material, became excessively large and resulted in part failure.

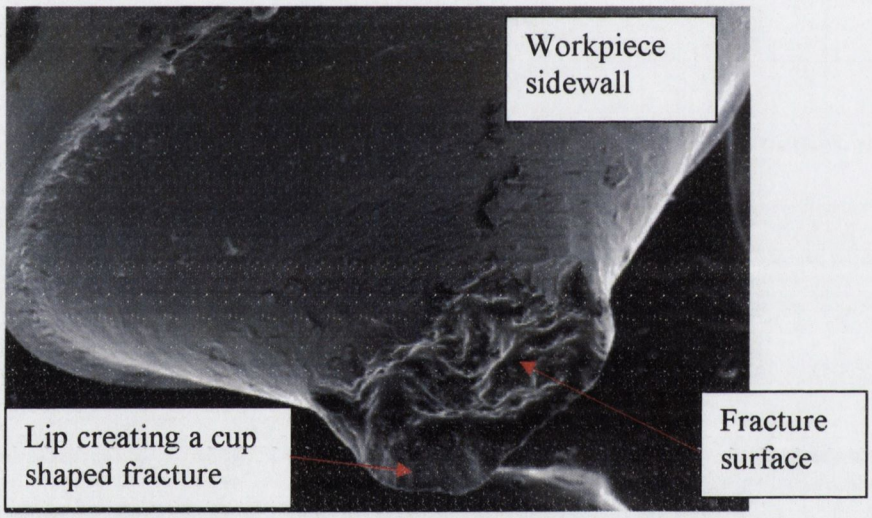

Figure 7.29: Ductile fracture surface of failed form rolled titanium part

This failure type was dubbed a double cup failure because the fractured surfaces of the failed workpiece had a lip around their edge that made them resemble a cup.

When the 1mm titanium wire was rolled with the ground dies it always failed just before it entered the sizing zone of the die. Both the 1mm diameter stainless steel and titanium workpieces also experienced this failure when they were rolled with the 2mm milled die set but the failure was more sporadic. Sometimes, without any changes having been made to the form rolling machine, successive parts would roll without and then with failure. The majority of the 1mm workpieces rolled with the 2mm milled dies failed during rolling.

7.5.3 Explaining the Development of Internal Failures Using FEA Damage Values

The FEA package DEFORM can predict damage values and regions of the workpiece with high damage values are more likely to fail than those with lower values.

Location and Development of Damage with the workpiece

The damage distribution within a workpiece was found to vary with the shape of the die feature and the area reduction experienced by the workpiece. To analyse this further a series of workpieces were deformed using different die geometries and the resulting damage plots and distributions are shown in Figure 7.30. The creation of damage plots is explained in Chapter 6.

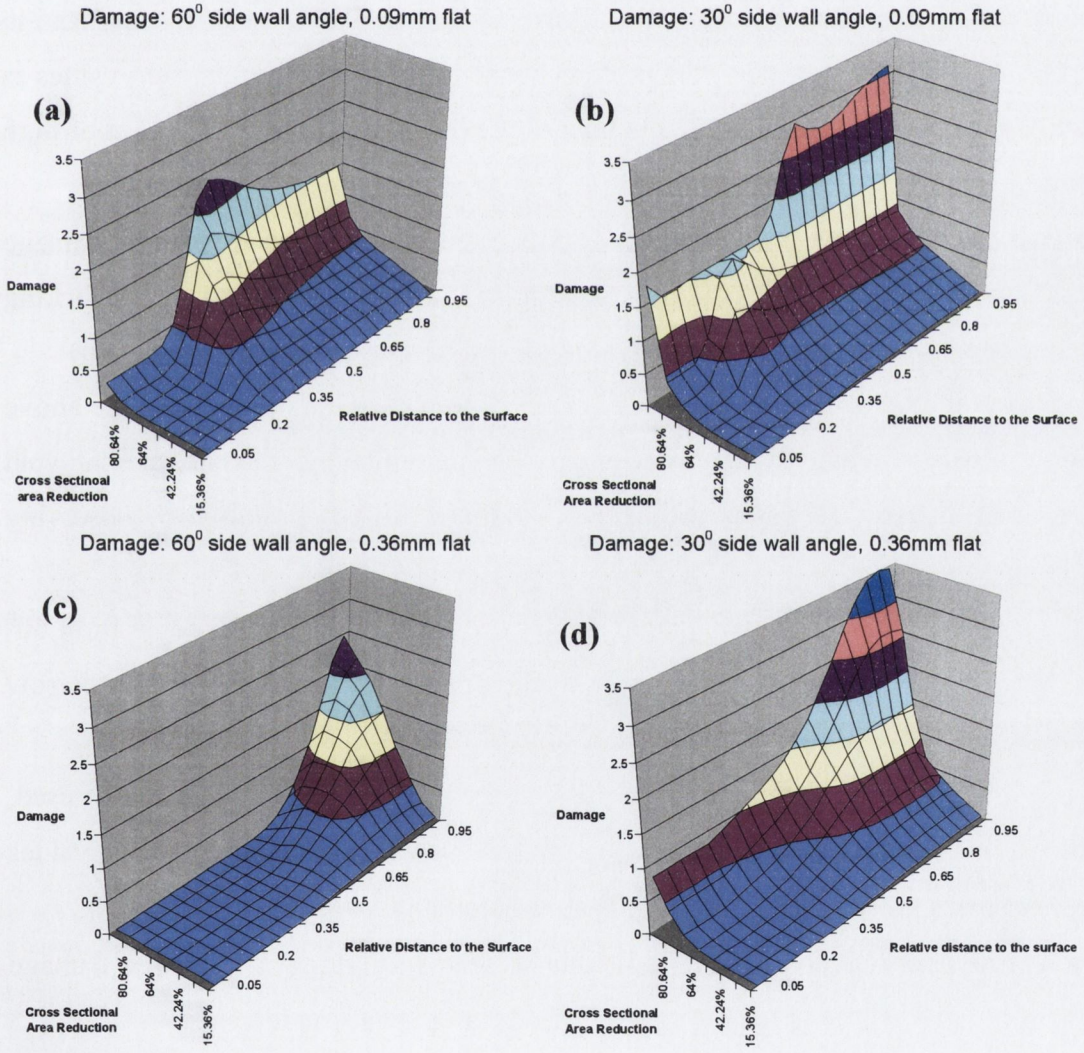

Figure 7.30: Damage plots showing the variation of damage with die penetration

Observations on Damage plots

- The workpieces deformed by die sets that have large sidewall angles of 60^0 retain a dead metal zone (i.e. a region of zero damage and zero plastic strain) under the tip of the groove for the duration of the forming process as shown in Figure 7.30(a, c).
- For the dies having wide flats of 0.36mm, Figure 7.30(c, d), the damage is concentrated at the centre of the workpiece and the damage values are higher than for workpieces deformed by die sets that have narrower flats of 0.09mm, as shown in Figure 7.30(a, b). In addition the small flat produces damage values over a greater proportion of the workpiece, and the highest damage values are just under the dead metal zone. The presence of the maximum damage values at the surface of the workpiece is significant because they are likely to interact with surface defects such as laps which could lead to part failure. Furthermore, the volume of material affected by high damage values is much larger thereby increasing the likelihood of a defect occurring in a region of high damage.
- Small sidewall angles of 30^0, Figure 7.30(c, d) result in lower workpiece damage values, however, at large penetrations, necking of the workpiece occurs. This necking results in the large increase in damage values at end of the stroke in Figure 7.30(b)

Consequently, for improved die design, a number of points can be drawn from the above information. When the aim of the die design is to minimise the risk of internal void formation, then the damage values within the workpiece can be minimised by observing the following points:

- Use the smallest possible sidewall angle e.g. by decreasing the sidewall angle from 60^0 to 30^0 the maximum damage values in the workpiece are reduced by 10% for a narrow flat and 20% for a wide flat for an area reduction of 63%.
- If a large sidewall angle is required then the smallest possible flat width should be used, e.g. by decreasing the flat width from 0.36mm to 0.09mm the maximum damage values in the workpiece are reduced by 37%, for an area reduction of 63%.
- Minimise the area reduction because as can be seen in Figure 7.30(a-d) the damage values increase for all the groove geometries as the area reduction increases.

7.6 Micro-Form Rolling and FEA

A number of problems associated with the FEA of form rolling are outlined in Chapter 5 of this thesis. The solutions to these problems will be answered briefly before moving on to discuss problems peculiar to the micro-form rolling process in more detail.

1. **Modelling the complex deformation mechanism**
   Although 2D FEA captures some aspects of the form rolling Process, it misses the torsional and twisting nature of the process. Therefore, 3D FEA simulations were performed to understand the complex triaxial stress state present in a form rolled workpiece.
2. **Volume loss due to workpiece rotation**
   An additional software tool, the Rigid Super Element RSE, was developed by DEFORM that helps alleviate this problem.
3. **Localised deformation on a large workpiece**
   Due to the small size of the feature formed on to micro-form rolled parts a very fine mesh is required. However, the workpiece is large compared to the feature and if a fine mesh was used for the entire workpiece several hundred thousand nodes would be required and the simulation times would be very long. To reduce the total number of nodes used to mesh the workpiece while maintaining a fine mesh where required the meshing tools described in the Chapter 6 were used to concentrate the mesh in the region of deformation.
4. **Long die stroke length**
   A form rolling operation is performed over a very large die stroke, which means a large number of small simulation steps are required to capture the relative movement of the die and the workpiece. In order to minimise this problem, the largest possible step size should be used. It was found that the most appropriate step size was one four hundredth of a workpiece rotation. This step size is still relatively small, and when it is considered that the workpiece may undergo ten or more rotations during a die stroke a large number of simulations steps are required. Because of the large number of steps form rolling simulations are very time intensive.
5. **Contact conditions and rotation of the workpiece**
   Slippage of the workpiece is a problem when modelling the form rolling process. To overcome this problem a high friction factor of m=1 was used, Pater et al [55]

who used 3D FEA to simulate the form rolling process used the same friction factor. Increasing the contact area between the die and the workpiece can also improve traction and, therefore, the rotation of the workpiece. This is achieved by moving the dies radially into the workpiece before starting the die stroke.

The geometry of the micro-form rolling dies used in this research differs from traditional rolling dies in three ways and these three differences had an effect on the FEA analysis of the process:

- The small size of the die feature, due to its small spreading angle, resulted in a very small contact area that led to undesired rotation and slipping of the workpiece.
- The wide flat on the die feature created a large amount of tangential material flow in the workpiece which resulted in very large waveforms on the workpiece
- The lack of a sizing zone on the die allowed a simplified 2D simulation method to be used

Each of these factors will be discussed in greater detail in the following section.

7.6.1 Undesired Rotation of the Workpiece in 3D FEA

When simulating a form rolling process the central axis of the workpiece should form a right angle with the direction of die movement, see Figure 7.31.

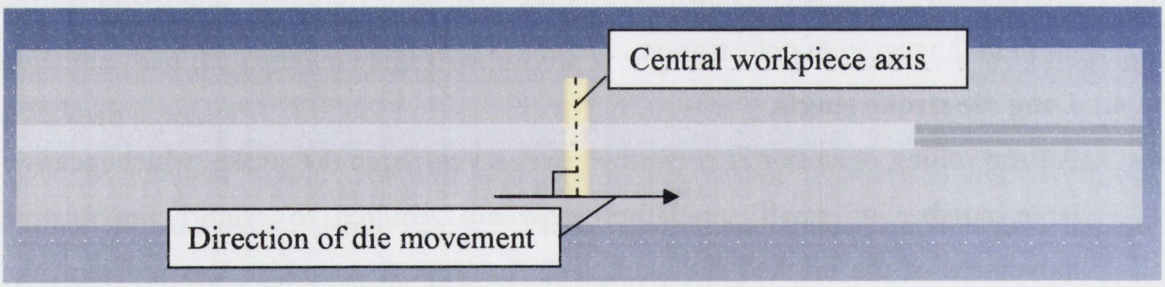

Figure 7.31: Alignment of workpiece axis and die movement under correct operating conditions

However, when simulating the form rolling of a narrow groove, the workpiece had a tendency to rotate around an axis in the centre of the groove that is perpendicular to the die surface, as shown in Figure 7.32.

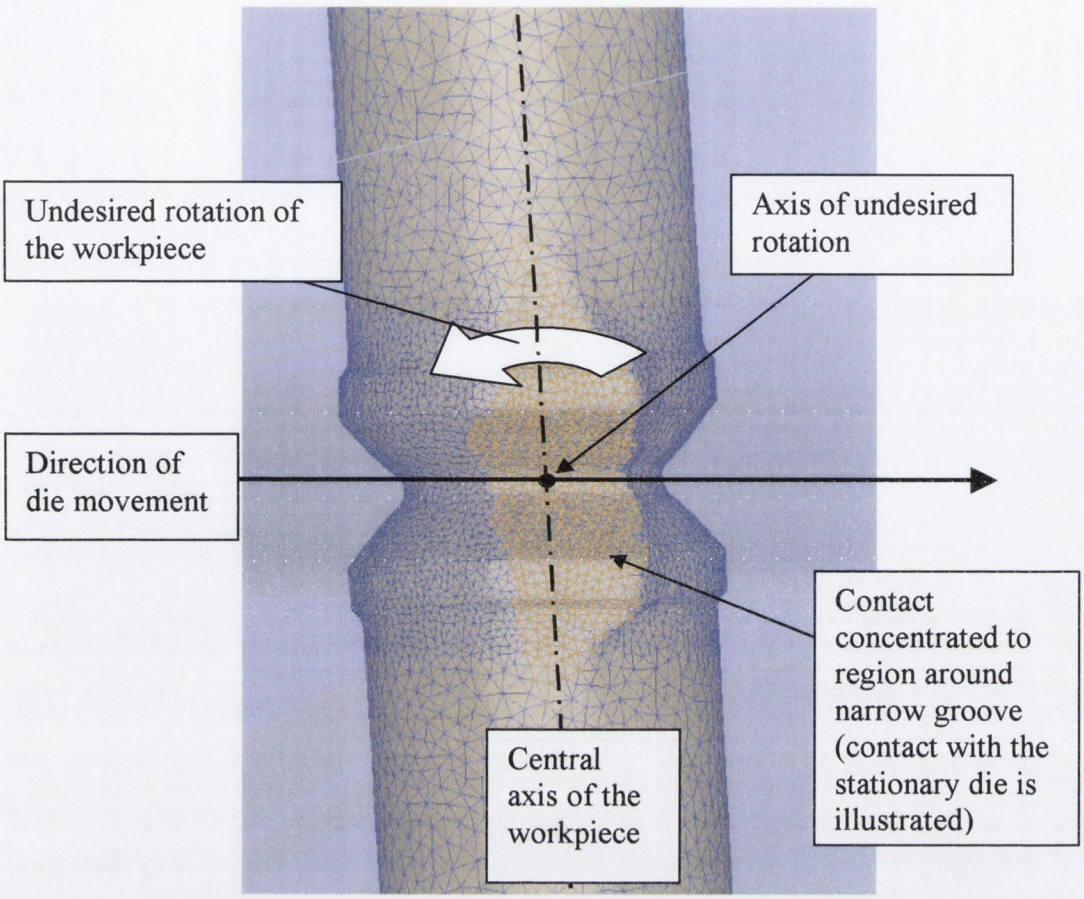

Figure 7.32: Undesired rotation of the deforming workpiece around point of symmetry

This workpiece rotation is undesirable because its severity increases with continued rolling and it leads to slippage of the workpiece. It also increases the simulation times because it increases the complexity of the forming process. Undesired workpiece rotation was also observed in several experimental rolling trials, particularly when smaller diameter workpieces were being rolled. However, the form rolling machine could be adjusted to eliminate this undesired rotation or reduce it to such a degree that it did not lead to workpiece slippage. This adjustment was through a trial and error process in which the machine settings were repeatedly adjusted. This process was feasible because it only took several minutes to implement each adjustment. However, each 3D FEA simulation took several days to run and a trial and error approach was not appropriate for the simulations. Therefore, the simulations were initialised with boundary conditions (bcc) that prevented the undesired rotation of the workpiece.

For this rotation to occur, the workpiece must overcome turning moments that are a product of the frictional forces and their distance from the point of rotation. When simulating the form rolling of a narrow groove, the contact between the workpiece and the

die is concentrated in a small region around the groove and, therefore, the moment preventing the unwanted rotation is small.

During actual deformations in experimental trials, the contact area did not decrease to such an extent because there was always a certain amount of elastic deformation in the workpiece which would retain contact between it and the die. The 3D FEA of the process does not facilitate the use of an Elasto-plastic workpiece and, therefore, several simulation techniques were examined to help solve this problem. These included:

- An obvious solution is the use of the rotational FEA method as the workpiece is prevented from rotating in any direction, by bcc located on the end faces of the workpiece.
- The use of friction strips and knurled regions have also been used with limited success, these methods will know be briefly discussed:

Knurling: The application of knurled surfaces to form rolling dies to improve traction between the die and the workpiece has been referred to in the literature reviewed [15]. Therefore in several simulations, knurled regions were added to the form rolling dies, see Figure 7.33. These regions were positioned near the start of the die to provide increased traction at the start of the stroke when the die feature was at its smallest and, therefore, providing only a small amount of traction.

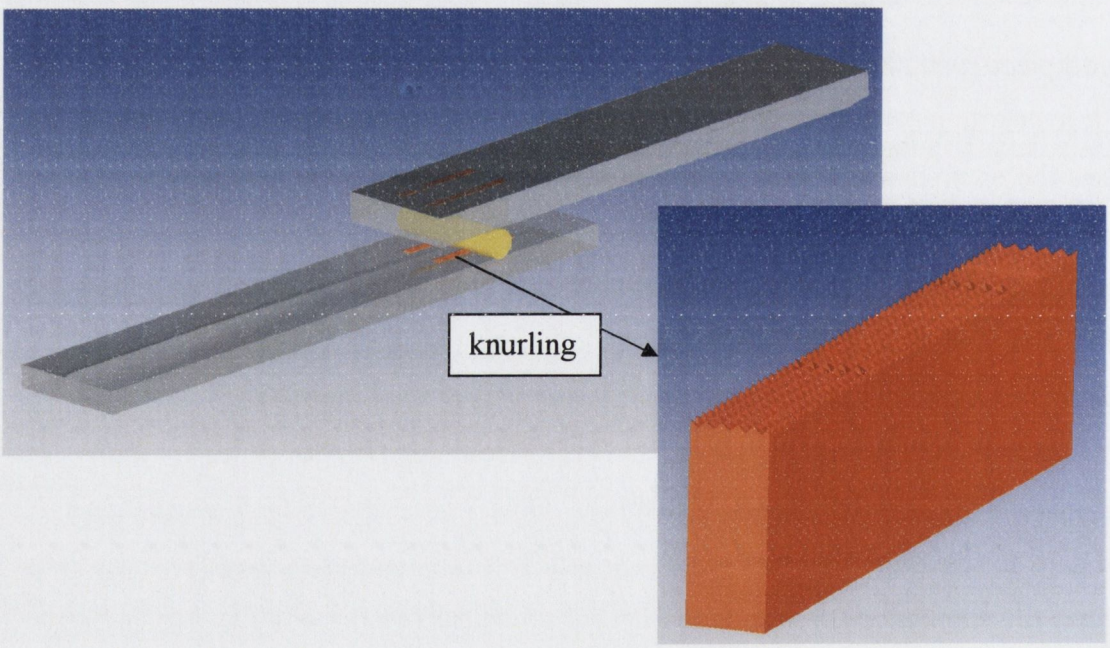

Figure 7.33: The position of the knurling on the die and a close up of the knurled surface.

Although the knurled objects helped to improve traction, they did require a fine workpiece mesh and, therefore, simulation times were increased. The knurling was positioned at the

start of the die and when the workpiece moved out of this zone slippage and unwanted rotation of the workpiece tended to occur.

Friction strips: In some simulations, die regions with higher levels of friction were positioned to aid traction and to prevent slippage and the undesired rotation of the workpiece, see Figure 7.34.

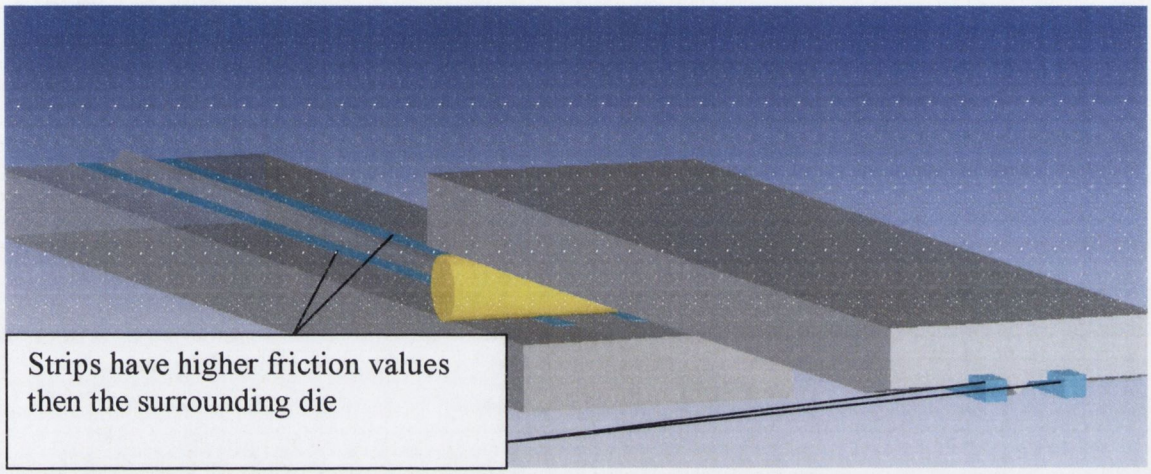

Figure 7.34: Picture showing the friction strips in an FEA simulation

Again, while this method tended to prevent unwanted rotation of the workpiece at the start of the process, its effectiveness decreased with continued rolling.

- When the form rolling process being modelled uses a die with a symmetrical feature, a ½ symmetry model can be used as demonstrated by Fang et al [33]. The boundary conditions required when using such a ½ symmetry simulation prevents the undesired rotation because the face of symmetry must be restrained from moving axially, thereby, preventing the unfavourable rotation of the workpiece as illustrated in Figure 7.35.

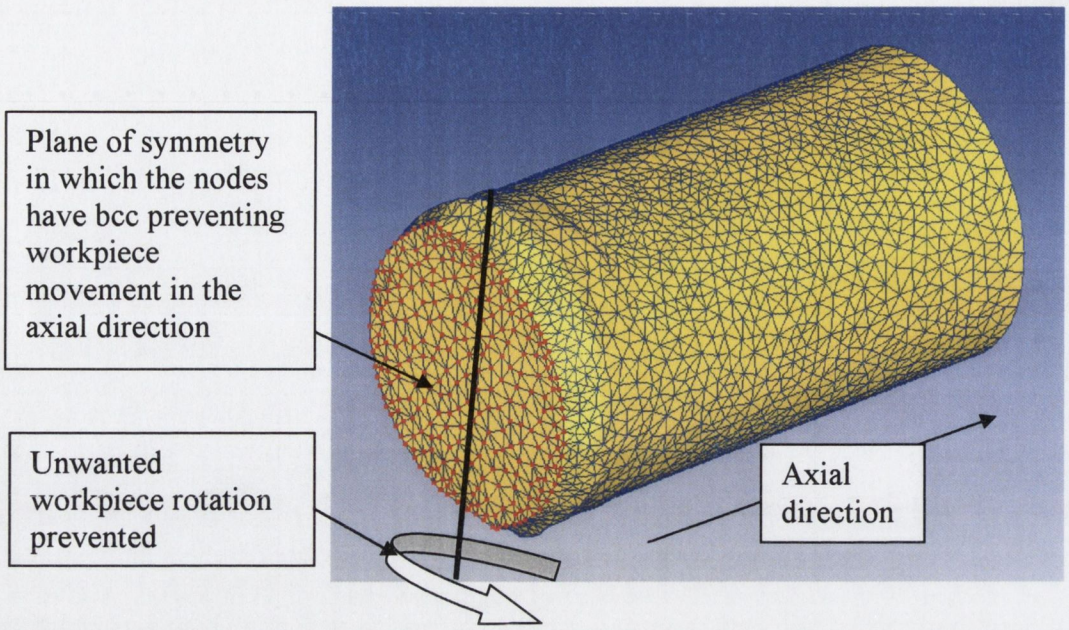

Figure 7.35: A ½ symmetry model showing the axial boundary conditions used to prevent unwanted workpiece rotation

7.6.2 2D Sequential versus Single Stroke Simulation

Traditionally, 2D form rolling simulations are carried out using a sequential simulation method in which the workpiece is assumed to be deformed by a series of dies that gradually deform the workpiece to the required feature geometry. This method is described in greater detail in Chapter 5. However, due to the geometry of the dies used in this project a simpler simulation approach could be taken in which the workpiece is formed in a single stroke with a die that has the required workpiece geometry. This method is advantageous as it is easier to setup because only one die section has to be drawn and positioned in the FEA simulation. It is also less computationally intensive because only one die stroke is necessary.

In order to validate that the single stroke simulation was sufficiently accurate for modelling the process, the results obtained from the simulation were compared to those from a sequential simulation, in which a 0.45mm stainless steel wire was deformed by a 0.45mm die set. Both simulations assumed plane strain conditions. The die loads, workpiece geometry and workpiece stresses were compared and the results obtained are described below:

Die Load

Figure 7.36 shows that the loads predicted by each simulation are very similar; the loads rapidly increase to 50N and then gradually increases to a maximum of just under 200N. The sequential simulation load comprised of 9 individual loads one for each die profile that deformed the workpiece. Excluding the zero values, there is on average a 1.3% difference between the loads for the two simulation types.

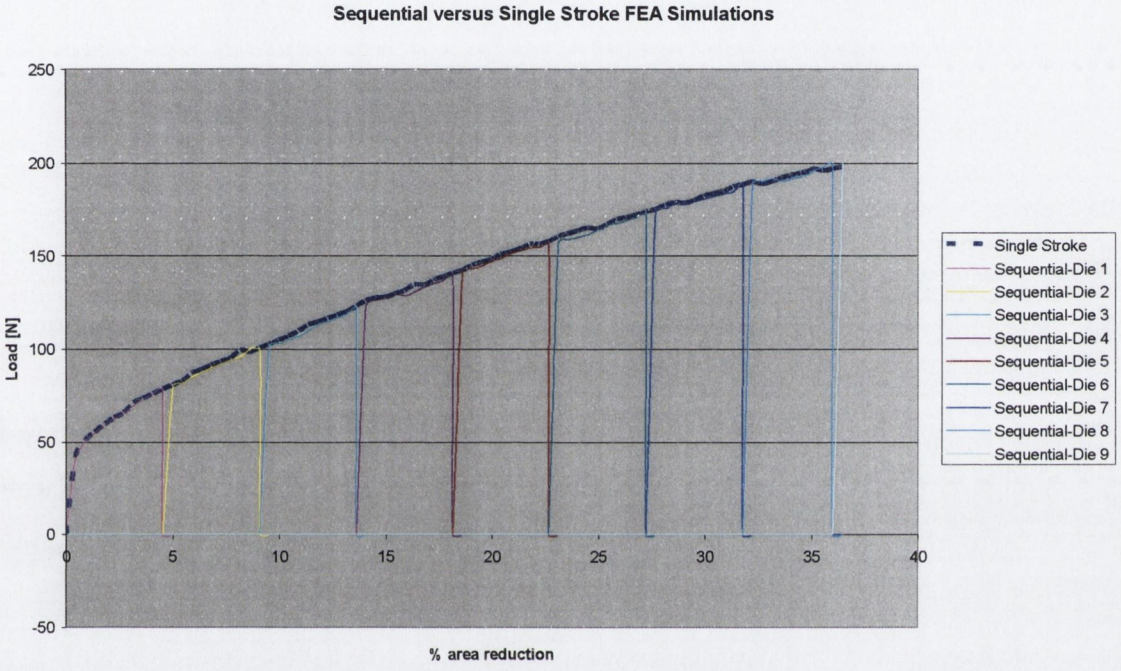

Figure 7.36: Graph of radial die load for sequential and single stroke simulation

Effective Stress in the Workpiece

The effective stress in the workpiece at the maximum area reduction of 60% using both simulation methods were compared using visual and quantitative methods. The stress distributions within the workpiece are shown in Figure 7.37. Again it is evident that they are very similar. The stress is at a maximum where the groove contacts the workpiece and drops off with increasing distance from the groove.

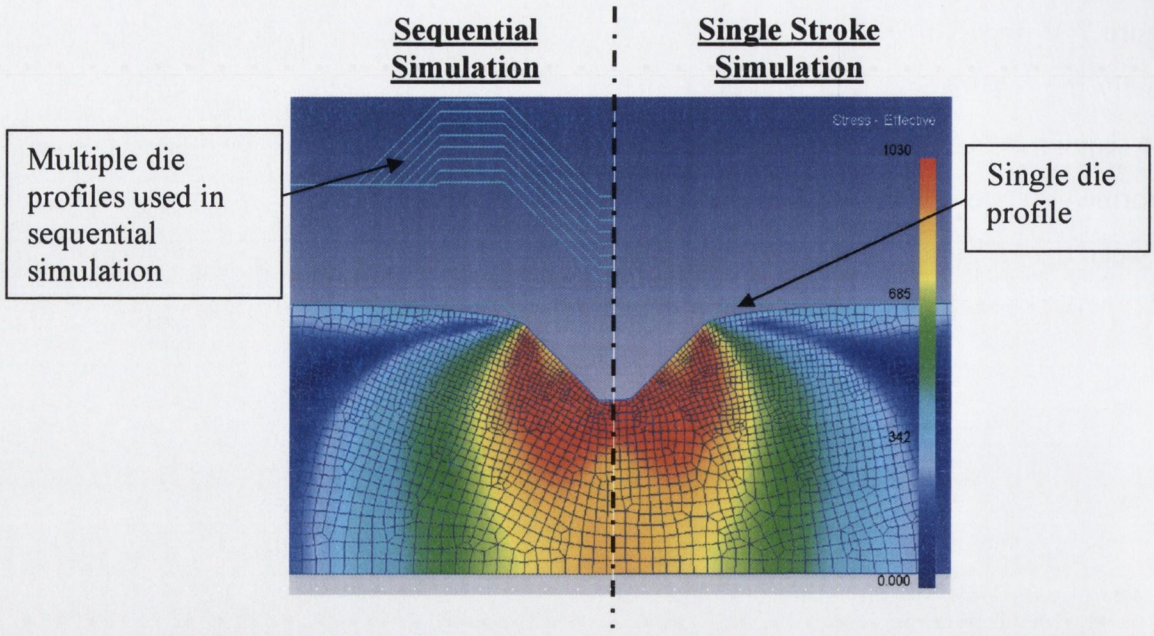

Figure 7.37: Stress Distribution in workpiece for sequential and single stroke simulation

Table 7.4 below surmises the effective stress data obtained for the simulations, it shows that the minimum, maximum, average and standard deviation for the stresses compare well for each simulation. For example, the average stress in the single stroke simulation is only 1.25% lower than the average stress predicted by the sequential simulation.

	Sequential Simulation	Single Stroke Simulation
Min. Stress [N]	0.0555	0.0583
Max. Stress [N]	1030	1020
Average Stress [N]	322	318
Standard Deviation [N]	341	322

Table 7.3: Table of stresses in workpiece for sequential and single stroke simulation

The Shape of the formed Workpiece

Figure 7.38(a-c) shows the shapes of the workpiece at the maximum area reduction of 60%. Figure 7.38(a) shows the outline of the final workpiece geometry when a sequential simulation is used while Figure 7.38(b) shows the outline of the final workpiece geometry when a single stroke simulation is used. Again, the similarity between the produced shapes is clear.

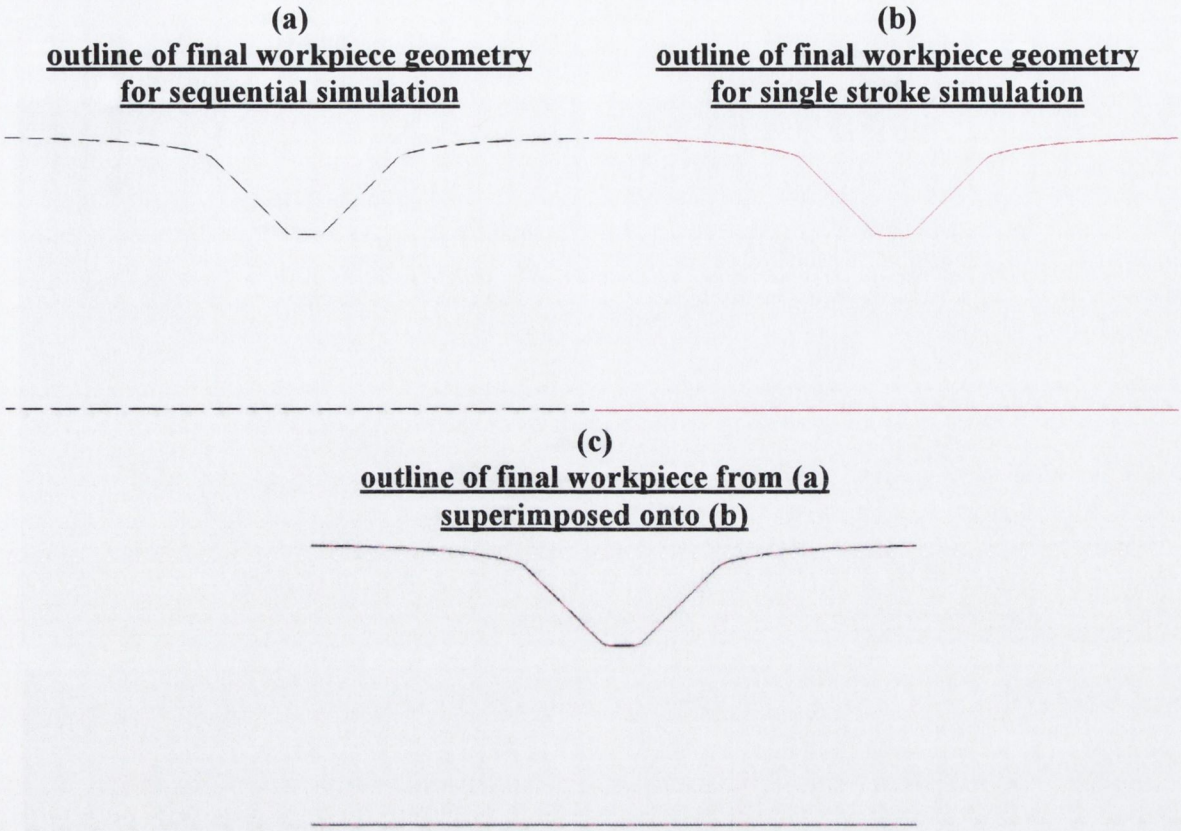

Figure 7.38: The shape of a workpiece following sequential and single stroke simulation

From the comparisons made above it is clear that single stroke simulation method is sufficiently accurate for modelling a form rolling process in which the flat size is assumed to be constant.

When the flat width of the die feature remains constant for the duration of the form rolling stroke the tip of the die geometry always fits into the groove, see Figure 7.39(a). This prevents material being forced into the groove by the die and the possible formation of laps, see Figure 7.39(b). A sequential simulation is, therefore, not required.

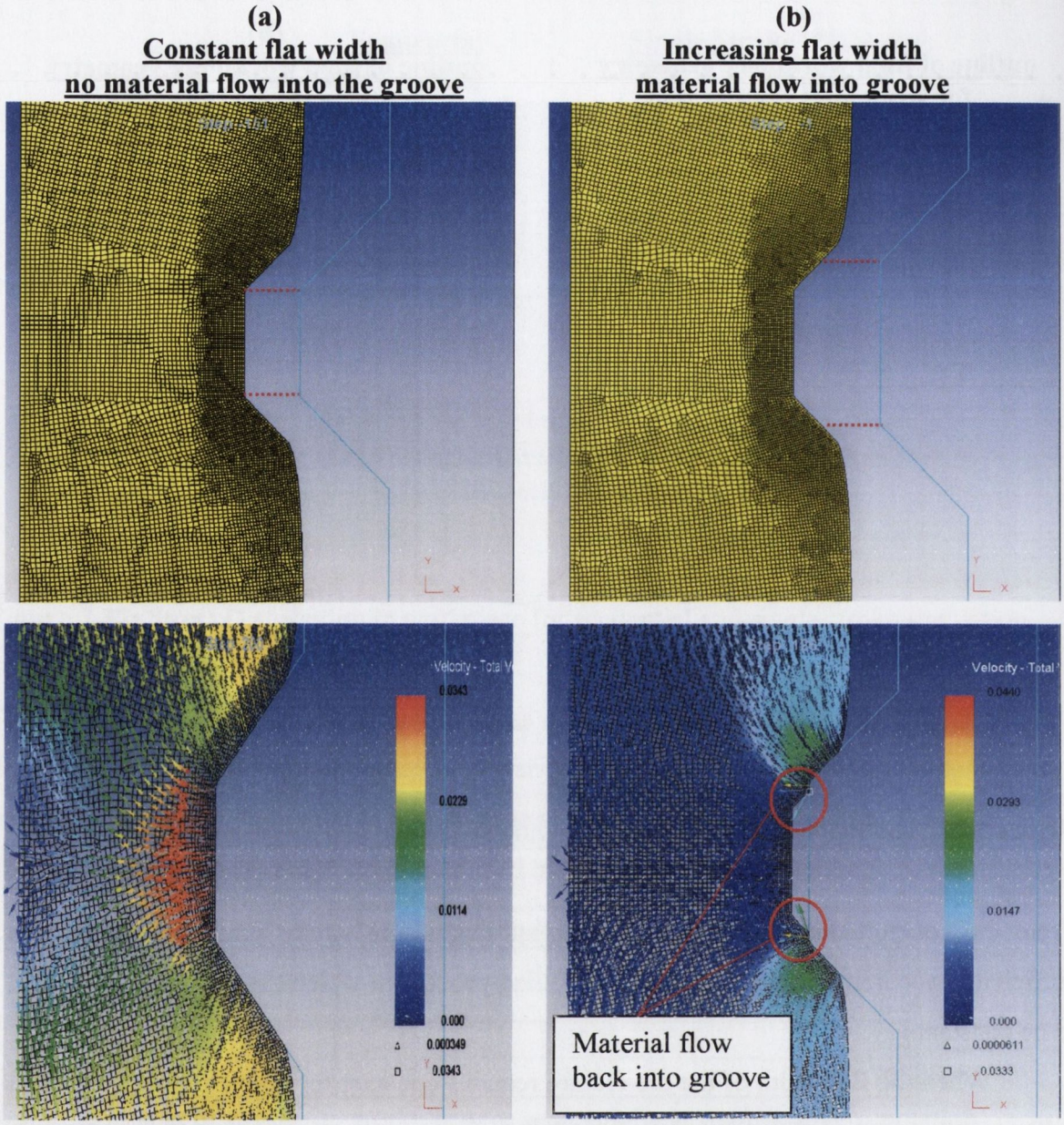

Figure 7.39: Situations in which sequential or single stroke simulations are appropriate

7.6.3 Limitations of 2D FEA

2D FEA simulations of the form rolling process allow new die designs to be analysed very quickly compared to 3D simulations and, therefore, they are a useful tool in the form rolling die design process. However, there are a number of limitations associated with 2D simulations and these are discussed in the following section.

No Restriction on the Axial Flow of Workpiece Material

For the majority of a 2D form rolling simulation, the only part of the die in contact with the workpiece is the actual die feature, see Figure 7.40. The remainder of the die face only

comes into contact with the workpiece at the end of the rolling stroke. However, in reality there will always be some portion of the workpiece in contact with the die face.

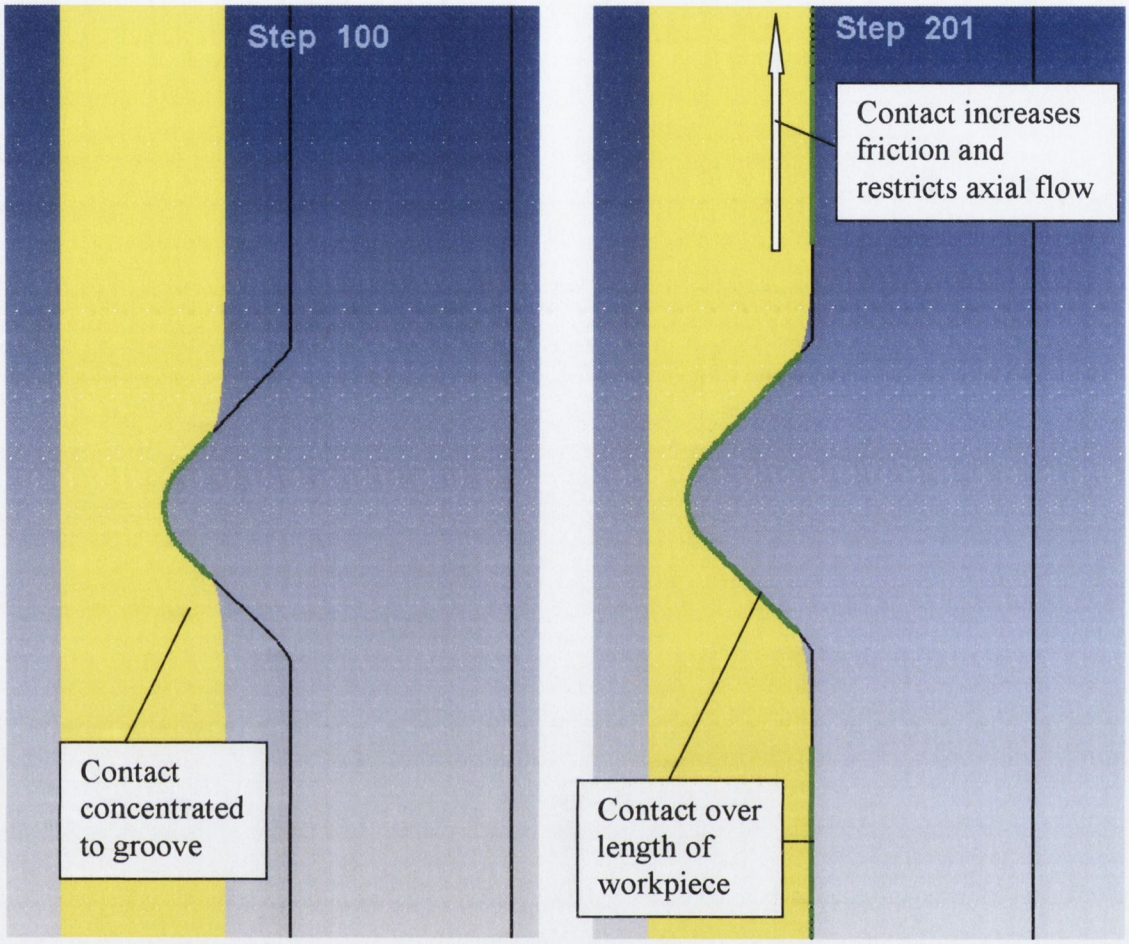

Figure 7.40: Die/workpiece contact conditions in 2D FEA simulations of the form rolling process

When the workpiece is in contact with the die face, there is an increased amount of interfacial friction resisting the axial flow of the workpiece and, therefore, the amount of axial flow of the workpiece material is reduced. Restraining axial flow of the workpiece material has a significant effect on the development of the workpiece shape because, it tends to trap workpiece material in the groove region so the workpiece accurately assumes the die feature geometry. However, in 2D FEA simulations the material finds it easier to flow axially and the geometry of the workpiece groove and die feature deviate. This problem becomes more pronounced when ground die sets are analysed because they have trenches on the side of the feature into which workpiece material flows radially away from the workpiece centre to fill. The filling and the subsequent emptying of these trenches can

be predicted by 3D FEA, as shown in Figure 7.41 but cannot be replicated in 2D simulations.

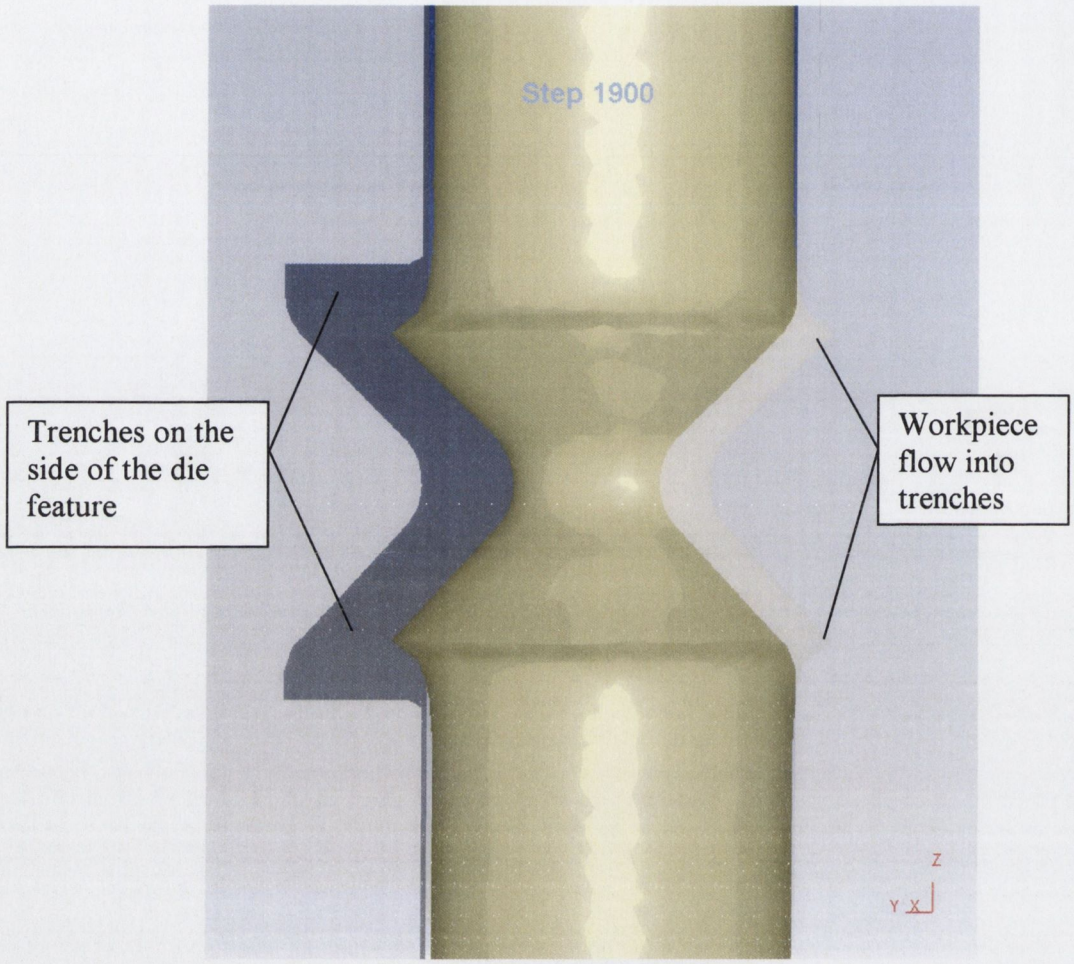

Figure 7.41: Flow into die trenches as predicted by 3D FEA

Form rolled parts that were removed before reaching the die sizing zone where the workpiece material is forced out of the trenches, also exhibited evidence of radial flow into the trenches.

Significant Torsional Stresses that cannot be predicted by 2D FEA

Due to the rotational nature of the process, the workpiece experiences torsional stresses that twist and strain the workpiece. Therefore, 2D simulations have significantly lower effective strains than 3D simulations particularly in the surface region of the workpiece where the torsional strains are at their highest. This is discussed in greater detail later in this Chapter.

The Waveform cannot be analysed using 2D FEA

The waveform has a large effect on the deformation of the workpiece and in controlling the rotation of the workpiece. It is, therefore, important to garner as much information as possible on this feature. The waveform is most evident when a transverse workpiece section is analysed. However, 2D FEA of the form rolling process analyses the deformation on the central longitudinal axis of the workpiece and, therefore, provides no information on the waveform.

7.7 Rolling Loads Predicted by FEA Simulations

Figure 7.42 below shows the normal die load predicted using FEA for a 2mm diameter stainless steel workpiece rolled with the 2mm die set. The drop in the rolling load observed after approximately half a workpiece revolution is typical of load plots calculated using FEA simulations.

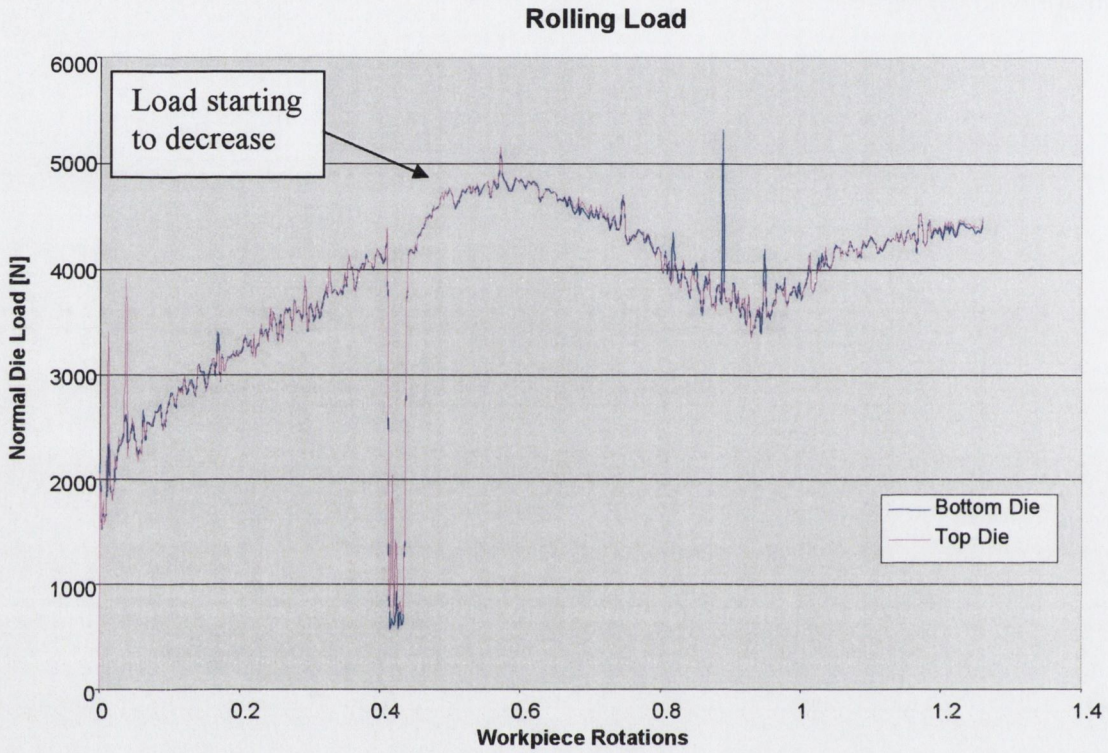

Figure 7.42: FEA simulation showing the drop in rolling load after ½ a revolution

However, the relevant literature would indicate that the load would be expected to increase for the duration of the knifing zone. To determine why the die load decreased in such a manner a more detailed understanding of the rolling load was required. This was achieved using a composite die which assumed the die to be divided into five segments and allowed the load in each of these segments to be determined individually. When a rolling die is examined three regions are evident, the die feature and two flats one on either side of the feature. The largest segment consisted of the die feature and one flat region, the other segments divided the remaining flat into four segments. These segments are shown in Figure 7.43.

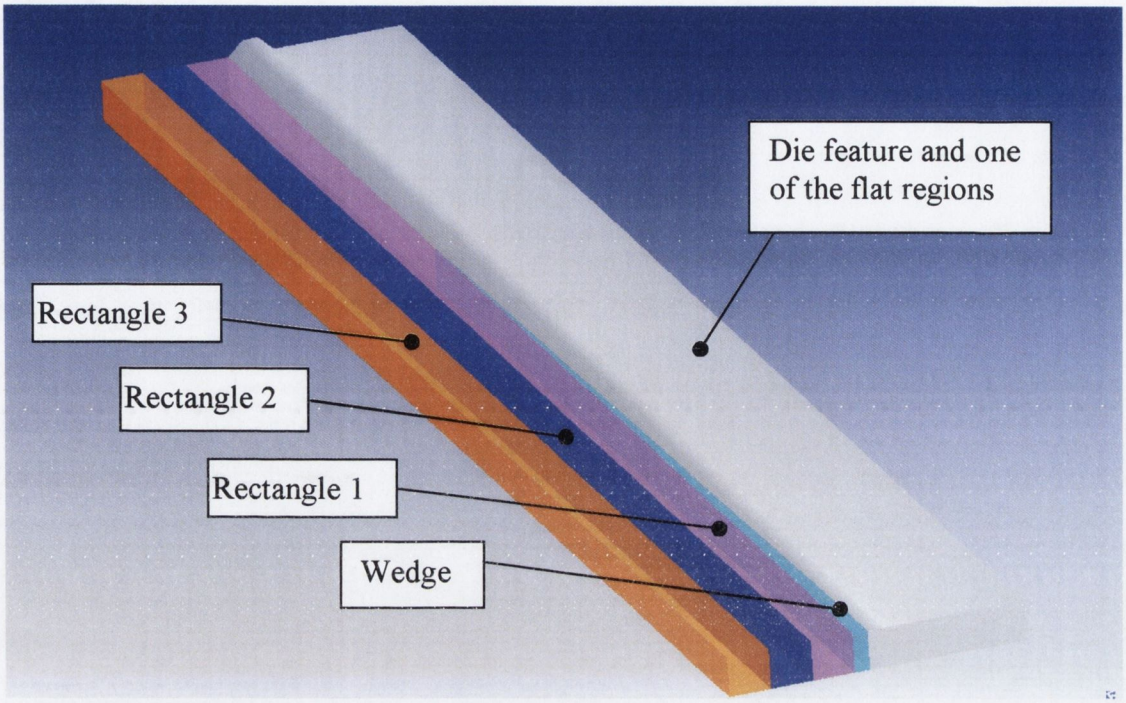

Figure 7.43: The segmented die used to calculate the load in several die regions

The load that the die feature was responsible for could be determined by subtracting the rolling load applied by the rectangles and the wedge away from the load applied by the die feature and one of the flat regions. The loads predicted for these die segments are shown in Figure 7.44 below.

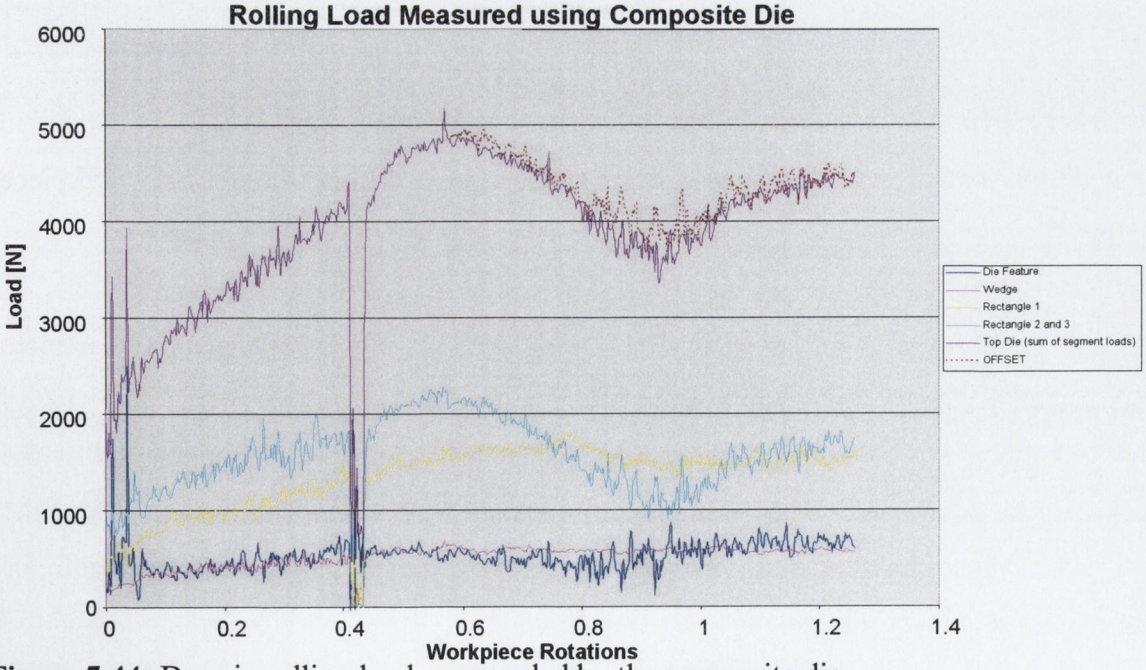

Figure 7.44: Drop in rolling load as recorded by the composite die

The OFFSET line was created by offsetting the load of rectangle 2 and 3 to coincide with the Top Die line and it clearly illustrates that the drop in the rolling load is due to the drop in load recorded by rectangles 2 and 3. This was due to a decreasing contact area between the die and workpiece which is a result of the manner in which the FEA simulation was setup. At the start of the simulation, the dies penetrate a small distance radially into the workpiece (less than 1% of the workpiece radius) and this generates a large die/workpiece contact area which provides sufficient traction to rotate the workpiece, as shown in Figure 7.45 (a, b). During the first half rotation, the contact area increases in size. However, because a plastic workpiece is used after half a rotation the radius of the workpiece is reduced to that of the new die gap and the contact area is significantly reduced, see Figure 7.45(c).

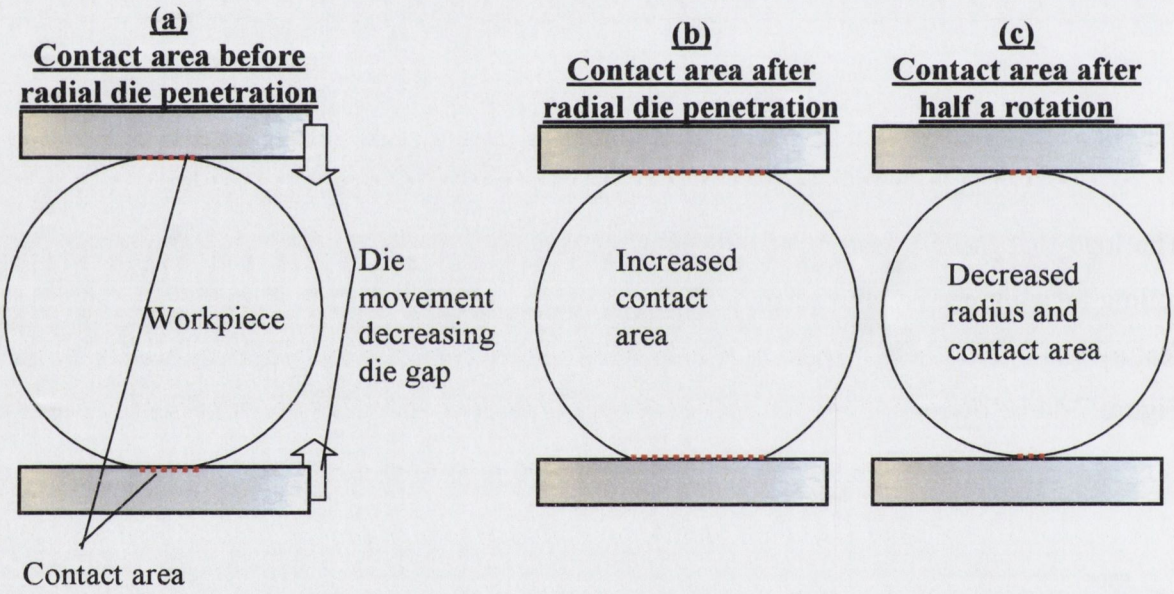

Figure 7.45: Variation in the die/workpiece contact areas during the first half workpiece rotation

The load decreases with further rolling until the workpiece has experienced one complete rotation after which the load begins to increase again.

Consequently, the load determined using a composite die demonstrates that the wedge feature on the die is only responsible for a small proportion of the rolling load at the start of the rolling stroke. For example after, one workpiece revolution it is responsible for only 15% of the total rolling load.

7.8 Stress and Strain Distributions Predicted using FEA

The 3D FEA simulations forming the basis of the stress and strain plots discussed in the following section, were simulated using the rotating die method in which the dies rotate around a stationary workpiece.

7.8.1 Laminar Strain Pattern in a Form Rolled Part as Predicted by FEA

Pater et al predicted a laminar strain pattern in form rolled workpieces with very large strains on the surface decreasing towards the centre of the workpiece. This laminar strain pattern was observed during 3D FEA simulations using DEFORM. Figure 7.46 below clearly shows the laminar strain pattern typical of the rolling process as determined by 3D FEA. The largest strain is located near the surface of the workpiece and the strain level decreases progressively towards the workpiece centre.

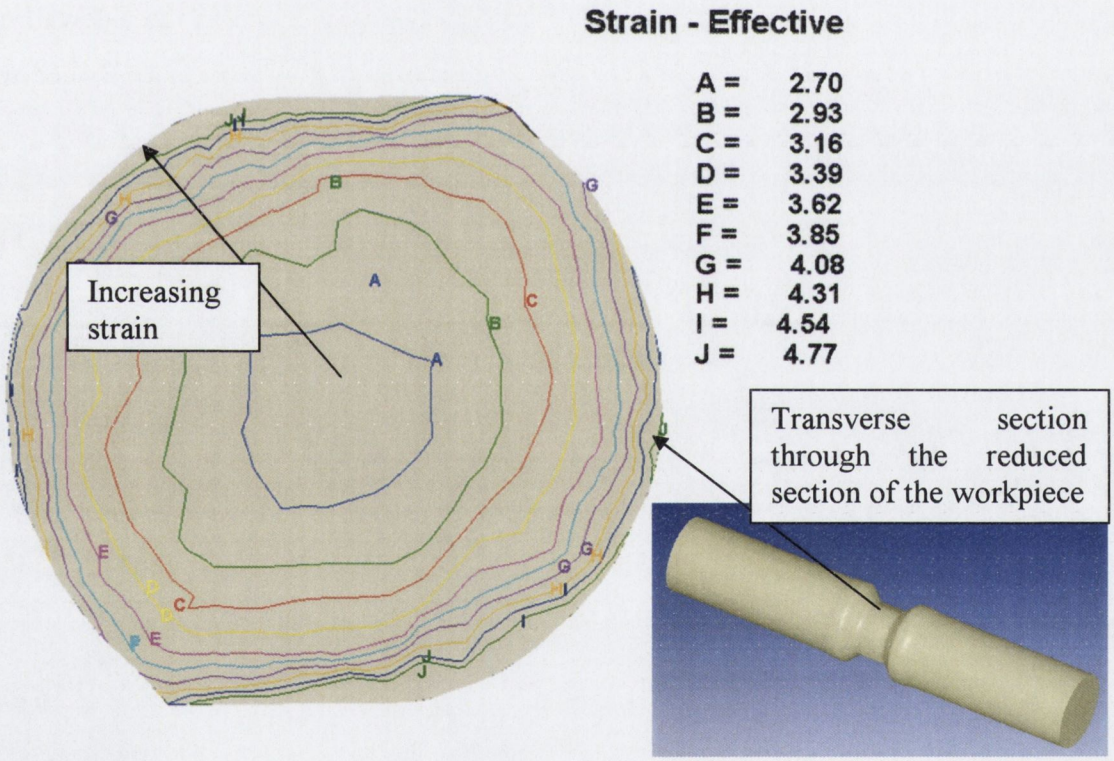

Figure 7.46: Illustration of the laminar strain pattern typical of a form Rolled part. In this instance it is a 1mm stainless steel workpiece rolled with the 2mm milled die set to an area reduction of 60%

A laminar strain pattern was also observed on the sidewall of the workpiece, with the largest strain located near the tip of the groove, as shown in Figure 7.47. This laminar

strain pattern on the groove sidewall is a result of increased workpiece area reduction towards the tip of the groove.

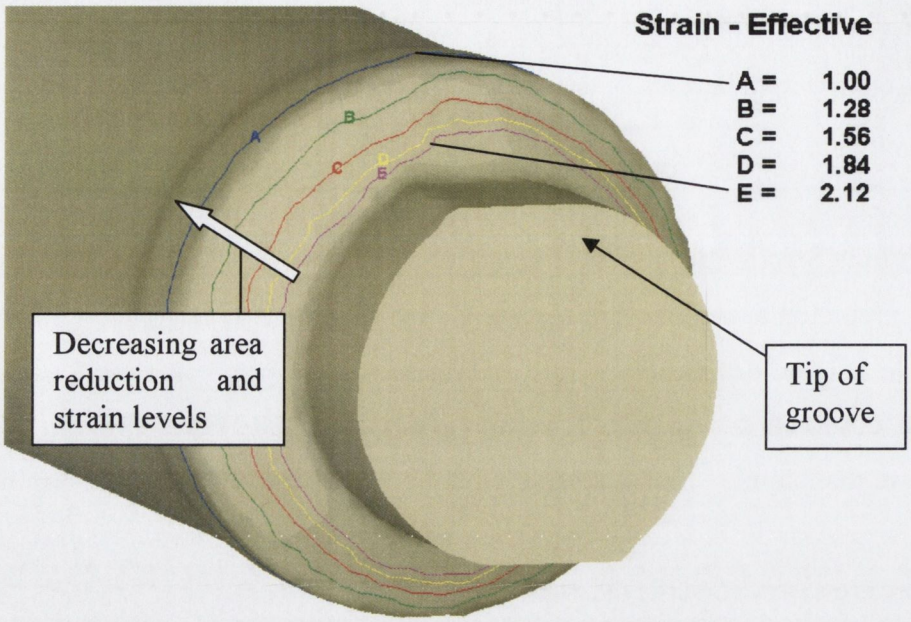

Figure 7.47: Illustration of the laminar strain pattern typically found in the sidewall of a From Rolled workpiece. In this instance it is a 1mm stainless steel workpiece Rolled with the 2mm milled die set to an area reduction of 60%

The effective strain predicted using both plane strain and axisymmetric 2D FEA simulations are shown in Figure 7.48.

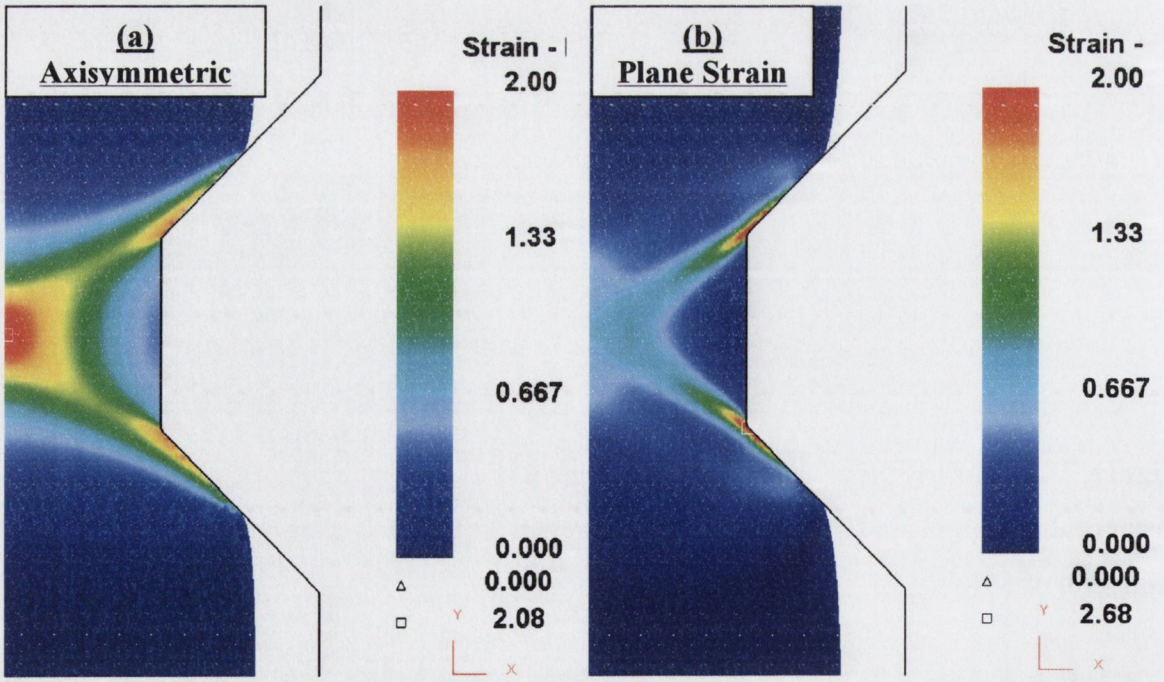

Figure 7.48: Distributions of the strains predicted by plane strain and axisymmetric FEA simulations

While the figures show a laminar strain pattern, the strains are lower than those predicted using 3D FEA and the maximum strain value is located at the centre of the workpiece instead of at the surface.

Both of the workpieces experienced the same level of die penetration. However, the axisymmetric workpiece does undergo a greater area reduction of 60% compared to the 36.8% reduction experienced by the plane strain workpiece. The axisymmetric model has larger strain values than the plane strain model which can be explained by the greater area reduction it has experienced. Both of the 2D simulations predict strain levels that are significantly lower than those predicted by the 3D simulation particularly in the surface region.

The strain levels in the centre of the axisymmetric model and the 3D model are quite similar at 2.4 and 2.7. However, closer to the surface of the workpiece, the difference in strain levels varies much more significantly at 0.5 for the 2D axisymmetric simulation and 4.5 for the 3D simulation. This indicates that, in addition to the straining of the workpiece caused by area reduction which can be predicted by the 2D FEA, there is straining of the workpiece due to the rotational nature of the form rolling process that can only be predicted by 3D FEA.

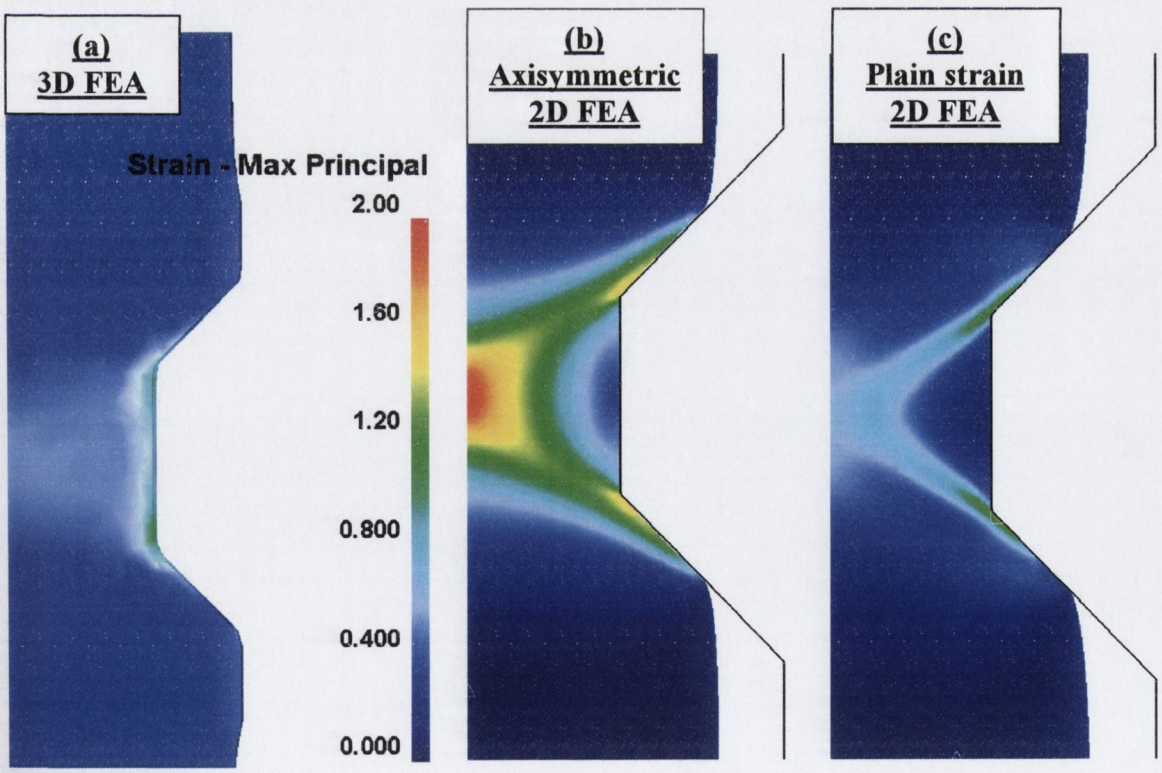

Figure 7.49: The maximum principal strains predicted by 2D and 3D FEA form rolling Simulations

Therefore, to examine the rotational deformation of the workpiece, a series of tracking points or a tracking line was placed in the workpiece. Before the workpiece was deformed these points formed a straight line across its diameter. As the workpiece was deformed, it caused a distortion of the tracking line which highlighted the flow of workpiece material, see Figure 7.50.

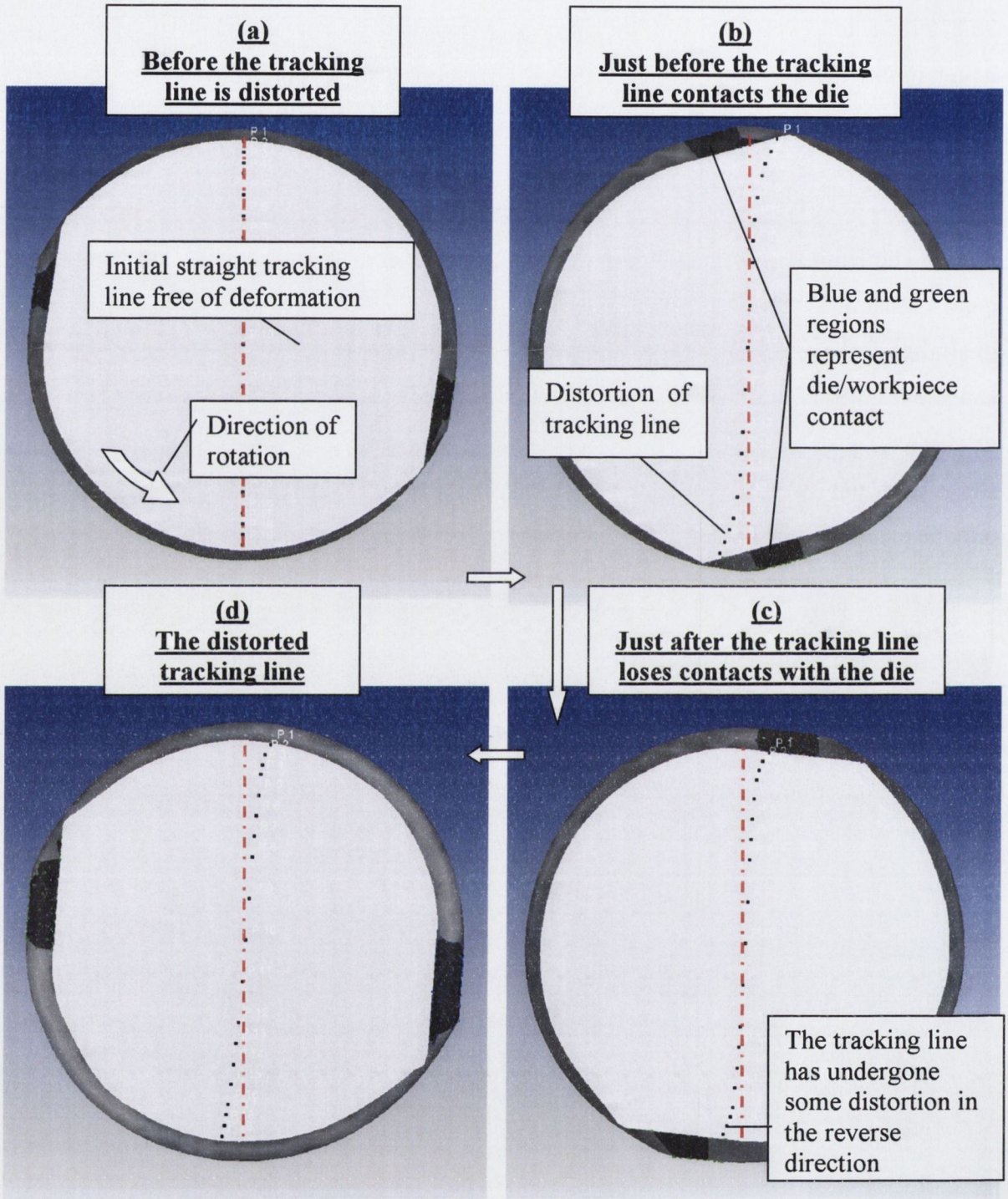

Figure 7.50: The distortion of a tracking line located along the diameter of the workpiece due to tangential deformation

During each die workpiece contact, the tracking line experienced two distinct movements. Before the tracking line contacted the die, the ends of it were distorted in a direction opposite to workpiece rotation and then before the tracking line lost contact with the die the direction of distortion was reversed. These two movements are illustrated in Figure 7.50. In Figure 7.50 the magnitude of tracking line distortion in the reverse direction is much smaller than the initial distortion. However, as the level of area reduction increases the magnitude of the distortion in the reverse direction also increases and it eventually exceeds the magnitude of the initial distortion, as shown in Figure 7.51.

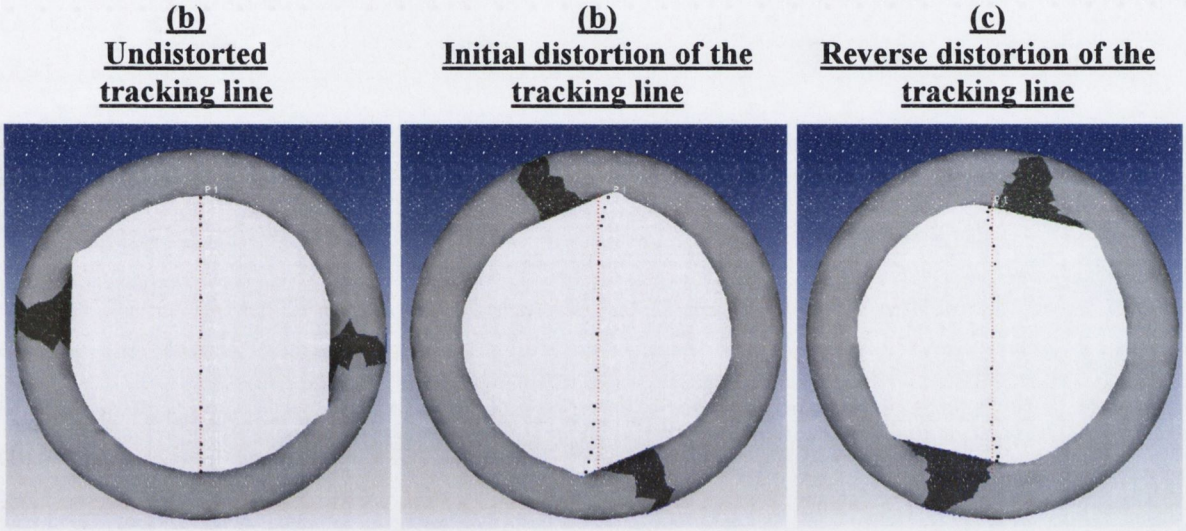

Figure 7.51: Increased area reduction of the workpiece leading to increased distortion of a tracking line located along the diameter of the workpiece

Figure 7.51 also shows that the level of tracking line distortion per die/workpiece contact increases with increased area reduction. The total distortion of the workpiece is the sum of the distortion experienced during each die/workpiece contact.

Nefedov [29] performed rolling trials in which a bolt was screwed into a workpiece. The screw performed the same function as the tracking lines used in FEA simulations as it recorded the distortion experienced by the workpiece. The geometry of the distorted tracking line and the bolt are very similar. In both cases the distortion is concentrated towards the workpiece surface. The concentration of the workpiece distortion towards the surface is also evident when the strain levels within the workpiece are examined. Figure 7.52 shows the effective strain levels within the workpiece, it shows a constant value of strain in the central undistorted portion of the workpiece and rapidly increasing strain levels as the surface of the workpiece is approached.

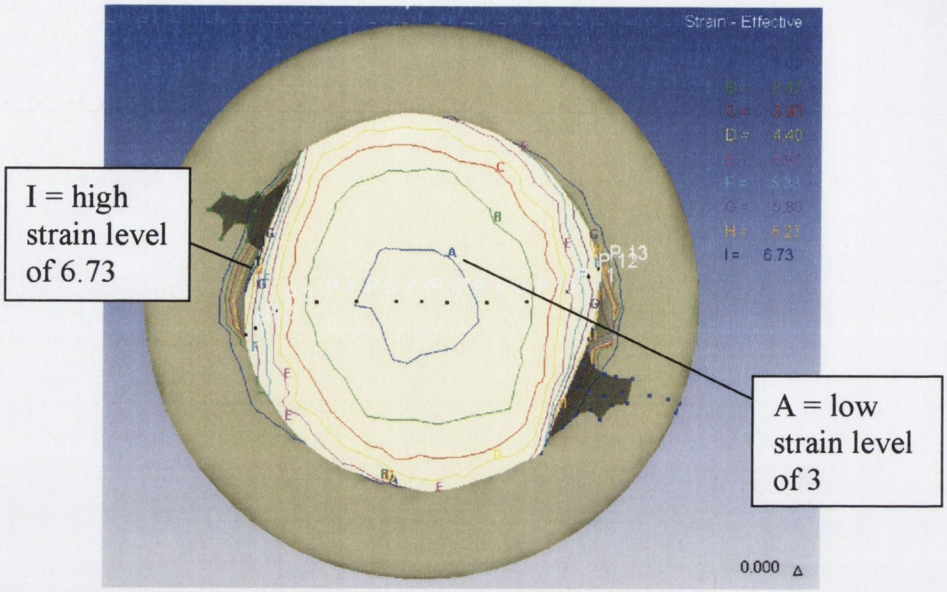

Figure 7.52: Lower levels of effective strain in the centre of a form rolled workpiece where tangential deformation is low

At very large area reductions the tangential deformation stretches across the entire diameter of the workpiece as shown in Figure 7.53.

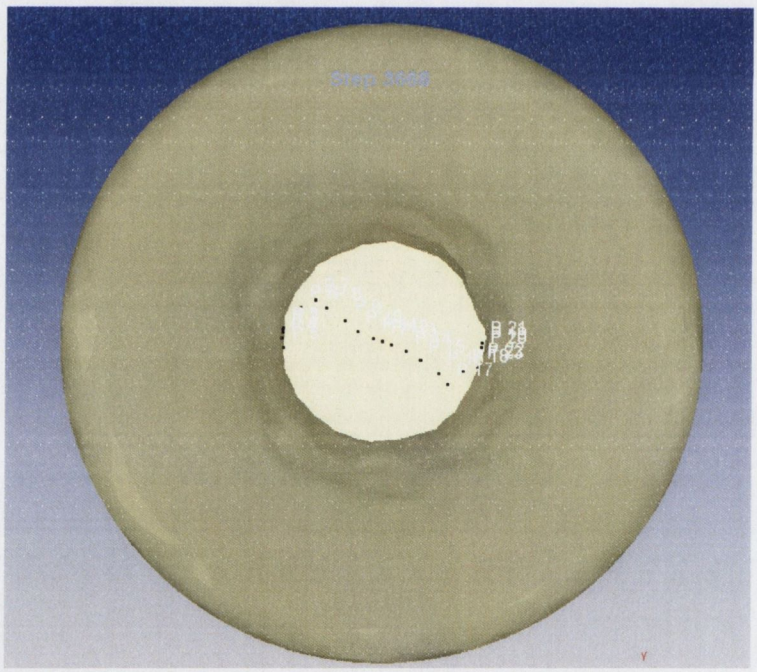

Figure 7.53: Tangential deformation across the entire diameter of the workpiece at a large area reduction

The laminar strain pattern has already been noted in the literature but it has not previously been attributed to the repeated working of the surface region due to the rotational nature of the process. As the workpiece rotates material is initially

deformed in a direction opposite to workpiece rotation before being deformed in the reverse direction. This results in the very large effective strains predicted by the 3D FEA simulations.

The distortion of the surface region of the workpiece during form rolling, has certain similarities to redundant work, which is the additional shearing that a workpiece must under go during deformation due to the necessity of a metal to flow in particular fashion. The additional shearing is not required for the actual net change in the workpiece geometry, but it is required for the material to deform in a mode necessitated by the die geometry. It increases the force needed to deform the workpiece. The additional shearing distorts the internal structure of the workpiece, which can be observed by examining the distortion of a grid within the workpiece. Initially the grid has an orthogonal pattern; however, during deformation it is distorted before being returned to an orthogonal pattern. When FEA is used to predict redundant work it appears as two regions of shear strain rate operating in opposite directions, the first region distorts the workpiece structure and the second returns it to an orthogonal pattern. When the predicted shear strain rate pattern in a transverse section of a from rolled part is examined, two regions of shear strain rate operating in opposite directions are observed, as illustrated in Figure 7.54

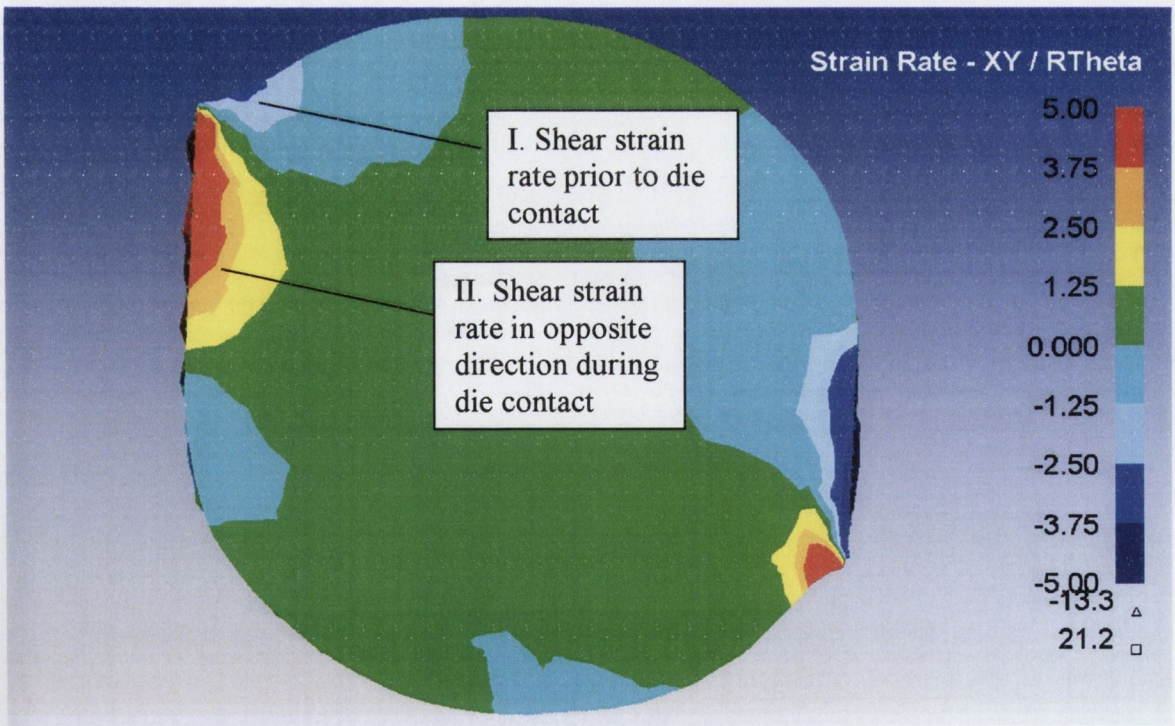

Figure 7.54: Shear strain rate within a workpiece during form rolling

There is a region of high shear strain rate immediately prior to die contact and there is a counteracting region of high shear strain rate acting in the opposite direction where the workpiece contacts the die. The remainder of the workpiece has lower values of strain rate.

However, in form rolling the distortion is a result of the rotation of the workpiece relative to the die, which has the effect of trapping material and displacing it in the tangential direction, rather than the material requiring additional shearing to deform as in the case of redundant work.

7.8.2 **Stress Distribution in a Form Rolled part as predicted by FEA**

The FEA simulations used by Fang et al [33] predicted a tensile maximum principal stress in the centre of the workpiece where the hydrostatic stress was also at is lowest. This was a significant prediction as both of these conditions can contribute to crack initiation. In the die/workpiece contact area both the maximum principal and the hydrostatic stresses were compressive. Eyres [32] and Pater [55] also predicted tensile stresses in centre of the workpiece.

The form rolling stress distribution described above was predicted for the wide variety of rolling conditions examined during the research for this thesis. Figures 7.55 illustrates the predicted stresses within a workpiece formed with a narrow round, and Figure 7.56, illustrates the predicted stresses within a workpiece formed with a wide flat. Both figures show that the maximum principal stress and the hydrostatic stress are tensile for small and large area reductions of 20% and 60 % respectively. This indicates that the form rolling process is tensile in nature, irrespective of area reduction and groove geometry, and, therefore the development of internal failures in from rolled parts is a major concern. The figures also illustrate that the tensile stresses increase as the area reduction experienced by the workpiece increases

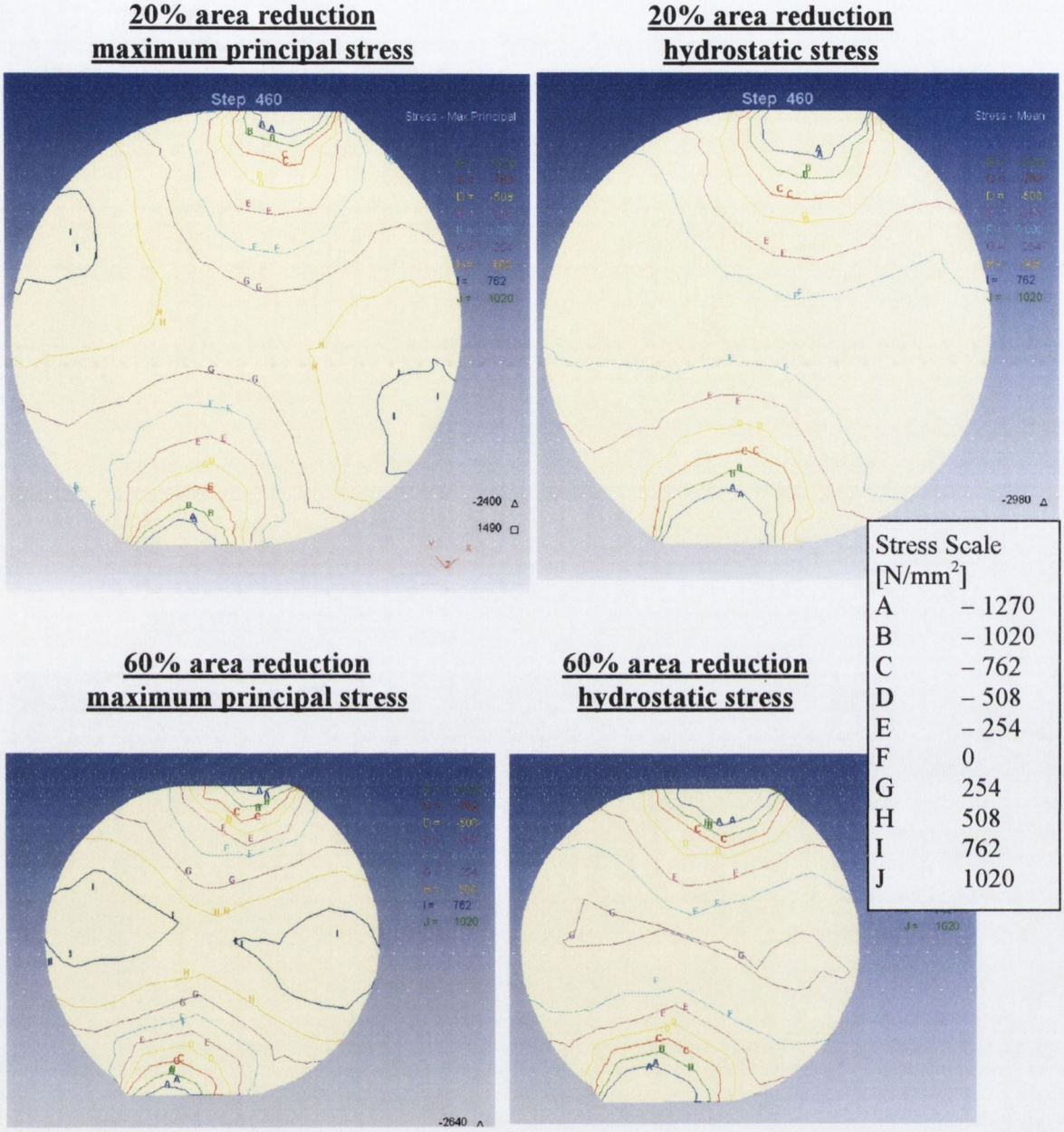

Figure 7.55: Tensile hydrostatic and maximum principal stress in a From Rolled part with a wide groove

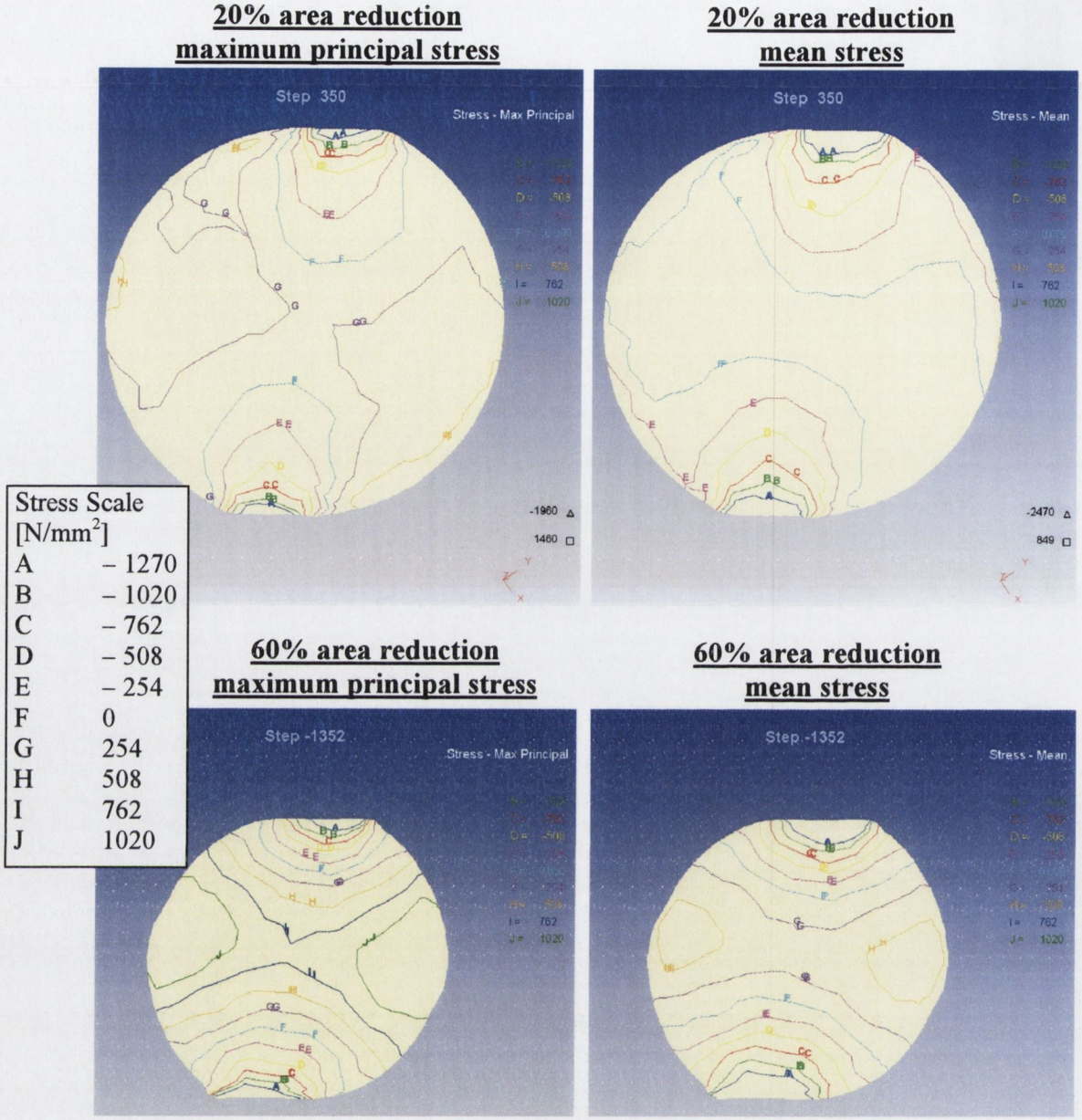

Figure 7.56: Tensile hydrostatic and maximum principal stress in a From Rolled part with a narrow groove

To develop a better understanding of the effect that die geometry and workpiece area reduction have on the micro-form rolling process, the stresses in the radial, tangential and axial directions as predicted by 3D FEA simulations were also investigated. Two die geometries are examined the 2mm ground and the 2mm milled die sets. Each of these die sets produced the same area reduction, however, their geometries are quite different and this affects the deformation mechanism. The main difference in the geometries of the dies is the shape of the tip of the feature. The ground die has a narrow round tip while the

milled die has a wider flat tip. Figure 7.57 shows the predicted stresses in the workpiece as it deformed by the 2mm ground die set.

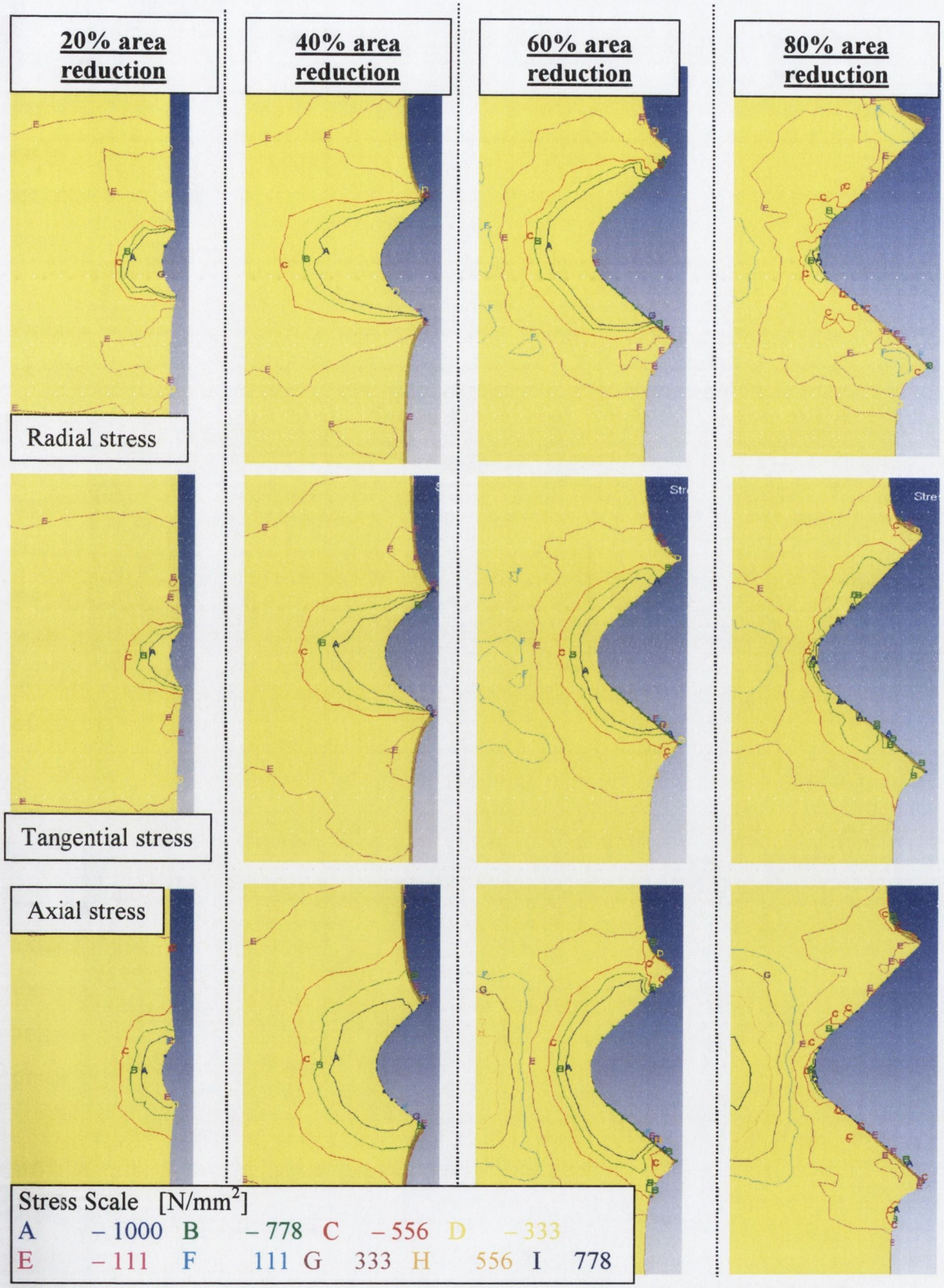

Figure 7.57: The stress distributions in the radial, tangential and axial directions for an increasing area reduction when using the ground die set with a narrow round

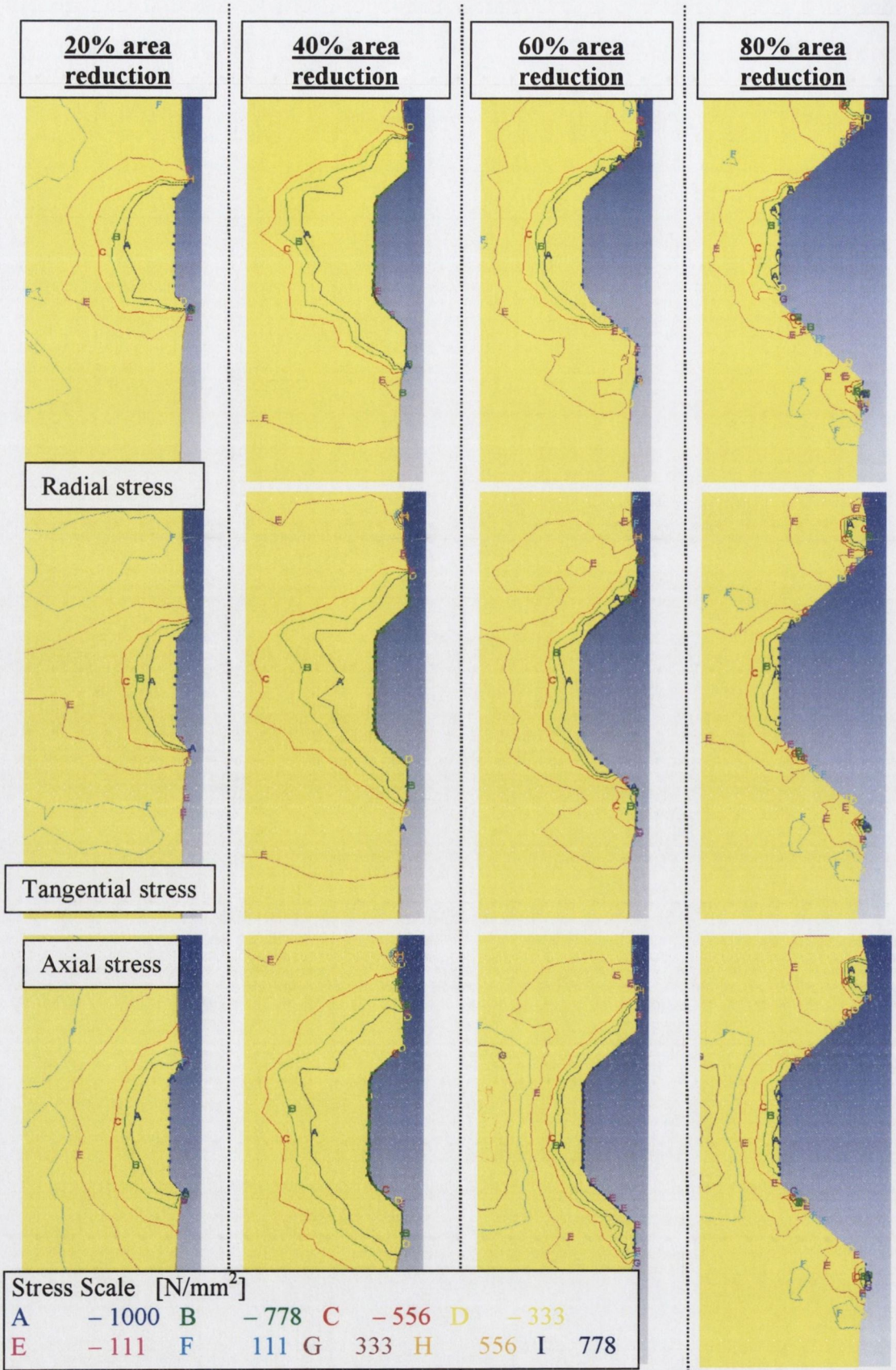

Figure 7.58: The stress distributions in the x, y and z directions for an increasing area reduction when using the milled die set with a wide flat

Figure 7.57 shows the development of a triaxial stress state along the central axis of the workpiece under groove tip. No tensile stresses are present at an area reduction of 40%, however, by 60%, there are tensile stresses in the radial, tangential and axial directions. This highlights that the deformation mechanism experienced by the workpiece is dependent on the area reduction it has experienced. The magnitude of the stresses in the radial and the tangential direction remain constant while the stresses in the axial direction increase. Also as the area reduction increases the tensile stresses become more concentrated under the groove tip, therefore a failure is most likely to occur in this region.

The workpiece formed with the wide flat also becomes more tensile as the area reduction increases however a triaxial stress state does not develop along the central axis, as illustrated in Figure 7.58. The magnitude of the compressive stresses in the radial and the tangential direction decrease as the area reduction increases, although they remain compressive in contrast to the workpiece deformed with the ground dies. The axial stress is tensile as with the ground dies; this is inevitable as the length of the workpiece is increased during the rolling process. The increased level of compressive stress in the centre of the workpiece is due to the large flat width on the die. Whether the workpiece is deformed with the wide flat or the narrow round, the stresses near the surface are compressive, however, due to the large size of the wide flat this compression is retained into the centre of the workpiece.

The triaxial stress state within the workpiece was also examined used 2D FEA simulations the results of which are now presented using stress region diagrams. Nefedov et al [29] explained the deformation mechanism of the workpiece by dividing it into four stress regions which were determined by whether the stresses in the radial tangential and axial directions were compressive or tensile. The stress regions used by Nefedov simplified the visualisation of the complex triaxial stress state in a form rolled workpiece and they are, therefore, used to describe the stresses predicted by the Finite Element Analysis of the process.

As mentioned previously, the stress state within the deforming workpiece varies with groove geometry and the level area reduction. Figure 7.59 (a-d) shows the stress distribution within workpieces deformed by a selection of dies and whose cross sectional areas are reduced to different degrees. In the graphs, the letters C and T indicate compressive and tensile stress respectively, while x (radial), y (axial) and z (tangential) represent the directions of these stresses.

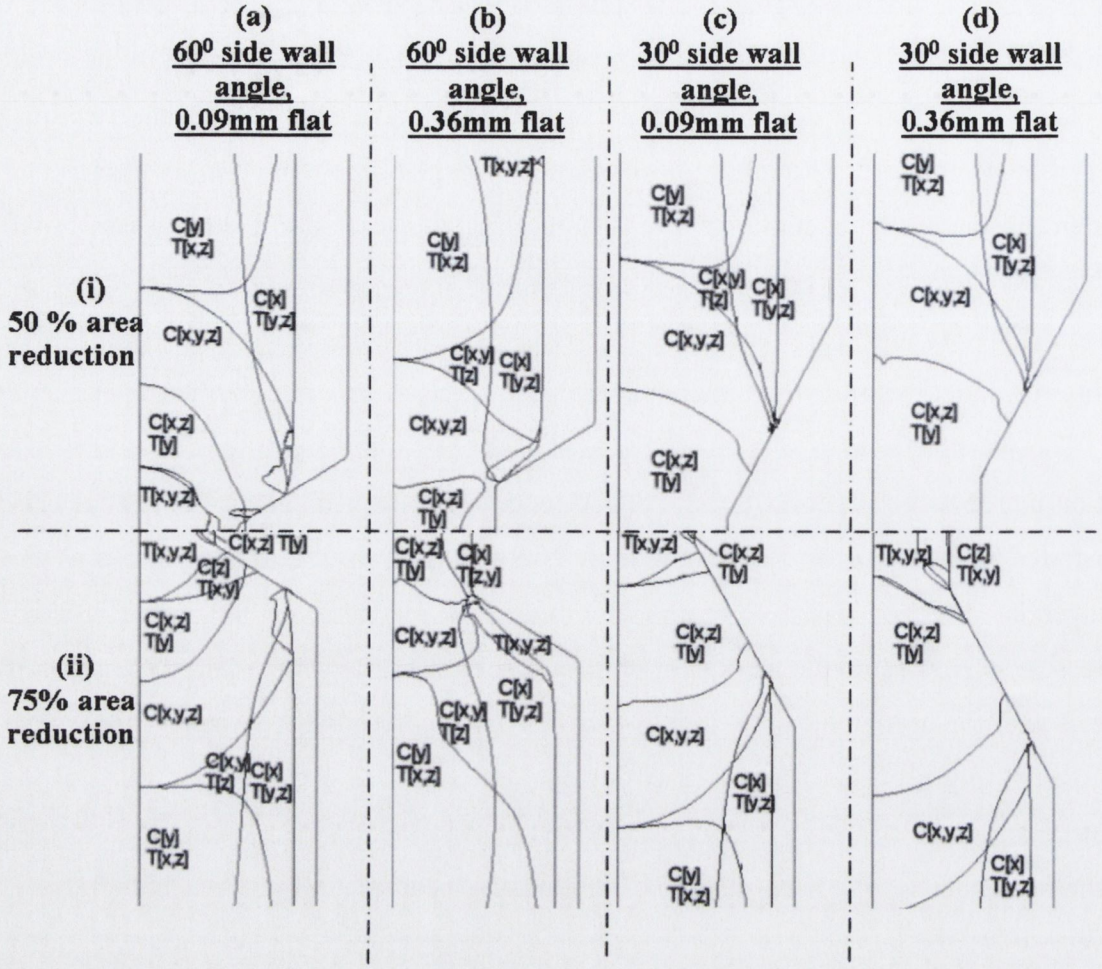

Figure 7.59: Variation of stress distribution within the workpiece as a function of die geometry and cross sectional area reduction.

Figure 7.59(a-d) shows four distinct types of die groove geometry:

1. Narrow groove flat and a large sidewall angle shown in Figure 7.59(a).
2. Wide groove flat and a large sidewall angle shown in Figure 7.59 (b).
3. Narrow groove flat and a small sidewall angle shown in Figure 7.59 (c).
4. Wide groove flat and a small sidewall angle shown in Figure 7.59 (d).

A number of interesting points can be noted from these stress distributions:

- The stress distributions within workpieces deformed by dies with a sidewall angle of 60^0 do not change with increasing area reduction. So the stress patterns for 50% and 75% cross sectional area reduction are very similar.
- The stress distributions within the workpieces deformed by dies with a sidewall angle of 30^0 changes with increased area reduction, and they tend to become more tensile. In this case the central region of the workpieces

changes from having a tensile stress in only one direction (55% reduction) to having tensile stresses in all three directions (75% reduction).

- The stress distributions within a workpiece deformed by a die with sidewall angles of 60^0 and a narrow flat of 0.09mm are more tensile than those deformed with a wide flat of 0.36mm, there are now three tensile stress components in the central region of the workpiece compared with one. This indicates that the flat width is having an influence on the deformation experienced by the workpiece.
- For both the 50% and 75% reduction in area the stress distributions within a workpiece deformed by a die with a sidewall angle of 30^0 and a narrow flat of 0.09mm are very similar to those deformed with a wide flat of 0.36mm. This indicates that the angle rather than the flat size is the dominant factor in the deformation process.

From the observations above it can be concluded that the workpiece will be deformed by one of two different deformation mechanisms depending on both the die geometry and level of cross sectional area reduction.

Indentation

The workpieces shown in Figure 7.59(b(i, ii)), 7.59(c(i)) and 7.59(d(i)) experienced an indentation like process in which the stresses are predominantly compressive except for axial tension. In region I of Figure 7.60, the die penetrates into the workpiece compressing it radially and tangentially while simultaneously forcing the metal to flow axially.

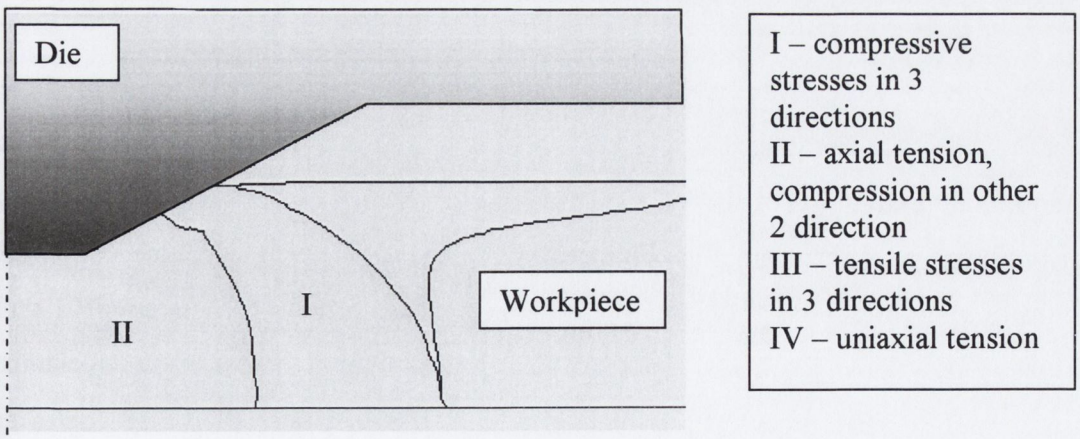

Figure 7.60: Indentation deformation mechanism

In Region II of Figure 7.60, the material is compressed radially by the penetration of the die into the workpiece while the axial flow of material in region I pulls on the material resulting in axial stretching and tensile stresses.

Spreading and stretching

Figure 7.59(a(i, ii)), 7.59 c(ii)) and 7.59(d(ii)) indicate that the workpiece material experienced a spreading and stretching process. Spreading arises as material, newly deformed by the sidewall of the die, is forced to flow axially by the increasing penetration of the die. This is evident in the figures as a region of three dimensional compression, region I of Figure 7.61. This axial flow pulls on the remainder of the material in contact with the sidewall of the die resulting in tensile assisted compression of the workpiece i.e. the workpiece is deformed through a combination of both axial tension (from the spreading region) and radial compression (caused by the penetration of the die into the workpiece), region II. A stretching zone results in the area of the workpiece under the die flat, region III, which experiences tensile stresses acting in three directions.

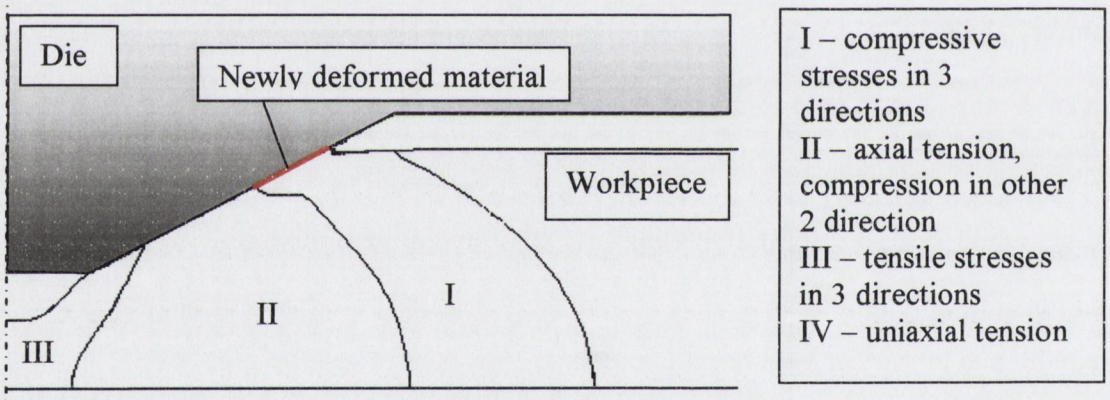

Figure 7.61: Spreading and stretching deformation mechanism

These deformation mechanisms have some similarities with those predicted by Nefedov [29] for a transverse helical rolling process. However, Nefedov's stress distributions predict a region of uniaxial tension which is missing from the stress distributions predicted by the FEA simulations. This tensile region is located in the reduced section of the workpiece and is a result of an applied force which is used to pull the workpiece through the rollers. The spreading and stretching deformation mechanism is more similar to that predicted by Nefedov as it predicts the other three deformation regions.

The indentation like process seems to arise when the workpiece loses contact with the sidewall of the die and, therefore, the spreading effect of the sidewall is lost. The

axial flow of material in workpieces that have lost contact with the sidewall, is a result of the reduction in the diameter increasing the length of the workpiece. This was described in greater detail earlier in this chapter, and a constant volume approach was used to estimate the increase in length with diameter reduction. However when the workpiece retains contact with the die sidewall, the axial flow of material is controlled by their relative lateral movement. This is illustrated by DEFORM plots showing the axial workpiece velocities in Figure 7.24.

7.9 Development of a Larger Waveform on One Side of the Workpiece

During form rolling, workpiece material or a 'waveform' builds up where the workpiece contacts the dies. In several FEA simulations, one of the waveforms was larger then the other. This is problematic as it can lead to the bending of the workpiece and uncontrolled workpiece slip.

When unequal waveforms develop on the workpiece, there is also evidence of workpiece slippage. The slippage is apparent by measuring the position of the workpiece relative to the two dies. If there is no slippage, the workpiece will be equidistant from the start of both dies. However, when slippage is present the workpiece will be further from the start of one die relative to the other. Therefore the workpiece has experienced a degree of slippage along the surface of the die it has travelled furthest along and sticking to the die surface along which it has travelled the lesser distance.

The slippage can be further explained by examining the workpiece velocities. As explained earlier in Chapter 3, rotational and the translational velocities can be represented by the following equations:

$$V_{w,trans} = V_{die,move}/2 \qquad (3.10)$$

$$\omega_w = V_{die,move}/2r_o \qquad (3.11)$$

These equations assumed that there was no interfacial slippage between the stationary die and the workpiece and therefore the velocity of the workpiece where it was in contact with the stationary die was zero. However if there is interfacial slip this velocity is not zero and the velocity profiles and the equations change to those shown below.

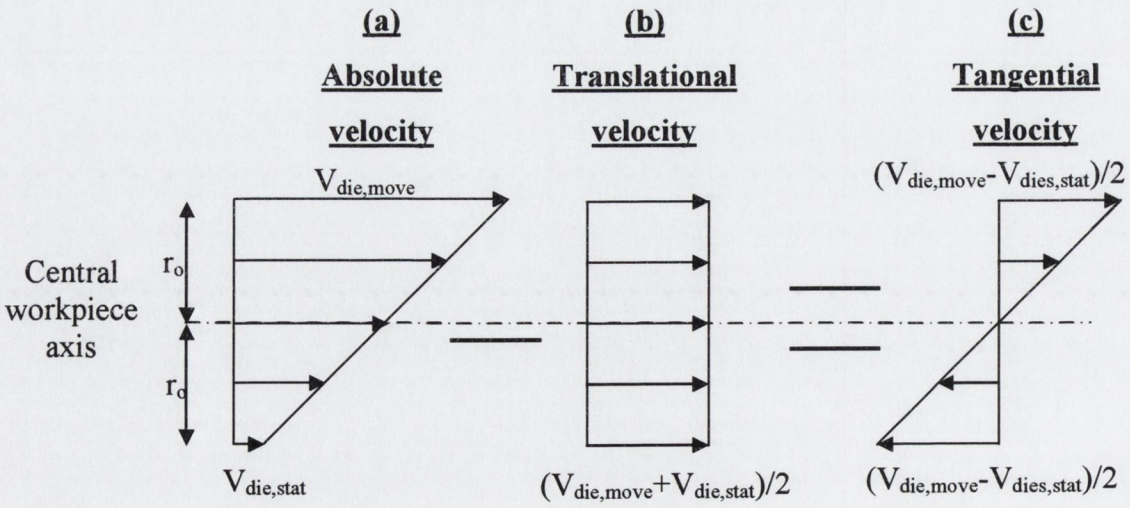

Figure 7.62: Velocity components of the rotating workpiece

$$V_{w,trans} = (V_{die,move}+V_{die,stat})/2 \quad (7.16)$$

$$\omega_w = (V_{die,move} - V_{die,stat})/2r_o \quad (7.17)$$

These new equations indicate an increase in the translational velocity and a decrease in the rotational velocity of the workpiece due to slippage along the stationary die. This is supported by the results of an examination of the workpiece velocities predicted by the 3D FEA simulations.

The slippage leads to the creation of lips on the workpiece where it separates from the die feature and as the workpiece rotates this lip comes into contact with the other waveform and increases its size, as shown in Figure 7.63

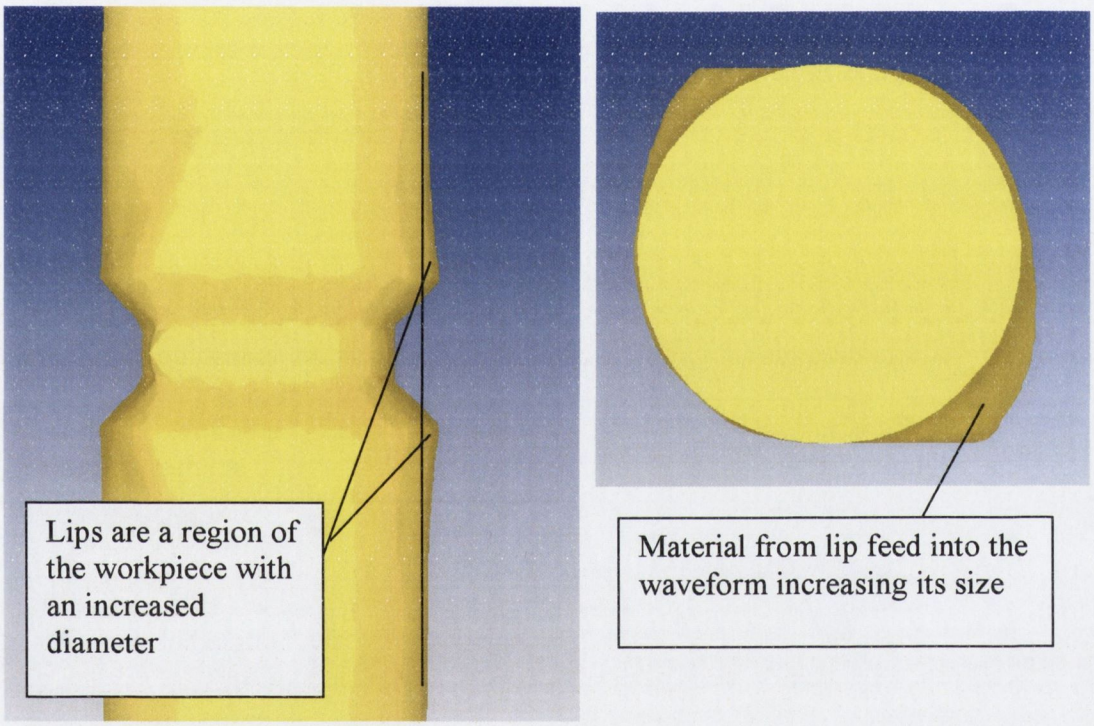

Figure 7.63: Workpiece lips due to the workpiece sliding along the stationary die

The creation of the lip is due to the workpiece slipping along the die feature which causes material to be pulled into the lip. When there is no workpiece slippage, contact is largely a result of the ironing out of the waveform and so die/workpiece contact is concentrated to the side of the workpiece, on which the waveform is located, see Figure 7.64(a). However, when slippage is present, the contact region increases in length, as shown in Figure 7.64(b).

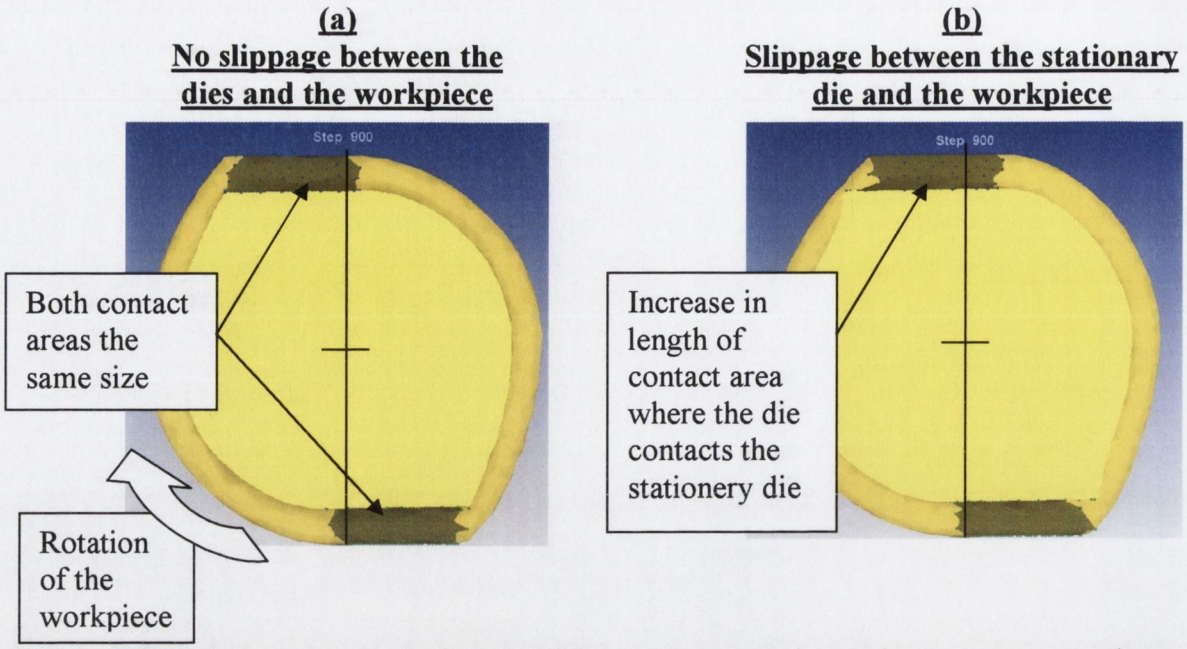

Figure 7.64: The increase in the length of the stationary die/workpiece contact area due to the slippage of the workpiece along the stationary die.

An example of this problem in the case of a 2mm SS workpiece being rolled by the 2mm milled dies will now be given. In this case, the workpiece slips along the stationary die while sticking to the moving die

- After one rotation the workpiece is equidistant from the start of both dies and there is no evidence of lips, see Figure 7.65.

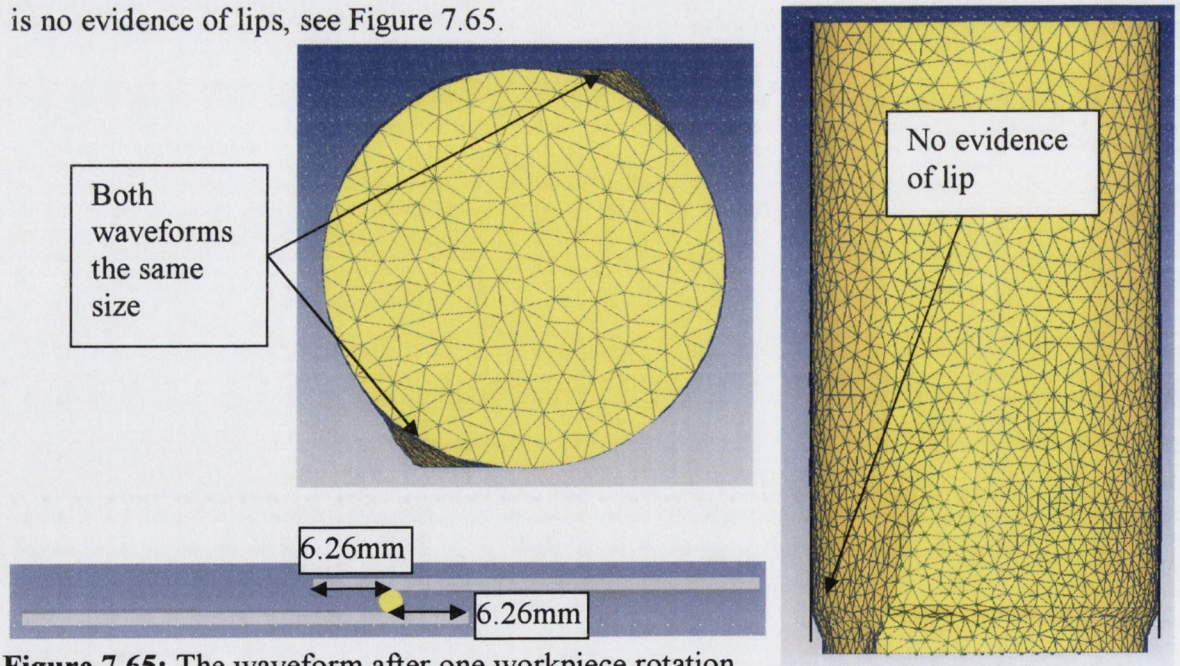

Figure 7.65: The waveform after one workpiece rotation

- Half a rotation later and the workpiece has travelled further along the stationary die compared with the moving die and the waveform in contact with the moving dies is larger then the one in contact with the stationary die. There is also evidence of lips, see Figure 7.66.

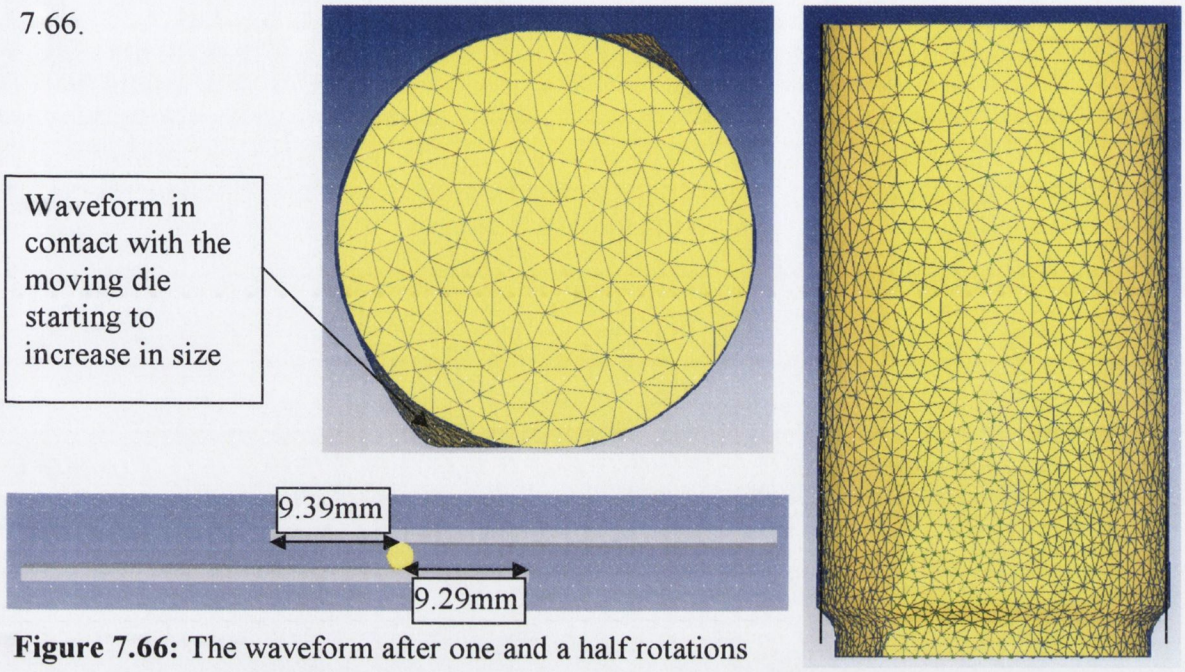

Figure 7.66: The waveform after one and a half rotations

- After two and a half rotations the problem has become much more pronounced, as shown in Figure 7.67.

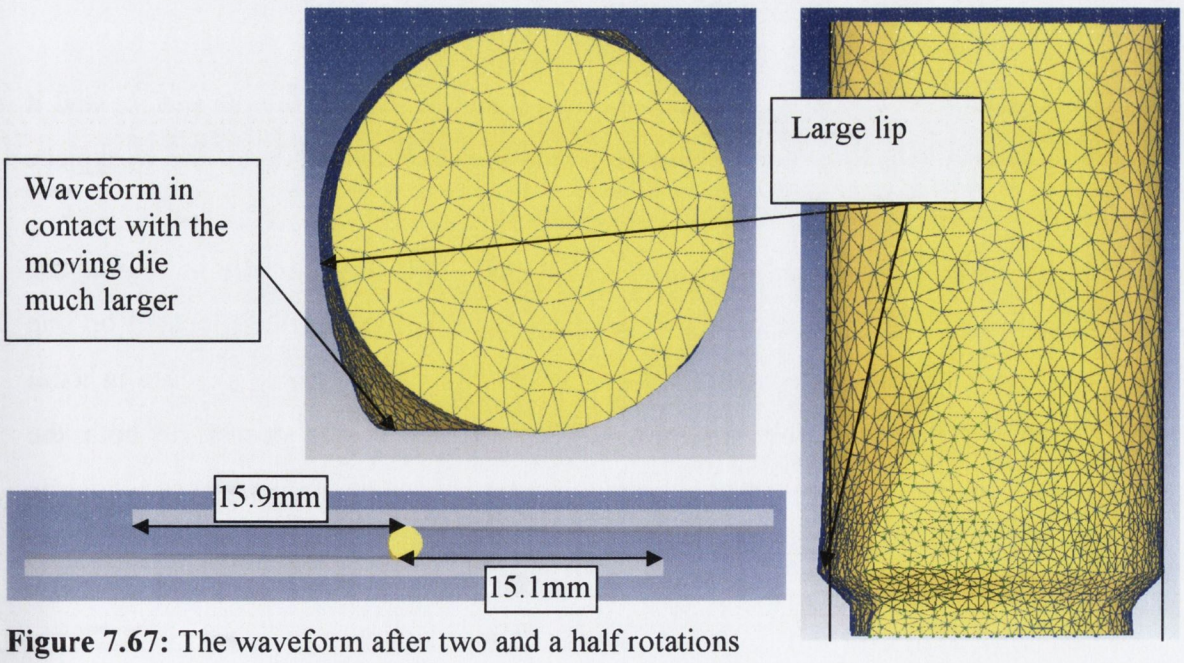

Figure 7.67: The waveform after two and a half rotations

Evidence of the workpiece sliding along one of the dies can also be found when the velocities and contact conditions of the workpiece are examined.

Furthermore, with continued rolling, and an increasing mismatch between the waveforms, bending of the workpiece tends to occur as illustrated in Figure 7.68.

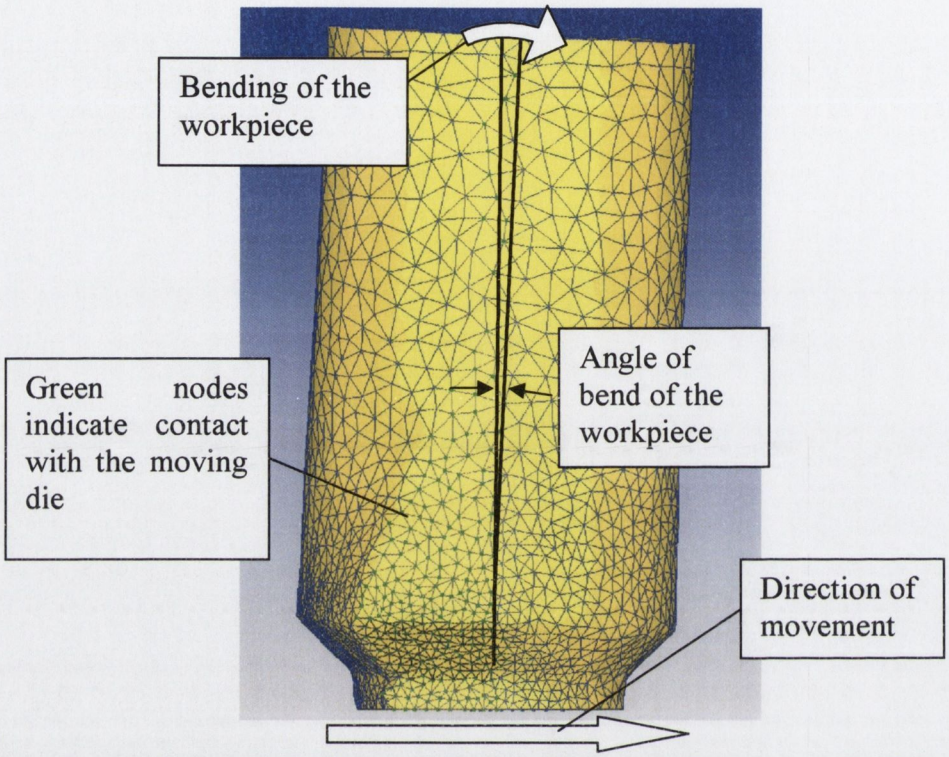

Figure 7.68: The bending of the workpiece due to the mismatch in the size of the waveforms

This bending of the workpiece occurs on a plane parallel to the die surface and it results in the ends of the workpiece being displaced ahead of the middle of the workpiece in the direction of workpiece translation, see Figure 7.69.

As the material in the large waveform is ironed out it flows axially increasing the length of the workpiece. But because all the material in the waveform is located on one side of the workpiece this side of the workpiece experiences a greater increase in axial length than the other, and, therefore, bending of the workpiece occurs. If both the waveforms were the same size the axial material in both sides of the workpiece would be equal and workpiece bending would not occur.

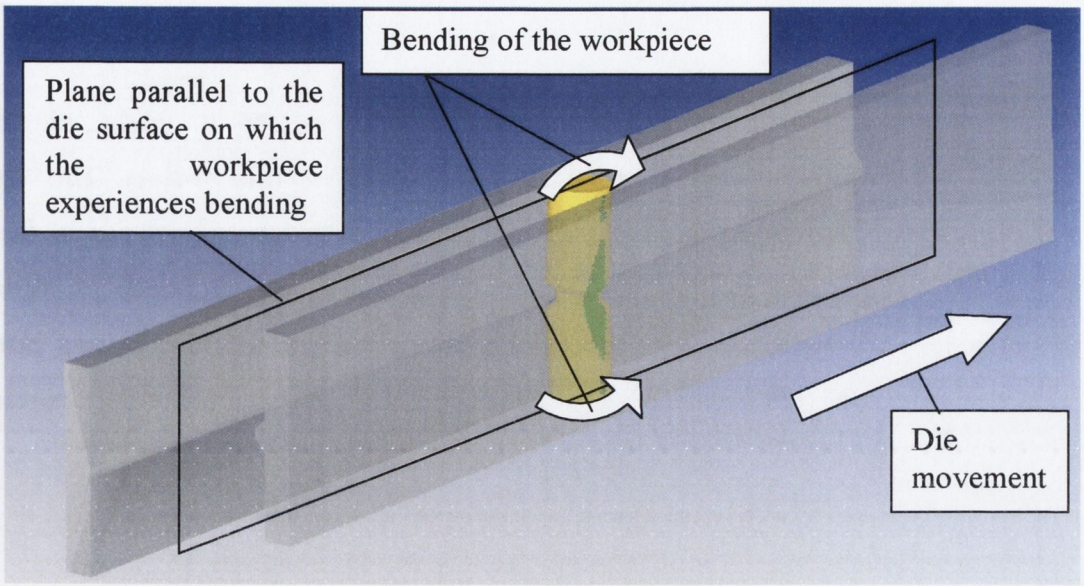

Figure 7.69: The plane on which the workpiece bends when one waveform becomes much larger then the other.

It is difficult to show experimentally that this is a contributor to workpiece slippage as it is very difficult to gain access to the part during the rolling stroke, to examine the development of lips and unequal waveforms and by the end of the die stroke, these problems are likely to have been ironed out.

7.10 One-Die Rolling

The viability of the novel one-die rolling process, in which one of the wedge dies is replaced with a flat traction block, has been proven during this project. This die configuration was used to roll a variety of die/workpiece combinations and has in fact proven to be more successful than traditional form rolling under certain conditions. Wire diameters ranging from 0.45 to 2mm where rolled using the process and it was also modelled using DEFORM 3D. Figure 6.32 shows parts that were rolled using the one-die rolling process.

7.10.1 Importance of the Viability of One-Die Rolling for Micro-Form Rolling

Under certain conditions, which are described in this section, all the deformation experienced by a workpiece may be due to only one die, resulting in what is in effect a one-die rolling process. Therefore, the viability of one-die rolling takes on important connotations for the viability of micro-form rolling as a whole. This effect is primarily a result of the small spreading angles used on the rolling dies which means that the successive die geometries encountered by the workpiece as it rotates between the dies are dimensionally very similar to each other. Therefore, if one of the dies deforms the workpiece to a greater extent than specified, it is possible that the other die will not deform the workpiece at all. This could arise if the starting point of the moving die is set incorrectly, or if due to manufacturing problems, there is a difference between the geometries of the dies. The likelihood of these events occurring increases with the miniaturisation of the process and the conditions under which they would arise are discussed below.

Out of specification groove width in the knifing zone

Circumstances leading to one-die rolling in the knifing zone of a two wedge die arrangement are unlikely because both the width and depth of the feature are increasing. However the area of workpiece/die contact may be restricted to the tip of the groove, resulting in a situation that is in effect a one-die rolling process. The die dimension most likely to be out of specification is the flat width, f, which is regularly wider then specified.

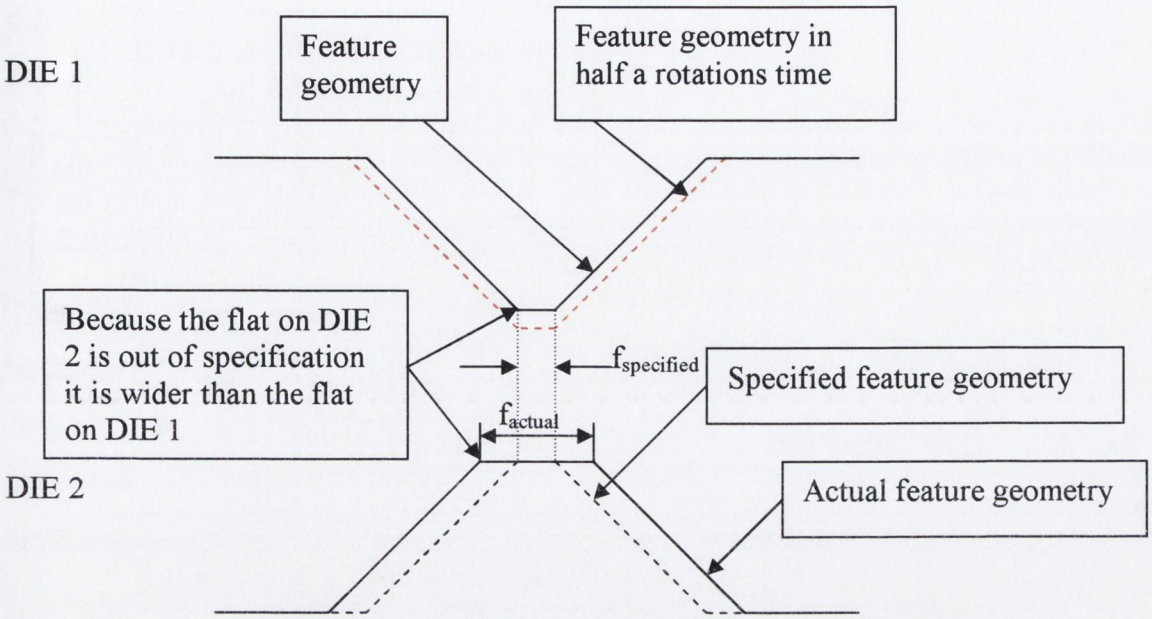

Figure 7.70: The conditions that lead to one-die rolling in the knifing zone

In Figure 7.70 the solid black lines represent the actual die geometries in the region of workpiece contact. The dashed black lines represent the specified geometry of die 2 while the dashed red line represents the geometry of die 1 in half a rotations time when the region of the workpiece currently in contact with die 2 will contact it.

For the sidewalls of die 1 to contact the sidewalls of the workpiece, the increase in width in half a rotation, Δw must be equal to or greater than amount the groove width is out of speciation, w_{error}, see Figure 7.71. If it does not increase by this amount, then only the ΔR region of the die will contact the workpiece, and a situation approaching one-die rolling will occur.

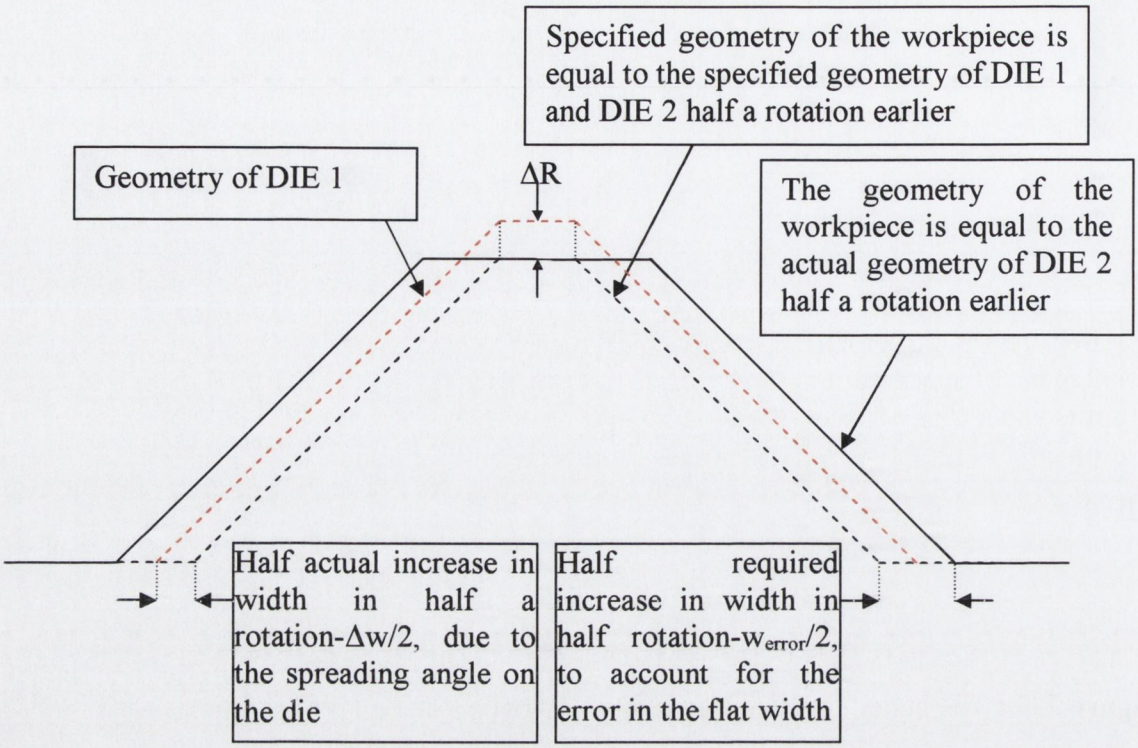

Figure 7.71: The die geometries that lead to one-die rolling in the knifing zone

i.e. if $\Delta w < w_{error}$ one-die rolling will be approached (7.18)

The equation for determining the increase in width can be calculated as follows.

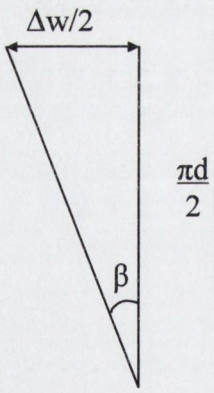

While:

$$\tan\beta = \frac{\Delta w/2}{\pi d/2} \quad (7.19)$$

$$\Delta w = \tan\beta \cdot \pi d \quad (7.20)$$

Figure 7.72: Determining the increase in feature width over half a rotation

Combining equations 7.18 and 7.20:

If $\tan\beta \cdot \pi d < w_{error}$ one-die rolling will be approached. (7.21)

For example, for the 0.45mm die set with a 45° sidewall angle and a 0.8° spreading angle there was a 0.075mm difference in the flat widths between the stationary and the moving die. This gives:

$$\Delta w = \tan\beta \cdot \pi d = \tan 0.8 \cdot \pi 0.45 = 0.019mm$$

w_{error} = 0.075mm

$$\therefore \Delta w < w_{error}$$

Therefore, rolling conditions approaching one-die rolling will occur and the problem will be magnified if a smaller diameter wire is used as this will further decrease the value of Δw. This die set suffers from a particularly large w_{error} and even if the spreading angle was increased to 3°, Δw would still be less than w_{error}, and the rolling conditions would approach those of one-die rolling.

Incorrect starting position in the knifing zone

If the starting position of the moving die is set incorrectly the workpiece will contact the pair of dies at different points along their lengths and because the feature geometry increases along the length of the die one side of the workpiece will encounter a larger die geometry than the other. In this case the profiles of DIE 1 and DIE 2 that are in contact with the workpiece will differ as illustrated in Figure 7.73 below.

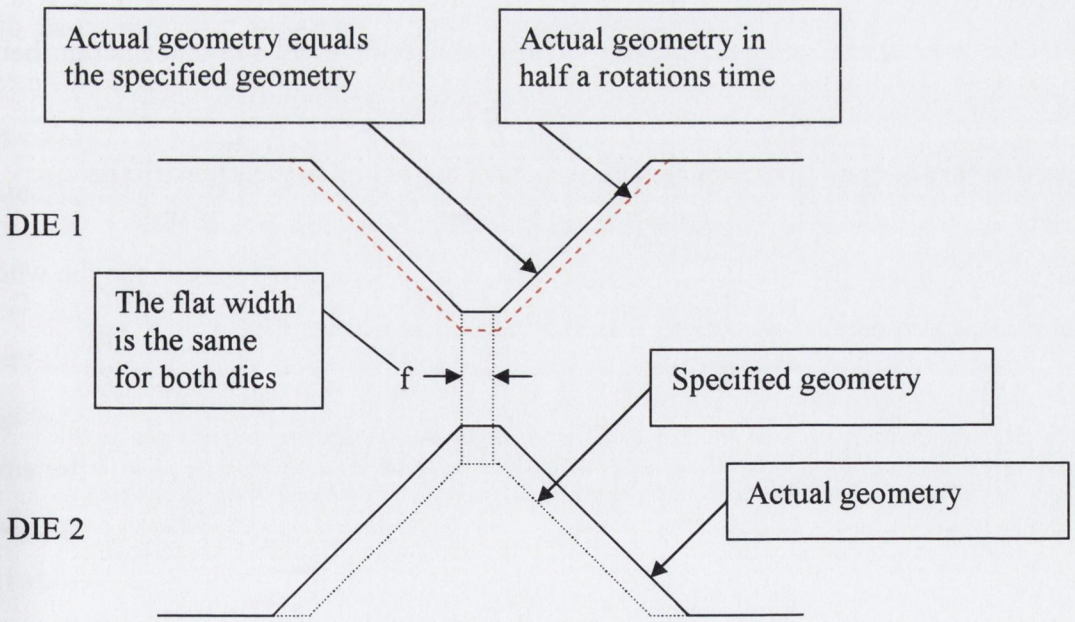

Figure 7.73: Incorrect starting position of the moving die that can lead to one-die rolling

In this case the error in the width of the tool is a function of the spreading angle of the die and the magnitude of the error in the starting position of the moving tool, $start_{error}$, as illustrated below.

Where:

$$\tan\beta = \frac{w_{error}/2}{start_{error}} \qquad (7.22)$$

$$w_{error} = 2\tan\beta \cdot start_{error} \qquad (7.23)$$

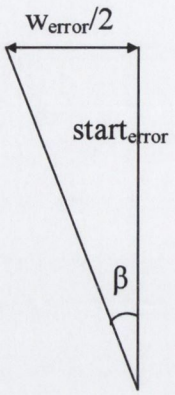

Figure 7.74: Determining error in the flat width when the starting position of the dies is set incorrectly

As already shown, the increase in the width of the die feature in half a rotation, Δw, is equal to $\tan\beta \cdot \pi d$. Now, if Δw is set equal to w_{error}, the $start_{error}$ becomes $\pi d/2$. Therefore, if the starting position of the dies is off-set by an amount equivalent to half a workpiece circumference, $\pi d/2$ or more, the actual geometry of die 1 in half a rotations time will be smaller then the current geometry of die 2. This will result in all the deformation being carried out by die 1.

Incorrect starting position in the spreading zone or one width being out of spec

This error only applies to dies that have spreading zones, which are areas of the die where the feature height remains constant but the flat width increases.

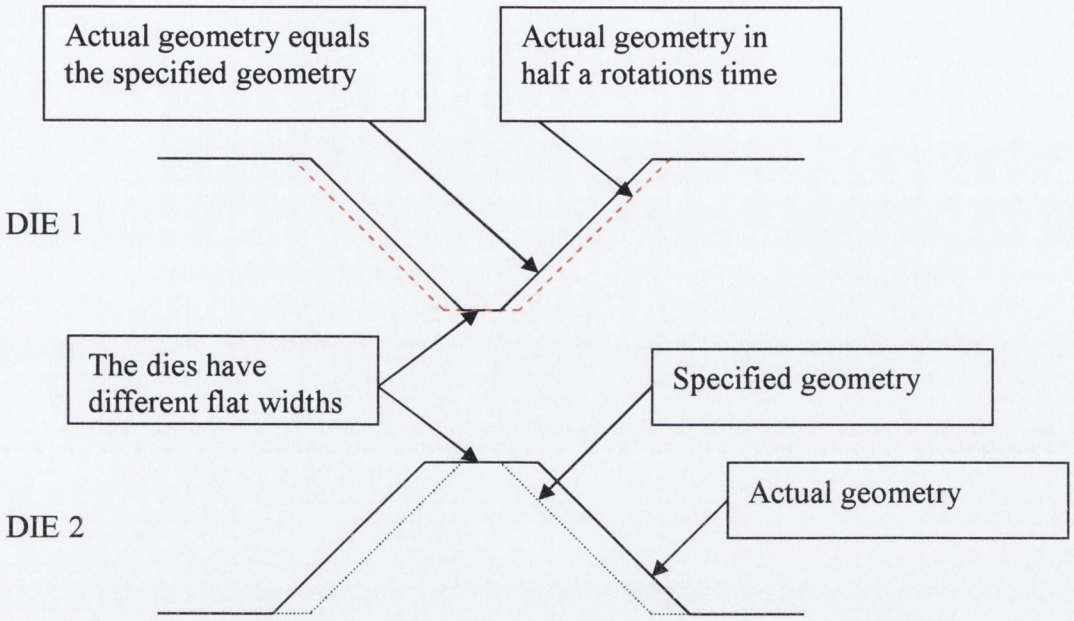

Figure 7.75: Circumstances leading to one-die rolling in the spreading zone

Figure 7.75 above illustrates the circumstances that can lead to one-die rolling in the spreading zone of a rolling process. Due to machining errors, or the starting position of the moving die being set incorrectly, DIE 2 could be wider than specified and this results in the forming of a groove that is wider than specified on one side of the workpiece. However, if DIE 1 is within specification, then, due to the very small spreading angle, its width in half a rotation will still be less then the width of DIE 2. Therefore, all the deformation will be performed by DIE 2 and the conditions of one-die rolling will have been established. This condition will arise if the difference in flat widths of the two dies is greater then the increase in the flat width of DIE 1 in half a rotation.

7.10.2 **Development of Workpiece Shape during One-Die Rolling**

In one-die rolling, one flat die and one wedge die are used and because of the difference in the geometries of these dies, the development the groove in the workpiece is quite different compared with traditional rolling. Where the workpiece contacts the flat die, material flows back into the groove because there is no die feature to resist its flow and this results in a decrease in the size of the workpiece groove. As well as forming the groove geometry, the wedge die must also remove the material that flowed into the groove when it was in contact with the flat die. The flow of material into the workpiece groove can be seen when a velocity vector plot is examined as shown in Figure 7.76.

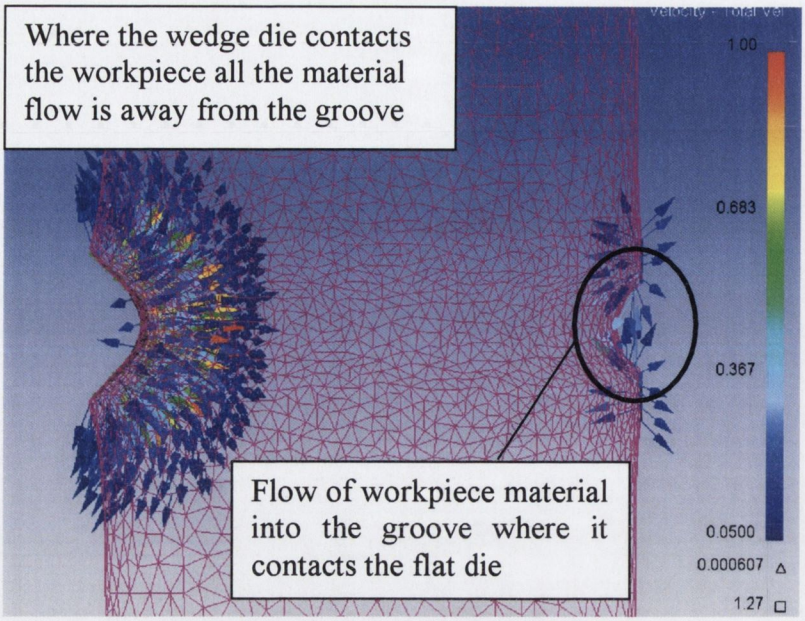

Figure 7.76: Velocity vector plot of one-die rolling process

7.10.3 **Possibility of Lap Formation**

Both the milled dies and the ground dies are potentially susceptible to the problem of lap formation for different reasons. As shown in Figure 7.77, the ground dies contain trenches on either side of the feature and a large amount of workpiece material is displaced into these valleys creating lips. These lips are ironed out when they come into contact with the flat die which resulted in the flow of material into the groove and a reduction in its size, as shown in Figure.7.77.

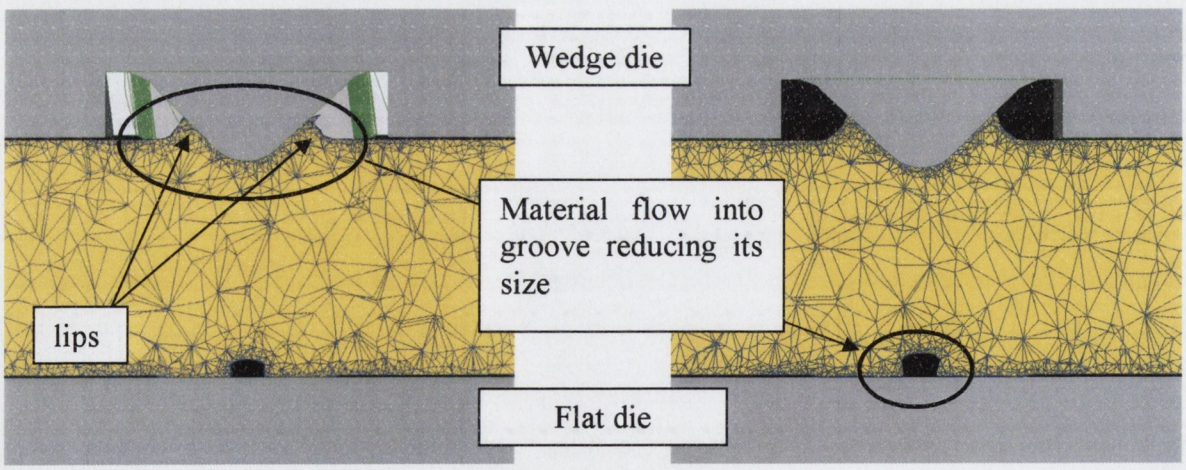

Figure 7.77: Sections through workpiece at half rotation intervals, illustrating flow of workpiece material into groove on contact with featureless die

However, due to the rounded tip of the die feature, it generally fits inside the remaining groove and forces material axially without the formation of laps. Also, the long sizing zone

tends to promote the formation of the correct groove shape by the end of the rolling stroke. The milled dies do not have trenches on either side of the feature and therefore workpieces rolled with them form smaller lips and less material is displaced back into the groove on contact with the flat die. However, the large flat on the groove tip is more likely to catch material and force it axially into the workpiece creating laps. The ironing out of these lips also leaves markings on the flat die, particularly if a lower strength tool steel such as P20 is used, see Figure 7.78.

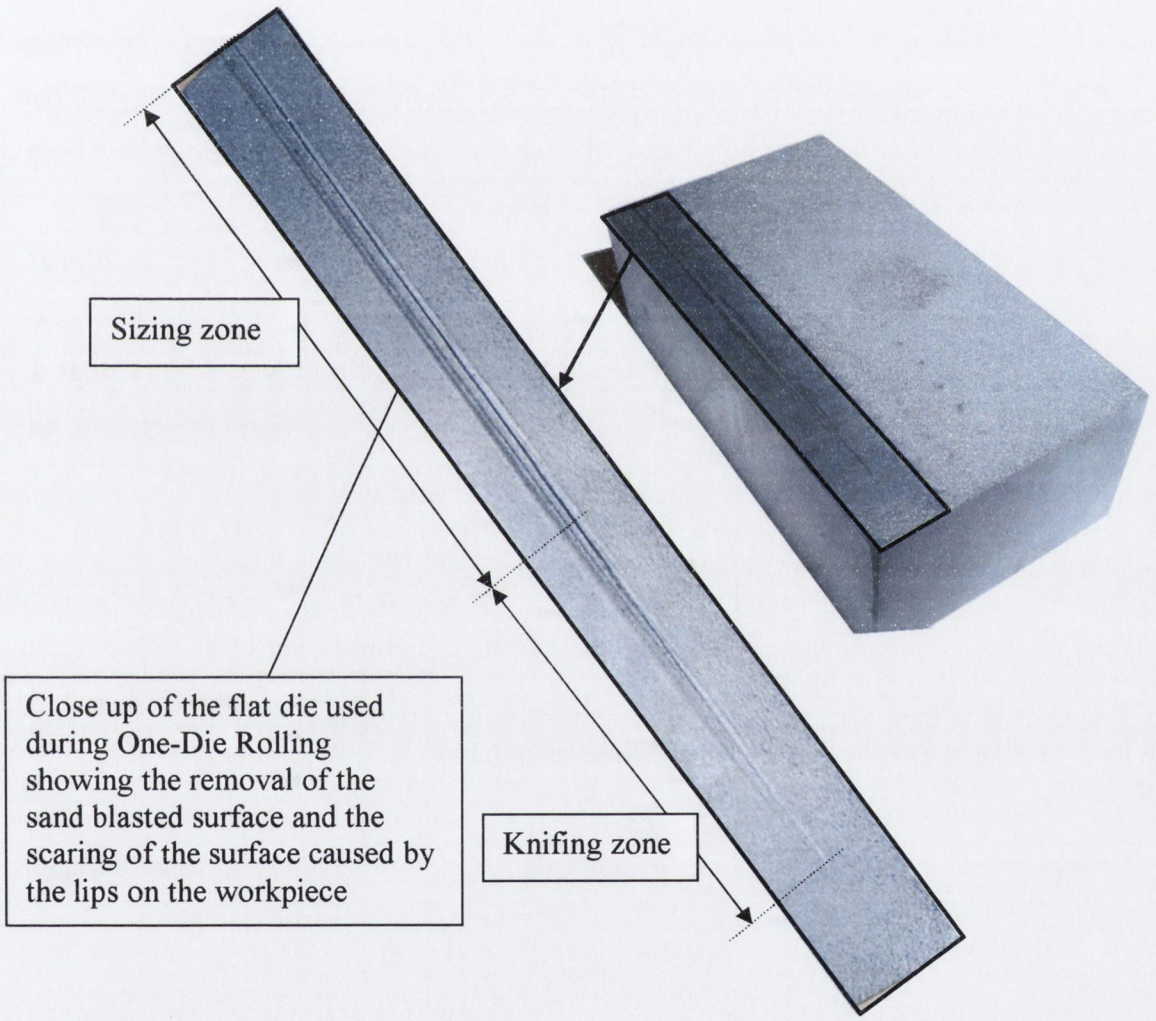

Figure 7.78: Evidence of lips on the scarred surface of the flat die

7.10.4 **Quality of Parts Produced using One-Die Rolling**

The parts produced using the one-die rolling technique are, in general, inferior to parts produced using traditional rolling. There are three reasons why the quality of the parts differs:

1. The surface quality of the groove itself is inferior for one-die rolling due to flaking and scarring along the sidewall and at the tip of the groove. For a given die set, the surface quality decreased as the diameter of the workpiece was decreased. This could be due to the increasing number of workpiece rotations with increasing miniaturisation and, therefore, the increased number of times workpiece material will be forced from the lips into the groove.
2. Due to the rough traction surface on the flat die, the surface quality of the workpiece for one-die rolling is inferior to that of traditional rolling. The workpiece tends to have a cratered surface. This problem becomes more acute as the workpiece diameter decreases and the scale of the surface roughness approaches that of the feature being produced. This problem could be alleviated somewhat by using a flat die with a smooth, EDM free region, near the end of the stroke where the cratered workpiece surface could be ironed out.
3. However the quality of the rolled part does increase in one area. For traditional form rolling, particularly when using ground dies, the lips that form on either side of the groove are often not completely ironed out. Therefore the workpiece has a diameter slightly larger then the rest of the wire in a region around the groove, as illustrated in Figure 7.79.

Figure 7.79: Profile of workpiece with ironed out lips

However with one-die rolling this region of increased diameter does not form to any great extent due to the lips being ironed out repeatedly by the flat die.

Although the quality of the parts rolled using the one-die rolling technique is inferior to those rolled using the traditional form rolling technique they still possess the improved material properties that the form rolling provides compared to machining such as the formation of beneficial flow lines and work hardening.

7.10.5 **Advantages and Disadvantages of the One-Die Rolling Process**

Apart from the advantages discussed earlier, such as easier setup and decreased machining costs, another other advantage became apparent when performing one-die rolling.

- For example some parts of the form rolling machine, associated with the feeding of the workpiece between the dies have to redesigned to match the geometry of the die set being used. However, if a flat moving die is used instead of a wedge tool, then these parts don't have to be redesigned.

As mentioned earlier, parts produced using one-die rolling tend to have inferior surface quality compared to that produced using traditional form rolling. In addition, the process appears to be less stable in the sizing zone and the workpiece can twist resulting in misshaped feature geometry.

CHAPTER 8

CONCLUSIONS

CHAPTER 8

CONCLUSIONS

Tooling Design Analysis Method using 2D and 3D FEA

- 2D and 3D FEA simulations were used to analyse micro-form rolling die designs and they predicted much of what was observed during experimental rolling trials:
  - Damage values predicted the location of failures within the experimentally rolled parts.
  - **Loss of contact between the die and workpiece in the sidewall region and the subsequent deviation of the workpiece groove geometry from the die geometry was predicted. This phenomenon has not been previously discussed in the literature.**
  - The effect of die geometry and increasing area reduction on metal flow and defects was also predicted using FEA.

- By analysing the stress and strain distributions predicted by FEA simulations of the micro-form rolling process some observations can be made:
  - The literature predicted a laminar strain pattern in the workpiece in which maximum values were located at the surface. **This pattern was confirmed during this research and, using 3D FEA, this laminar strain pattern was, for the first time, attributed to the rotational nature of the process.**
  - The literature predicted tensile hydrostatic stresses and maximum principal stresses in the centre of the workpiece and these stress conditions were observed for the wide range of die geometries used in this research.
  - When the stresses were divided into directional components, it was found that the axial stress was the largest tensile stress. Also, that the die geometry and area reduction determined whether a tri-axial tensile stress state developed in the centre of the workpiece.

- Some limitations associated with 2D FEA also became apparent during this research. They were associated with the inability of 2D FEA to model the rotational nature of the form rolling process:

- 2D FEA simulations were unable to predict the large surface strains that are a result of the rotational nature of the process.
- 2D FEA could not be used to model the waveform.
- Also, workpieces modelled using 2D FEA tended to experience excessive axial workpiece material flow.

- Due to the geometry of the die features used in this research, a simplified 2D FEA simulation could be used. A sequential 2D simulation approach is usually used to model the form rolling process and it uses a series of die profiles which gradually deform the workpiece to the final geometry. However, because the dies used in this research have a constant flat width, only one die profile was needed to model the process, thereby, improving the simulation setup and run times.

- Some factors that differentiated the 3D FEA of micro-form rolling from the FEA of macro-form rolling were also observed:
  - The small size of the die feature resulted in the die/workpiece contact being concentrated around the groove which could lead to undesired rotation of the workpiece. This could be prevented through the use of appropriate boundary condition in the FEA simulation.

The Effect of Die Geometry and Manufacturing Method on the Micro-Form Rolling Process

- **It is recommended that micro-form rolling dies are manufactured using a grinding process instead of a milling process for the reasons outlined below**:
  - The geometric accuracy and surface quality of ground dies was superior to that of milled dies. The main error associated with milled dies was that the feature widths were larger than specified. However, this allowed the micro-form rolling process using wide flats to be investigated and it proved to be quite different to rolling with narrower rounds.
  - The machining lines present on the milled dies were transferred to the workpiece decreasing its surface quality as compared to a workpiece rolled with a ground die set.

- Burrs resulting from milling also became more problematic with the miniaturisation of the die feature and they had a negative effect on die quality.
- The narrow curved feature geometry of the ground die set which prevented the formation of axial laps could not be replicated using milling.

- The prevention of lap formation on form rolled parts is an important aspect of die design. Both helical and axial laps can be present on form rolled parts. However, both can be prevented through careful die design:
  - **The lack of a spreading zone, in which the width of the groove is gradually increased, on the dies used in this research prevented the formation of helical laps.**
  - **The use of a groove with a narrow rounded tip prevented the formation of axial laps that were present on parts with wide groove geometries.**

Neither of the design parameters mentioned above have received much attention to date in the literature.

<u>The effect of Miniaturisation on the Form Rolling Process</u>

- During this research it was found that for a given die geometry, the quality of the parts produced using micro-form rolling decreased with reducing workpiece diameter:
  - Decreasing the workpiece diameter had the effect of increasing the area reduction experienced by the workpiece and this tended to decrease the surface quality of the part and increase the likelihood of part failure during the rolling stroke.
  - Internal failures were also found to develop in workpieces that had experienced very large cross sectional area reductions approaching 90%.
  - For a given groove flat width, the chances of die/workpiece separation in the sidewall region increased as the workpiece diameter decreases.
  - The stresses predicted by FEA simulations indicate that the process becomes more tensile as the area reduction experienced by the workpiece increases.
  - Small diameter workpieces were also more likely to develop internal axial failures than larger parts due to the large number of rotations they experienced.

A limit is, therefore, set on the maximum reduction in area possible without failure of between sixty and ninety percent.

The effect of Workpiece Material on Micro-Form Rolling

- **During this research stainless steel and titanium alloy workpieces were cold formed. This is significant because most of the current form rolling research focuses on hot working and experimental trials using lead.** It was discovered that both of these materials could be rolled to significant area reductions of over 60% and that stainless steel is more suited to the micro-form rolling process for the following reasons:
  - The surface quality of micro-form rolled stainless steel parts was superior to that of titanium parts which suffered from peeling.
  - Titanium parts were also more likely to fail during the rolling stroke.

The Limitations of Micro-Form Rolling

- Limitations with several aspects of the form rolling process became apparent during this research and they are discussed below:
  - As the workpiece diameter and die feature size decreased, setup of the rolling machine became more difficult because the smallest possible machine adjustments represented a significant proportion of the workpiece diameter or die feature.
  - Optical microscopes could not provide sufficiently clear images of micro-form rolled parts and, therefore, the use of a Scanning Electron Microscope provided the best method of observing and photographing the curved surfaces of a micro-form rolled part. Dimensions can subsequently be measured from these photographs. If the geometry is needed for a Finite Element simulation, the photograph can be imported into a graphics package and traced to ensure that the most accurate representation of the geometry is achieved.

The One-Die Rolling Process

- **The novel one-die rolling process which has not been previously mentioned in literature proved to be a viable process and was used to micro-form roll a range of die/workpiece combinations. Conclusions from these tests are listed below:**
  - The one-die rolling has cost and rolling machine setup advantages over traditional rolling.

- However, the surface quality of One-Die Rolled parts tends to be inferior to parts rolled using traditional form rolling.
- The stability of the process also decreases as undesired rotation and slippage of the workpiece becomes more likely.
- It was also determined that incorrect machine setup or out of specification dies could lead to conditions approaching one-die rolling.

CHAPTER 9

FUTURE WORK

CHAPTER 9

FUTURE WORK

Because micro-form rolling is a new process, a broad range of work could be carried out in the future. However, the most important work is that which will aid the commercialisation of the process. If micro-form rolling could be expanded to include a greater range of die designs and workpiece materials, it would be much more attractive and would become more of a rival to micro-machining. Some possibilities for future work in the areas of workpiece material and die design are discussed below.

The micro-form rolling dies used during this research had no spreading zone and parts produced, therefore, were free of laps. However, the maximum groove width that could be produced was small. The use of rolling dies with spreading zones would allow the production of parts with longer grooves and the investigation of the effect that helical laps have on micro-form rolled parts.

It would also be interesting to investigate the implications of using die features with profiles other than the triangular profile used in this research. For example, if a circular profile was used would the maximum area reduction before failure change and how would it affect the workpiece stresses predicted by FEA simulations?

As was discovered during this research, the workpiece material can have a big effect on the quality of micro-form rolled parts. Therefore, rolling trials using a broad range of materials should be performed to determine which materials are most suited to the process and the maximum area reduction that can be achieved before failure.

There was very little evidence of the size effect during this research because fine grained workpieces were used. It would be interesting to perform rolling trials with coarse grained workpieces to determine if the size effect became more pronounced and to determine whether it had an adverse effect on the quality of parts produced.

REFERENCES

[1] Sabbagh, D., *"Sales of handsets top 500 million"*, The Times, Business, pp. 31, March 11, 2004.

[2] Keepler, J., *"Whats a good number"*,Fastener Technology International, http://www.coldheadetmachinecorp.com, September 27 2004.

[3] rolflo, *"25 Years of Excellence"*,http://www.rolflo.com/index.html, September 27 2004.

[4] Orlomoski, R. W., *"Form rolling for increased profits"*, Wire Industry, pp. 734-736, 12, 1989.

[5] Geiger, M., Engel, U., Vollersten, F., Kals, R. and Mebner, A., *"Metal forming of micro parts for electronics"*, Production Engineering, pp. 15-18, 2, 1994.

[6] Kugler, *"http://www.kugler-precision.com/pdf_doc/maschinen/katalog_maschinen_en.pdf#search=%22kugler%20microturn%22"*,11th September 2006.

[7] Geiger, M., Kliener, M., Eckstein, R., Tiesler, N. and Engel, U., *"Microforming"*, CIRP ANNALS, pp. 445-462, 50, 2, 2001.

[8] Van Brussel, H., Peirs, J., Reynaerts, D., Delchambre, A., Reinhart, G., Roth, N. and Weck, M., *"Assembly of microsystems"*, CIRP ANNALS, pp. 451-472, 49, 2, 2000.

[9] Geiger, M., Messner, A. and Engel, U., *"Production of microparts - size effects in bulk metal forming, similarity theory-"*, Production Engineering, pp. 55-58, IV, 1, 1997.

[10] Engel, U. and Eckstein, R., *"Microforming-from basic research to its realisation"*, Journal of Materials Processing Technology, pp. 35-44, 125-126, 2002.

[11] Armstrong, R. W., *"On size effects in polycrystal plasticity"*, J. Mechs. Phys. Solids, pp. 196-199, 9, 1961.

[12] Miyazaki, S., Fujita, H. and Hiraoka, H., *"Effects of specimen size on the flow stress of rod specimens of polycrystalline Cu-Al alloy"*, Scripta Metallurgica, pp. 447-449, 13, 1979.

[13] Fu, X. P. and Dean, T. A., *"Past developments, current applications and trends in the cross wedge rolling process"*, International Journal of Machine Tools and Manufacture, pp. 367-400, 33, 3, 1993.

[14] *"Shaft forging the East German way"*, Metalworking Production, pp. 49-50, 19, 1969.

[15] Holub, J., *"Transverse hot rolling"*, Machinery, pp. 129-133, 102, 3, 1969.

[16] *"Wedge-rolling forming makes UK debut"*, Metalworking Production, pp. 43-45, 1, 1969.

[17] Hobdel, A. C. and Thomas, A., *"Approaches to cheaper forgings"*, Metal Forming pp. 17-25, 1969.

[18] EWM, *"The AF - series"*,http://www.ewmenn.de/english/programm/indexprogramm_e.html, September 27 2004.

[19] Sanmei, *"Micro rolling machine"*,http://www.sanmei-works.jp/english/seihin/index.html, September 27 2004.

[20] Profiroll, *"Thread and Profile Rolling Machine PW 10e"*,http://www.profiroll.de/en/thread_profile_rolling/machines/economical/pw_10e/, September 27 2004.

[21] Pater, Z., *"Tools optimisation in cross-wedge rolling"*, Journal of Materials Processing Technology, pp. 153-159, 139, 1-3, 2003.

[22] Pater, Z., Weronski, W., Kazanecki, J. and Gontarz, A., *"Study of process stability in cross wedge rolling"*, Journal of Materials Processing Technology, pp. 458-462, 92-93, 1999.

[23] Li, Q., Lovell, M. R., Slaughter, W. and Tagavi, K., *"Investigation of the morphology of internal defects"*, Journal of Materials Processing Technology, pp. 248-257, 125-126, 2002.

[24] Orlomoski, R. W., *"Making cylindrical parts by form rolling"*, Machine Design, pp. 125-127, November, 1986.

[25] Rolling, A. c. o. T. a. S., *"Thread Rolling"*, ASM Metals Handbook, pp. 130-143, Vol. 3 Machining, 1967.

[26] Pater, Z., *"Finite element analysis of cross wedge rolling"*, Journal of Materials Processing Technology, pp. 201-208, 173, 2006.

[27] Zhang, S. H., Li, M.-S., Xu, Y., Kang, D. C. and Li, C.-Z., *"Introduction to a new CNC ball-spinning machine"*, Journal of Material Processing Technology, pp. 112-114, 170, 2005.

[28] Sommer, H. H., *"The skew rolling mill a barstock rolling process based on high intensity forming"*, wire, pp. 49-53, 32, 2, 1982.

[29] Nefedov, A. A., Brezhnev, L. A., Sichevoi, A. P., Bystrikov, O. P. and Mil'man, E. A., *"A study of metal deformation under transverse helical rolling"*, STAL in English, pp. 371-374, 5, 1964.

[30] Eyres, G., MacGinley, T. and Monaghan, J., *"A finite element investigation into the failure of form rolling dies"*, International Manufacturing Conference 20, pp. 699-705, 2003.

[31] Eyres, G. and Monaghan, J., *"Designing forming tools using FEA"*, International Manufacturing Conference 19, pp. 717-724, 2002.

[32] Eyres, G. and Monaghan, J., *"Three-dimensional finite element analysis of a flat die form rolling process"*, International Manufacturing Conference 21, pp. 41-48, 2004.

[33] Fang, G., Lei, L. and Zeng, P., *"Three-dimensional rigid-plastic finite element simulations for the two-roll cross-wedge rolling process"*, Journal of Materials Processing Technology, pp. 245-249, 129, 2002.

[34] Teterin, P. K. and Luzin, Y. F., *"On the mechanism of metal rupture during cross rolling"*, STAL in English, pp. 758-760, 10, 1960.

[35] Kazanskaya, I. I., Panfilov, M. G. and Ippolitov, V. I., *"Reasons for the development of defects in tranverse helical rolling"*, STAL in English, pp. 709-711, 9, 1962.

[36] Dong, Y., Lovell, M. R. and Tagavi, K., *"Analysis of interfacial slip in cross sedge rolling: an experimentally verified finite-element model"*, Journal of Materials Processing Technology, pp. 273-281, 80-81, 1998.

[37] Dong, Y., Tagavi, K., Lovell, M. R. and Deng, Z., *"Analysis of stress in cross wedge rolling with application to failure"*, International Journal of Mechanical Sciences, pp. 1233-1253, 42, 2000.

[38] Deng, Z., Lovell, M. R. and Tagavi, K., *"Influence of material properties and forming velocity on the interfacial slip characteristics of cross wedge rolling"*, Journal of Manufacturing Science and Engineering, pp. 647-653, 123, 2001.

[39] Dong, Y., Tagavi, K. and Lovell, M. R., *"Analysis of interfacial slip in cross-wedge rolling: a numerical and phenomenological analysis"*, Journal of Materials Processing Technology, pp. 44-53, 97, 2000.

[40] Li, Q. and Lovell, M. R., *"On the critical friction of a two-roll cwr process"*, Journal of Materials Processing Technology, pp. 245-256, 160, 2005.

[41] Pater, Z., *"Theoretical method for estimation of mean pressure on contact area between rolling tools and workpiece in cross wedge rolling processes"*, Int. J. Mech. Sci, pp. 233-243, 39, 2, 1997.

[42] Pater, Z., *"A study of cross wedge rolling process"*, Journal of Materials Processing Technology, pp. 370-375, 80-81, 1998.

[43] Pater, Z., *"Numerical Simulation of the cross wedge rolling process including upsetting"*, Journal of Materials Processing Technology, pp. 468-473, 92-93, 1999.

[44] Pater, Z., *"Theoretical and experimental analysis of cross wedge rolling process"*, International Journal of Machine Tools and Manufacture, pp. 49-63, 40, 2000.

[45] Johnson, W. and Mamilis, A. G., *"A survey of some physical defects arising in metal working processes"*, 17th Int. MDTR Conf., pp. 607-621, 1977.

[46] Thompson, G. and Hawkyard, J. B., *"Crack formation in transverse rolling - a review"*, 1st International Conference on Rotary Metal-Working Processes, pp. 171-184, 1979.

[47] Tsuchikawa, T. and Ono, N., *"Surface roughening and failure during cold-form-rolling"*, 3rd International Conference on Rotary Metalworking Processes, pp. 333-343, 1984.

[48] Ishii, M., Takahashi, M. and Takeda, S., *"The development of a high-precision cross-rolling method"*, 3rd International Conference on Rotary Metalworking processes, pp. 345-352, 1984.

[49] Guifu, L., Guolu, Z. and Changwu, G., *"The study on the technological parameters and the load and power parameters on 3-roll cross wedge rolling"*, 3rd International Conference on Rotary Metalworking Processes pp. 333-343., 1984.

[50] Mockel, L. and Rotz, L., *"Transverse rolling"*, Metal Forming, pp. 279-284, 1968.

[51] Kusiak, J., *"Optimization techniques in computer simulation of metal forming processes"*, Dissertations Monographies 30, pp. n.a., 1995.

[52] Tsukamoto, H., Morimoto, K. and Juge, T., *"Cross roll method for the production of axi-symmetric shafts"*, Advance technology of plasticity, pp. 936-941, 2, 1984.

[53] Glab, R., Hahn, F., Kolbe, M. and Meyer, L. W., *"Processes of partial bulk metal-forming - aspects of technology and fem simulation"*, Journal of Material Processing Technology, pp. 174-178, 80-81, 1998.

[54] Orlomoski, R. W., *"Thread Rollers are part formers"*, Fastener Technology, pp. 49-52, 3/4, 1979.

[55] Pater, Z., Bartnicki, J. and Samolyk, G., *"Numerical modelling of cross-wedge rolling of ball pin"*, Journal of Materials Processing Technology, pp. 1235-1240, 164-165, 2005.

[56] Pater, Z., Gontarz, A. and Weronski, W., *"Cross-wedge rolling by means of one flat wedge and two shaped rolls"*, Journal of Materials Processing Technology, pp. 550-554, 177, 1-3, 2006.

[57] Armstrong, *"On size effects in polycrystal plasticity"*, J. Mech. Phys. Solids, pp. 196-199, 9, 1961.

[58] Miyazaki, S., Shibata, K. and Fujita, H., *"Effect of specimen thickness on mechanical properties of polycrystalline aggregates with various grains sizes"*, Acta Metallurgica, pp. 885-862, 27, 1979.

[59] Kals, R., Vollersten, F. and Geiger, M., *"Scaling effects in sheet metal forming"*, pp. 65-75, 1996.

[60] Geiger, M., Engel, U., Messner, A., Kals, R. and Vollersten, F., *"Design of micro-forming processes – fundamentals, materials data and friction behaviour"*, 9th International Cold Forging Congress, pp. 155-164, 1995.

[61] Tiesler, N. and Engel, U., *"Microforming - effects of miniaturisation"*, 8th International Conference on Metal Forming, pp. 2000.

[62] Bissacco, G., Hansen, H. N. and De Chiffre, L., *"Micromilling of hardened tool steel for mould making applications"*, Journal of Material Processing Technology, pp. 201-207, 167, 2005.

[63] Wong, C. C., Dean, T. A. and Lin, J., *"Incremental forming of cylindrical components using flow forming principles"*, Journal of Materials Processing Technology, pp. 60-66, 153-154, 2004.

[64] Buttimer, F., MacGinley, T. and Monaghan, J., *"Design and manufacture of groove forming tooling"*, International Manufacturing Conference 18, pp. 21-30, 2001.

[65] Fraunhofer-Institut für Werkzeugmaschinen und Umformtechnik IWU, C., *"Flat die cross rolling*
",http://www.simtop.fhg.de/cgi-bin/rmcat?72990303_e, 28 March 2006.

[66] Tseng, A. A., *"Material characterization and finite element simulation for forming miniature metal parts"*, Finite Element in Analysis and Design, pp. 251-265, 6, 7, 1990.

[67] Messner, A., Engel, U., Kals, R. and Vollersten, F., *"Size effect in the FE-simulation of micro-forming processes"*, Journal of Material Processing Technology, pp. 371-379, 45, 1994.

[68] Geibdorfer, S., *"Simulation of microforming processes"*, 3rd Erlangen Workshop on Microforming, pp. n.a., 2005.

[69] Cockroft, M. G. and Latham, D. J., *"Ductility and workability of metals"*, Journal of the Institute of Metals, pp. 33-39, 96, 1968.

[70] Kim, H. and Yamanaka, M., *"Prediction and elimination of ductile fracture in cold forgings using FEM simulation"*, Transactions of NAMRI/SME, pp. 63-69, 23, 1995.

[71] *"Selection of Material for thread rolling dies"*, ASM Speciality Handbook - Tool Materials, pp. 195-197, 1995.

[72] Uddeholm, *"AISI D2 Cold work tool steel"*,http://www.bucanada.ca/aisi_d2.pdf, 22 February 2007.

[73] Molinari, A., Straffelini, G., Tesi, B. and Bacci, T., *"Dry sliding wear mechanisms of the Ti6Al4V alloy"*, Wear, pp. 105-112, 208, 1997.

[74] Alam, M. O. and Haseeb, A. S. M. A., *"Response of Ti-6Al-4V and Ti-24Al-11Nb alloys to dry sliding wear against hardened steel"*, Tribology International pp. 357-362, 35, 2002.

[75] Askeland, D. R., *"Influence of crystal structure"*, The Science and Engineering of Materials, pp. 90-91, 1996.

APPENDIX: FORM ROLLING MACHINE SETUP SHEET

AF3 THREAD ROLLING MACHINE:
ADJUSTMENT SHEET FOR FORM ROLLING

General
Date: _____
Name: _____

Specifics
Material: _____
Diameter of blank: _____ Length of blank: _____
Head [Y/N]: ____
Features to be rolled: _____
Die dimensions: _____
Die number (name): _____
Traction surface: _____

Steps to be completed (mark off as completed)
1. remove old dies and put in new ones ☐
2. adjust position of keeperfinger ☐
3. change the feed finger ☐
4. adjust the feedfinger ☐
5. make tops of dies parallel ☐
6. rough adjustment of die gap ☐
7. adjust for misalignment ☐

run	A	B	C	D	E	F	G	H	I	J	K
setting											

8. if necessary adjust height of die to make features level ☐
9. adjust die match ☐

run		1		2		3		4		5		6	
Adjuster 1	Adjuster 2												
Adjuster 3	Adjuster 4												
Diameter													
Profile													
run		7		8		9		10		11		12	
Adjuster 1	Adjuster 2												
Adjuster 3	Adjuster 4												
Diameter													
Profile													

10. adjust feed rails for blanks ☐
11. adjust longitudinal position of the feedrails ☐
12. adjust the height and the opening angel of the keeperfinger ☐
13. put on feedrail spring ☐

Final working Setup

Adjuster 1	Adjuster 2	Adjuster 3	Adjuster 4	setting

Notes [1] _____

_____

_____

_____

APPENDIX: CONFERENCE PROCEEDINGS

Abstract for the IMC 23 Conference held in University of Ulster Jordanstown, Belfast on the 30th August-1st September 2006:

THE EFFECT OF DIE GEOMOETRY AND WORKPIECE DIAMETER ON THE MECHANICS OF MICRO FORM-ROLLING

Emmet Cregan[1], John Monaghan[1]

1. Dept. of Mechanical & Manufacturing Engineering, Trinity College Dublin, Ireland.

ABSTRACT

Form Rolling is a rotary forming process, in which the workpiece is rotated between a pair of flat dies. It can be used to form complex shapes on axisymmetric metal parts. Microparts are those with at least 2 sub-millimetre dimensions and the parts Form-Rolled during this research project fall within this category.

The research project reported on here aims to establish a better understanding of the effects that workpiece diameter, material, area reduction and die geometry have on the Micro Form-Rolling process and the quality of the formed parts. Particular emphasis was placed on the factors leading to internal failures, such as the area reduction experienced by the part during the forming process.

Micro Form-Rolling trials using a variety of die/workpiece combinations were carried out on a EWM AF3 Form Rolling machine. Ti 6AL 4V Titanium alloy and AISI 316 stainless steel workpieces were Rolled during this research and after Rolling they were mounted sectioned and then examined under a microscope to determine the presence, location and magnitude of any defects.

The Elasto-plastic FE packages DEFORM 2D and 3D were used to model the Micro Form-Rolling process. The stress distributions present in the workpiece during Rolling were examined to determine a better understanding of the mechanics of the process. Signs of failure were also monitored, high damage values were apparent in some simulations indicating where and when internal failure was likely to ensue.

KEYWORDS: (Micro, Form Rolling, FEA)

Abstract for the MED06 Conference held in DIT, Dublin on the 15th -16th March 2006:

AN EXPERIMENTAL AND FEA INVESTIGATION OF THE DEVELOPMENT OF INTERNAL DEFECTS IN THE MICRO FORM-ROLLING OF BIOCOMPATIBLE METALS

Emmet Cregan[1], John Monaghan[1]

1. Dept. of Mechanical & Manufacturing Engineering, Trinity College Dublin, Ireland.

Fax: 00 353 679 5554

e-mail: creganem@tcd.ie

ABSTRACT

Form-Rolling is a rotary forming process, in which the workpiece is rotated between a pair of flat dies. It is used to form near net shape axisymmetric metal parts. This paper investigates the development of internal defects during the Form-Rolling of microparts. Microparts are those that have 2 dimensions in the sub-millimetre range. The materials investigated were AISI 316 stainless steel (FE-Cr18-Ni10-Mo3) and ASTM Grade 5 titanium (Ti-6Al-4V). Both of these materials are biocompatible and are used in the manufacture of medical devices. Both Experimental and Finite Element Analysis of the process are discussed in this paper.

KEYWORDS: Form-Rolling, Finite Element Analysis (FEA), Micro.

Abstract for the IMC 22 Conference held in the Institute of Technology Tallaght, Dublin on the 31st August-2nd September 2005:

AN EXPERIMENTAL AND FEA INVESTIGATION OF THE MICROFORM ROLLING PROCESS

Emmet Cregan[1], John Monaghan[1]

1. Dept. of Mechanical & Manufacturing Engineering, Trinity College Dublin, Ireland.

ABSTRACT

Form Rolling is a rotary forming process, in which the workpiece is rotated between a pair of reciprocating flat dies. It is used to form net or near net shape axisymmetric metal parts. This paper investigates the application of the Form Rolling process to the production of microparts, defined as those having two or more dimensions in the sub-millimetre range.

It is suspected that as the parts being Form Rolled become smaller the characteristics of the process will change due to what is termed the "size effect" phenomenon. The "size effect" dictates that as the diameter to grain size ratio of a part becomes small the material flow strength decreases. Microform Rolling trials were carried out on a Form Rolling machine purchased for this research project. The trials involved Form Rolling geometrically similar features onto stainless steel wire samples of different diameters. The parts formed and the loads produced during the forming process were investigated for any scale dependent factors.

The Microform Rolling process was also modelled using Finite Element Analysis. The FE packages DEFORM 2D and 3D were used. 2D simulations used multi-object workpieces in which individual grains were represented by objects whose geometries were determined from actual grain structures.

KEYWORDS: Form Rolling, Finite Element Analysis (FEA), Microforming.

APPENDIX: POSTER PRESENTATION

Poster for the 2006 Sir Bernard Crossland Symposium at TCD, Dublin on the 29th and 30th of March 2006:

Mechanics of Micro Form-Rolling

Emmet Cregan[1], John Monaghan[1]

1. Dept. of Mechanical & Manufacturing Engineering, Trinity College Dublin, Ireland.

INTRODUCTION

Form-Rolling is a rotary forming process, in which the workpiece is rotated between a pair of flat dies, it can be used to form complex shapes on axisymmetric metal parts.

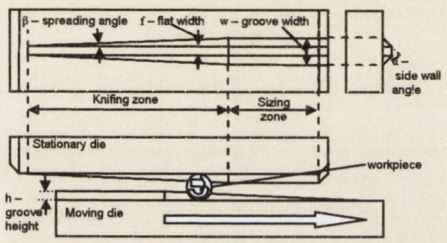

Figure 1: The Form-Rolling Process and the main die features

Microparts can be defined as "parts or structures with at least two dimensions in the submilimeter range" [1]. The parts Form-Rolled during this research fall into this category see figure 2.

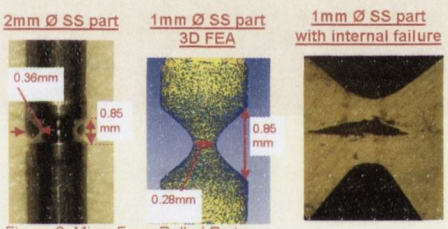

Figure 2: Micro Form-Rolled Parts

THEORY

Form-Rolling is a rotary metal forming process which includes a complex 3D stress state. The two predominant stresses are radial compressive stresses due to the penetration of the die into the workpiece and axial tensile stresses due to the deformed material being forced to flow axially. Torsional stresses also arise due to the contact conditions. The tensile stresses inherent in the process can lead to the failure of the part through the opening of internal voids or the necking of the part.

Microforming is subject to a "size effect" that differentiates it from Macroforming. It arises because of the large proportion of surface grains present in a micropart.

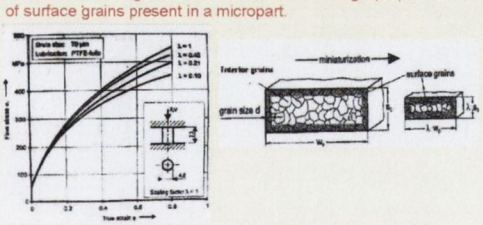

Figure 3: Decreasing flow strength with increasing proportion of surface grains [2, 3]

Elastoplastic Finite Element Analysis

FEA simulations have been used to analyse the deformation of the workpiece, necking is apparent in the simulations while internal failures can be predicted through the use of damage algorithms, see Figure 4. Damage values are a function of the stress state in the workpiece, if they exceed a critical value then failure of the part is likely to ensue.

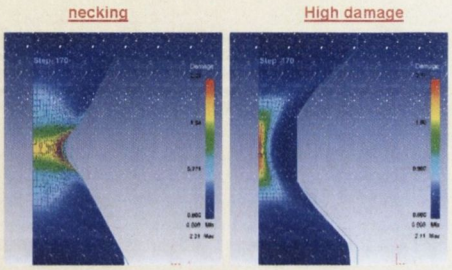

Figure 4: Prediction of Failure

Attempts have also been made to model the influence of the "size effect" in the Micro Form-Rolling Process, through the use of surface layers and meshed objects representing the grains.

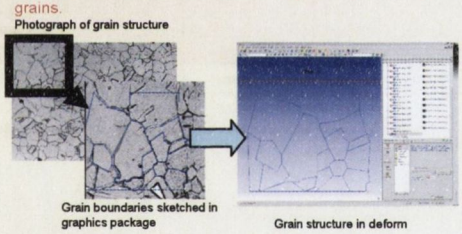

Figure 5: Grain to FEA

RESULTS

- Parts which experience large area reductions of over 60% are vulnerable to failure.
- Die geometry plays an important roll in the type of failure experienced by the part.

FUTURE WORK

Micro Form-Rolling trials with a variey of die/workpiece combinations are to be undertaken to develop a better understanding of the effects that workpiece diameter, material, area reduction and die geometry have on the forming process and the quality of the formed part.

REFERENCES

1. M. Geiger et al 2001. Microforming. *CIRP ANNALS*. 445-462
2. F. Vollersten et al 2004. State of the art in micro forming and investigations into micro deep drawing. *Journal of Materials Processing Technology*. 151: 70-79.
3. M. Geiger et al 1997. Production of microparts. *Production Engineering*. 4: 1: 55-58.

ACKNOWLWDGEMENTS

The authors are grateful to the Materials Ireland, Materials Processing Research Centre (MPRC) at Trinity College Dublin for their technical support to date